INVESTIGATIONS OF REVERSIBLE THERMOCHROMISM IN THREE-COMPONENT SYSTEMS

by

Alexander N. Bourque

Submitted in partial fulfilment of the requirements
for the degree of Doctor of Philosophy

at

Dalhousie University
Halifax, Nova Scotia
March 2014

Table of Contents

List of Tables xi
List of Figures xiv
Abstract xxxviii
List of Abbreviations and Symbols Used xxxix
Acknowledgements xliii

Chapter 1 Introduction 1

1.1 Colour in Chemistry 1
1.2 Chromic Materials 5
1.3 Thermochromism 10
1.4 Thermochromism in Organic Compounds 11
1.4.1 Bianthrone and Crowded Ethenes 11
1.4.2 Schiff Bases 13
1.4.3 Spiro Compounds 14
1.4.4 Liquid Crystals 17
1.4.5 Polymers and Oligomers 21
1.4.6 Charge-Transfer Complexes 23
1.5 Inorganic Thermochromism 24
1.6 Summary of Thermochromism 26

Chapter 2 Rewritable Three-Component Thermochromic Mixtures 27

2.1 Introduction to Three-Component Thermochromic Mixtures 27
2.1.1 Colour Former - Crystal Violet Lactone (CVL) 28
2.1.2 Colour Developer – Alkyl Gallates 35
2.1.3 Co-Solvent - Primary Alkyl Alcohols 41
2.1.3.1 Polymorphism in Primary Alkyl Alcohols 44
2.1.3.2 Structures of Primary Alkyl Alcohols 47
2.1.3.3 Thermodynamic Parameters of Primary Alkyl Alcohols 49
2.2 Binary Interactions in Three-Component Systems 51

2.2.1 Dye:Developer Interactions 52
2.2.1.1 Formation of Metastable Aggregate Structures 52
2.2.1.2 Examples of Binary Dye:Developer Interactions 54
2.2.1.2.1 CVL:Alkyl Gallate Binary Mixtures 54
2.2.1.2.2 Binary Complexes of CVL with Bisphenol A 60
2.2.2 Binary Developer:Solvent Interactions 62
2.2.2.1 Introduction to Binary Developer:Solvent Interactions 62
2.2.2.2 Alkyl Gallate:Primary Alcohol Binary Mixtures 62
2.3 A Look Ahead 68

Chapter 3 Experimental Methods 71

3.1 Materials 71
3.1.1 Research at Dalhousie University 71
3.1.2 Research Internship at Toshiba Co. Research and Development Centre (RDC) 72
3.2 Sample Preparation 73
3.2.1 Three-Component Mixture Preparation 73
3.2.1.1 Gram-Scale (Bulk) Mixture Preparation 73
3.2.1.2 Microgram-Scale Sample Preparation 75
3.2.1.3 Milligram-Scale Sample Preparation 76
3.2.2 Binary Sample Preparation 76
3.2.3 Synthesis of Intermediate Chain Length Alkyl Gallates 76
3.2.4 Ink-Jet Printer (IJP) Ink Preparation – Toshiba Co. RDC 78
3.3 Experimental Techniques 78
3.3.1 Colour Determination 78
3.3.1.1 Experimental Setup of Heat/Cool Cycling Experiments 79
3.3.1.2 Observational Spectroscopy 81
3.3.1.3 Colour Photo Analysis 82
3.3.1.4 Colour Space Conversions 84
3.3.2 Differential Scanning Calorimetry (DSC) 87
3.3.2.1 DSC Apparatus 88

3.3.2.2 DSC Calibration 91
3.3.3 Technologies for Toshiba Co. RDC Internship 92
3.3.3.1 Ink-Jet Printer 92
3.3.3.2 Colour Erasers 93
3.3.3.3 Colour Analyzer 94
3.3.3.4 Print Test Sheet and Over-Write Testing 95

Chapter 4 Influence of the Solid Solvent on the Thermochromic Behaviour of DDG-Containing Mixtures 97

4.1 Introduction and Background 97
4.1.1 Gross and Fine Features of Thermochromic Behaviour 99
4.1.1.1 Gross Features of Thermochromic Behaviour 100
4.1.1.2 Fine Features of Thermochromic Behaviour 100
4.2 Results and Discussion 101
4.2.1 CVL:DDG:TD-OH Mixtures 102
4.2.1.1 Introduction to Studies on CVL:DDG:TD-OH Mixtures 102
4.2.1.2 Observational Spectroscopy Results 103
4.2.1.2.1 Gross Features of CVL:DDG:TD-OH Mixtures 103
4.2.1.2.2 Fine Features of CVL:DDG:TD-OH Mixtures 105
4.2.1.3 Colour Photo Analysis of CVL:DDG:TD-OH Mixtures 109
4.2.1.3.1 Gross Features of CVL:DDG:TD-OH Mixtures 109
4.2.1.3.2 Fine Features of CVL:DDG:TD-OH Mixtures 111
4.2.1.4 Conclusions Concerning CVL:DDG:TD-OH Mixtures 116
4.2.2 CVL:DDG:HD-OH Mixtures 118
4.2.2.1 Introduction to Studies on CVL:DDG:HD-OH Mixtures 118
4.2.2.2 Observational Spectroscopy Results for CVL:DDG:HD-OH Mixtures 119
4.2.2.2.1 Gross Features of CVL:DDG:HD-OH Mixtures 119
4.2.2.2.2 Fine Features of CVL:DDG:HD-OH Mixtures 124
4.2.2.3 Colour Photo Analysis of CVL:DDG:HD-OH Mixtures 128
4.2.2.3.1 Gross Features of CVL:DDG:HD-OH Mixtures 129

4.2.2.3.2 Fine Features of CVL:DDG:HD-OH Mixtures 132
4.2.2.4 Conclusions Concerning CVL:DDG:HD-OH Mixtures 135
4.2.3 CVL:DDG:OD-OH Mixtures 137
4.2.3.1 Introduction to Studies on CVL:DDG:OD-OH Mixtures 137
4.2.3.2 Gross Features of CVL:DDG:OD-OH Mixtures 138
4.2.3.3 Fine Features of CVL:DDG:OD-OH Mixtures 141
4.2.3.4 Conclusions Concerning CVL:DDG:OD-OH Mixtures 142
4.3 Summary of the Influence of Solvent Alkyl Chain Length 144

Chapter 5 Influence of Developer Chain Length on Thermochromic Behaviour 148

5.1 Introduction 148
5.2 Experimental Results and Discussion 150
5.2.1 Octadecyl Gallate (ODG) Mixtures 150
5.2.1.1 CVL:ODG:TD-OH Mixtures 151
5.2.1.1.1 Gross Features of CVL:ODG:TD-OH Mixtures 151
5.2.1.1.2 Fine Features of CVL:ODG:TD-OH Mixtures 153
5.2.1.1.3 Conclusions Concerning CVL:ODG:TD-OH Mixtures 155
5.2.1.2 CVL:ODG:HD-OH Mixtures 156
5.2.1.2.1 Gross Features of CVL:ODG:HD-OH Mixtures 156
5.2.1.2.2 Fine Features of CVL:ODG:HD-OH Mixtures 158
5.2.1.2.3 Conclusions Concerning CVL:ODG:HD-OH Mixtures 160
5.2.1.3 CVL:ODG:OD-OH Mixtures 161
5.2.1.3.1 Gross Features of CVL:ODG:OD-OH Mixtures 161
5.2.1.3.2 Fine Features of CVL:ODG:OD-OH Mixtures 161
5.2.1.3.3 Conclusions Concerning CVL:ODG:OD-OH Mixtures 164
5.2.1.4 Summary of Thermochromic Behaviour in CVL:ODG:Alcohol Mixtures 165
5.2.2 Octyl Gallate (OG) Mixtures 168
5.2.2.1 CVL:OG:TD-OH Mixtures 168
5.2.2.1.1 Gross Features of CVL:OG:TD-OH Mixtures 168

5.2.2.1.2 Fine Features of CVL:OG:TD-OH Mixtures....172
5.2.2.1.3 Conclusions Concerning CVL:OG:TD-OH Mixtures....174
5.2.2.2 CVL:OG:HD-OH Mixtures....174
5.2.2.2.1 Gross Features of CVL:OG:HD-OH Mixtures....174
5.2.2.2.2 Fine Features of CVL:OG:HD-OH Mixtures....176
5.2.2.2.3 Conclusions Concerning CVL:OG:HD-OH Mixtures....178
5.2.2.3 CVL:OG:OD-OH Mixtures....179
5.2.2.3.1 Gross Features of CVL:OG:OD-OH Mixtures....179
5.2.2.3.2 Fine Features of CVL:OG:OD-OH Mixtures....180
5.2.2.3.3 Conclusions Concerning CVL:OG:OD-OH Mixtures....182
5.2.2.4 Summary of Thermochromic Behaviour in CVL:OG:Alcohol Mixtures....183
5.2.3 Propyl Gallate (PG) Mixtures....184
5.2.3.1 Introduction to Studies of PG-Containing Mixtures....185
5.2.3.2 Gross Features of PG-Containing Mixtures....186
5.2.4.3 Fine Features of PG-Containing Mixtures....189
5.2.3.4 Conclusions Concerning PG-Containing Mixtures....191
5.2.4 Gallic Acid (GA) Mixtures....192
5.2.4.1 Introduction to Studies of GA-Containing Mixtures....192
5.2.4.2 Gross Features of Behaviour in GA-Containing Mixtures....193
5.2.4.4 Summary of Thermochromic Behaviour in CVL:GA:Alcohol Mixtures....197
5.3 Summary of the Influence of Developer Chain Length....198

Chapter 6 Thermochromic Behaviour in Mixtures Containing Other Developers and Solvents....202

6.1 Introduction and Background....202
6.1.1 Summary of Variable Alkyl Chain Length Experiments....202
6.1.2 Other Phenolic Developers....203
6.1.2.1 Bisphenol A (BPA)....204
6.1.2.2 2,4-Dihydroxybenzophenone (DHB)....204

6.1.3 Other Solvent – Octadecanethiol 205
6.2 Experimental Results and Discussion 206
6.2.1 CVL:BPA:HD-OH Mixtures 206
6.2.1.1 Introduction to Studies on CVL:BPA:HD-OH Mixtures.....206
6.2.1.2 Gross Features of CVL:BPA:HD-OH Mixtures 206
6.2.1.3 Fine Features of CVL:BPA:HD-OH Mixtures 210
6.2.1.4 Conclusions Concerning CVL:BPA:HD-OH Mixtures.....212
6.2.2 CVL:DHB:HD-OH Mixtures 214
6.2.2.1 Introduction to Studies on CVL:DHB:HD-OH Mixtures.....214
6.2.2.2 Gross Features of CVL:DHB:HD-OH Mixtures 215
6.2.2.3 Fine Features in CVL:DHB:HD-OH Mixtures.....219
6.2.2.4 Conclusions Concerning CVL:DHB:HD-OH Mixtures 222
6.2.3 CVL:DDG:OD-SH Mixtures.....224
6.2.3.1 Introduction to Studies on CVL:DDG:OD-SH Mixtures 224
6.2.3.2 Gross Features of CVL:DDG:OD-SH Mixtures.....225
6.2.3.3 Fine Features of CVL:DDG:OD-SH Mixtures 230
6.2.3.4 Conclusions Concerning CVL:DDG:OD-SH Mixtures.....233
6.2.4 Binary Phase Diagram Determination 234
6.2.4.1 Introduction to Binary Phase Diagram Determination 234
6.2.4.2 Binary Phase Diagram Determination for BPA:HD-OH Mixtures 236
6.2.4.3 Binary Phase Diagram Determination for DHB:HD-OH Mixtures.....239
6.2.4.4 Binary Phase Diagram Determination for DDG:OD-SH Mixtures 240
6.2.4.5 Summary of Binary Phase Diagram Determination 242
6.3 Conclusions Regarding Thermochromism in Mixtures Containing BPA, DHB, or OD-SH.....243

Chapter 7 Ternary Thermochromic Phase Diagrams 248

7.1 Introduction and Background 248
7.2 Ternary Thermochromic Phase Diagram Determination.....252
7.2.1 Thermochromic Phase Diagrams of ODG-Containing Mixtures 252
7.2.1.1 CVL:ODG:TD-OH Thermochromic Phase Diagram 252

7.2.1.2 CVL:ODG:HD-OH Thermochromic Phase Diagram.....253
7.2.1.3 CVL:ODG:OD-OH Thermochromic Phase Diagram.....254
7.2.1.4 Summary of CVL:ODG:Alcohol Thermochromic Phase Diagrams 256
7.2.2 Thermochromic Phase Diagrams of DDG-Containing Mixtures 257
7.2.2.1 CVL:DDG:TD-OH Thermochromic Phase Diagram 258
7.2.2.2 CVL:DDG:HD-OH Thermochromic Phase Diagram.....260
7.2.2.3 CVL:DDG:OD-OH Thermochromic Phase Diagram.....265
7.2.2.4 Summary of CVL:DDG:Alcohol Thermochromic Phase Diagrams 266
7.2.3 Thermochromic Phase Diagrams for OG-Containing Mixtures.....267
7.2.3.1 CVL:OG:TD-OH Thermochromic Phase Diagram 268
7.2.3.2 CVL:OG:HD-OH Thermochromic Phase Diagram.....269
7.2.3.3 CVL:OG:OD-OH Thermochromic Phase Diagram.....271
7.2.3.4 Summary of CVL:OG:Alcohol Thermochromic Phase Diagrams 272
7.2.4 Thermochromic Phase Diagrams of PG-Containing Mixtures.....273
7.2.4.1 CVL:PG:TD-OH Thermochromic Phase Diagram.....274
7.2.4.2 CVL:PG:HD-OH Thermochromic Phase Diagram 275
7.2.4.3 CVL:PG:OD-OH Thermochromic Phase Diagram 278
7.2.4.4 Summary of CVL:OG:Alcohol Thermochromic Phase Diagrams 280
7.2.5 Thermochromic Phase Diagrams for CVL:BPA:HD-OH and CVL:DHB:HD-OH Mixtures 281
7.2.5.1 Thermochromic Behaviour of BPA- and DHB-Containing Mixtures 281
7.2.5.2 Thermochromic Phase Diagrams for BPA- and DHB-Containing Mixtures 282
7.2.5.3 Summary of Thermochromic Phase Diagrams for BPA- and DHB-Containing Mixtures 287
7.2.6 Thermochromic Phase Diagram for CVL:DDG:OD-SH Mixtures 289
7.3 Conclusions Regarding Thermochromic Phase Diagram Determination 292

Chapter 8 Thermally Erasable Ink-Jet Printer Inks 296

8.1 Introduction and Background 296

8.1.1 Thermally Erasable Laser-Jet Toner - e-blue™ 296
8.1.1.1 Background 296
8.1.1.2 Composition and Function 296
8.1.1.3 Technical Problems with Erasable Printing Inks 298
8.1.2 Thermally Erasable Ink-Jet Printer Inks 300
8.1.2.1 Composition and Function 300
8.1.2.2 Colour Density Threshold Values 302
8.2 Results and Discussion 303
8.2.1 Enhancement of the Colour Density of IJP Inks 303
8.2.1.1 IJP Inks Containing CVL 303
8.2.1.2 IJP Inks Containing Blue 63 and Blue 203 305
8.2.1.3 IJP Inks Containing Blue C4OH, Blue C6NH2 and PS-Blau 307
8.2.2 Effectiveness of Erasing – IJP Inks 310
8.2.2.1 IJP Inks Containing CVL 311
8.2.2.2 IJP Inks Containing Blue 63 and Blue 203 312
8.2.2.3 IJP Inks Containing Blue C4OH, Blue C6NH2 and PS-Blau 313
8.2.3 Modification of the Viscosity of IJP Inks 314
8.2.3.1 IJP Inks Containing CVL Modified With PVA 315
8.2.3.2 IJP Inks Containing Blue C4OH Modified With PVA 317
8.2.4 Best Ink Prepared During the Internship 319
8.3 Conclusions Regarding Thermally Erasable Ink-Jet Printer Inks 323

Chapter 9 Summary, Conclusions, and Future Work 325

9.1 Summary of Reversible Thermochromism in Three-Component Mixtures 325
9.1.1 Influence of the Solvent Alkyl Chain Length 325
9.1.2 Influence of the Developer Alkyl Chain Length 328
9.1.3 Other Developer and Solvent Components 331
9.1.4 Influence of the Solvent Rotator Phase 334
9.1.5 Melt-Lightened vs. Melt-Darkened Thermochromism and Maximum Colour Contrast 336

9.2 General Conclusions Concerning Reversible Thermochromic Behaviour in Three-Component Mixtures 340
9.3 Conclusions Regarding Thermally Erasable Ink-Jet Printer Inks 342
9.4 Future Work 343
9.4.1 Compilation of Thermochromic Phase Diagrams Using Combinatorial Methods 344
9.4.2 Structural Analysis Using X-Rays 344
9.4.3 Thermal Analysis 346
9.4.4 Extension of Design Rules 346
References 348
Appendix 365
Permissions for Reproduced Figures 365

List of Tables

Table 1.1. Chromic phenomena and associated stimuli. 6

Table 2.1. Melting points and alkyl chain lengths of various alkyl gallate developers. 36

Table 2.2. Melting points, solid-solid phase transition temperatures, and alkyl chain lengths of various alkyl alcohol solvents. 44

Table 2.3. Long spacing of primary alcohol polymorphs in Å.[148,150,160] 49

Table 2.4. Thermodynamic data for the phase transitions of 1-tetradecanol.[156] 49

Table 2.5. Thermodynamic data for the phase transitions of 1-hexadecanol.[156] 50

Table 2.6. Thermodynamic data for the phase transitions of 1-octadecanol.[149] 50

Table 2.7. The stoichiometry of dye:developer complexes formed in equilibrium mixtures of CVL with PG, OG, and DDG.[110] 60

Table 2.8. Compound formation and eutectic data for binary mixtures of PG, OG, and DDG with TD-OH, HD-OH, and OD-OH; all data were obtained from DSC studies during heating runs at 5 K min^{-1}.[110] 66

Table 4.1. Melting points, solid-solid phase transition temperatures, and alkyl chain lengths of various alkyl alcohol solvents. 99

Table 5.1. Melting points and alkyl chain lengths of various alkyl gallate developers. 149

Table 7.1. The colour designation of thermochromic samples as a function of colour density. 251

Table 7.2. The colour density and colour contrast values obtained *via* colour photo analysis for ODG-containing mixtures, with the samples demonstrating the highest colour contrast for each ternary system. 257

Table 7.3. The colour density and colour contrast values obtained *via* observational spectroscopy for DDG-containing mixtures, showing data for the samples demonstrating the highest colour contrast for each ternary system. 267

Table 7.4 The colour density and colour contrast values obtained *via* colour photo analysis for DDG-containing mixtures, showing data for the samples demonstrating the highest colour contrast for each ternary system. 267

Table 7.5. The colour density and colour contrast values obtained *via* colour photo analysis for OG-containing mixtures, showing data for the samples demonstrating the highest colour contrast for each ternary system listed in the table. 273

Table 7.6. The colour density and colour contrast values obtained *via* colour photo analysis for PG-containing mixtures, showing data for the samples demonstrating the highest colour contrast for each ternary system listed in the table. 280

Table 7.7. The colour density and colour contrast values obtained *via* colour photo analysis for PG-containing mixtures, showing data for the samples demonstrating the highest colour contrast for each ternary system. 289

Table 7.8. The colour density and colour contrast values obtained *via* observational spectroscopy for CVL:DDG:OD-SH mixtures, showing data for the samples demonstrating the highest colour contrast for each compositional range studied listed in the table. 292

Table 8.1. The compositions of CVL inks. 304

Table 8.2. The compositions of Blue 63 and Blue 203 inks. 307

Table 8.3. The compositions of blue C4OH, blue C6NH2 and PS-Blau 203 inks. 309

Table 9.1 Colour contrast values and equilibrium solid and melt colour densities obtained *via* colour photo analysis for melt-darkened thermochromic mixtures. The samples listed demonstrated the highest colour contrast observed here for each ternary system. 337

Table 9.2 Colour contrast values and equilibrium solid and melt colour densities obtained *via* observational spectroscopy for melt-lightened thermochromic mixtures. The samples listed demonstrated the highest colour contrast observed here for each ternary system. 338

Table 9.3 Colour contrast values and equilibrium solid and melt colour densities obtained *via* colour photo analysis for melt-lightened thermochromic mixtures. The samples listed demonstrated the highest colour contrast observed here for each ternary system. Note: the CVL:DDG:HD-OH mixture was measured without the use of a white reference material for brightness normalization and, therefore, the colour densities are artificially high. 339

Table 9.4 Colour contrast values and equilibrium solid and melt colour densities obtained *via* colour photo analysis for melt-lightened mixtures containing BPA and DHB. A sample from the low solvent concentration regime (*e.g.* $z \leq 100$) and high solvent concentration regime (*e.g.* $z \geq 150$) is listed for both systems. 339

Table 9.5 Colour contrast values and equilibrium solid and melt colour densities obtained *via* colour photo analysis for melt-lightened thermochromic mixtures. The samples listed demonstrated the highest colour contrast observed here for each ternary system. 340

List of Figures

Figure 1.1. Phenolphthalein converts from a colourless form (in acidic environments) to a pink/fuchsia colour (in basic environments) due to a ring-opening reaction in the presence of hydroxide ions.[24] 8

Figure 1.2. The halochromic equilibrium of crystal violet lactone showing the colourless spiropyran form of CVL (left) and the strongly coloured merocyanine form of CVL (right).[25] The colour images of thermochromic samples, shown at the bottom right of the figure, show different colour densities due to varying concentrations of the ring-opened, MC form of CVL.....9

Figure 1.3. The structure of (a) bianthrone and (b) dixanthylene; both become more planar as the temperature is increased due to the expansion of the central alkene bond. (c) Bulky groups at the 1, 1', 8, and 8' positions prevent the two aromatic moieties from becoming planar, resulting in non-thermochromic compounds.....12

Figure 1.4. The keto-enol equilibrium responsible for thermochromism and photochromism in Schiff bases.....13

Figure 1.5. Schematic representation of the tautomeric ring-opening equilibrium between the spiropyran (SP) form and the merocyanine (MC) form of a spiro compound.....15

Figure 1.6. The ring-opening equilibrium of the acid-sensitized fluoran dye, S-205. The MC form of the dye is black in colour.....16

Figure 1.7. (a) The structure of cholesterol (where R = OH) and (b) the thermochromic temperature ranges for some cholesteric liquid crystals, where the R-groups form ester linkages with the parent cholesterol molecule.....18

Figure 1.8. (a) The structure of (*S*)-4-(2-methylbutyl)phenol and (b) the thermochromic temperature ranges for some derivatives of (*S*)-4-(2-methylbutyl)phenol, where the R-groups form carbon-carbon or ether linkages with the parent molecule.....18

Figure 1.9. Pitch length corresponds to the distance between layers A and B, over which the orientational director of the layer (represented by an arrow) has made a complete rotation about the central helical axis. Reproduced with permission from *Journal of Chemical Education*, 1999, 76(9), 1201-1205. Copyright (1999) American Chemical Society.[38] 19

Figure 1.10. An illustrative depiction of the colour change associated with changes in pitch length of a chiral nematic phase liquid crystal above the *S*-*N** transition.[72].....21

Figure 1.11. (a) The thermochromic polymer poly(3-hexylthiophene) is an important material for organic electronic applications due to its high electrical conductivity. (b) Thermochromic polydiacetylenes have garnered substantial interest due to their tuneable colour *via* R-group modification. 22

Figure 1.12. The components of an intensely coloured thermochromic charge-transfer system, (a) electron-rich dialkoxynaphthalene derivatives and (b) electron-poor 1,4,5,8-naphthalenetetracarboxylic diimide derivatives.[89] 24

Figure 1.13. The thermochromic equilibrium of aqueous $CoCl_2$ solutions, where a change in ligand coordination geometry elicits a colour change from red to blue on heating. 26

Figure 2.1. The crystal structure of crystal violet lactone (CVL). The unit cell is monoclinic in the $P2_1/n$ space group with four molecules per unit cell. Reproduced with permission from reference 112 (*Journal of Crystallographic and Spectroscopic Research*, 1984, 14(2), 121-128).....29

Figure 2.2. Crystal violet lactone (CVL) and its ring-opened resonance forms. The open form displays zwitterionic or quinonoid-stabilized resonance structures. The type of stabilization depends on the strength of the intermolecular interaction causing the ring-opening reaction.[114] HA represents the acidic developer added to initiate ring-opening.....31

Figure 2.3. (a) The UV-Vis absorption spectrum of leuco-CVL in acetonitrile shows a major band at 280 nm. (b) CVL in acetonitrile acidified with acetic acid shows a major band at 605 nm and a shoulder at 570 nm. Reproduced with permission from reference 25 (*Journal of Photochemistry*, 1987, 37, 379-390).....32

Figure 2.4. (a) The change in absorbance with increased solvent polarity. A maximum in colour density is reached at 7 vol% acetone. (b) The ratio (C_{max}/C_o) of the concentration of the coloured form at the absorption maximum, C_{max}, to the initial dye concentration, C_0, depends on the dielectric constant of the solvent. Adapted from reference 119. 34

Figure 2.5. The structure of gallic acid (R = H) and its associated esters (R = C_nH_{2n+1}).....35

Figure 2.6. The crystal structure of propyl gallate dihydrate is monoclinic, $P2_1/c$, Z = 4, with a = 7.872 Å, b = 7.560 Å, c = 19.836 Å, and with β =101.03º. Reproduced with permission from reference 136 (*Acta Crystallographica E*, 2002, E58, o245-o247). 37

Figure 2.7. The crystal structure of octyl gallate dihydrate is triclinic, *P-1*, Z = 2, with a = 6.617 Å, b = 9.956 Å, c = 14.088 Å and with α = 79.08º, β = 85.58º, and γ = 70.80º. Reproduced with permission from reference 138 (*Acta Crystallographica E*, 1990, B46, 519-524).....39

Figure 2.8. The packing behaviour in even- and odd-numbered primary alcohols in (a) the (β) phase and (b) the tilted (γ) phase. The grey spheres represent the

hydroxyl groups and the black spheres represent the carbon chains (omitting hydrogen atoms). Unfavourable end-group packing in the tilted phases precludes the formation of γ-phases in odd-numbered primary alcohols with n > 14. The β phases do not demonstrate differences in end-group packing between even- or odd-numbered alcohols. Adapted from reference 159. 45

Figure 2.9 The crystal structures of (a) the β-phase of 1-heptadecanol and (b) γ-phase of 1-octadecanol. (a) The β-phase of 1-heptadecanol is characterized by head-to-head bilayer stacking in which the hydroxyl groups form a plane and the alkyl chains are oriented in a nearly perpendicular fashion to the hydroxyl plane. (b) The γ-phase of 1–octadecanol is characterized by a head-to-head bilayer structure in which the alkyl chains are oriented at an angle of approximately 60° to the hydroxyl plane. Large spheres represent oxygen atoms, small spheres represent carbon atoms, and hydrogen atoms are omitted for clarity. Adapted from reference 160. 48

Figure 2.10. Schematic representation of the two types of proposed structures for the metastable phases of binary dye:developer mixtures employed in rewritable thermochromic systems, and the proposed structure of the colourless equilibrium phase. (a) A coloured metastable structure in which alkyl chains give rise to long-range lamellar order, and the heads of the alkyl chains (*e.g.*, the hydroxyl or phenolic protons) interact with the dye molecules. (b) A colourless, equilibrium structure in which the dye and developer have become phase-separated. (c) A thermally quenched, glassy metastable state in which there is no long-range order associated with the alkyl chains of the developer. Reproduced with permission from reference 110 (D. C. MacLaren, *PhD Thesis*, Dalhousie University, 2003). 53

Figure 2.11. A CVL:DDG mixture where $x_{CVL} = 0.17$ showing (a) an as-solidified glassy form of the mixture and (b) the partially crystalline form of the mixture after annealing at 65 °C for 30 minutes. Reproduced with

permission from reference 110 (D. C. MacLaren, *PhD Thesis*, Dalhousie University, 2003). 55

Figure 2.12. A comparison of the (a) crystallites formed during annealing of the x_{CVL} = 0.17 mixture showing consistent morphological features with (b) crystallites of pure DDG. Reproduced with permission from reference 110 (D. C. MacLaren, *PhD Thesis*, Dalhousie University, 2003). 55

Figure 2.13. DSC thermograms on heating of glassy mixtures of CVL and DDG. The lack of a crystallization event at x_{CVL} = 0.33 indicates that there is no free DDG in the mixture at (and above) this composition. Reproduced with permission from reference 110 (D. C. MacLaren, *PhD Thesis*, Dalhousie University, 2003). 56

Figure 2.14. Raman spectra of crystal violet lactone:dodecyl gallate mixtures (CVL:DDG) showing the formation of a complex at x_{CVL} = 0.25. The relative intensities of the carboxylate carbonyl modes at 1359 cm^{-1} and 720 cm^{-1}, the $C{=}NR_2$ mode at 1584 cm^{-1}, and the $C\text{-}NR_2$ mode at 918 cm^{-1} reach maximum values when x_{CVL} = 0.25. Reproduced with permission from reference 110 (D. C. MacLaren, *PhD Thesis*, Dalhousie University, 2003). 58

Figure 2.15. The stoichiometry of the coloured DDG_3:CVL complex was determined by Job's method of continuous variation. The 3DDG:CVL stoichiometry of the coloured complex was supported by both (a) the carboxylate carbonyl vibrations and (b) the $C\text{-}NR_2/C{=}NR_2$ vibrations. The error bars indicate spread over three sets of samples. Reproduced with permission from reference 164 (*Journal of Materials Chemistry*, 2003, 13, 1695-1700). 59

Figure 2.16. Binary phase diagrams determined on (a) heating and on (b) cooling for 1-tetradecanol (TD) and dodecyl gallate (DDG, also known as lauryl gallate, LG) mixtures. Note the formation of a binary compound, $(LG)_2$•TD

(= 2DDG:TD-OH), at x_{LG} = 0.67. Reproduced with permission from reference 110 (D. C. MacLaren, *PhD Thesis*, Dalhousie University, 2003). 64

Figure 2.17. The binary phase diagram determined on heating for 1-hexadecanol (HD) and propyl gallate (PG) mixtures. Boundaries are added as a guide to the eye. The system is characterized by a eutectic at x_{LG} = 0.15 ± 0.05, 318 ± 1 K. No compound formation was observed for this binary system. Reproduced with permission from reference 110 (D. C. MacLaren, *PhD Thesis*, Dalhousie University, 2003). 65

Figure 3.1. The method of preparation of bulk samples. Far right: both samples contain CVL as the dye and DDG as the developer. The blue sample contains HD-OH as the solvent while the white sample contains TD-OH as the solvent, demonstrating how the colour of the solid state depends on choice of solvent. 74

Figure 3.2. Microgram samples of CVL:DDG:OD-SH prepared in Teflon vial caps. Heating of the samples produced inhomogeneous blue colouration. The diameter of the vial caps is 8 mm. 75

Figure 3.3. The *trans*-esterification reaction of tetradecanol (TD-OH) with gallic acid (GA) produces tetradecyl gallate (TDG). 77

Figure 3.4. The experimental setup used during heat/cool cycling experiments. The heating rate was controlled by the hot plate and the cooling rate was controlled by the addition of ice to the water bath. The temperature was recorded by a mercury thermometer held in the water bath and the samples were held in the bath by a sheet of aluminium. 80

Figure 3.5. The colour scale used throughout this work to define the colour intensity of bulk three-component thermochromic mixtures. The values on the figure indicate the colour density (*CD*) of each colour as measured in the *Lab** colour space. 82

Figure 3.6. Top: a colour density versus temperature plot showing the colour change behaviour in the CVL:DDG:TD-OH ternary system at various concentrations. Lines are added as a guide to the eye. Bottom: colour photographs of the sample at a composition of [1:8.7:86.4] (mole ratios are normalized to CVL content) showing the change in observed colour. At room temperature, the colour density is very low and the sample is white/colourless. As the sample melts, the colour changes to blue and there is an increase in the colour density. 83

Figure 3.7. Samples were removed from the water bath, imaged with a digital camera, and analyzed with the image analysis software ImageJ. 84

Figure 3.8. The CIE *Lab** colour space. The *a** axis spans red to green, the *b** axis spans yellow to blue and the *L** axis, referred to as the lightness, spans *L** = 0 which is black to *L** = 100 which is white.[185,] 85

Figure 3.9. Schematic diagram of a power-compensated DSC apparatus. The separated sample (S) and reference (R) chambers have their own heaters and thermometers, which are linked through a feedback circuit that minimizes the temperature differential between S and R (ΔT_{SR}). If $\Delta T_{SR} = 0$, the average temperature amplifier controls the heating profile. If $\Delta T_{SR} \neq 0$, at which point a thermal event is occurring, both the differential temperature amplifier and the average temperature amplifier will heat S and R to minimize ΔT_{SR}. Adapted from references 189 and 191. 89

Figure 3.10. Left: the modified Canon 8600 printer that was used to print thermally erasable IJP inks. Right: the cartridge holder showing substantial modification to prevent auto shut-off features from functioning.....93

Figure 3.11. The Konica Minolta Chroma Meter CR300 used to analyze the colour of printed images.....94

Figure 3.12. (a) The standard “print test sheet” showing image analysis rectangles and printed text. (b) "Over-write” print test sheets showing the first printed image and the location of the overwrite images. Note that there is a new “fresh printing” rectangle on this page for comparison with the over-write printed image. 96

Figure 4.1. The structure of gallic acid (R = H) and associated gallic acid esters (R = alkyl chain) used in this work. 99

Figure 4.2. Colour density versus temperature plots obtained *via* observational spectroscopy for CVL:DDG:TD-OH samples in the $[1:y:90]$ (top) and $[1:y:60]$ (bottom) compositional ranges. The molar ratios of the three components are given on the figure. Heating rates during these experiments were dT/dt = 1 K min^{-1}. T_{fus} represents the melting point of the pure solvent. Lines are added as a guide to the eye. Error in *CD* was estimated to be +/- 0.15. Note: data were only collected to 80 °C for the $[1:y:90]$ samples. 104

Figure 4.3. Colour density versus temperature plots obtained *via* colour photo analysis for samples in the CVL:DDG:TD-OH system. The molar ratios of the three components are given on the figure. Heating rates during these experiments were dT/dt = 1 K min^{-1}. T_{fus} represents the melting point of the pure solvent. Lines are added as a guide to the eye. Error in *CD* was estimated to be +/-0.15.....110

Figure 4.4. Colour photographs (a) on heating and (b) on cooling of the CVL:DDG:TD-OH sample at a composition of $[1:9:90]$. Note the formation of colour upon melting (T > 42 °C) and reduction in colour density upon solidification (T < 36 °C). 112

Figure 4.5. Colour photographs of the CVL:DDG:TD-OH sample at a composition of $[1:10:189]$. Note the high transparency of the molten phase of the

mixture, as well as the lack of colour formation on solvent melting ($T \geq 40$ °C) and the appearance of colour upon solidification ($T \leq 30$ °C). 113

Figure 4.6. Colour photographs of the CVL:DDG:TD-OH sample at a composition of [1:3.5:45.5]. Note the formation of colour upon melting ($T \geq 50$ °C) and loss of colour upon solidification ($T \leq 30$ °C). 114

Figure 4.7. Colour density versus temperature plots obtained *via* observational spectroscopy for CVL:DDG:HD-OH samples in the [1:y:90] (top), [1:y:60] (middle), and [1:y:30] (bottom) compositional ranges. The molar ratios of the three components are given on the figure. Heating rates during these experiments were dT/dt = 1 K min^{-1}. T_{fus} represents the melting point of the pure solvent. Lines are added as a guide to the eye. Error in *CD* was estimated to be +/-0.15. Note: data were only collected to 70 °C for the [1:y:30] samples. 120

Figure 4.8. Colour density versus temperature plots obtained *via* observational spectroscopy for samples in the CVL:DDG:HD-OH system (where $z < 30$). The molar ratios of the three components are given on the figure. Heating rates during these experiments were dT/dt = 1 K min^{-1}. T_{fus} represents the melting point of the pure solvent. Lines are added as a guide to the eye. Error in *CD* was estimated to be +/-0.15. 123

Figure 4.9. Colour photographs of the CVL:DDG:HD-OH sample at a composition of [1:0.5:23]. The yellow colour of the melt is due to insoluble *leuco*-CVL.....126

Figure 4.10. Colour density versus temperature plots obtained *via* colour photo analysis for samples in the CVL:DDG:HD-OH system. Note that these data were not normalized with a reflective white standard material. The molar ratios of the three components are given on the figure. Heating rates during these experiments were dT/dt = 1 K min^{-1}. T_{fus} represents the melting point

of the pure solvent. Lines are added as a guide to the eye. Error in *CD* was estimated to be +/-0.15.....130

Figure 4.11. Colour photographs of CVL:DDG:HD-OH samples at a variety of compositions; (a) [1:3:96], (b) [1:5:94], (c) [1:3:46], and (d) [1:0.5:23].....131

Figure 4.12. Colour density versus temperature plots obtained *via* observational spectroscopy for CVL:DDG:OD-OH samples in the [1:*y*:100] (top), [1:*y*:90] (middle), and [1:*y*:80] (bottom) compositional ranges. The molar ratios of the three components are given on the figure. Heating rates during these experiments were d*T*/d*t* = 1 K min^{-1}. T_{fus} represents the melting point of the pure solvent. Lines are added as a guide to the eye. Note: data were only collected to 70 °C for the [1:*y*:100] samples. Error in *CD* was estimated to be +/-0.15.....139

Figure 5.1. Colour density versus temperature plots obtained via colour photo analysis for samples in the CVL:ODG:TD-OH system. The molar ratios of the three components are given on the figure. Heating rates during these experiments were dT/dt = 1 K min^{-1}. T_{fus} represents the melting point of the pure solvent. Lines are added as a guide to the eye. Error in *CD* was estimated to be +/-0.15.....152

Figure 5.2. Colour photographs of CVL:ODG:TD-OH samples at compositions of (a) [1:6.4:26.7] and (b) [1:3.6:59].....153

Figure 5.3. Colour density versus temperature plots obtained *via* colour photo analysis for samples in the CVL:ODG:HD-OH system. The molar ratios of the three components are given on the figure. Heating rates during these experiments were d*T*/d*t* = 1 K min^{-1}. T_{fus} represents the melting point of the pure solvent. Lines are added as a guide to the eye. Error in *CD* was estimated to be +/-0.15.....157

Figure 5.4. Colour photographs of the CVL:ODG:HD-OH samples at compositions of (a) [1:5.8:48.5] and (b) [1:6.1:25.8].....158

Figure 5.5. Colour density versus temperature plots obtained *via* colour photo analysis for samples in the CVL:ODG:OD-OH system. The molar ratios of the three components are given on the figure. Heating rates during these experiments were dT/dt = 1 K min^{-1}. T_{fus} represents the melting point of the pure solvent. Lines are added as a guide to the eye. Error in *CD* was estimated to be +/-0.15.....161

Figure 5.6. Colour photographs of the CVL:ODG:OD-OH samples at compositions of (a) [1:5.2:87]and (b) [1:5.9:25.2].....163

Figure 5.7. Colour density versus temperature plots obtained *via* colour photo analysis for samples in the CVL:OG:TD-OH system. The molar ratios of the three components are given on the figure. Heating rates during these experiments were dT/dt = 1 K min^{-1}. T_{fus} represents the melting point of the pure solvent. Lines are added as a guide to the eye. Error in *CD* was estimated to be +/-0.15.....169

Figure 5.8. Colour photographs of CVL:OG:TD-OH samples at a composition of (a) [1:6.2:103.2] and (b) [1:5.7:23.6].....170

Figure 5.9. Binary phase diagram determined on heating for tetradecanol (TD) and octyl gallate (OG) mixtures. Note the lack of compound formation and the formation of a single eutectic. Reproduced with permission from reference 110 (D. C. MacLaren, *PhD Thesis*, Dalhousie University, 2003). 172

Figure 5.10. Colour density versus temperature plots obtained *via* colour photo analysis for samples in the CVL:OG:HD-OH system. The molar ratios of the three components are given on the figure. Heating rates during these experiments were dT/dt = 1 K min^{-1}. T_{fus} represents the melting point of the

pure solvent. Lines are added as a guide to the eye. Error in *CD* was estimated to be +/-0.15.....175

Figure 5.11. Colour density versus temperature plots obtained *via* colour photo analysis for samples in the CVL:OG:OD-OH system. The molar ratios of the three components are given on the figure. Heating rates during these experiments were dT/dt = 1 K min^{-1}. T_{fus} represents the melting point of the pure solvent. Lines are added as a guide to the eye. Error in *CD* was estimated to be +/-0.15.....180

Figure 5.12. Colour photographs of the CVL:OG:OD-OH sample at a composition of [1:1.9:23.1]. 181

Figure 5.13. Colour density versus temperature plots obtained *via* colour photo analysis for samples in the CVL:PG:TD-OH system. The molar ratios of the three components are given on the figure. Heating rates during these experiments were dT/dt = 1 K min^{-1}. T_{fus} represents the melting point of the pure solvent. Lines are added as a guide to the eye. Error in *CD* was estimated to be +/-0.15.....186

Figure 5.14. Colour density versus temperature plots obtained *via* colour photo analysis for samples in the CVL:PG:HD-OH system. The molar ratios of the three components are given in the figure. Heating rates during these experiments were dT/dt = 1 K min^{-1}. T_{fus} represents the melting point of the pure solvent. Lines are added as a guide to the eye. Error in *CD* was estimated to be +/-0.15.....187

Figure 5.15. Colour photographs of the CVL:PG:HD-OH sample at a composition of [1:6.2:99.0]. Note the loss of colour on melting ($T \geq 50$ °C), the reappearance of colour upon solidification of the developer ($T < 58$ °C), and further intensification of the colour on solidification of the solvent ($T = 48$ °C). 188

Figure 5.16. Colour density versus temperature plots obtained *via* colour photo analysis for samples in the CVL:PG:OD-OH system. The molar ratios of the three components are given on the figure. Heating rates during these experiments were dT/dt = 1 K min^{-1}. T_{fus} represents the melting point of the pure solvent. Lines are added as a guide to the eye. Error in *CD* was estimated to be +/-0.15.....189

Figure 5.17. The structure of gallic acid (GA).....193

Figure 5.18. Colour density versus temperature plots obtained *via* colour photo analysis for samples in the CVL:GA:TD-OH system. The molar ratios of the three components are given on the figure. Heating rates during these experiments were dT/dt = 1 K min^{-1}. T_{fus} represents the melting point of the pure solvent. Lines are added as a guide to the eye. Error in *CD* was estimated to be +/-0.15.....194

Figure 5.19. Colour density versus temperature plots obtained *via* colour photo analysis for samples in the CVL:GA:HD-OH system. The molar ratios of the three components are given on the figure. Heating rates during these experiments were dT/dt = 1 K min^{-1}. T_{fus} represents the melting point of the pure solvent. Lines are added as a guide to the eye. Error in *CD* was estimated to be +/-0.15.....195

Figure 5.20. Colour density versus temperature plots obtained *via* colour photo analysis for samples in the CVL:GA:OD-OH system. The molar ratios of the three components are given on the figure. Heating rates during these experiments were dT/dt = 1 K min^{-1}. T_{fus} represents the melting point of the pure solvent. Lines are added as a guide to the eye. Error in *CD* was estimated to be +/-0.15.....196

Figure 5.21. Colour photographs of the CVL:GA:OD-OH sample at a composition of [1:6.2:102.8].....197

Figure 6.1. Structure of bisphenol A.....204

Figure 6.2. Structure of 2,4-dihydroxybenzophenone. 205

Figure 6.3. Colour density versus temperature plots obtained *via* colour photo analysis for CVL:BPA:HD-OH samples in the (top) low solvent concentration regime and (bottom) high solvent concentration regime. The molar ratios of the three components are given on the figure. Heating rates during these experiments were dT/dt = 1 K min^{-1}. T_{fus} represents the melting point of the pure solvent. Lines are added as a guide to the eye. Error in *CD* was estimated to be +/-0.15. Note that data for the high concentration regime were only collected to 90 °C.....207

Figure 6.4. Colour photographs of CVL:BPA:HD-OH samples at various compositions; (a) [1:8:91], (b) [1:6.1:95.4], (c) [1:16:1985], and (d) [1:4:2000].....208

Figure 6.5. Colour photographs of CVL:BPA:HD-OH samples at low solvent concentrations (a) [1:1:23] and (b) [1:1.3:47]. 210

Figure 6.6. Colour photographs of the CVL:BPA:HD-OH sample at a composition of [1:8:91]. Note the gradual loss of colour on heating beginning around 40 to 42 °C before colour is completely lost upon solvent melting. On cooling, colour did not reappear with solvent solidification (T < 50 °C), instead requiring conversion to the LO-phase of the solvent (46 to 40 °C) for the full reappearance of colour.....211

Figure 6.7. Colour density versus temperature plots obtained *via* colour photo analysis for samples in the CVL:DHB:HD-OH system in the low solvent concentration (top) and high solvent concentration (bottom) regimes. The molar ratios of the three components are given on the figure. Heating rates during these experiments were dT/dt = 1 K min^{-1}. T_{fus} represents the melting

point of the pure solvent. Lines are added as a guide to the eye. Error in *CD* was estimated to be +/-0.15. 216

Figure 6.8. Colour photographs of CVL:DHB:HD-OH samples at various compositions: (a) [1:8:91], (b) [1:6:93], and (c) [1:16:1685].....217

Figure 6.9. Colour photographs of CVL:DHB:HD-OH samples at compositions of (a) [1:0.2:16] and (b) [1:1:48]. Both samples demonstrate high melt opacity due to low solvent concentrations.....220

Figure 6.10. Colour density versus temperature plots obtained *via* observational spectroscopy for samples in the CVL:DDG:OD-SH system with $z \approx 1900$ to 2100. The molar ratios of the three components are given on the figure. Heating rates during these experiments were $dT/dt = 1$ K min^{-1}. T_{fus} represents the melting point of the pure solvent. Lines are added as a guide to the eye. Error in *CD* was estimated to be +/-0.15.....226

Figure 6.11. Colour density versus temperature plots obtained *via* observational spectroscopy for samples in the CVL:DDG:OD-SH system with $z \approx 900$ to 1000. The molar ratios of the three components are given on the figure. Heating rates during these experiments were $dT/dt = 1$ K min^{-1}. T_{fus} represents the melting point of the pure solvent. Lines are added as a guide to the eye. Error in *CD* was estimated to be +/-0.15.....227

Figure 6.12. Colour density versus temperature plots obtained *via* observational spectroscopy for CVL:DDG:OD-SH samples in the (top) $z \approx 650$ to 715 and (bottom) $z = 500$ compositional ranges. The molar ratios of the three components are given on the figure. Heating rates during these experiments were $dT/dt = 1$ K min^{-1}. T_{fus} represents the melting point of the pure solvent. Lines are added as a guide to the eye. Error in *CD* was estimated to be +/-0.15.....229

Figure 6.13. Binary phase diagram determined by DSC on heating for 1-hexadecanol (HD-OH) and bisphenol A (BPA) mixtures. Note the lack of compound formation. 237

Figure 6.14. Binary phase diagram determined by DSC on heating for 1-hexadecanol (HD) and 2,4-dihydroxybenzophenone (DHB) mixtures. Note the lack of compound formation. 240

Figure 6.15. Binary phase diagram determined by DSC on heating for 1-octadecanethiol (OD-SH) and dodecyl gallate (DDG) mixtures. Note the invariance in the melting and solid-solid phase transition temperatures of OD-SH and the nearly invariant melting transition temperature of DDG. 241

Figure 7.1. A ternary thermochromic phase diagram of the CVL:DDG:TD-OH system (note: LG ≡ DDG, TD ≡ TD-OH). The thermochromic behaviour of thermally quenched samples deposited onto paper *via* ink jet printing is mapped onto the ternary phase diagram to identify which type of behaviour occurs within specific compositional regions of the phase diagram. Here thermochromic samples became coloured after thermal quenching into a metastable solid state, and colour was lost after standing at room temperature, after which the decoloured equilibrium solid state was returned. Reproduced with permission from reference 181 (H. Tang, *MSc Thesis*, Dalhousie University, 2007). 249

Figure 7.2. A portion of the ternary thermochromic phase diagram of the CVL:ODG:TD-OH system, showing the melt colouration. The equilibrium solids were all colourless. 253

Figure 7.3. A portion of the ternary thermochromic phase diagram of the CVL:ODG:HD-OH system, showing the melt colouration. The equilibrium solids were all colourless. 254

Figure 7.4. A portion of the ternary thermochromic phase diagram of the CVL:ODG:OD-OH system, showing the melt colouration. The equilibrium solids were all colourless. Samples with high developer concentrations (*e.g.*, when $x_{ODG} > 6\%$) demonstrated melt-darkened thermochromism in which (a) the solid state was colourless and (b) the melt was coloured. Samples with high solvent concentration and low developer concentrations (*e.g.*, when $x_{ODG} < 4\%$ and $x_{OD\text{-}OH} > 94\%$) were (c) colourless in the solid state and (d) colourless in the melt. In the schematic diagrams, the number of dye and developer molecules is shown as being the same for both the solid and melt but, for the ease of drawing, the number of solvent molecules is not conserved. 255

Figure 7.5. A portion of the ternary thermochromic phase diagram of the CVL:DDG:TD-OH system, showing the melt colouration. The equilibrium solids were all colourless. 259

Figure 7.6. A portion of the ternary thermochromic phase diagram of the CVL:DDG:HD-OH system. Samples with high developer concentrations (*e.g.*, when $x_{DDG} > 7\%$) were coloured in (a) the solid state and (b) formed darker molten phases on heating, demonstrating melt-darkened behaviour. Samples with low developer concentrations (*e.g.*, when $x_{DDG} < 5\%$) were (c) coloured in the solid state and (d) became decoloured upon melting, demonstrating melt-lightened thermochromism. In between these regions (*e.g.*, when $x_{DDG} = 6$ to 7%), samples were sometimes not thermochromic. In the schematic diagrams, the number of dye and developer molecules is shown as being the same for both the solid and melt but, for the ease of drawing, the number of solvent molecules is not conserved. 262

Figure 7.7. A close-up view of the solvent-rich region of the ternary thermochromic phase diagram of CVL:DDG:HD-OH mixtures. In this region, the colouring behaviour was observed to change from melt-lightened behaviour (when $x_{DDG} \leq 5\%$) to melt-darkened behaviour (when $x_{DDG} > 7\%$). In the

intermediate region ($x_{DDG} \approx 6$ to 7%), the colour contrast between the equilibrium solid and the melt was near zero. 263

Figure 7.8. A portion of the ternary thermochromic phase diagram of the CVL:DDG:OD-OH system. Samples with high developer concentrations (*e.g.*, when $x_{DDG} > 10\%$) demonstrated melt-darkened thermochromism. Samples with low developer concentrations (*e.g.*, when $x_{DDG} < 5\%$) demonstrated melt-lightened thermochromism. In between these regions (*e.g.*, when $x_{DDG} \approx 6\%$), samples were sometimes not thermochromic. 265

Figure 7.9. A portion of the ternary thermochromic phase diagram of the CVL:OG:TD-OH system. Samples with high developer concentrations (*e.g.*, when $x_{OG} \approx 18\%$) demonstrated melt-darkened thermochromism. Samples with low developer concentrations (*e.g.*, when $x_{OG} < 8\%$) demonstrated melt-lightened thermochromism. In between these regions (*e.g.*, when $x_{OG} \approx$ 11%), a non-thermochromic sample was obtained. 269

Figure 7.10. A portion of the ternary thermochromic phase diagram of the CVL:OG:HD-OH system. Samples with high developer concentrations (*e.g.*, when $x_{OG} \approx 18\%$) demonstrated melt-darkened thermochromism. Samples with low developer concentrations (*e.g.*, when $x_{OG} < 8\%$) demonstrated melt-lightened thermochromism. In between these regions (*e.g.*, when $x_{OG} \approx 10\%$), a non-thermochromic sample was obtained. 270

Figure 7.11. A portion of the ternary thermochromic phase diagram of the CVL:OG:OD-OH system. Samples with high developer concentrations (*e.g.*, when $x_{OG} \approx 19\%$) demonstrated melt-darkened thermochromism. Samples with low developer concentrations (*e.g.*, when $x_{OG} < 11\%$) demonstrated melt-lightened thermochromism. No non-thermochromic samples were obtained for this ternary system. 272

Figure 7.12. A portion of the ternary phase diagram of the CVL:PG:TD-OH system. Samples with high developer concentrations (*e.g.*, when $x_{PG} \approx 18\%$) demonstrated melt-darkened thermochromism. Samples with low developer concentrations (*e.g.*, when $x_{PG} < 8\%$) demonstrated melt-lightened thermochromism. In between these regions (*e.g.*, when $x_{PG} \approx 10\%$), a non-thermochromic sample was obtained. 275

Figure 7.13. A portion of the ternary thermochromic phase diagram of the CVL:PG:HD-OH system. Samples with high developer concentrations (*e.g.*, when $x_{PG} \approx 7\%$) were coloured in (a) the solid state and (b) retained colour upon melting, yielding melt-darkened thermochromism at very large developer concentrations ($x_{PG} > 18\%$). Samples with low developer concentrations (*e.g.*, when $x_{PG} < 4\%$) were coloured in (c) the solid state and (d) became decoloured upon melting. demonstrating melt-lightened thermochromism. 277

Figure 7.14. A portion of the ternary thermochromic phase diagram of the CVL:PG:OD-OH system. Samples with high developer concentrations (*e.g.*, when $x_{PG} \approx 18\%$) demonstrated melt-darkened thermochromism. Samples with low developer concentrations (*e.g.*, when $x_{PG} < 8\%$) demonstrated melt-lightened thermochromism. In between these regions (*e.g.*, when $x_{PG} \approx 10\%$), a non-thermochromic sample was obtained. 279

Figure 7.15. A portion of the ternary thermochromic phase diagram of the CVL:BPA:HD-OH system, showing the melt phase(s) at relatively low solvent concentrations (where $z \approx 25$ to 100). 283

Figure 7.16. A portion of the ternary thermochromic phase diagram of the CVL:DHB:HD-OH system, showing the melt phase(s) relatively low solvent concentrations (where $z \approx 15$ to 100). 284

Figure 7.17. A portion of the ternary thermochromic phase diagram of the CVL:BPA:HD-OH system at high solvent concentration (where $z \approx 160$ to 2250). Melt-lightened behaviour was observed for all compositions. 286

Figure 7.18. A portion of the ternary phase diagram of the CVL:DHB:HD-OH system at high solvent concentration (where $z \approx 160$ to 2650). Melt-lightened behaviour was observed for all compositions. 287

Figure 7.19. A portion of the ternary thermochromic phase diagram of the CVL:DDG:OD-SH system at very high solvent concentrations (where $z \geq 500$). Melt-darkened thermochromism was obtained at relatively high CVL and DDG concentrations (*e.g.*, when $x_{CVL} > 0.2\%$ and $x_{DDG} \geq 0.4\%$). Samples with low developer concentrations (*e.g.*, when $x_{DDG} < 0.5\%$) demonstrated melt-lightened thermochromism. Some samples were non-thermochromic at high developer concentrations (*e.g.*, when $x_{DDG} \approx 0.8\%$). 290

Figure 8.1. The structure of the e-blue^{TM} dye, blue 203. (a) The leuco form of blue 203. (b) The ring-opened form of blue 203, which is formed in the presence of an acidic developer. 297

Figure 8.2. (a) Laser-jet toner is deposited on the surface of the page, incident light is reflected back to the observer, and little light intensity is lost to scattering within the page. (b) IJP inks penetrate deeply into the page due to the high mobility of the volatile solvent. Dye molecules found deep in the page appear with less contrast due to scattering of light within the page, and reflective losses from the surface of the page further reduce image colour density.[220] 301

Figure 8.3. The structure of the phenolic developer, bisphenol F. 304

Figure 8.4. Colour density fade of CVL-containing IJP inks as a function of time. Rapid colour loss was observed within the first few days after printing. Note: lines are added as a guide to the eye. 305

Figure 8.5. The structures of (a) blue 63 and (b) blue 203. The highlighted regions indicate the structural differences between the two leuco dyes. 306

Figure 8.6. Colour fade of blue 63 and blue 203 inks as a function of time. CVL ink #5 is presented for comparison. Although little colour fade was observed in these inks, the initial colour density was low. Note: lines are added as a guide to the eye. 307

Figure 8.7. The structures of the leuco dyes (a) blue C4OH, (b) blue C6NH2, and (c) PS-blau. The highlighted regions indicate the structural differences between blue C4OH and blue C6NH2. 308

Figure 8.8. Colour fade of inks containing blue C4OH, blue C6NH2 and PS-blau as a function of time. CVL ink #5 is presented for comparison. Initial colour densities in the blue C4OH and blue C6NH2 inks exceeded the $CD = 0.4$ threshold, and colourfastness was substantially better than in CVL inks. Note: lines are added as a guide to the eye. 310

Figure 8.9. Colour density versus time after erasing for CVL inks. The erasing of these samples was carried out using the "iron-eraser". Initial colour densities before erasure were $CD \approx 0.35$ to 0.40. Note: lines are added as a guide to the eye. 312

Figure 8.10. Colour density versus time after erasing for inks containing blue 63 and blue 203. All three inks show good colour erasure and maintain the erasure over time. Initial colour densities before erasure were $CD \approx 0.25$ to 0.30. CVL ink #5 is shown for comparison. Note: lines are added as a guide to the eye. 313

Figure 8.11. Colour density versus time after erasing for inks containing blue C4OH, blue C6NH2 and PS-blau. The three inks show fairly poor colour erasure and do not maintain the erased state over time. Initial colour densities before erasure were $CD \approx 0.35$ to 0.45. The colour fade behaviour

of CVL ink #5 is shown for comparison. Note: lines are added as a guide to the eye. 314

Figure 8.12. Colour density fade as a function of time after printing of CVL-containing inks to which PVA was added. The legend indicates the concentration of PVA in the final ink mixture. There appears to be little correlation between PVA loading and colourfastness as all samples behave similarly. Note: lines are added as a guide to the eye. 316

Figure 8.13. Colour density after erasing for CVL inks containing PVA. The legend indicates the concentration of PVA in the final ink mixture. All of the samples demonstrate very good erasing and no colour reformation over time. Initial colour densities before erasure were $CD \approx 0.25$ to 0.40. Note: lines are added as a guide to the eye. 317

Figure 8.14. Colour density fade as a function of time after printing for blue C4OH inks modified with PVA. The legend indicates the concentration of PVA in the final ink mixture. There appears to be no correlation between PVA loading and colourfastness as all curves behave similarly. A CVL-containing ink, modified with PVA, is shown for comparison. Note: lines are added as a guide to the eye. 318

Figure 8.15. Colour density after erasing for blue C4OH inks modified with PVA. The legend indicates the concentration of PVA in the final ink mixture. All of the samples demonstrate good erasing with little colour reformation over time. Initial colour densities before erasure were $CD \approx 0.30$ to 0.40. A CVL-containing ink, modified with PVA, is shown for comparison. Note: lines are added as a guide to the eye. 318

Figure 8.16. Colour density fade as a function of time after printing for blue C4OH/DHB inks modified with PVA. The legend indicates the

concentration of PVA in the final ink mixture. Note: lines are added as a guide to the eye. 320

Figure 8.17. Colour density after erasing for blue C4OH/DHB inks modified with PVA. The legend indicates the concentration of PVA in the final ink mixture. All of the samples demonstrate very good erasing and essentially no colour reappearance over time. Initial colour densities before erasure were $CD \approx 0.35$ to 0.40. Note: lines are added as a guide to the eye. 320

Figure 8.18. The best ink prepared during the internship containing blue C4OH as the dye, DHB as the developer, PVA as a viscosity modifier, and acetic acid as a colour deepener. Note: lines are added as a guide to the eye. 321

Figure 8.19. (a) Printed image and (b) erased image created with the blue C4OH/DHB ink modified with both PVA and acetic acid. The printed image has good colour density and the text is sharp. The box marked (1) was used as a placeholder, so that when the ink is erased it was possible to record the colour density of the erased image. No residual shadows are observable on the erased image. 322

Figure 9.1. A stylized summary of the observed thermochromic behaviour of CVL:DDG:TD-OH mixtures at high solvent concentrations (*e.g.,* when $z \geq 80$). The equilibrium solid state was always colourless, and melt-darkened thermochromism could generate a coloured melt at high developer concentrations (*e.g.*, $y > 9$).....326

Figure 9.2. A stylized summary of the thermochromic behaviour of CVL:DDG:HD-OH and CVL:DDG:OD-OH mixtures at high solvent concentrations (*e.g.,* when $z \approx 80$ to 100). The equilibrium solid state usually was coloured, with melt-darkened thermochromism occurring at high developer concentrations (*e.g.*, $y \approx 6$ to 10), and melt-lightened thermochromism occurring at low developer concentrations (*e.g.*, $y \approx 0.5$ to 4).....327

Figure 9.3. A stylized summary of the observed thermochromic behaviour of CVL:ODG:solvent mixtures at low solvent concentrations (*e.g.,* when $z \approx 25$). The equilibrium solid state was always colourless, and melt-darkened thermochromism generated high melt colour density at high developer loading (*e.g.*, $y \approx 6$). 329

Figure 9.4. A stylized summary of the thermochromic behaviour of CVL:PG:alcohol and CVL:OG:alcohol mixtures at high solvent concentrations (*e.g.,* when $z \approx 85$ to 100). The equilibrium solid state always was coloured, with melt-lightened thermochromism occurring at virtually all developer concentrations (*e.g.*, $y \approx 0.5$ to 6), and complete decolourization of the melt occurring when $y \leq 2$. 330

Figure 9.5. A stylized summary of the thermochromic behaviour of CVL:BPA:HD-OH and CVL:DHB:HD-OH mixtures at low solvent concentrations (*e.g.,* when $z \leq 100$). The equilibrium solid state always was coloured, with melt-lightened thermochromism occurring at all compositions.....332

Figure 9.6. A stylized summary of the thermochromic behaviour of CVL:BPA:HD-OH and CVL:DHB:HD-OH mixtures at high solvent concentrations (*e.g.,* when $z > 100$). High solid-state colour densities were obtained at high developer ($y = 10$ to 16) and low solvent ($z \leq 500$) concentrations. Low solid state colour density was observed at very low developer (*e.g.* $y = 0.3$ to 0.5) and high solvent (*e.g.*, $z \approx 1000$) concentrations. 333

Figure 9.7. A stylized summary of the thermochromic behaviour of CVL:DDG:OD-SH mixtures at high developer loading ($y \approx 5$ to 6). Melt-darkened thermochromism was obtained at low solvent concentrations ($z \leq 500$). Melt-lightened thermochromism was obtained at high solvent concentrations *(*$900 \leq z \leq 2000$). Between these two regimes, $z \approx 700$, non-thermochromic behaviour was observed. 334

Abstract

Thermochromic materials undergo temperature-dependent colour changes. Although there are several origins of thermochromism, two distinct types of thermochromism are common in thermochromic mixtures. Melt-lightened thermochromism occurs when the colour density of a mixture decreases with increasing temperature, and is usually associated with colour loss upon mixture melting. Melt-darkened thermochromism occurs when the colour density of a mixture increases with increasing temperature, and is usually associated conversion from a decoloured solid state to a coloured melt.

Three-component thermochromic systems generally consist of a leuco dye (minor component), a phenolic colour developer (intermediate component), and a high melting-point organic solvent (dominant component). In these systems, the colouring behaviour is controlled by competing binary interactions, with the dye:developer interaction responsible for colour formation and the developer:solvent interaction responsible for colour erasure.

In the present study, three-component mixtures composed of CVL (dye), long-chain alkyl gallates (phenolic developer), and long-chain alkyl alcohols (long-chain solvent) were examined. The thermochromic behaviour (*i.e.*, melt-lightened vs. melt-darkened thermochromism) of these mixtures was examined as a function of the matching of the alkyl chain length of the gallate developer and alcohol solvent. When the alkyl chain lengths were well matched, the developer:solvent interaction dominated in the solid state and melt-darkened thermochromism was observed. When the alkyl chain lengths were poorly matched, the dye:developer interaction dominated in the solid state, and melt-lightened thermochromism was observed. The colour density of the molten state was determined by the developer:dye molar ratio, with high molar ratios yielding coloured melts and low molar ratios yielding decoloured melts.

Additional studies employing chemically dissimilar developers and solvents (*e.g.*, bisphenol A with 1-hexadecanol) yielded mixtures that displayed optimal melt-lightened thermochromism. The high solid-state colour density due to weak developer:solvent interactions provides further evidence that competing binary interactions are responsible for the colouring behaviour observed for three-component thermochromic systems.

Ternary thermochromic phase diagrams were used to define compositional regions of optimal thermochromic behaviour (*i.e.*, high colour contrast), providing a useful experimental tool for the rapid identification of ideal sample compositions. Additionally, an examination of the properties of thermally erasable ink-jet printer inks was carried out during the present study.

List of Abbreviations and Symbols Used

(***In order of appearance***)

HOMO – highest occupied molecular orbital

LUMO – lowest unoccupied molecular orbital

LED – light-emitting diode

E_g – band-gap energy

eV – electron volt

UV – ultraviolet

L – quantum mechanical box length

ΔE_N – energy of electronic transition

h – Planck's constant

N – quantized energy level

m_e – electron mass

CVL – crystal violet lactone, 3,3-bis(*p*-*N*,*N*-dimethylaminophenyl)-6-*N*,*N*-dimethylaminophthalide

SP – spiropyran

MC – merocyanine

BPA – bisphenol A, 2,2-bis(4-hydroxyphenyl)propane

TAM – triarylmethane

S-205 – 2'-anilino-6'-[ethyl(3-methylbutyl)amino]-3'-methyl*spiro*[*iso*benzofuran-1(3*H*),9'-[9*H*]xanthene]-3-one

*N** – chiral nematic phase of liquid crystalline materials

S – smectic phase of liquid crystal

T(S-N)* – smectic-to-chiral nematic phase-transition temperature

P3HT – poly-3-hexylthiophene

PDA – polydiacetylenes

PDAc-(12,8) – pentacosa-10,12-diynoic acid

HDCA-(11,4) –heneicosa-6,8-diynoic acid

DMAP – dimethylaminophenyl moiety

HOMO-1 – the 'HOMO minus one' energy level

UV-Vis – Ultraviolet and visible regions of the electromagnetic spectrum

ε – molar absorptivity

ε_{max} – the molar absorptivity at the absorbance maximum (λ_{max})

HCl – hydrochloric acid

C_{max} – concentration of coloured species at maximum absorbance

C_o – initial concentration of the dye

DHB – 2,4-dihydroxybenzophenone

T_{fus} – fusion temperature, also known as melting and/or freezing point

GA – gallic acid

PG – propyl gallate

OG – octyl gallate

DG – decyl gallate

DDG – dodecyl gallate

TDG – tetradecyl gallate

HDG – hexadecyl gallate

ODG – octyl gallate

pK_a – acid dissociation constant

TD-OH – 1-tetradecanol

HD-OH – 1-hexadecanol

OD-OH – 1-octadecanol

X_A – mole fraction of component A

DSC – differential scanning calorimetry

$\gamma_{sym(COO^-)}$ – symmetric wag deformation Raman mode of COO^- group

η_A – number of moles of component A

η_A / η_B – molar ratio of component A to component B

MM2PP – molecular motions calculation program

LG – lauryl gallate, also known as dodecyl gallate (DDG)

OD-SH – 1-octadecanethiol

DD-COOH – 1-dodecanoic acid

TD-COOH – 1-tetradecanoic acid

DD- NH_2 – 1-dodecylamine

TrD-NH_2 – 1-tridecylamine

HD- NH_2 – 1-hexadecylamine

OD- NH_2 – 1-octadecylamine

HD-COOH – 1-hexadecanoic acid

OD-COOH – 1-octadecanoic acid

p-TsOH – *para*-toluenesulfonic acid monohydrate

RDC – Toshiba Co. research and development centre

PGMME – propylene glycol monomethyl ether

PVA – poly(vinyl alcohol)

TLC – thin layer chromatography

IJP – ink-jet printer/printing

RGB – *RGB* colour space

R – red component of *RGB* colour space

G – green component of *RGB* colour space

B – blue component of *RGB* colour space

CIE – International Commission on Lighting

CIE *XYZ* – CIE *XYZ* colour space

X – *X* coordinate of CIE *XYZ* colour space

Y – *Y* coordinate of CIE *XYZ* colour space

Z – *Z* coordinate of CIE *XYZ* colour space

CIE *Lab** – CIE *Lab** colour space

*L** – lightness coordinate of CIE *Lab** Colour Space

*a** – red to green colour coordinate of CIE *Lab** colour space

*b** – yellow to blue colour coordinate of CIE *Lab** colour space

CD – colour density

CD_{Equil} – colour density of the equilibrium solid state

CD_{Melt} – colour density of the molten mixture

ΔCD – colour contrast, or change in colour density

var – variance in colour coordinates

var_X – variance in colour coordinate X

ΔT_{SR} – temperature difference between sample and reference pans

$\dot{Q}_S$ – power input to sample pan

$\dot{Q}_R$ – power input to reference pan

C_S – sample heat capacity

C_R – reference heat capacity

T_S – sample temperature

T_{ST} – sample thermometer temperature

R_S – electrical resistance of the thermometer

Acknowledgements

I would first like to acknowledge and thank my supervisor, Prof. Mary Anne White, whose guidance and support during my time at Dalhousie University has helped greatly in my development as a researcher and a scientist. I would like to than Prof. Bart Kahr of New York University, who served as my external examiner, for his time and effort, and for useful discussions regarding the solid state chemistry of dyes. I would also like to extend my gratitude to Michel Johnson who provided valuable technical support for the experimental work presented in this thesis. I would also like to thank the members of my supervisory committee, Prof. D. Jean Burnell, Prof. Jeff Dahn, and Prof. Peng Zhang for providing guidance in my research work and useful feedback regarding my progress towards completing my PhD. Additionally, I would like to acknowledge that all of the members of my supervisory committee were kind enough to allow me to use their laboratory space and research equipment during my time at Dalhousie University. I would like to thank NSERC for funding, in particular through the DREAMS program at Dalhousie University, which is funded through the CREATE program. I would also like to thank Toshiba for providing funding for my internship at Toshiba RDC in Kawasaki, Japan.

I would like to thank the members of the Prof. Mary Anne White research group, past and present: Dr. Andrew Ritchie, Dr. Kimberly Miller, Dr. Cathy Whitman, Carl Romao, Paul Allred, Jan Pöhls, Louis Desgrosseilliers, Jacy Conrad, Anthony Cerqueira, Adam Bent, John Niven, John Noel, Herman Stubeda, Dr. Ran Chen, Alex Safatli, and Hong Tang. In addition, I would also like to thank Mike Boutilier, Richard Conrad, and Brian Millier for their technical support as well as Cheryl Coolen, Giselle Andrews, Sean Hartwell, Cheryl Stanton, and Deanna Wentzell for administrative support.

A special thank you is extended to Dr. Kenji Sano (my supervisor), Yumiko Sekiguchi (my instructor), Hideyuki Tsuji (group leader), Dr. Akiko Hirao (unit leader), and Akihiro Matsui (my Japanese twin) for their support and guidance during my internship with Toshiba during the summer of 2011. I also extend my gratitude to the other members of the Organic Materials Laboratory at Toshiba RDC for their support: BinBin Huang, Shinetsu Fujieda, Toshihiro Imada, Arisa Yamada, and Shoko Yoshida.

Finally, I would like to thank my family and friends for helping to support me emotionally through the long process that is graduate school, and for providing some levity during the process of writing this thesis. In particular I would like to thank my parents, Dave and Bernie Bourque, my brother Greg, and my sister Danielle. I would also like to extend my gratitude to Mike Plume, Derek Jones, Johnnie Walker, and Courtney Calahoo for their unwavering support during my time at Dalhousie.

Chapter 1 Introduction*

1.1 Colour in Chemistry

Colour has long played an important role in shaping our view of the world, from early efforts to modify the colour of textiles with dyes and pigments found in nature, through the invention of the written word and the development of long-lasting inks that could be used to maintain permanent written records, to more recent applications such as high-performance visual display media including flat-screen televisions[1] and Imax® image projection systems,[2] and the development of advanced synthetic dyes and pigments for textile and printing applications that are able to respond to external stimuli such as light, heat, and pH changes.[3,4]

There are numerous sources of colour in our world, and the colour observed relies on three important factors: the spectral intensity of the incident light beam (*i.e.*, the relative intensities and distribution of frequencies of the incident beam), the modifications that occur upon interaction of the light beam with a physical system (*e.g.*, light scattering from a solid object), and the way in which our optical system perceives the light.[5,6] Colour can arise from numerous sources: colour by emission from a source, colour due to absorption or transmission of specific frequencies of light from an incident beam, colour arising from scattering processes (*e.g.*, the colour of the sky is due to

* Sections 1.1 – 1.5 were adapted from: M. A. White and A. Bourque, *Colorant, Thermochromic*, in press in *Encyclopedia of Color Science and Technology*, R. Luo (Ed.), Springer, New York, USA, **2013**. A. Bourque's contributions to the work were: writing drafts of each section of the review, preparing figures, and general editing. The review chapter has been modified from its original version to fit the context of this thesis.

Rayleigh scattering), and light dispersion effects (*e.g.*, the splitting of a white light beam into component colours by a prism).[5,7]

Black-body radiation is an example of colour generated by emission of light. Black-body radiation occurs when a thermally excited material emits radiation in the visible region of the electromagnetic spectrum.[5,7,8] Fluorescence and phosphorescence are types of photoluminescence. Fluorescence occurs when an electron is promoted from a low-lying molecular orbital (*e.g.*, the highest occupied molecular orbital (HOMO)) to a high-energy molecular orbital (*e.g.*, the lowest unoccupied molecular orbital (LUMO)) *via* the absorption of high-energy light. Subsequent decay of the electron from the excited state, usually through a lower energy intermediate state, to the ground state is accompanied by the emission of a photon at an energy lower than that of the incident photon.[5,7,8] Phosphorescence occurs when an electron is promoted to an excited state *via* light absorption, then undergoes intersystem crossing from a singlet excited state to a triplet excited state. The intersystem crossing process prevents rapid re-emission (*i.e.*, fluorescence), increasing the lifetime of the excited state and delaying the emission of the photon. As such, phosphorescent light emission can continue well after the initial excitation.[5,7,8]

Perhaps the most ubiquitous example of emissive colour generation today is the light-emitting diode (LED).[9] In these devices, electrons are promoted to higher energy levels *via* stimulation with electrical energy, and the subsequent decay of the high-energy electrons to low-energy electronic states generates photons with a narrow frequency distribution.[7,8] The colour of an LED is defined by the energy band gap, E_g, of the

semiconductors used in the device, and since band-gap energies are easily tuneable by semiconductor doping, many colours are available for LED devices.[7,8]

Colour by transmission/absorption/reflection is most pertinent to the research presented in this thesis. These processes rely on the removal of specific wavelengths of light from a polychromatic incident light source by absorptive processes occurring within a material of interest.[5] For a semiconductor, the energy band gap, which separates the low-energy valence band from the high-energy conduction band, will determine which frequencies of light are absorbed. Any frequency of light that is higher in energy than the band gap (*i.e.,* at shorter wavelengths) will be absorbed by the material, with the absorbed light energy promoting an electron from the valence band to the conduction band. This process is exploited in silicon photovoltaic cells, where the low band-gap energy of silicon (E_g = 1.1 eV), allows for the absorption of photons with energies greater than 1.1 eV.[7,10] The visible light spectrum spans a broad energy range extending from 1.6 eV (red) to 3.3 eV (violet), therefore all of these frequencies of light can be absorbed by silicon, making it extremely useful for photovoltaic applications.[7]

The colour of inorganic materials is generated through two main types of interaction. Most transition metal complexes become coloured due to interactions of light with the central metal ion and the ligands attached to the metal centre. The ligands generate a local electronic field, called the crystal field, which causes previously degenerate metal d-orbitals to split.[7] Crystal field splitting allows the electrons to undergo relatively low-energy transitions between the energy levels, giving rise to colour formation by absorption of visible frequencies of light.[7,8] A second type of colour generation in inorganic solids is due to the presence of point defects, called *F*-centres (or

colour centres), in a crystalline lattice. The electronic field of the crystal is modified in such a way that single charges, or pairs of charges, can migrate to the surface of the crystal, leaving electrons (or holes) in the defect sites, subsequently giving rise to significantly lowered excitation energies, often in the visible region of the electromagnetic spectrum.[7,8]

In materials made from absorptive small molecules, such as dye molecules, the absorption of light energy occurs due to the promotion of electrons from occupied molecular orbitals (*e.g.*, the HOMO) to higher energy unoccupied molecular orbitals (*e.g.*, the LUMO).[11] Molecules that absorb light are called chromophores, meaning *colour bearer*.[12] Sometimes the chromophore does not absorb light in the visible spectrum (*e.g.*, UV-absorbers, etc.) and might need to be coupled with another material to tune the absorption energy of the chromophore. These colour modifiers, call auxochromes, meaning *colour increaser*, modify the electronic structure of the chromophore by either adding or removing electronic density of the chromophore.[8,12] This is the basis of "push-pull" systems and the use of electron–donating and –withdrawing groups that are sometimes added to aromatic chromophores to modify the colour of organic dyes.[13]

Simple, unsaturated organic molecules typically absorb photons in the UV region of the spectrum. The incorporation of π-bonding into organic molecules generates molecular orbitals that are closer in energy than σ-orbitals.[11] The degree of delocalization experienced by electrons in the π-bonding motif will directly control the energy gap between the frontier molecular orbitals (*i.e.*, the energy gap between the HOMO and LUMO), with longer conjugation lengths corresponding to narrow energy gaps between molecular orbitals.[14] As the conjugation length increases and the energy gap between the

frontier molecular orbitals narrows, the absorption energy of the valence electrons moves from the UV region into the visible region of the spectrum.[8,11] Organic dyes typically have extended π-bonding networks, which allow for long conjugation lengths and small HOMO-LUMO transition energies, producing strong solid-state colouration.[14] The reduction in the HOMO-LUMO transition energy can be estimated using the 1-dimensional quantum mechanical equation for a particle in a box of length, L:[15]

$$E_n = \frac{h^2 n^2}{8 m_e L^2} \qquad (1.1)$$

where E_n is the energy of the n^{th} energy level, h is Planck's constant, n is the principal quantum number (1,2,3...), and m_e is the electron mass. The energy of the electronic transition from the n to n+1electronic state, ΔE, is then determined by

$$\Delta E = E_{n+1} - E_n = \frac{(2n+1)h^2}{8 m_e L^2}. \qquad (1.2)$$

As the electron density is further dispersed across the molecule through increased conjugation (*i.e.*, L increases), the HOMO-LUMO gap is reduced (*i.e.*, ΔE_N decreases) into the visible region and colour forms in the compound.[7,15,16]

1.2 Chromic Materials

Chromic materials are defined as materials that undergo distinct colour changes in response to the influence of external stimuli, particularly when the colour change is reversible and controllable.[3] Many external stimuli can be used to induce colour changes in chemical systems; a few are listed in

Table 1.1.[3] Thermochromic, photochromic and ionochromic materials are the most frequently observed types of chromic materials, although many other types of chromic materials have found niche applications in industrial settings (particularly as sensors).[17] Thermochromic compounds are discussed in greater depth later in this chapter (sections 1.3 – 1.5) and multi-component thermochromic mixtures will be discussed in Chapter 2; the remainder of this section is dedicated to the discussion of some important chromic materials currently on the market.

Table 1.1. Chromic phenomena and associated stimuli.

Chromic Phenomenon	Stimulus
Thermochromism	Heat
Photochromism	Light
Ionochromism (halochromism)	Ions (protons)
Electrochromism	Electric potential
Solvatochromism	Solvents
Vapochromism	Vapours
Mechanochromism	Mechanical action

The best-known commercial application of photochromic materials is in Transitions® lenses, which undergo photochromic darkening when exposed to UV radiation from the sun.[18] A photochromic *cis-trans* isomerization reaction causes the lens to become more strongly absorbing in the UV-visible region of the spectrum, thereby protecting the eyes of the wearer from intense, and potentially harmful, solar radiation.

Photochromic materials are also suitable for use in sensor applications where rapid detection of stray electromagnetic radiation can provide workers an extra measure of safety.[19,20] Of course the most important photochromic material on the planet, as far as human beings should be concerned, is retinal (also known as retinaldehyde or Vitamin A aldehyde). Retinal, a polyene, undergoes an all-*cis* to all-*trans* photoisomerization reaction when eyes are exposed to light, thereby changing the absorption spectrum of retinal, allowing for the physiological detection of changes in light intensity.[21] This process forms the basis for colour detection in animals, with the detection of different colours reliant on the associated proteins to which retinal is attached (*i.e.*, cones and rods).[22]

Ionochromic materials have been exploited for many years in the form of pH indicators. The pH-sensitive dyes undergo structural modifications in the presence of hydrogen ions (acids) or hydroxide ions (bases), which can cause dramatic changes in the colour of the dye. Litmus paper, which is impregnated with a mixture of dyes extracted from lichens, turns red in the presence of acid and blue in the presence of base.[23] Figure 1.1 shows the colour-changing equilibrium of phenolphthalein, a pH indicator well-known to students. Phenolphthalein is colourless at acidic conditions, but as the pH increases to basic conditions, a ring-opening reaction extends conjugation across the three aromatic moieties of phenolphthalein through resonance, shifting the absorption maximum into the visible region and producing the strongly coloured form of the dye.[8] Phenolphthalein demonstrates *halochromism*, a form of ionochromism, where the colour of the dye is sensitive to the hydrogen ion concentration (*i.e.*, pH-sensitive).[24]

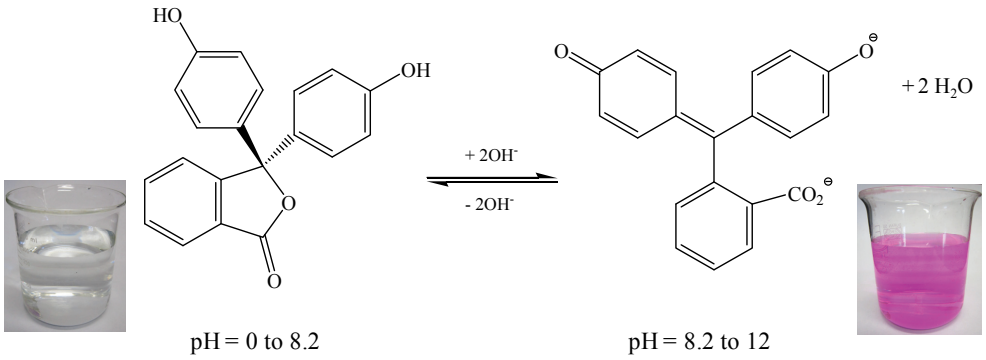

Figure 1.1. Phenolphthalein converts from a colourless form (in acidic environments) to a pink/fuchsia colour (in basic environments) due to a ring-opening reaction in the presence of hydroxide ions.[24]

Another important example of halochromic behaviour is observed in the colour-forming reaction of the leuco dye crystal violet lactone (CVL), shown in Figure 1.2.[25] The closed-ring form of CVL, referred to as the spiropyran (SP) form, is colourless due to the presence of a central sp^3 carbon atom, called a *spiro centre*, which limits conjugation lengths in the closed-ring form of CVL.[11] Reaction of *leuco*-CVL with an acidic compound causes cleavage of the lactone ring and generates the ring-opened form (see Figure 1.2, right), which contains a central sp^2 hybridized carbon atom. The ring-opened form is in resonance with three additional cationic forms, two with the positive charge localized on the dimethyl ammonium moieties, and one with the charge localized on the central carbon atom.[25]

The ring-opened structure is called the merocyanine (MC) form and is intensely blue/violet in colour.[26] The π-electron density becomes delocalized over the entire molecule as a result of the multiple resonance structures, and in doing so causes the energy of electronic transitions between frontier orbitals to fall within the orange region of the visible spectrum, producing blue colouration by virtue of the strong absorption of

orange wavelengths.[11,26] A more in-depth discussion on the chemistry of crystal violet lactone is presented in section 2.1.1.

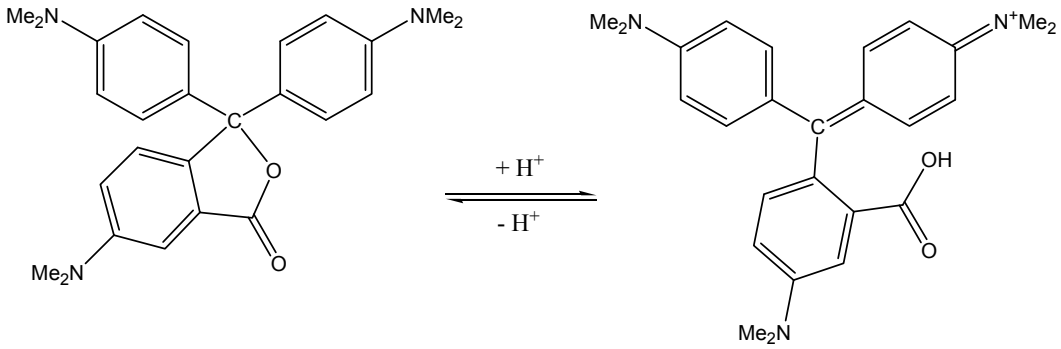

Spiropyran (SP) form

Merocyanine (MC) form

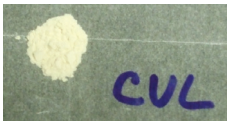

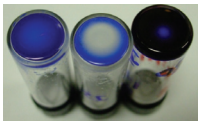

Figure 1.2. The halochromic equilibrium of crystal violet lactone showing the colourless spiropyran form of CVL (left) and the strongly coloured merocyanine form of CVL (right).[25] The colour images of thermochromic samples, shown at the bottom right of the figure, show different colour densities due to varying concentrations of the ring-opened, MC form of CVL.

The future of chromic materials lies in the development of new technologies. An important emergent area of research in the field of electrochromism focuses on creating textiles with electrically controlled, colour-changing fabrics towards developing "chameleonic camouflage".[8] These chameleon suits could use body-mounted cameras to map out the colour scheme of the surrounding environment, then manipulate electrochromic fibres embedded in their fabrics to match the colour scheme of the environment, providing an unprecedented level of cloaking and camouflage in combat situations.[27,28]

1.3 Thermochromism

Thermochromism is defined as the temperature dependence of the electronic absorption spectrum of a compound, generally while in the liquid or solid state.[29,30] In recent years, thermochromism has been extended to include multi-component systems that, as a whole, undergo colour changes in response to temperature changes.[31] Strictly speaking, reversibility is considered to be an essential requirement for thermochromic behaviour, although there are important applications of thermochromic materials in which an irreversible colouring reaction is specifically desired.[32] For this reason, colour changing materials which show irreversible colouring behaviour are often included in discussions about thermochromism. In the present work, reversible thermochromism is shortened to "thermochromism" for simplicity, while irreversible colour changes are specifically referred to as "irreversible thermochromism".

The most important commercial application of a material that changes colour with the application of heat is thermal receipt paper.[33] In thermal receipt paper, an acid-sensitive, colour-changing dye (*e.g.*, a fluoran dye) is microencapsulated in a polymer shell and embedded into the receipt paper.[34,35] An acidic developer that contains phenolic protons (*e.g.*, bisphenol A, BPA) is added directly to the page, but is not able to develop colour due to the encapsulation of the dye.[33] Upon application of heat, the microcapsules containing the dye rupture, releasing the dye and initiating a colour-forming reaction between the dye and developer.[36] Since the creation of a permanent record of the sales transaction is the intended goal, irreversibility of the process is explicitly desired. Recent examples of thermochromic products include Hypercolor™ T-shirts,[37,38] Pilot's FriXion™ pens and highlighters,[39,40] and Toshiba's e-blue™ erasable laser jet toner.[41,42]

1.4 Thermochromism in Organic Compounds

Thermochromism is most prevalent in organic compounds where subtle modifications in the molecular environment, frequently due to temperature-induced structural changes, can alter the delocalized π-electronic structure of the molecule and give rise to dramatic changes in colour.[15] There are three general mechanisms for organic thermochromism: (1) structural modifications that do not involve bond cleavage (*e.g.*, stereoisomerism),[43] (2) physical responses to temperature changes that cause light interference effects in large intermolecular systems (*e.g.*, liquid crystals),[44] and (3) reversible, thermally induced chemical modifications, referred to as *thermal tautomerism*,[31] such as ring-opening reactions (*e.g.*, spiropyrans)[45] and keto-enol equilibria (*e.g.*, Schiff bases)[46] that alter the electronic structure of the molecule. Ring-opening reactions are the most important to the present study.

1.4.1 Bianthrone and Crowded Ethenes

One of the earliest examples of reversible thermochromism in organic compounds was reported for bianthrone and related compounds, called the crowded ethenes.[29] Figure 1.3 shows the structure of bianthrone and dixanthylene, two early examples of compounds in this class.[47,48] Crowded ethenes contain two polycyclic aromatic moieties separated by a double bond. At room temperature, each anthrone moiety is slightly bent preventing coplanarity of the two anthrone moieties. This isolates the π-bonding motifs of each anthrone moiety causing each unit to act as an individual chromophore. A proposed mechanism for the observed thermochromic behaviour in crowded ethenes suggests that as the temperature is increased, the central double bond weakens and the π-electron

density becomes delocalized over the two anthrone moieties. This results in the formation of a biradical species, with the electronic absorption spectrum of each chromophore modified by the presence of a radical electron, which results in a colour change.[49]

Another proposed mechanism is based on the thermal expansion of the central double bond. As temperature is increased, the central double bond expands and weakens, allowing the two non-coplanar anthrone moieties to rotate into a more planar arrangement. The enhanced coplanarity extends the π-bonding conjugation length over the entire molecule, decreasing the absorption energy of the π-electrons and thereby changing the colour of the compound. If, however, bulky groups are placed at the R-positions shown in Figure 1.3 (c), steric hindrance prevents rotation about the central bond axis, resulting in compounds that are non-thermochromic.[50]

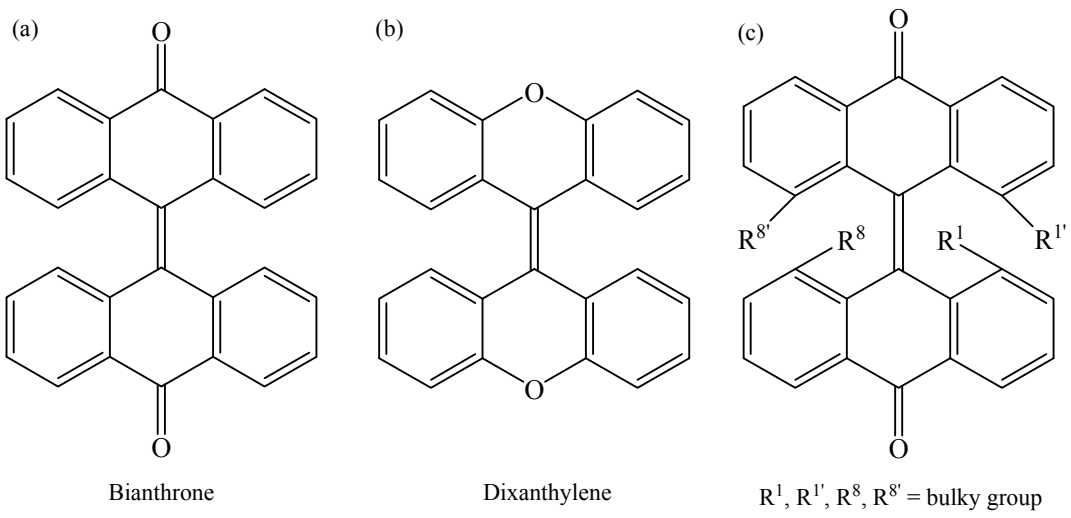

Figure 1.3. The structure of (a) bianthrone and (b) dixanthylene; both become more planar as the temperature is increased due to the expansion of the central alkene bond. (c) Bulky groups at the 1, 1', 8, and 8' positions prevent the two aromatic moieties from becoming planar, resulting in non-thermochromic compounds.

1.4.2 Schiff Bases

Schiff bases, also known as salicylidene-anilines, are formed by the condensation of an aromatic amine (*e.g.*, aniline) with either an aldehyde or a ketone (*e.g.*, salicylaldehyde).[51] Such compounds exist in a state of equilibrium between two forms, the *enol-imine* and *keto-enamine* forms. Figure 1.4 shows the keto-enol equilibrium; for salicylidene-aniline, the enol-imine form is more stable at room temperature than the keto-enamine form.[51] Increasing the temperature allows for an intramolecular tautomerization reaction to occur, whereby the proton from the hydroxyl oxygen migrates to the nitrogen atom of the imine bond, followed by electronic rearrangement yielding a ketone and an enamine moiety. Due to this electronic rearrangement, the keto-enamine has a more extended π-bonding structure than the parent enol-imine, reducing the energy of electronic transitions of the π-electrons and changing the colour of the compound.[19]

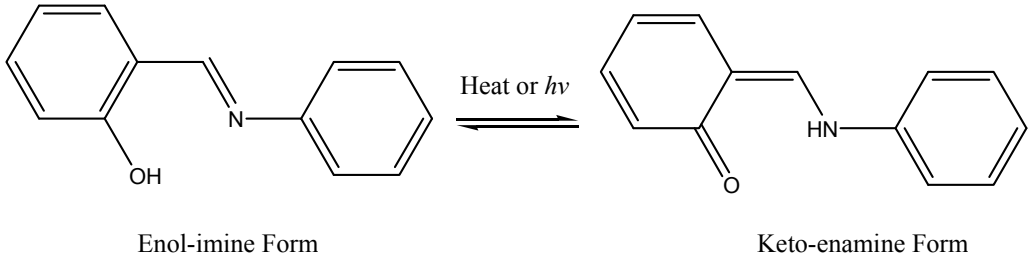

Figure 1.4. The keto-enol equilibrium responsible for thermochromism and photochromism in Schiff bases.

Substituent effects play a critical role in determining which form of the keto-enol equilibrium will dominate at a given temperature. Recent studies demonstrate the vast variability in this family of compounds, where the addition of electron–donating and –withdrawing groups and other ring substitutions can be used to push the keto-enol equilibrium in either direction.[51,52] To switch between forms, energy sufficient to exceed

the activation energy of the tautomeric reaction must be added to the system; the two main energy sources for converting between forms are heat and light. For many years, thermochromism and photochromism were thought to be mutually exclusive in Schiff bases;[12] however, recent studies have indicated that Schiff bases are almost always thermochromic and are occasionally photochromic in the solid state.[51,53]

1.4.3 Spiro Compounds

Spiro compounds are arguably the most important class of compound employed in thermochromic applications.[31] This is due not only to the inherent thermochromic properties of some spiro compounds,[54] but also due to the fact that many chromic materials use triarylmethane dyes (TAM dyes)[55] and fluoran dyes[56] to serve as the functional dye in multi-component thermochromic mixtures (*e.g.*, TAM dyes are used in carbonless copy paper,[38] fluoran dyes are used in thermal receipt paper,[57] etc.).[58] In addition to TAM and fluoran dyes, this class of compounds includes the spiropyrans,[59] spironaphthalenes,[60] and spirooxazines.[61,62] Some spiro compounds, so named for the "spiro" central sp^3 tetrahedral carbon centre that all members share, are subject to numerous tautomeric equilibria including lactim-lactam, acid-base, and the aforementioned keto-enol equilibria.[54,55,63]

Molecular rearrangement reactions (*i.e.*, tautomeric equilibria) can have significant impacts on the colour of these compounds. In general, the thermochromic behaviour of spiro compounds arises from the conversion of the sp^3 spiro carbon centre to an sp^2 carbon centre. On conversion to the sp^2 carbon centre, π-bonding electron density of the molecule can become delocalized over a larger portion of the molecule through

extended conjugation and resonance, yielding electronic transitions that fall in the visible region of the spectrum, producing colour.[11] Figure 1.5 shows an example of thermal tautomerism, in which the spiropyran (SP) form is converted to the merocyanine (MC) form *via* ring-opening of the pyran ring. Since the spiropyran form contains the spiro carbon centre, which prevents conjugation across the entire molecule, the spiropyran form is usually colourless. The merocyanine form, which has longer conjugation lengths arising from the influence of the central sp^2 carbon, is deeply coloured (*e.g.*, violet, red, blue) for nearly all members of this family.[4,54]

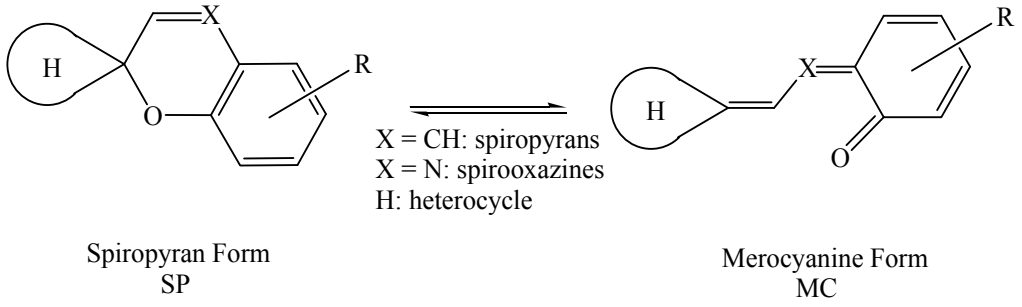

Figure 1.5. Schematic representation of the tautomeric ring-opening equilibrium between the spiropyran (SP) form and the merocyanine (MC) form of a spiro compound.

Leuco (from the Greek, meaning "white") dyes are able to change from colourless to intensely coloured upon conversion from the SP form to the MC form.[4] The two most important classes of leuco dyes are the triarylmethane (TAM) and fluoran dyes. Compounds from each of these classes find applications in commercial products ranging from inks and paints,[64,65,66,67] to dyed textiles,[20,68] and other chromic materials such as sensors.[69,70] The fluoran dye S-205 (Figure 1.6) is widely used as a black colouring agent in thermal paper.[34,57,71] Since the colouring reaction requires the presence of an acidic developer, compounds such as bisphenol A are used to develop the MC form of the dye.[57] Although the colouring reaction on thermal paper is irreversible, the commercial

importance of thermal paper is such that it should be included in any discussion regarding thermochromism.[8,31]

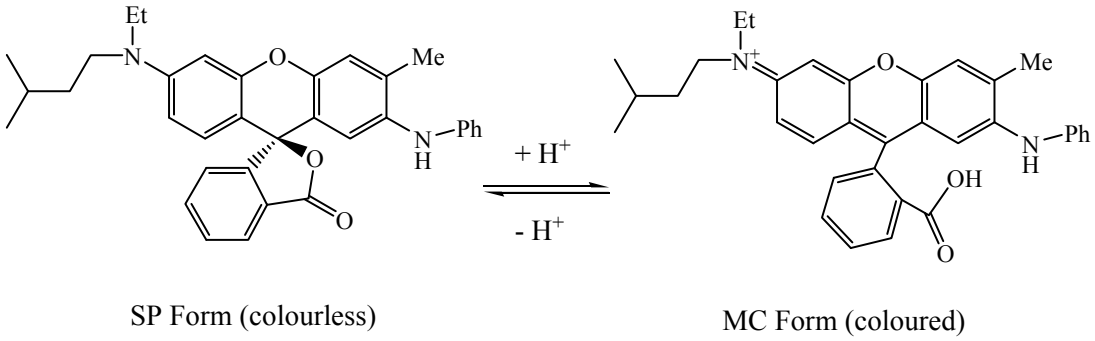

Figure 1.6. The ring-opening equilibrium of the acid-sensitized fluoran dye, S-205. The MC form of the dye is black in colour.

Triarylmethane (TAM) dyes also contain a spiro carbon centre, although in TAM dyes the spiro carbon centre segregates the π-electron density of three aromatic moieties instead of two (as for spiropyrans and fluorans).[54,55] The small size of the three segregated aromatic moieties causes the conjugation lengths in the colourless SP form to be very short, meaning that electronic absorptions have energies in the UV region, causing the SP form to be white in the solid state.[5,7] Many spiropyrans and fluoran dyes have longer conjugation lengths in the SP form compared to TAM dyes, which causes the so-called "colourless" SP form to actually demonstrate colouration. Since the absorptions still occur at relatively high energy (*i.e.*, blue/violet absorptions), the native colour of the SP form of many spiropyran and fluoran dyes is yellow.[8,54]

Crystal violet lactone (CVL) is a commercially relevant TAM *leuco* dye which undergoes a colour change from white to intense blue/violet in the presence of an appropriate developer (*e.g.*, BPA) or in acidic solutions.[25] CVL was mentioned earlier in this chapter (section 1.3) as an important material for carbonless copy paper.[25,33] The

ring-opening equilibrium for converting between the SP and MC forms of CVL was shown in Figure 1.2.[25] CVL is of central importance to the research presented in this thesis as CVL was used as the colouring agent in all investigations concerning three-component thermochromic mixtures discussed herein, and a more complete discussion of the properties of CVL is presented in Chapter 2.

1.4.4 Liquid Crystals

An important example of thermochromic behaviour arising from purely physical interactions is the thermochromic liquid crystals. Liquid crystals can be found in a wide variety of products including thermometers, food-spoilage warning indicators, 'stress testers', and mood rings.[25] Although thermochromic effects have been identified in numerous liquid crystalline compounds, only two major classes of liquid crystals have been widely exploited for use in commercial products: the esters of cholesterol and the esters of (*S*)-4-(2-methylbutyl)phenol.[72]

The liquid crystalline phase of matter was first identified by Reinitzer while studying the properties of the esters of cholesterol.[73] Figure 1.7 shows the structure of cholesterol and the thermochromic temperature range for a few series of cholesterol esters. The thermochromic phase of liquid crystals was historically referred to as the "cholesteric liquid crystal phase"; however, this name has been replaced by the more accurate descriptor "chiral nematic phase", which reinforces the fact that the thermochromic phase is chiral in nature.[72]

(a)

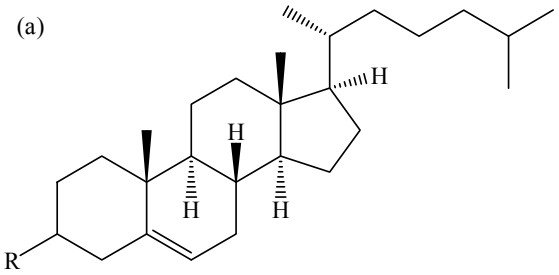

(b)

R	Temperature Range of Colour Change[72]
CH_3CO_2 to $C_8H_{13}CO_2$	94 to 113 °C
CH_3OCO_2 to $C_6H_{13}OCO_2$	94 to 108 °C
$C_7H_{15}OCO_2$ to $C_9H_{19}OCO_2$	77 to 81 °C

Figure 1.7. (a) The structure of cholesterol (where R = OH) and (b) the thermochromic temperature ranges for some cholesteric liquid crystals, where the R-groups form ester linkages with the parent cholesterol molecule.

Figure 1.8 shows the structure of the liquid crystalline compound (*S*)-4-(2-methylbutyl)phenol, the esters of which are used in a wide range of commercial products.[72,74] The advantages of this compound over cholesteric liquid crystals include the reduced cost of production and a broader range of thermochromic temperatures (including near-physiological, near-ambient, and near water-freezing temperatures).[72]

(a)

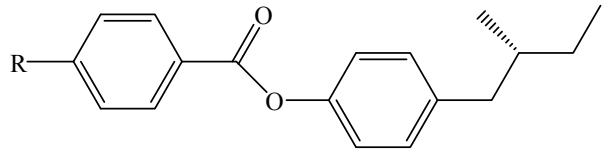

(b)

R	Temperature Range of Colour Change[72]
C_5H_{11} & C_8H_{17}	-5 to 0 °C
$C_6H_{13}O$ to $C_{10}H_{21}O$	35 to 50 °C
C_5H_{11}-Ph to C_7H_{15}-Ph	130 to 140 °C

Figure 1.8. (a) The structure of (*S*)-4-(2-methylbutyl)phenol and (b) the thermochromic temperature ranges for some derivatives of (*S*)-4-(2-methylbutyl)phenol, where the R-groups form carbon-carbon or ether linkages with the parent molecule.

Thermochromic behaviour in these materials is rooted in the special optical properties of the chiral nematic phase (abbreviated here as *N**). The chiral nematic phase is composed of calamitic (*i.e.*, rod-shaped) liquid crystals, which demonstrate short-range orientational order in the direction of the long-axis of the molecules but lack long-range positional order.[31,72] Within a given layer in the liquid crystalline structure, the long axes of the molecules will tend to be preferentially oriented in one direction. This direction is

called the *director*. Due to the lack of long-range order in the chiral nematic phase, the director rotates slightly from layer-to-layer, yielding a helical structure.[72] The orientation of the director is normal to the direction of the principal optical axis of the chiral nematic phase. Eventually the director makes a full revolution about the central optical axis, returning to its original orientation. The shortest distance between two layers that have the director pointing in the same direction is called the *pitch length*.[38] Figure 1.9 shows a schematic representation of the rotation of the director with respect to the principal optical axis (in the vertical direction) of the chiral nematic phase. The initial orientation of the director (layer A, Figure 1.9) is returned after a full revolution about the vertical axis (layer B, Figure 1.9), over a distance corresponding to the pitch length of the chiral nematic phase.[38]

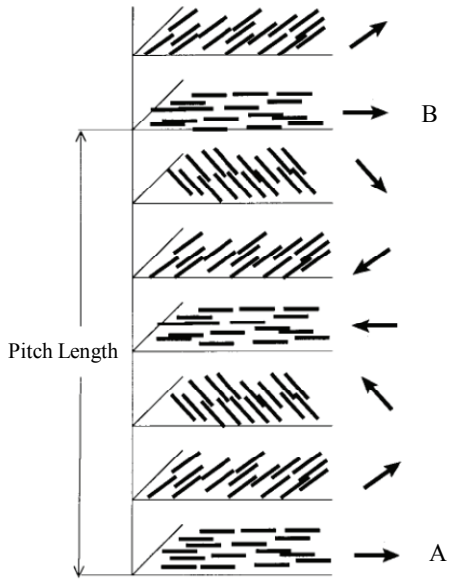

Figure 1.9. Pitch length corresponds to the distance between layers A and B, over which the orientational director of the layer (represented by an arrow) has made a complete rotation about the central helical axis. Reproduced with permission from *Journal of Chemical Education*, 1999, 76(9), 1201-1205. Copyright (1999) American Chemical Society.[38]

Colour can arise in the chiral nematic phase of liquid crystals as a result of constructive interference of light reflected from layers that have the same director orientation.[72] Light that reflects from layer A can constructively interfere with light reflected from layer B when the extra distance travelled by the light (reflected from layer A compared with layer B) is equal to an integer number of wavelengths of the incident light beam. Wavelengths of light that do not satisfy this condition will not constructively interfere on reflection and are either transmitted or absorbed by the material.[72] This behaviour is akin to Bragg diffraction in layered crystalline solids, and in this way chiral nematic phase liquid crystals behave as a type of diffraction grating or, more precisely, a monochromator.[31]

Due to thermal expansion the pitch length of the chiral nematic phase, and therefore the observed colour of the liquid crystal, is critically dependent on temperature.[72] In addition, thermochromism can be influenced by a phase transition. In many cases, the smectic (*S*) to chiral nematic (*N**) phase transition is exploited.[72] As the liquid crystal is heated from the smectic phase to the nematic phase, the loss of long-range orientational ordering causes a shortening of the pitch length with a concomitant decrease in the wavelength of light constructively reflected by the liquid crystals. Therefore, as the temperature is increased above the smectic-to-nematic phase transition temperature, *T*(*S*-*N**), the colour of reflected light changes from red to blue, as shown in Figure 1.10.[72,75] In commercial applications, the liquid crystal material is usually printed onto a black backing material. The black backing material absorbs any light that is not reflected (*i.e.*, transmitted light) preventing this light from reflecting back towards the

liquid crystal layer, because reflected polychromatic light would obscure the monochromating effect of the liquid crystal.[72,75]

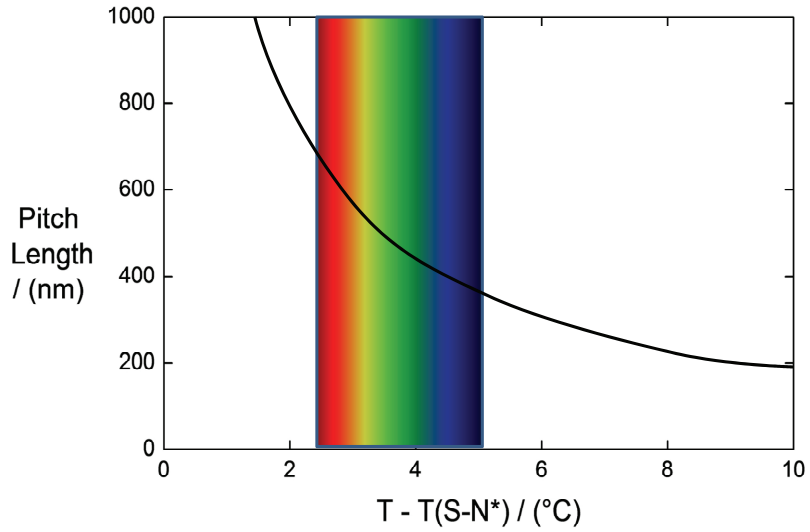

Figure 1.10. An illustrative depiction of the colour change associated with changes in pitch length of a chiral nematic phase liquid crystal above the *S*-*N transition.[72]**

1.4.5 Polymers and Oligomers

Conjugated organic polymeric and oligomeric materials can demonstrate a wide variety of colours due to the high degree of electronic delocalization present in these types of molecules.[76,77] As for conjugated small molecules, conjugated polymeric materials also are subject to thermally induced structural modifications that can result in dramatic colour changes, yielding thermochromic behaviour.[6,76] Common thermochromic polymers include the polythiophenes (Figure 1.11 (a)),[77,78] the polydiacetylenes (Figure 1.11 (b)),[79,80,81] and the σ-conjugated polysilanes.[82]

Poly-3-hexylthiophene (P3HT, see Figure 1.11 (a) where R = C_6H_{13}) is employed as a conducting layer in many organic electronic applications.[31] The large conjugation length results in a substantial reduction of the energy of electronic transitions, which

gives P3HT drastically improved electrical conductivity over most organic materials.[77] At room temperature, polythiophenes adopt a *trans*-planar structure in which the thiophene rings lie in the same plane. Side-chain groups attached to the thiophene rings aid in the stabilization of the main polymer backbone through side-chain interactions. Increasing the temperature causes the side-chain interactions to weaken, allowing the thiophene rings to rotate out of coplanarity, reducing the conjugation length of the delocalized electronic structure, and thereby changing the colour of the polymer.[6,31] Regioregular poly-3-hexylthiophenes undergo a reversible colour change from red-violet to yellow on heating.[83]

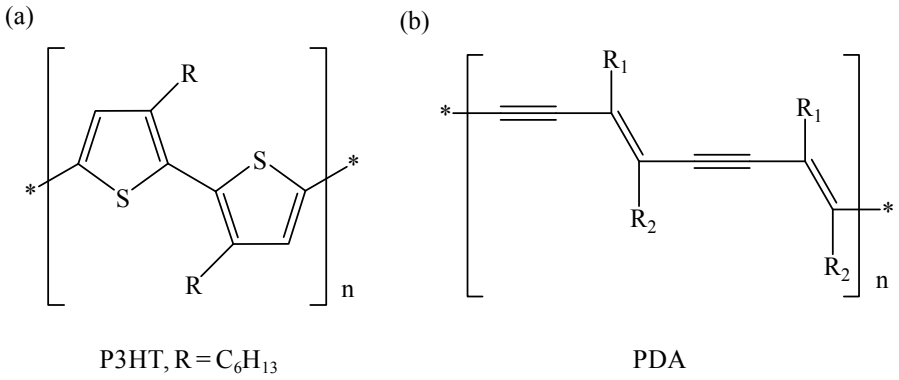

Figure 1.11. (a) The thermochromic polymer poly(3-hexylthiophene) is an important material for organic electronic applications due to its high electrical conductivity. (b) Thermochromic polydiacetylenes have garnered substantial interest due to their tuneable colour *via* R-group modification.

The physical properties of polydiacetylenes (PDA, see Figure 1.11 (b)) can easily be modified by substitution at the side-chain positions.[84] At low temperatures, the side-chain groups interact with each other to form extended hierarchical structures that prevent the backbone from twisting, which would result in a decrease in conjugation length. Again, as the temperature is raised, the side-chain interactions weaken and the polymer backbone is able to rotate, disrupting the planarity of the conjugated backbone, reducing

the overall conjugation length.[77] This causes an increase in the electronic transition energies thereby modifying the absorption spectrum of the polymer, and subsequently the colour.[6] Some examples of thermochromic PDA derivatives include PDAc-(12, 8), where $R_1 = (CH_2)_{11}CH_3$ and $R_2 = (CH_2)_7CH_3$, which is blue at room temperature and red at 70 °C,[85,86] and HDCA-(11,4), where $R_1 = (CH_2)_{11}COOH$ and $R_2 = (CH_2)_4COOH$, which changes from black to orange at 60 °C.[81]

1.4.6 Charge-Transfer Complexes

Charge transfer occurs when strong electron-donating compounds come into close proximity with electron-withdrawing compounds.[87] The strength of the charge-transfer interaction is strongly dependent on the intermolecular distance that separates the two molecules; changing the temperature of a supramolecular architecture based on charge-transfer complexes can therefore have significant impacts on the colour of the system.[88]

An example of thermochromism in supramolecular charge-transfer architectures is the intensely coloured charge-transfer complex formed from mixing electron-rich dialkoxynaphthalene derivatives with electron-poor derivatives of 1,4,5,8-naphthalenetetracarboxylic diimide (Figure 1.12).[89] When melted together, the two components form a supramolecular architecture due to intermolecular π-π stacking interactions. A columnar mesophase forms in the melt, which is intensely reddue to electronic absorptions associated with the charge-transfer band. Cooling the melt below the freezing point of the diimide causes the latter to precipitate inhomogeneously, disrupting the strongly coloured charge-transfer complex and returning the mixture to a colourless solid.[89]

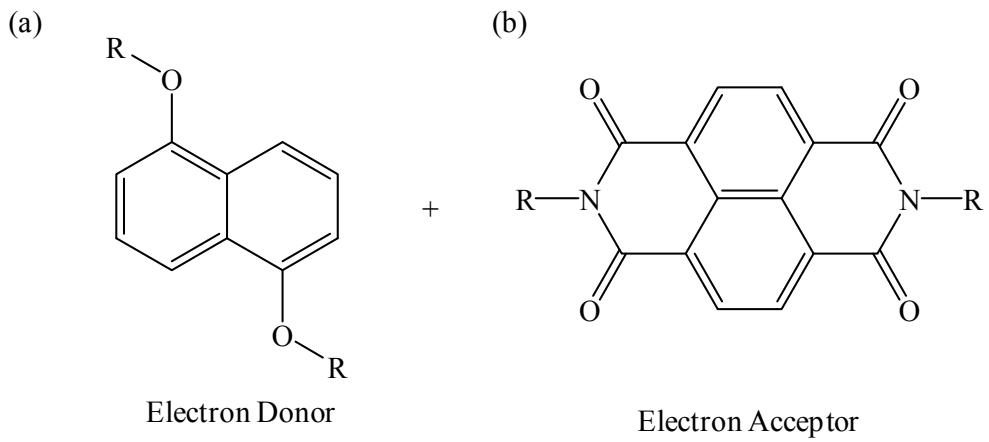

Figure 1.12. The components of an intensely coloured thermochromic charge-transfer system, (a) electron-rich dialkoxynaphthalene derivatives and (b) electron-poor 1,4,5,8-naphthalenetetracarboxylic diimide derivatives.[89]

1.5 Inorganic Thermochromism

Inorganic thermochromism can arise from a number of sources.[90] These include temperature-dependent changes in ligand geometry, the solvation sphere of a dissolved compound, metal coordination, band-gap energy (*e.g.*, semiconductors), reflectance properties, the arrangement and distribution of defects in the crystalline solid (*e.g.*, *F*-centres), and most importantly through phase transitions of a solid inorganic material.[3,5,7,16]

Vanadium(IV) dioxide (VO_2) is among the most interesting inorganic thermochromic materials owing to a solid-solid phase transition that occurs at 68 °C.[91,92] Below 68 °C, vanadium dioxide behaves as a semiconductor and transmits infrared light. At 68 °C, vanadium dioxide undergoes a semiconductor-to-metal phase transition, which changes the optical properties to infrared reflective.[93] This feature has made vanadium dioxide a prime candidate for use in smart coatings on buildings. A thin film of VO_2 can

be applied to the exterior of the building to allow transmission of visible light while blocking infrared light, which causes substantial warming of the building.[93] This mechanism could reduce the cooling requirements for the building and, since inorganic materials are generally much more resistant to photo-induced decomposition than organic materials, these materials could have substantially extended lifetimes compared to other types of building coatings such as paints.[94]

Another example of thermochromism arising from a phase transition is observed for Ag_2HgI_4.[95] The room temperature crystal structure is tetragonal, and the material is dark red. Heating a crystal of Ag_2HgI_4 to 50 °C causes a first-order phase transition of the crystal from tetragonal to cubic, coupled with a colour change to orange. As the material is further heated to 75 °C, a gradual second-order, order-disorder phase transition causes mobilization of silver ions in the crystalline lattice, which is coupled with a colour change to black. Across the 25 to 75 °C temperature range, the material changes from red to orange to black.[31,95]

An example of thermochromic behaviour associated with changes in the solvent sphere of a dissolved transition metal compound is seen in aqueous solutions of $CoCl_2$ (see Figure 1.13).[96,97] At room temperature, the Co(II) metal centre demonstrates octahedral geometry, which imparts a light rose-red colouration on the solution. Heating the mixture promotes conversion of the metal centre coordination geometry from octahedral to tetrahedral, which is accompanied by a colour change from red to dark blue.[97]

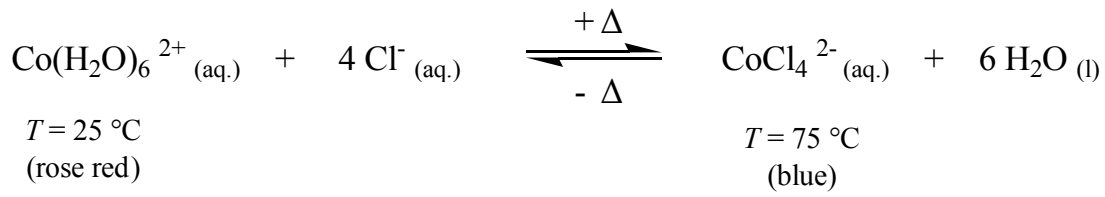

Figure 1.13. The thermochromic equilibrium of aqueous $CoCl_2$ solutions, where a change in ligand coordination geometry elicits a colour change from red to blue on heating.

1.6 Summary of Thermochromism

Thermochromism is observed in many chemical systems ranging from small organic molecules to highly conjugated polymers, crystalline inorganic solids, multi-component charge transfer complexes, and liquid crystalline materials. Such thermochromic materials belong to a broader class of materials called chromic materials, which undergo colour changes in response to the influence of external stimuli. Chapter 2 introduces the concept of multi-component thermochromic systems, the study of which is the main focus of this work.

Chapter 2 Rewritable Three-Component Thermochromic Mixtures

2.1 Introduction to Three-Component Thermochromic Mixtures

Chapter 1 presented numerous examples of thermochromic behaviour in pure compounds and some intermolecular systems, but did not focus on thermochromic behaviour arising from chemical reactions occurring in multi-component systems. These multi-component thermochromic systems will henceforth be referred to as *thermochromic mixtures*.[3,16,98]

The number of components present in a thermochromic mixture depends on the desired application. Three-component thermochromic mixtures have been studied in some depth over the past two decades due to their potential applications in rewritable printing technologies,[58,99,100,101,102,103] and are the main focus of the present research. Three-component thermochromic mixtures are comprised of a *colour former*, a *colour developer*, and a *co-solvent* (referred to as *solvent*).[16,31] Control of the competitive binary interactions between the colour former, colour developer, and co-solvent has been implicated as an important tool in modifying the colouring behaviour in thermochromic mixtures.[101,102]

All thermochromic mixtures contain a colour former and colour developer, and most employ a solvent component that is used to gain more control over the colouring behaviour. Some applications of thermochromic mixtures require the use of additional components such as UV-absorbers (to protect against photo-degradation)[104] and colour

erasers (to initiate colour erasure),[105] but the present study is limited to three-component mixtures.

2.1.1 Colour Former - Crystal Violet Lactone (CVL)

The colour former usually is a *leuco* dye, with common examples being the TAM dye crystal violet lactone (CVL, Figure 1.2)[99,106,107] and the fluoran dye S-205 (Figure 1.6).[57] To ensure good colour contrast between the coloured and decoloured states of the mixture, the dye should have both a colourless and a deeply coloured form. Leuco dyes that switch between a colourless spiropyran (SP) form and a deeply coloured merocyanine (MC) form satisfy this condition.[54] Additional chemical characteristics of the dye include high molar extinction coefficients to give strong colouration at low dye concentrations,[54] low cost of dye preparation to ensure commercial viability,[108] and good chemical stability of both the coloured and colourless forms to prevent decomposition of the dye under working conditions.[54,106,109,110]

3,3-*bis*(*p*-*N*,*N*-dimethylaminophenyl)-6-*N*,*N*-dimethylaminophthalide, more commonly known as crystal violet lactone (CVL), is a triarylmethane leuco dye that can change colour from colourless to blue/violet in the presence of an electron acceptor, or in acidic environments.[25,111,112] CVL was used as the colour former in all of the thermochromic mixtures examined in the present work.

Figure 2.1 shows the crystal structure of CVL at 298 K. The unit cell of CVL is monoclinic, the space group is $P2_1/n$, and the unit cell contains four molecules of CVL.[112] In the leuco form, the lactone ring is coplanar with its attached phenyl ring to within 3°.[112] Conjugation between the two dimethylaminophenyl (DMAP) rings and the

phthalide moiety is limited because the phthalide group is nearly perpendicular to the two DMAP rings, with dihedral angles of 119.1° to (C_2-C_7) and 92.6° to (C_{14}-C_{17}).[112] The DMAP rings take on a tilted "propeller" configuration where they tilt away from each other due to steric interactions between the protons attached to the carbon atoms *ortho* to the central carbon (C_3, C_4, C_{15} and C_{19}). The dihedral angle between the two DMAP rings is 69.0°.[112,113]

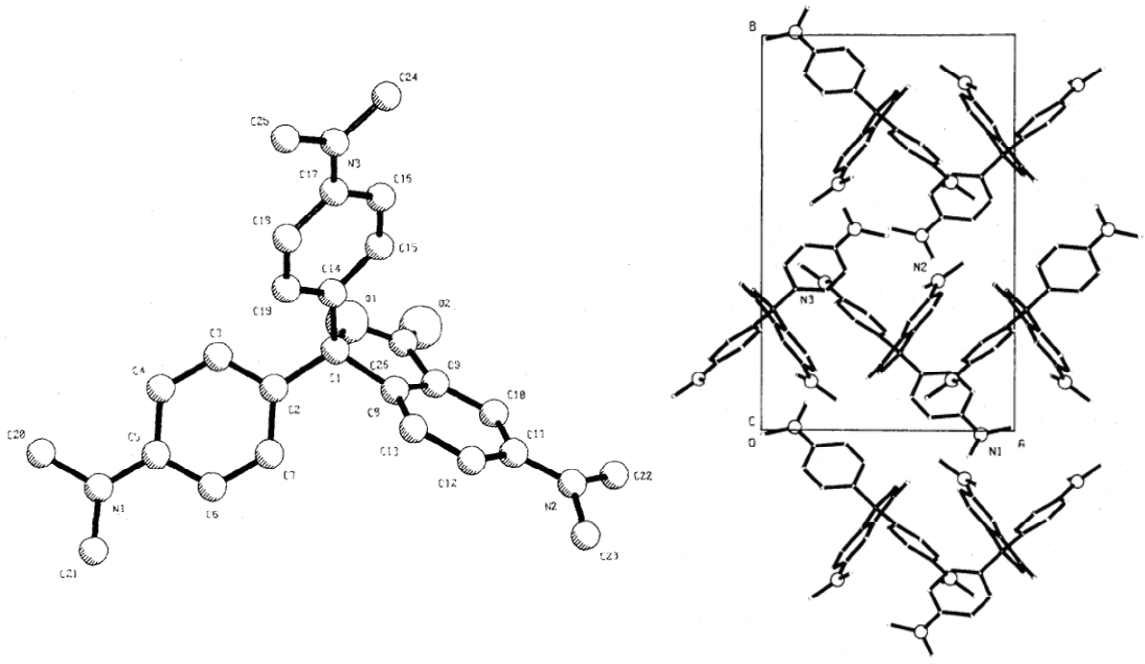

Figure 2.1. The crystal structure of crystal violet lactone (CVL). The unit cell is monoclinic in the $P2_1/n$ space group with four molecules per unit cell. Reproduced with permission from reference 112 (*Journal of Crystallographic and Spectroscopic Research*, 1984, 14(2), 121-128).

Figure 2.2 shows the colour-forming reaction of CVL, in which the lactone ring undergoes ring-opening in the presence of an acidic compound or, more generally, an electron acceptor.[25,54] The spiro carbon centre present in the leuco form of CVL prevents conjugation between the three distinct aromatic moieties. Upon protonation of the ester functionality and subsequent ring-opening, the central spiro carbon changes coordination

from four bonds to three.[114] This creates a cation that is stabilized by resonance with the three aromatic moieties. In each quinonoid resonance structure, one nitrogen atom donates free electron density to the delocalized structure, generating an iminium cation and extending the conjugation through the central sp^2 carbon.[115,116] In this way, the π-electron density becomes delocalized across the entire molecule, extending conjugation lengths and reducing the energy of electronic transitions into the visible region of the spectrum.[11,25,114]

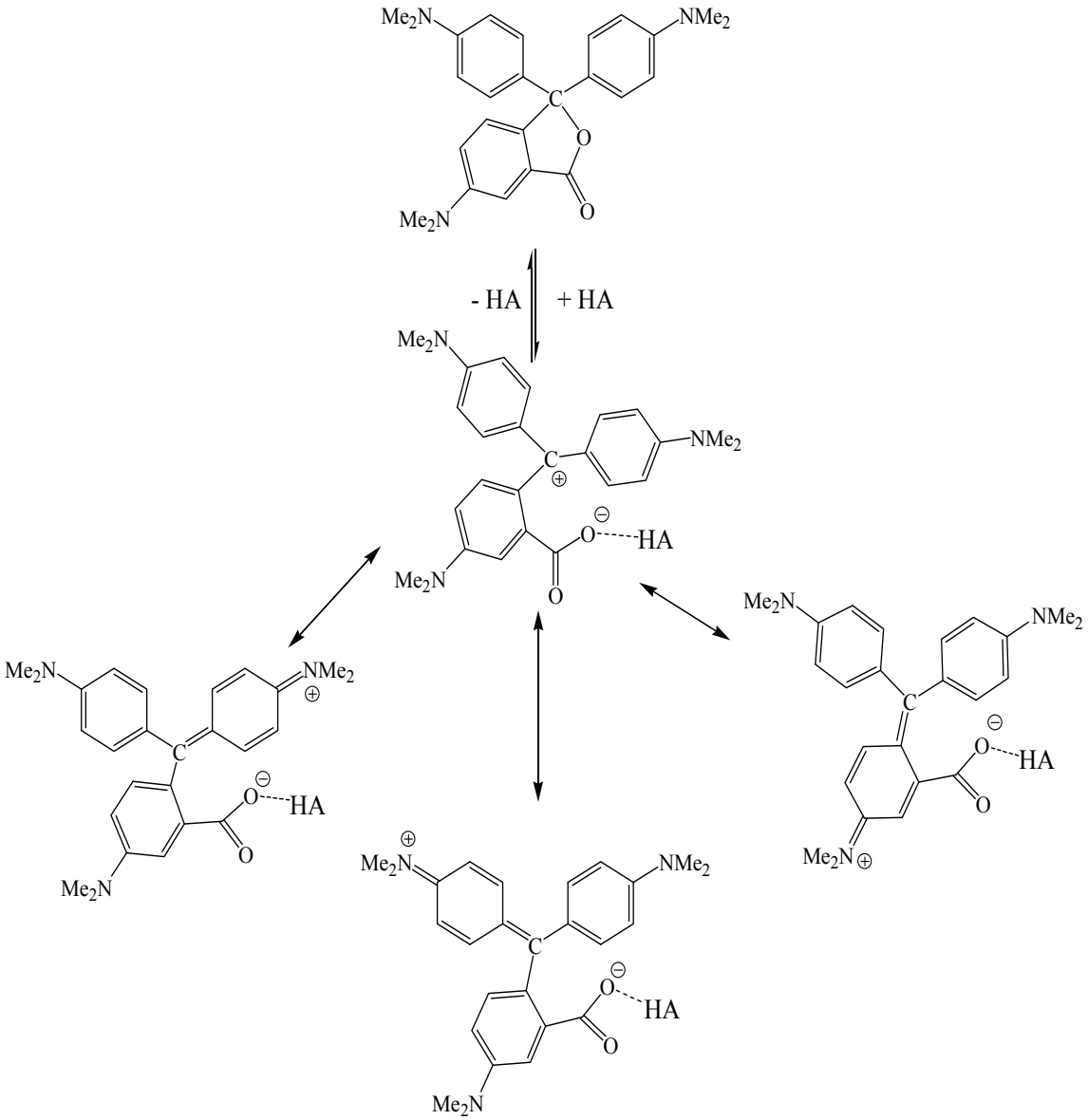

Figure 2.2. Crystal violet lactone (CVL) and its ring-opened resonance forms. The open form displays zwitterionic or quinonoid-stabilized resonance structures. The type of stabilization depends on the strength of the intermolecular interaction causing the ring-opening reaction.[114] HA represents the acidic developer added to initiate ring-opening.

Figure 2.3 shows the absorption spectrum of CVL in acetonitrile.[25] In the leuco form, the absorption maximum is observed at 280 nm. Conversion to the coloured form *via* acidification with acetic acid causes the absorption maximum to shift to 605 nm, with a shoulder at 570 nm.[25] The major band (605 nm) is attributed to the excitation of π-

bonding electrons from the HOMO to the π*-antibonding LUMO.[25,117] The shoulder at 570 nm is attributed to excitation of electrons from the HOMO-1 orbital to the LUMO. The band at 380 nm is attributed to a CVL radical species.[25,117]

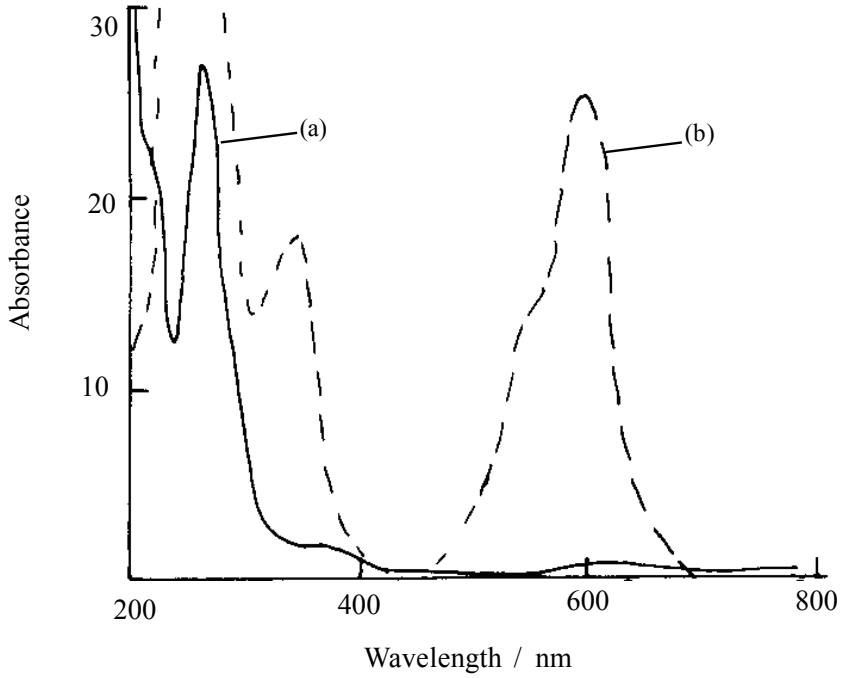

Figure 2.3. (a) The UV-Vis absorption spectrum of leuco-CVL in acetonitrile shows a major band at 280 nm. (b) CVL in acetonitrile acidified with acetic acid shows a major band at 605 nm and a shoulder at 570 nm. Reproduced with permission from reference 25 (*Journal of Photochemistry*, 1987, 37, 379-390).

Much of the research on the chemistry of CVL was focused on understanding the ring-opening equilibrium of CVL in solution.[25,106,113,114] The molar absorptivity, ε, of CVL in acidified acetonitrile showed a maximum of 2.8×10^4 mol^{-1} cm^{-1} at 605 nm in a solution of 90% acetic acid.[25] This value was substantially lower than that of crystal violet, the parent molecule of CVL, which showed an ε of 1.09×10^5 L mol^{-1} cm^{-1} at 586 nm in acetonitrile acidified with acetic acid.[25] This four-fold difference in ε_{max} indicates that CVL is largely in the leuco form, even in highly acidic environments.[25] As the concentration of acetic acid was further increased, ε_{max} was substantially reduced to ~ 1.4

x 10^4 L mol^{-1} cm^{-1} at 95% acetic acid and finally to ~8 x 10^3 L mol^{-1} cm^{-1} at 99% acetic acid.[25] Similar behaviour was observed in *d*-DMSO solutions acidified with HCl.[118] The colour loss observed at very low pH is due to the formation of a weakly coloured, cationic CVL species or, in the case of acidification with HCl, the formation of an HCl salt.[25,118]

Another important consideration regarding the ring-opening equilibrium in solution is the effect of the solvent. Solution-based studies on another TAM dye, blue 203, demonstrated that modifying the polarity of the solvent changed the concentration of the colour-forming species in solutions of toluene modified with aprotic polar solvents.[119] In these mixtures, the dye was mixed in a 1:1 molar ratio with a colour developer (ethyl gallate) to generate the ring-opened form of the dye, and the polarity of the solvent was modified with acetone, tetrahydrofuran, acetonitrile, or propylene carbonate.[119] Figure 2.4 (a) shows the change in absorbance as a function of acetone concentration for an equimolar blue 203:ethyl gallate mixture.[119] The concentration of the coloured species was highly dependent on the polarity of the solvent, increasing nearly monotonically up to 7 % acetone, after which the concentration of the coloured species decreased.[119]

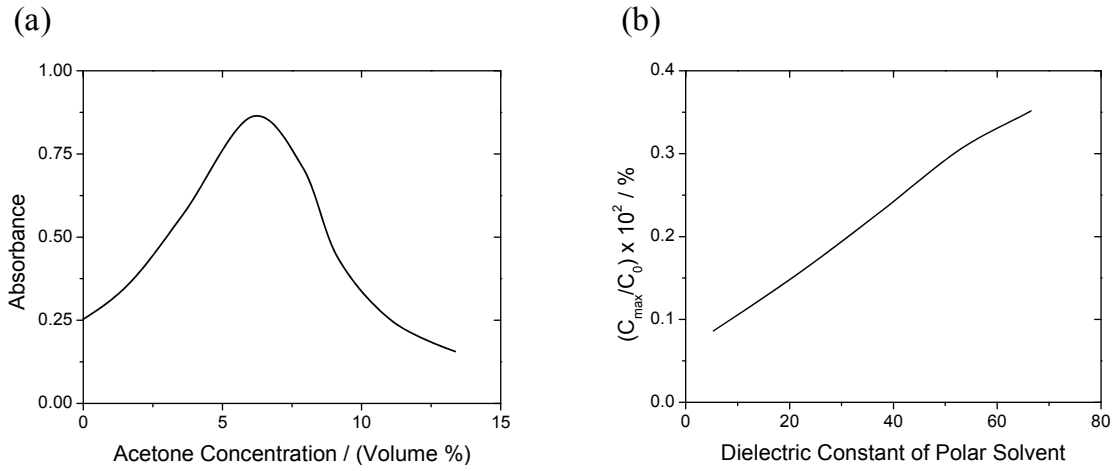

Figure 2.4. (a) The change in absorbance with increased solvent polarity. A maximum in colour density is reached at 7 vol% acetone. (b) The ratio (C_{max}/C_0) of the concentration of the coloured form at the absorption maximum, C_{max}, to the initial dye concentration, C_0, depends on the dielectric constant of the solvent. Adapted from reference 119.

Figure 2.4 (b) shows how the ratio (C_{max}/C_0) of the concentration of the coloured species measured at the absorbance maximum, C_{max}, to the initial concentration of the dye, C_0, changes as a function of dielectric constant of the solvent.[119] The concentration of the coloured form of the dye increases as the dielectric constant of the solvent is increased, indicating that the coloured zwitterionic form of the dye is more stabilized by solvents with high dielectric constant.[119] This behaviour was also reported for solutions of rhodamine B, a halochromic fluoran dye, in which the ring-opened zwitterionic form of the dye was most stable in solvents with high dielectric constants.[115,120] In general, polar protic solvents best stabilized the ring-opened charged form of the dye due to the formation of hydrogen-bonding networks and the dielectric/polarizability properties of the solvent.[25,115-120]

2.1.2 Colour Developer – Alkyl Gallates

The colour developer, usually an electron-accepting compound (*e.g.*, an acid), is added to generate the coloured form of the dye. Many of the dyes employed in thermochromic mixtures are halochromic and therefore require the addition of weakly acidic or basic developers to gain control over the colouring reaction.[4] Developers employed in thermochromic mixtures often contain phenolic protons, including the developers discussed in the present work such as the alkyl gallates, bisphenol A (BPA), and 2,4-dihydroxybenzophenone (DHB).[16] Alternatively, aliphatic developers containing carboxylic acid or phosphonic acid functionalities have also been employed in thermochromic mixtures.[71,121,122,123,124]

Alkyl gallates were chosen for use in the present study for a number of reasons including their relatively low pK_a values, their large number of available phenolic protons, their availability in various alkyl chain-lengths and ease of preparation *via* one-step synthesis, their compatibility with alcoholic solvents, and their use in previous studies on similar systems.[101,102,110,125,126,127] Figure 2.5 shows the general structure of gallic acid and its associated esters.

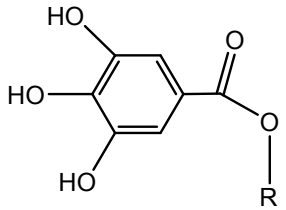

Gallic Acid: R = H
Gallic Acid Esters: R = C_nH_{2n+1}

Figure 2.5. The structure of gallic acid (R = H) and its associated esters (R = C_nH_{2n+1}).

Several gallate developers were used in the present study to effect changes in the colouring behaviour of thermochromic mixtures by changing the length of the developer

alkyl chain. Table 2.1 lists the names, abbreviations, alkyl chain lengths, and melting points for the gallate developers used in this work. The melting point of the gallate developer decreased with increasing chain length from gallic acid (T_{fus} = 251 to 252 °C) to octyl gallate (T_{fus} = 101 to 104 °C). The melting points of alkyl gallates with even-numbered alkyl chains do, however, begin to level off at chain lengths of eight carbon atoms or longer, eventually falling in the range of ~95 to 105 °C.[128,129,130,131]

Table 2.1. Melting points and alkyl chain lengths of various alkyl gallate developers.

Name	Abbreviation	Alkyl Chain	Melting Point / (°C) Literature[128-131]	Melting Point / (°C) Present Result[†]
Gallic Acid	GA	H	251 – 252	254 – 260 (decomp)
Propyl Gallate	PG	C_3H_7	146 – 149	149 – 151
Octyl Gallate	OG	C_8H_{17}	101 – 104	95 – 98
Decyl Gallate	DG	$C_{10}H_{21}$	94 – 95	91 – 94
Dodecyl Gallate	DDG	$C_{12}H_{25}$	96 – 97	97 – 99
Tetradecyl Gallate	TDG	$C_{14}H_{29}$	97 – 99	95 – 98
Hexadecyl Gallate	HDG	$C_{16}H_{33}$	99 – 101	94 – 95
Octadecyl Gallate	ODG	$C_{18}H_{37}$	102 – 104	102 – 104

Alkyl gallates are weakly acidic compounds. The pK_a for the first proton dissociation of PG (hydroxyl proton in the 4-position) is 7.22.[132] Calculated literature pK_a values for OG and DDG are 7.82 ± 0.20 and 7.93 ± 0.25, respectively.[133] The low pK_a values compared to other phenolic compounds are due to the *para* electron-accepting ester functionality.[125,134] Due to the relatively low acidity of this type of developer, the

[†] The melting points obtained in the present work were recorded on a melting point apparatus.

cationic form of CVL, which forms at very low pH values, generally cannot be generated by alkyl gallates.[25,131] This is beneficial for the development of thermochromic mixtures as the cationic form of CVL, which is less intensely coloured than the zwitterionic form, is not formed even at high developer concentrations.[25,112]

Crystal structures of the higher alkyl gallates (12 carbon alkyl chain and higher) have not been reported in the literature, although methodologies for crystallizing alkyl gallates have been reported in the patent literature.[135] Furthermore, no crystal structures for pure alkyl gallates containing short alkyl chains were found in the literature, although the crystal structures of propyl, butyl, and octyl gallate dihydrates have been reported.[136,137,138] The crystal structures of propyl gallate dihydrate and octyl gallate dihydrate are shown in Figure 2.6 and Figure 2.7, respectively.[136,138]

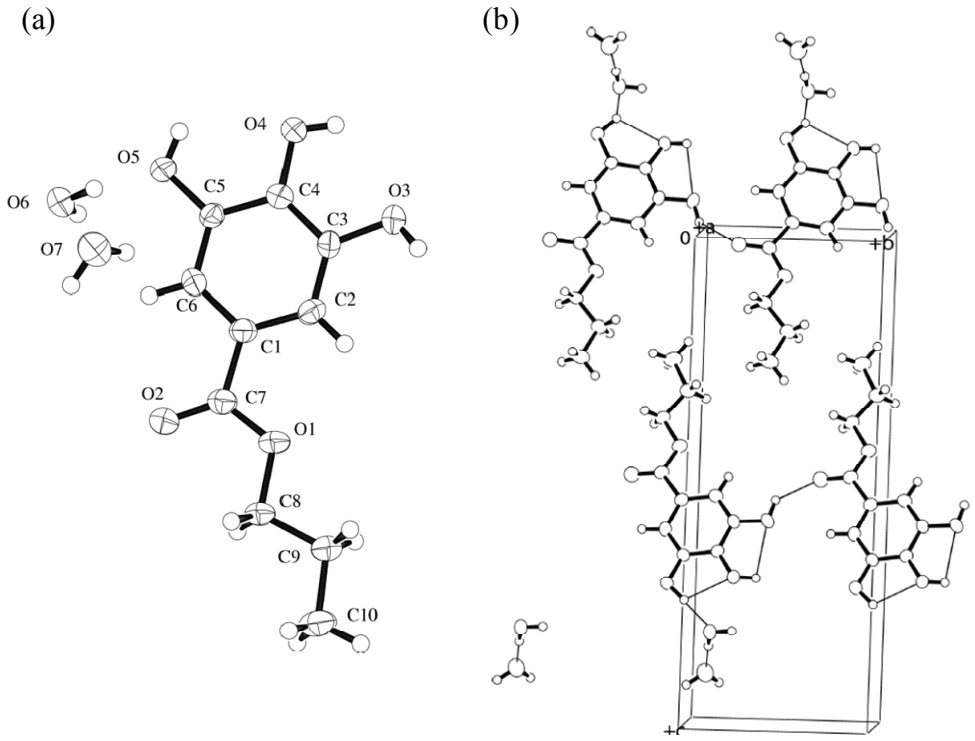

Figure 2.6. The crystal structure of propyl gallate dihydrate is monoclinic, $P2_1/c$, $Z = 4$, with a = 7.872 Å, b = 7.560 Å, c = 19.836 Å, and with β =101.03°. Reproduced with permission from reference 136 (*Acta Crystallographica E*, 2002, E58, o245-o247).

Propyl gallate (PG) dihydrate forms a monoclinic unit cell in the space group $P2_1/c$, with four molecules per unit cell, and unit cell parameters of a = 7.872 Å, b = 7.560 Å, c = 19.836 Å, and with β = 101.03°.[136] The molecule is planar to within 2° and the alkyl chains adopt an extended *trans* zig-zag pattern. No phenyl stacking was observed in the structure, and the methyl end-groups interact with each other.[136] The hydroxyl groups are oriented in the same direction with intramolecular hydrogen-bonding interactions occurring between the 3,4 and 4,5 hydroxyl groups, in addition to intermolecular interactions between the 3-hydroxyl proton and the carbonyl oxygen of the ester linkage.[136]

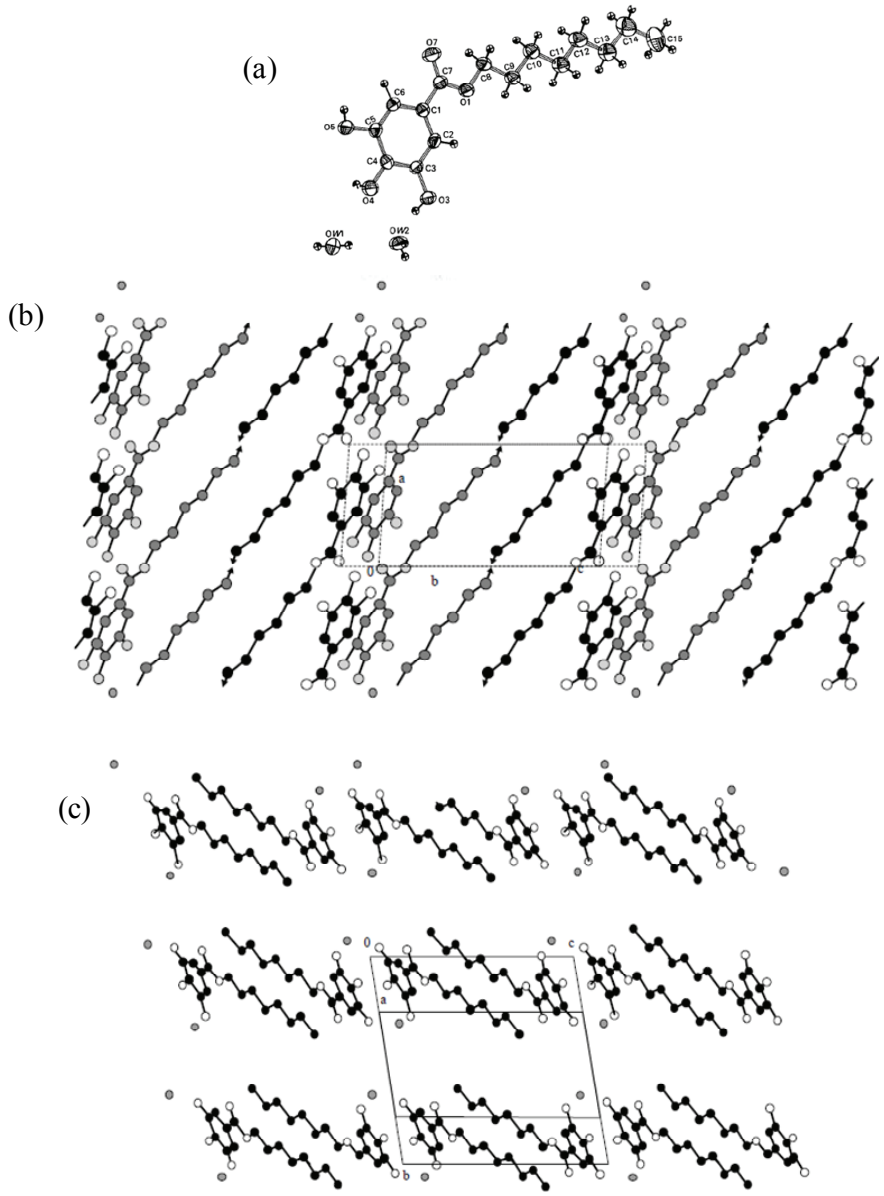

Figure 2.7. The crystal structure of octyl gallate dihydrate is triclinic, *P-1*, *Z* = 2, with *a* = 6.617 Å, *b* = 9.956 Å, *c* = 14.088 Å and with *α* = 79.08º, *β* = 85.58º, and *γ* = 70.80º. Reproduced with permission from reference 138 (*Acta Crystallographica E*, 1990, B46, 519-524).

Octyl gallate (OG) dihydrate is triclinic in the P-1 space group. The unit cell contains two molecules, and the unit cell parameters are a = 6.617 Å, b = 9.956 Å, and c = 14.088 Å, with α = 79.08°, β = 85.58°, and γ = 70.80°.[138] The phenyl group is co-planar (to within 3°) with the alkyl chain, and the alkyl chains adopt a *trans* zig-zag pattern. In

contrast to the PG crystal structure, in which no π-stacking was observed, OG shows π-stacking of the aromatic rings.[138] The π-stacking interaction is stabilized by the interdigitized arrangement of the alkyl chains, which allows for the formation of a head-to-head bilayer structure with the alkyl chains localized in the regions between the planes formed by the aromatic head groups.[138] Hydrogen bonding between the phenolic protons is similar to that observed in PG, where intramolecular 3,4 and 4,5 hydrogen bonding, and intermolecular hydrogen bonding between the ester carbonyl and the 4-hydroxyl proton, was observed. [136,138]

The most important feature of alkyl gallates, as far as their applications in thermochromic mixtures are concerned, is the change in physical properties associated with changing alkyl chain lengths.[136,138] The crystal structure of octyl gallate dihydrate, which serves as a model for the expected crystal form of dodecyl gallate (which contains a 12 carbon atom alkyl chain), shows that the organization of the alkyl chains plays an important role in defining the overall structure of the crystal.[138] Due to the packing of the alkyl chains in the crystal, the aromatic rings and hydroxyl groups become oriented in an arrangement that favours the formation of intermolecular π-stacking and hydrogen-bonding interactions.[138] Short-chain gallates, which do not undergo such efficient packing of the alkyl chains, are prevented from undergoing π-stacking interactions due to steric considerations.[136]

Since alkyl chain length plays such a crucial role in defining the physical characteristics of the alkyl gallates, selection of appropriate chain lengths for the developer component of thermochromic mixtures is critical to controlling the colouring behaviour of such mixtures.[101,110] In particular, modifying the degree of alkyl chain

length matching of the alkyl chains (*i.e.*, the similarity in alkyl chain length) attached to the developer and to the co-solvent component (which will be discussed in the following section) can be used to gain control over the type of colouring behaviour observed in three-component mixtures.[101] Studies on the influence of modifying the length of the developer alkyl chain (and also the solvent alkyl chain) are central to the present research.

2.1.3 Co-Solvent - Primary Alkyl Alcohols

The co-solvent, hereafter referred to as the *solvent*, generally makes up 50 to 99% of the thermochromic mixture by mass.[3,31,100,105] High-melting organic solvents (where T_{fus} = 40 to 80 °C), such as long-chain aliphatic alcohols, alkanes, and esters, are commonly employed as solvents in thermochromic mixtures.[3,31,100,101,121] The solvent functions as an interaction medium for the dye and developer, and can be used to control the colour-change temperature of the mixture.[3,16,31,101] It can also influence the thermochromic behaviour of three-component mixtures, as shown in this thesis.

In general, the role of the solvent falls into one or more of four categories.[110] First, when the melting point of the solvent ($T_{fus,solvent}$) is lower than that of the bulk mixture (*i.e.*, that of the dye-developer mixture, $T_{fus,mixture}$), the solvent provides a liquid medium to aid in the phase-separation of the developer from the metastable structures formed by the dye and developer.[3,16,110] In this case, the melting point of the solvent is used to control the decolourization temperature of the mixture, and the decolourization temperature can be easily adjusted by changing the solvent concentration. In this

application, the solvent is a minor component of the mixture (0.5 to 10 mass%) as compared to a standard thermochromic mixture (50 to 90 mass%).[3,16,139]

Second, when the solvent component constitutes a large portion of the thermochromic mixtures (50 to 90 mass%), the melting point of the bulk mixture is primarily determined by the melting point of the solvent ($T_{fus,solvent} \sim T_{fus,mixture}$).[3,100,101,110] If the solvent is highly crystalline, for example in long-chain carboxylic acids, the solvent component can provide nucleation sites for the phase separation of the developer from a coloured dye:developer complex, and can lower the activation energy of the phase-separation process, resulting in increased rates of decolourization.[110] The term "decolourization accelerating agent" has been used to describe the solvent when employed in this role.[3,110,140]

Third, if the solvent and developer are chemically compatible and a metastable dye:developer aggregate is present (particularly in the solid state), then molecules of the solvent could incorporate themselves into the dye:developer aggregate structure.[110,141] Addition of the solvent molecules to the aggregate could influence the cohesive properties and stability of the aggregate, thereby modifying decolourization temperatures and phase-separation rates of the metastable structures.[110,121,141]

Fourth, and most relevant to the present work, if the developer and solvent demonstrate strong attractive interactions, it is possible for the solvent to disrupt dye:developer interactions completely, giving rise to a decoloured state.[101,142,143] The formation of colour in three-component thermochromic mixtures is dependent on the competition between three binary interactions: the dye:developer, developer:solvent, and dye:solvent interactions.[101,102] If the dye:developer interaction is strongly attractive,

decolourization of the mixture can be difficult due to the lack of phase separation of the dye and developer on thermal quenching.[100,101] In such cases, the addition of a solvent, which forms an attractive developer:solvent interaction, can be used to disrupt the dye:developer aggregate and can cause phase separation of the dye and developer.[101,110]

Previous studies regarding the nature of the developer:solvent interaction showed that developer:solvent compound formation is possible in mixtures containing developer and solvent components with alkyl chains that are similar in length.[101,110] In such an instance, the formation of a developer:solvent compound essentially sequesters the developer from the dye, thereby preventing colour formation in the mixture.[101,102,110,143]

One additional factor that can influence colouring behaviour in three-component systems is the polymorphic nature of the solid state of long-chain aliphatic compounds. The role played by each of the solid polymorphs of the aliphatic solvent has not been examined in depth in the literature.[110] The role of the solvent component in the thermochromic behaviour of three-component mixtures is central to this work.

Primary aliphatic alcohols were used as the solvent component for the majority of the work presented here; Table 2.2 lists some of the physical properties of the alcohols used in this work.[144,145,146,147] The subsections of section 2.1.3 expand on some of the important chemical properties and physical characteristics of aliphatic alcohols.

Table 2.2. Melting points, solid-solid phase transition temperatures, and alkyl chain lengths of various alkyl alcohol solvents.

Name	Abbreviation (used here)	Alkyl Chain	Melting Point / (°C)[144-147]	Solid-Solid Phase Transition Temperature / (°C)[144-147]
1-Tetradecanol	TD-OH	$C_{14}H_{29}$	36 – 38	33 – 36
1-Hexadecanol	HD-OH	$C_{16}H_{33}$	48 – 50	43 – 46
1-Octadecanol	OD-OH	$C_{18}H_{37}$	56 – 59	52 – 55

2.1.3.1 Polymorphism in Primary Alkyl Alcohols

The higher primary alcohols ($C_nH_{(2n+1)}OH$, $n > 12$) display polymorphism in the solid state.[144,145,148] Most importantly, they can exist in an orientationally disordered solid phase, called a rotator phase, at temperatures just below their melting point.[145,148,149] The rotator phase of primary alcohols is characterized by enhanced values of molar heat capacity,[149] ionic conductivity,[150] and dielectric constant[151] relative to the low-temperature solid phase and the high-temperature liquid phase.

Three solid phases are observed in primary alcohols with alkyl chains greater than 12 carbons atoms in length. All three of the phases are characterized by a head-to-head bilayer structure, with the terminal hydroxyl groups forming an extensive hydrogen-bonding network at the ends of the chains.[148,149,150,152,153,154,155]

A monoclinic phase, formed at the lowest temperatures, has the long axis of the molecule nearly perpendicular to the continuous plane formed by hydrogen bonds between the hydroxyl end-groups.[148,152,154,155] This phase has been referred to in the literature as both the low-temperature ordered phase (LO-phase) and the β-phase; the terminology LO-phase will be used later in this work to distinguish between the low-temperature ordered phase and the rotator phase. The β-phase is the thermodynamically

stable, low-temperature phase for DD-OH and TD-OH, and for the odd-numbered primary alcohols with chains longer than 12 carbon atoms.[150,156,157] This phase is sometimes referred to as a vertical phase (all chain vectors are aligned vertically).

Another monoclinic phase, referred to as the γ-phase, also can be formed at low temperature. In the γ-phase, the long axis of the molecule is tilted about 60° to the normal of the hydroxyl plane,[148-150,153,155,158] and this phase is only observed in longer-chain alcohols (n > 12) with even-numbered chain lengths. The exclusion of the tilted phase from the phase behaviour of odd-numbered primary alcohols is due to energy considerations.[153,159] This odd-even β-γ phase behaviour is also observed in paraffins and can be explained by examining the packing behaviour of the end groups of the molecule, as shown in Figure 2.8.[159]

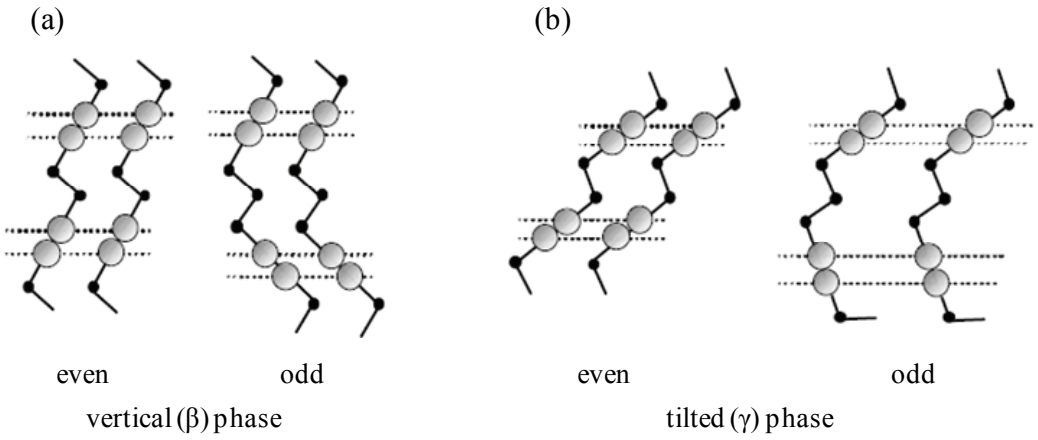

Figure 2.8. The packing behaviour in even- and odd-numbered primary alcohols in (a) the (β) phase and (b) the tilted (γ) phase. The grey spheres represent the hydroxyl groups and the black spheres represent the carbon chains (omitting hydrogen atoms). Unfavourable end-group packing in the tilted phases precludes the formation of γ-phases in odd-numbered primary alcohols with n > 14. The β phases do not demonstrate differences in end-group packing between even- or odd-numbered alcohols. Adapted from reference 159.

When the number of carbon atoms in the alkyl chain is even, the packing distances for the end groups are slightly shorter in the tilted phase than in the vertical

phase.[145,150,160] In odd-numbered alcohols, the extra carbon atom in the chain forces the end group to adopt a higher energy conformation with its neighbour than is observed in the case of even-numbered alcohols, preventing formation of the γ-phase in odd-numbered primary alcohols.[148,152,159]

The third solid polymorph observed in long-chain primary alcohols is an orientationally disordered phase in which the long axis of the molecule is tilted slightly from the normal to the hydroxyl plane (7°),[161] and in which rotation occurs about the long axis of the molecule.[144,148,156] This phase has been referred to in the literature as the α-phase or as the rotator phase (R-phase); the terminology R-phase will be used later in this work to distinguish between the rotator and low-temperature ordered phases. The α-phase exists immediately below the melting point of the pure alcohol.[144,148] The entropy of the various alcohol phases increases as follows: $S_{\gamma} < S_{\beta} < S_{\alpha} < S_{liquid}$.[150]

Although the end-group packing is similar for the β- and γ-phases, the lateral-chain packing of the alkyl groups in the tilted γ-phase is closer than in the vertical β-phase.[159] Enhanced packing of the lateral-chain groups is dependent on the length of the alkyl chain, and as the chain length increases the lateral-chain packing interactions become dominant and make the γ-phase the more thermodynamically stable, low-temperature solid phase.[144,160] This behaviour is akin to the changes in crystal packing observed for the aforementioned alkyl gallates (*vide supra*, section 2.1.2),[136,138] in which the increase in alkyl chain length from propyl gallate to octyl gallate was responsible for the formation of lateral-chain interactions in the octyl gallate crystal structure.[138] It is not unreasonable to assume that by matching the lengths of the alkyl chains attached to the

solvent and developer, respectively, attractive lateral-chain interactions between the two components could be obtained.[101,110]

The rotator phase (α-phase) is observed in alcohols with carbon chain lengths greater than 13 carbon atoms, and imparts a translucent, waxy appearance to the solid alcohol.[144,148] This is in contrast to the opaque, crystalline appearance of the low-temperature solid phases.[144-146] Transition of the rotator phase (R-phase) to a low-temperature ordered phase (LO-phase) upon cooling usually requires nucleation, and can display sub-cooling.[160] This sub-cooling can be enhanced by the presence of impurities and/or the addition of other long-chain aliphatic compounds (*e.g.*, longer or shorter primary alcohols, paraffins, *etc.*) resulting in a dramatic increase in the apparent stability of the rotator phase.[148,155,162]

2.1.3.2 Structures of Primary Alkyl Alcohols

The difference in structure between the β- and γ-phases of the higher primary alcohols with alkyl chain lengths between 14 and 20 carbons can be described by comparing the crystal structures of 1-heptadecanol (Figure 2.9 (a)) and 1-octadecanol (Figure 2.9 (b)).[153,160] The β-phases of TD-OH, HD-OH and OD-OH are monoclinic ($P2_1/c$) with eight molecules per unit cell and two molecules in an asymmetric unit cell. The two conformers include one molecule in an all-*trans* configuration (analogous to the γ-phase) and one molecule with an all-*trans* skeletal carbon configuration, with the C-C-C-O(H) torsional angle in a *gauche* configuration.[153,160,163] The γ-phases of HD-OH and OD-OH are monoclinic (C2/*c*) with eight molecules per unit cell. The γ-phases are

characterized by an all-*trans* configuration of the skeletal carbons of the alkyl chain.[153,155,160]

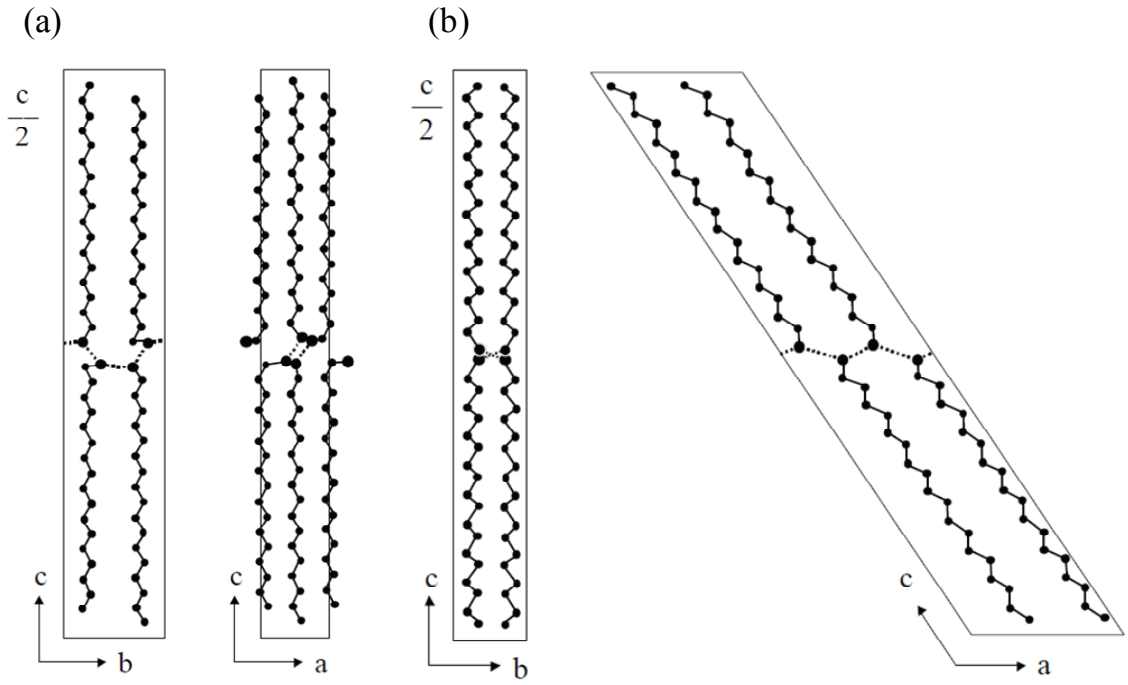

Figure 2.9 The crystal structures of (a) the β-phase of 1-heptadecanol and (b) γ-phase of 1-octadecanol. (a) The β-phase of 1-heptadecanol is characterized by head-to-head bilayer stacking in which the hydroxyl groups form a plane and the alkyl chains are oriented in a nearly perpendicular fashion to the hydroxyl plane. (b) The γ-phase of 1–octadecanol is characterized by a head-to-head bilayer structure in which the alkyl chains are oriented at an angle of approximately 60° to the hydroxyl plane. Large spheres represent oxygen atoms, small spheres represent carbon atoms, and hydrogen atoms are omitted for clarity. Adapted from reference 160.

Although no crystal structural data exist for the rotational phases of primary alcohols, authors have used XRD to compare the spacing of the molecules in the α-phase (rotator) with the β- and γ-phases.[148,150] A summary of the long spacing of the α-, β-, and γ-phases of the three normal alcohols used in the current work is presented in Table 2.3.

Table 2.3. Long spacing of primary alcohol polymorphs in Å.[148,150,160]

Alcohol	Abbreviation (used here)	α-phase	β-phase	γ-phase
1-Tetradecanol	TD-OH	38.9	39.6	33.05
1-Hexadecanol	HD-OH	43.83	44.9	37.27
1-Octadecanol	OD-OH	48.93	50.28	41.6

2.1.3.3 Thermodynamic Parameters of Primary Alkyl Alcohols

Thermodynamic data for the polymorphic transitions of 1-tetradecanol (TD-OH) are shown in Table 2.4. The low-temperature ordered β-phase transforms to the α-phase (rotator) at 311.2 K with a transition enthalpy change of 23.8 kJ mol^{-1}, and can be annealed to form the metastable γ-phase if heated at very slow rates.[156] Mosselman *et al.* produced a heating curve for TD-OH showing two arrests.[156] At slow heating rates (< 0.03 K min^{-1}) a β-γ transition was observed. This transition had a very small enthalpy of transition (1.8 kJ mol^{-1}), and was obscured by the more substantial β-α phase transition at 311.2 K when the heating rate was increased.[156]

Table 2.4. Thermodynamic data for the phase transitions of 1-tetradecanol.[156]

$\Delta_{trs}H$ / (kJ mol^{-1})	T_{trs} / K	Initial Phase	Final Phase
1.8	306	Crystalline, β	Crystalline, γ (metastable)
23.8	311.2	Crystalline, β	Crystalline, α
25.1	310.8	Crystalline, α	Liquid
47.0	311.2	Crystalline, γ (metastable)	Liquid

Thermodynamic data for the polymorphic transitions of 1-hexadecanol (HD-OH) and 1-octadecanol (OD-OH) are given in Table 2.5 and Table 2.6, respectively. The transition of the stable low-temperature γ-phase, to the metastable β-phase is very slow, and was not observed by most authors.[149,156] Only the γ-α and α-liquid phase transitions were consistently observed for the HD-OH and OD-OH systems. [149,156]

Table 2.5. Thermodynamic data for the phase transitions of 1-hexadecanol.[156]

$\Delta_{trs}H$ / (kJ mol^{-1})	T_{trs} / K	Initial Phase	Final Phase
21.7	315.8	Crystalline, γ	Crystalline, α
33.06	321.81	Crystalline, α	Liquid

Table 2.6. Thermodynamic data for the phase transitions of 1-octadecanol.[149]

$\Delta_{trs}H$ / (kJ mol^{-1})	T_{trs} / K	Initial Phase	Final Phase
25.60	324.55	Crystalline, γ	Crystalline, α
41.07	334.2	Crystalline, α	Liquid

The data presented in Tables 2.4 to 2.6 indicate that one solid-solid phase transition could be expected in thermochromic mixtures containing each of the primary alcohol solvents. In the case of 1-tetradecanol, the low-temperature ordered phase should be a β-phase that transitions to an α-phase (rotator phase) just prior to solvent melting.[148,156] In the case of both 1-hexadecanol and 1-octadecanol, the low-temperature ordered phase should be a γ-phase that transitions to an α-phase prior to solvent melting.[148,149,156] No effort was made here towards distinguishing the form of the low-temperature ordered phases (*i.e.*, distinguishing the β- and γ-forms) in three-component

mixtures, and as such all low-temperature ordered phases are referred to as LO-phases in subsequent sections of this thesis. The formation of the rotator phase (hereafter referred to the R-phase) was based on visual changes in the appearance of the mixture, with conversion to a shiny, translucent appearance indicating the formation of the rotator phase.[148]

2.2 Binary Interactions in Three-Component Systems

Based on a series of studies on the thermochromic properties of three-component thermochromic mixtures containing CVL, alkyl gallates, and primary alcohols, MacLaren, Tang, and White devised a set of design rules for preparing thermochromic mixtures based on the observation that competition between binary interactions controls the colouring behaviour in such mixtures.[101,102,110,143,164]

For example, if the strength of the binary dye:developer interaction is greater than the strength of the binary developer:solvent interaction, then the developer will generate the ring-opened form of the dye and the mixture will be coloured.[143] Conversely, if the developer:solvent interaction is stronger, the developer is not free to interact with the dye and no colour will be observed in the mixture.[101,143] In rewritable three-component thermochromic mixtures, competition between the binary interactions plays a central role in determining the colouring behaviour of the mixtures.[101,143]

2.2.1 Dye:Developer Interactions

2.2.1.1 Formation of Metastable Aggregate Structures

Binary dye:developer interactions have been extensively studied by researchers in both academia and industry due to the important role these interactions play in the generation of colour in multi-component thermochromic mixtures.[3,16,41,42,58,64,65,71,99-111,119,122,139-143,164,165] Much of the experimental work carried out by industrial research groups in the area of rewritable thermal printing has been focussed on identifying suitable colour-forming compositions. Although many examples of reversibly thermochromic mixtures have been described, considerably less information regarding the mechanism of colour formation in binary dye:developer mixtures has been reported.[9,33,41,42,121-124] Nevertheless, many research groups have suggested that the formation of metastable, binary dye:developer aggregate structures is central to the formation of the coloured state in rewritable thermochromic mixtures.[122,141,166,167,168] It has also been hypothesized that conversion of the metastable aggregate structure to an equilibrium, phase-separated structure is responsible for colour erasure in such mixtures.[71,100, 102,110]

In rewritable thermochromic mixtures, the dye and developer are thought to form metastable, binary complexes that are held together by weak intermolecular interactions such as H-bonding and van der Waals forces.[71,100,101,169,170,171,172,173] The structures of metastable coloured phases have been observed to vary from featureless, amorphous (*i.e.*, glassy) mixtures to more ordered structures of dye:developer aggregates.[71,100,101,169-173] Figure 2.10 shows proposed structures for two metastable coloured phases and a decoloured equilibrium phase that might form in binary thermochromic mixtures.[122,165]

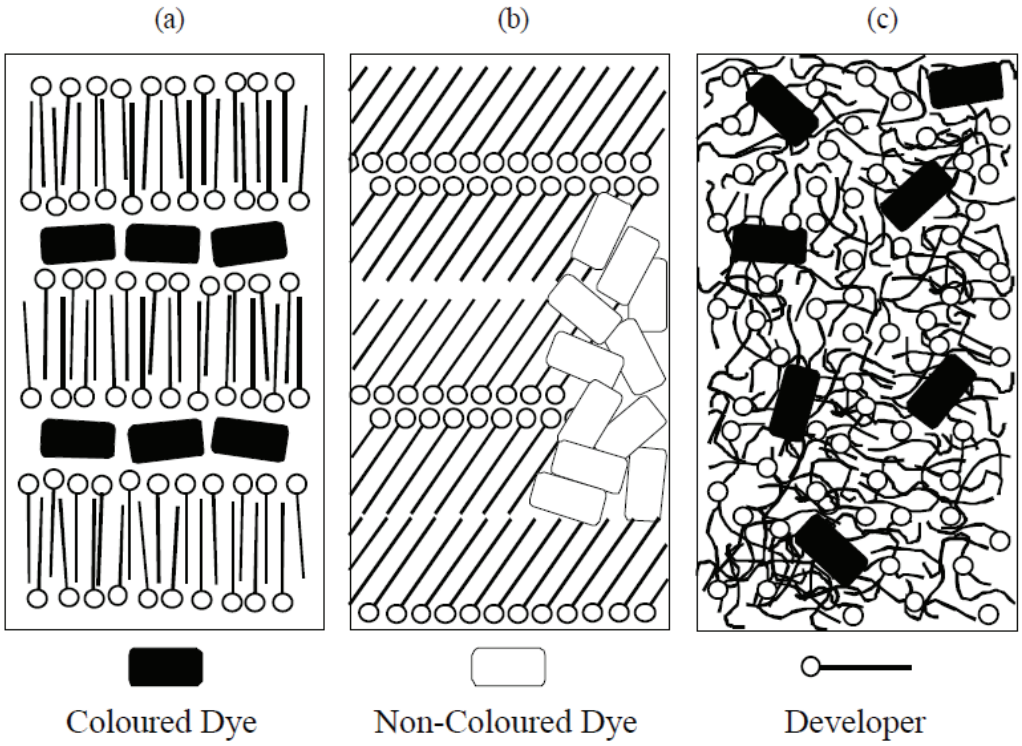

Figure 2.10. Schematic representation of the two types of proposed structures for the metastable phases of binary dye:developer mixtures employed in rewritable thermochromic systems, and the proposed structure of the colourless equilibrium phase. (a) A coloured metastable structure in which alkyl chains give rise to long-range lamellar order, and the heads of the alkyl chains (*e.g.*, the hydroxyl or phenolic protons) interact with the dye molecules. (b) A colourless, equilibrium structure in which the dye and developer have become phase-separated. (c) A thermally quenched, glassy metastable state in which there is no long-range order associated with the alkyl chains of the developer. Reproduced with permission from reference 110 (D. C. MacLaren, *PhD Thesis*, Dalhousie University, 2003).

Depending on the developer structure and the thermal history of the sample, binary dye:developer mixtures can adopt an ordered coloured form (Figure 2.10 (a)), in which the alkyl chains of the developer form long-range ordered lamellar structures, or a disordered glassy structure (Figure 2.10 (c)), in which a thermally quenched, molten mixture retains the disordering in the alkyl chains as the mixture is rapidly cooled.[110,122,165] Both of these coloured phases are metastable with respect to the decoloured equilibrium phase (Figure 2.10 (b)), which undergoes phase separation of the dye and developer, leading to colour loss.[110,122,165]

It is thought that possibly long alkyl chains attached to the developer play an important role in the formation of metastable aggregate structures,[102,110] similar to those described in Figure 2.10, where van der Waals interactions between the alkyl chains allow for the formation of large supramolecular structures.[71,121,141,173] It is further thought that the long alkyl chains support the formation of the metastable complex in the coloured state, and the high degree of crystallinity in their pure state allows for efficient phase-separation of the dye and developer upon decolourization of the mixture.[71,121,141,173] The binary dye:developer interactions of CVL with some alkyl gallates, and also with bisphenol A, are described in the following sections.

2.2.1.2 Examples of Binary Dye:Developer Interactions

2.2.1.2.1 CVL:Alkyl Gallate Binary Mixtures

The binary dye:developer system most relevant to the present work is that of CVL:alkyl gallate mixtures. MacLaren and White carried out a series of studies regarding the competition between binary interactions in three-component thermochromic mixtures containing crystal violet lactone as the dye, alkyl gallates (in particular dodecyl gallate, DDG) as the developer, and higher primary alcohols as the solvent.[101,110,143,164] Raman spectroscopy, differential scanning calorimetry, and optical microscopy were used to study the binary dye:developer interaction and to gain information about the stability and stoichiometry of CVL:alkyl gallate complexes.[101,110,143,164]

Melting of binary mixtures of CVL and DDG produced dark blue-coloured, viscous liquids that became more viscous with increasing mole fraction of CVL, x_{CVL}.[110] Upon cooling, the liquids solidified as glassy solids and maintained strong colouration.

Partial crystallization of the glass was observed after ageing at room temperature over the period of several hours to several days, and crystallization could be dramatically hastened by annealing at 65 to 75 °C.[110] Figure 2.11 shows a CVL:DDG mixture, where x_{CVL} = 0.17, at (a) room temperature after solidification and (b) after annealing at 65 °C for 30 minutes. The morphology of the crystals formed after annealing, shown in Figure 2.12 (a), was consistent with that of crystals of pure DDG, shown in Figure 2.12 (b).[110]

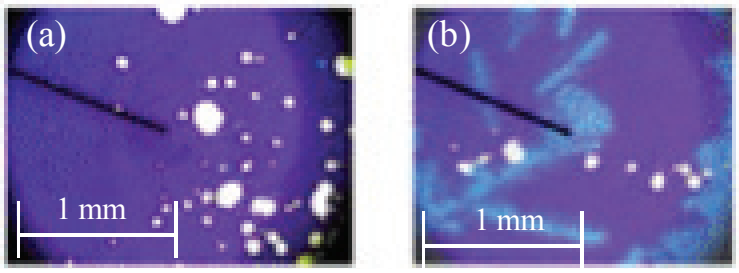

Figure 2.11. A CVL:DDG mixture where x_{CVL} = 0.17 showing (a) an as-solidified glassy form of the mixture and (b) the partially crystalline form of the mixture after annealing at 65 °C for 30 minutes. Reproduced with permission from reference 110 (D. C. MacLaren, *PhD Thesis*, Dalhousie University, 2003).

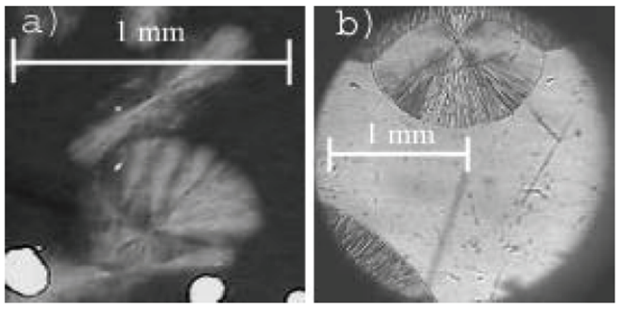

Figure 2.12. A comparison of the (a) crystallites formed during annealing of the x_{CVL} = 0.17 mixture showing consistent morphological features with (b) crystallites of pure DDG. Reproduced with permission from reference 110 (D. C. MacLaren, *PhD Thesis*, Dalhousie University, 2003).

Differential scanning calorimetry (DSC) was used to analyze the crystallization behaviour of glassy CVL:DDG mixtures in an effort to identify the composition above which no free DDG could crystallize from the mixture.[110] The lack of DDG

crystallization from an annealed binary mixture indicated that there was no free DDG in the mixture, implying that all of the developer was complexed with the dye. Figure 2.13 shows DSC thermograms on heating for mixtures with $0.13 \leq x_{CVL} \leq 0.33$.[110,164] At a composition of $x_{CVL} = 0.33$, no crystallization of DDG was observed indicating that at this mixing ratio all of the DDG was complexed with CVL.[110]

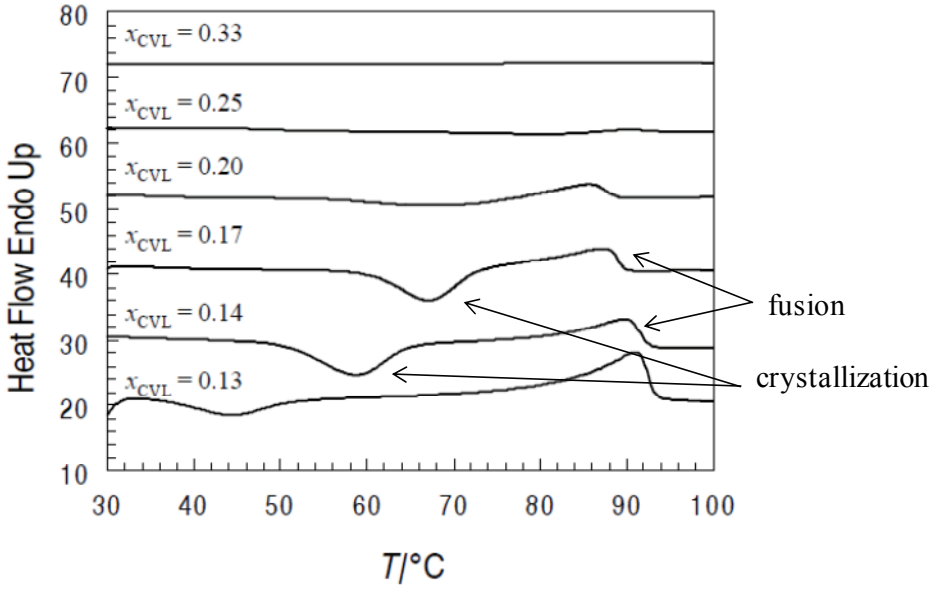

Figure 2.13. DSC thermograms on heating of glassy mixtures of CVL and DDG. The lack of a crystallization event at $x_{CVL} = 0.33$ indicates that there is no free DDG in the mixture at (and above) this composition. Reproduced with permission from reference 110 (D. C. MacLaren, *PhD Thesis*, Dalhousie University, 2003).

Vibrational spectroscopy was used to follow the ring-opening reaction of CVL as the lactone carbonyl bond dramatically changes vibrational frequency upon conversion from the lactone form to the ring-opened form.[174] Information regarding the stoichiometry of the binary CVL:DDG complex was obtained by employing Job's method of continuous variation, in which sequential increases in the concentration (*i.e.*, mole fraction) of one of the components was coupled with changes in the relative intensity of specific vibrational frequencies.[175,176] In the case of CVL:DDG mixtures, the

vibrational frequencies of interest associated with the ring-opened form of the dye include the symmetric carboxylate vibration at 1359 cm^{-1} and the wag deformation ($\gamma_{sym(COO^-)}$) at 720 cm^{-1}, and the C=NR_2 asymmetric vibration at ν = 1584 cm^{-1} and C-NR_2 vibration at 918 cm^{-1}.[110,177,178]

Figure 2.14 shows the Raman spectra of CVL:DDG mixtures across a wide compositional range.[110,164] The carboxylate carbonyl vibrations at 1359 cm^{-1} and 720 cm^{-1} were first observed at x_{CVL} = 0.10 and increased in relative intensity until x_{CVL} = 0.25. Above x_{CVL} = 0.25, the relative intensity of these peaks was reduced as more CVL was added, indicating that the stoichiometry of the CVL:DDG complex is 1:3, since further addition of CVL resulted in the observation of vibrations associated with the free, ring-closed form of CVL. Similar behaviour was observed for the C=NR_2 vibration at 1584 cm^{-1} and the C-NR_2 vibration at 918 cm^{-1}, in which a maximum of the relative intensities of these vibrations was observed at x_{CVL} = 0.25.[110,164]

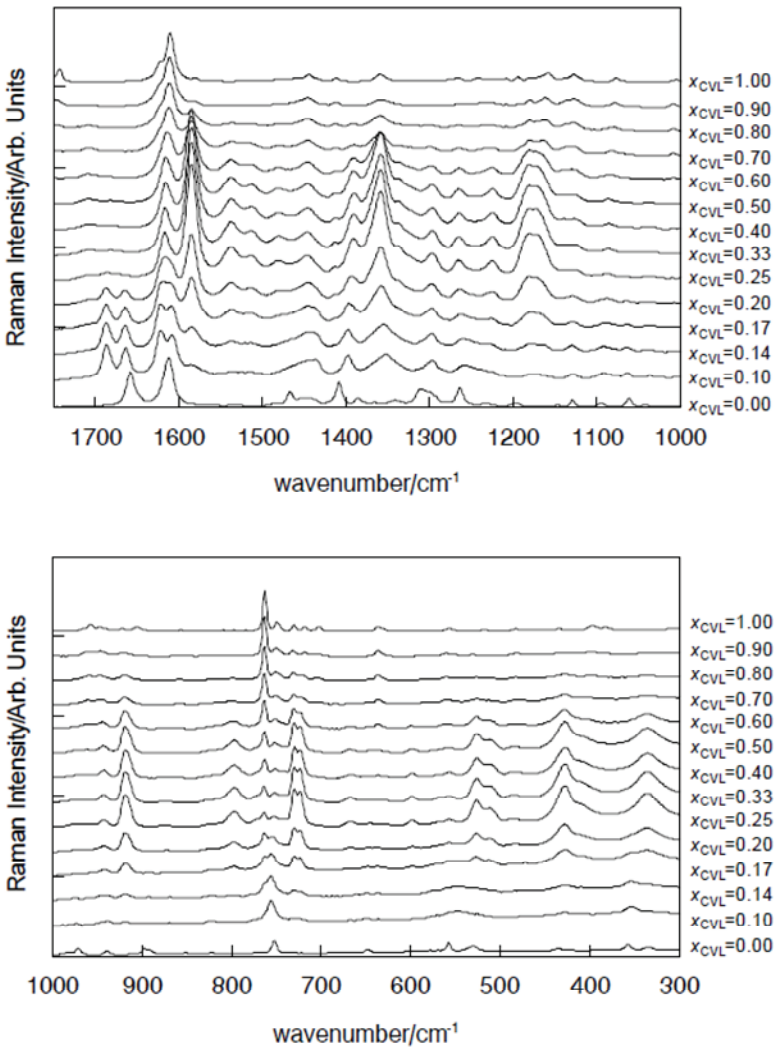

Figure 2.14. Raman spectra of crystal violet lactone:dodecyl gallate mixtures (CVL:DDG) showing the formation of a complex at x_{CVL} = 0.25. The relative intensities of the carboxylate carbonyl modes at 1359 cm^{-1} and 720 cm^{-1}, the C=NR$_2$ mode at 1584 cm^{-1}, and the C-NR$_2$ mode at 918 cm^{-1} reach maximum values when x_{CVL} = 0.25. Reproduced with permission from reference 110 (D. C. MacLaren, *PhD Thesis*, Dalhousie University, 2003).

The results of prior vibrational spectroscopy experiments were summarized by employing a modified version of Job's method of continuous variation.[175,176] The formation of a CVL:DDG complex can be written as:

$$\text{CVL} + y\ \text{DDG} = z\ \text{Complex} \qquad (2.1)$$

and Job's method states that if two components, A (*e.g.*, CVL) and B (*e.g.*, DDG), are mixed with continuously varying molar ratios, the maximum amount of complex will exist in the mixture where the mole ratio A to B, n_A/n_B, equals z of equation 2.1. A quantity proportional to the amount of complex, z (in this case, Raman intensity), plotted against the molar ratio, x_A/x_B, gives a maximum corresponding to the stoichiometric molar ratio of the complex.[175,176]

Using Job's method, MacLaren and White determined the molar ratio of the CVL:DDG complex to be 1:3.[110,164] In other words, three developer molecules were required to fully develop the ring-opened form of CVL, resulting in a 3DDG:CVL complex. Figure 2.15 shows the Job's plots for the carboxylate vibrations (Figure 2.15 (a)) and for the C-NR_2/C=NR_2 vibrations (Figure 2.15 (b)), both of which indicate a stoichiometry of 3DDG:CVL for the coloured complex.[110,164]

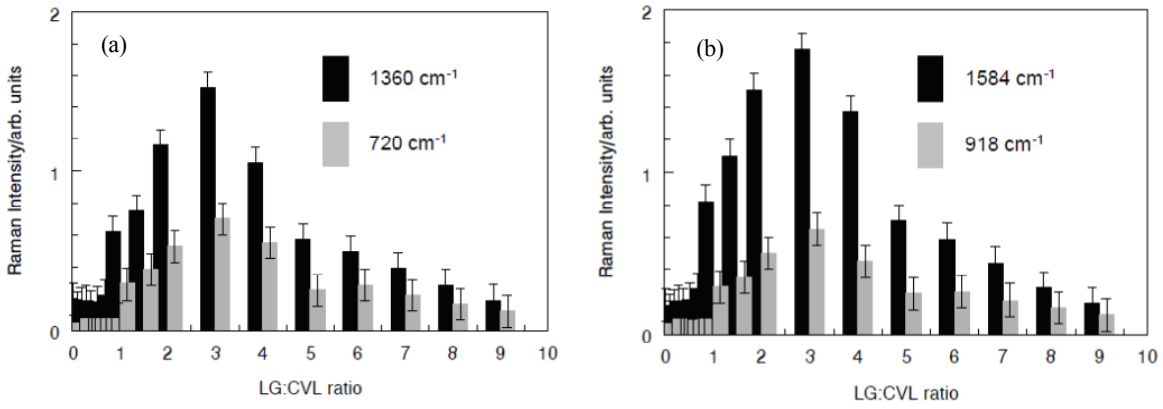

Figure 2.15. The stoichiometry of the coloured DDG_3:CVL complex was determined by Job's method of continuous variation. The 3DDG:CVL stoichiometry of the coloured complex was supported by both (a) the carboxylate carbonyl vibrations and (b) the C-NR_2/C=NR_2 vibrations. The error bars indicate spread over three sets of samples. Reproduced with permission from reference 164 (*Journal of Materials Chemistry*, 2003, 13, 1695-1700).

The previous methods of analysis, including visual observation of crystallization behaviour, differential scanning calorimetry, and vibrational spectroscopy, were extended to CVL:developer mixtures containing propyl gallate (PG) or octyl gallate (OG) as the developer component.[110] The results of these experiments are summarized in Table 2.7. Propyl gallate was shown to form a 2:1 complex with CVL and octyl gallate was shown to form a 4:1 complex with CVL. The 3DDG:CVL complex, with a 3:1 stoichiometry, fell between the molar ratios observed for PG and OG mixtures.[110]

Table 2.7. The stoichiometry of dye:developer complexes formed in equilibrium mixtures of CVL with PG, OG, and DDG.[110]

Developer	Abbreviation	Complex Type	Complex Stoichiometry
Propyl Gallate	PG	*x*PG:CVL	$x = 2$
Octyl Gallate	OG	*x*OG:CVL	$x = 4$
Dodecyl Gallate	DDG	*x*DDG:CVL	$x = 3$

2.2.1.2.2 Binary Complexes of CVL with Bisphenol A

The phenolic developer bisphenol A (BPA) has been employed as a developer in a number of studies of the thermochromic behaviour of multi-component mixtures.[57,58,100,103,174,175,176] Ibata *et al*. examined the formation of dye:developer complexes in mixtures of CVL and BPA.[174] The authors found that at a molar ratio of CVL:BPA = 2:1, roughly half of the molecules of CVL were in a form characterized by carbonyl vibrations associated with a –COOH functionality formed after opening of the lactone ring, while the other half remained in the ring-closed leuco form. Increasing the molar ratio to CVL:BPA = 1:5 resulted in the near-complete conversion of the –COOH form to a ring-opened form characterized by a negatively charged carboxylate group

(COO^-).[174] This examination of the complexation behaviour in CVL:BPA mixtures indicated that there are at least three possible forms of CVL in such mixtures, and the form observed is dependent on the molar ratio of the components and the strength of the interactions involved. In this system, the ring-closed form was more stable at low developer loading, the (–COOH) form was most stable at intermediate developer loadings (*e.g.* 2CVL:BPA), while the ($–COO^-$) form was more stable at high developer loadings (5BPA:CVL).[174]

Luthern and Peredes published two reports examining the molar ratio of dye:developer complexes in some three-component thermochromic mixtures.[175,176] In the first report, the authors examined the dye:developer ratio of CVL:BPA complexes formed in a three-component mixture containing 1-tetradecanol (TD-OH) as the solvent component.[175] They employed Job's method of continuous variation to determine that the maximum absorbance occurs at a molar ratio of 4BPA:CVL.[175] The observation that the the ring-opened form of CVL is best stabilized by four BPA molecules was supported by MM-2 calculations previously carried out for the same system by Takahashi *et al*.[179]

Luthern and Peredes noted that due to the requirement of four developer molecules to fully develop the colour of the dye, the developer was likely to be involved in separate interactions in addition to the colour-forming dye:developer interaction.[175,176] These other interactions, which might include hydrogen-bonding and π-stacking between multiple developer molecules, need to be overcome to allow the developer to interact with the dye.[175] The authors suggested those interactions could affect the colour-forming reaction through a variety of mechanisms, including (1) the efficiency of the interaction between BPA and CVL, which depends on the electron-acceptor strength of BPA, (2) a

competitive interaction between BPA and the solvent component, and (3) the formation of multiple complexes with varying stoichiometry simultaneous to the formation of the dye:developer complex.[175,176]

2.2.2 Binary Developer:Solvent Interactions

2.2.2.1 Introduction to Binary Developer:Solvent Interactions

Phase separation of the dye and developer has been implicated as an important mechanism in the colouring behaviour of rewritable thermochromic mixtures. In many cases, particularly in binary thermochromic mixtures, phase separation of the developer from the dye is either incomplete or inefficient, regardless of the structure of the coloured metastable phase. This problem necessitates the incorporation of an additional component into the mixture to aid in the decolourization process. In most practical applications, a solvent component is used to promote the phase separation of the dye:developer complex, thereby improving the thermochromic properties of the mixture by enhancing colour contrast between the coloured and decoloured states. As mentioned previously, common solvents include alcohols, alkanes, fatty acids, esters, and surfactants.

2.2.2.2 Alkyl Gallate:Primary Alcohol Binary Mixtures

MacLaren and White carried out a series of differential scanning calorimetry (DSC) studies on binary developer:solvent mixtures towards identifying the nature of the developer:solvent interactions that occur in three-component thermochromic systems.[101,110,143] The developers studied include the previously discussed alkyl gallates

(*e.g.*, PG, OG, and DDG) and the solvents studied include the higher primary alcohols (*e.g.*, TD-OH, HD-OH, and OD-OH).[110]

The phase diagrams for mixtures of dodecyl gallate (DDG, also known as lauryl gallate, LG) and TD-OH, HD-OH, and OD-OH, respectively, indicated the formation of a binary compound of the stoichiometry 2DDG:alcohol.[110,143] Binary compound formation was not, however, observed in the binary phase diagrams of PG:alcohol and OG:alcohol mixtures.[110]

Figure 2.16 shows the binary phase diagram for DDG:TD-OH mixtures (note: LG ≡ DDG).[110] The most prominent feature of the phase diagram is the formation of a congruently melting compound, 2DDG:TD-OH, at $x_{DDG} = 0.67$. This feature also was observed in the phase diagrams of DDG:HD-OH and DDG:OD-OH mixtures.[110,143] The formation of this compound indicates a strong interaction between the developer and the solvent when the alkyl chains attached to both molecules are of a similar length.[101,110,143]

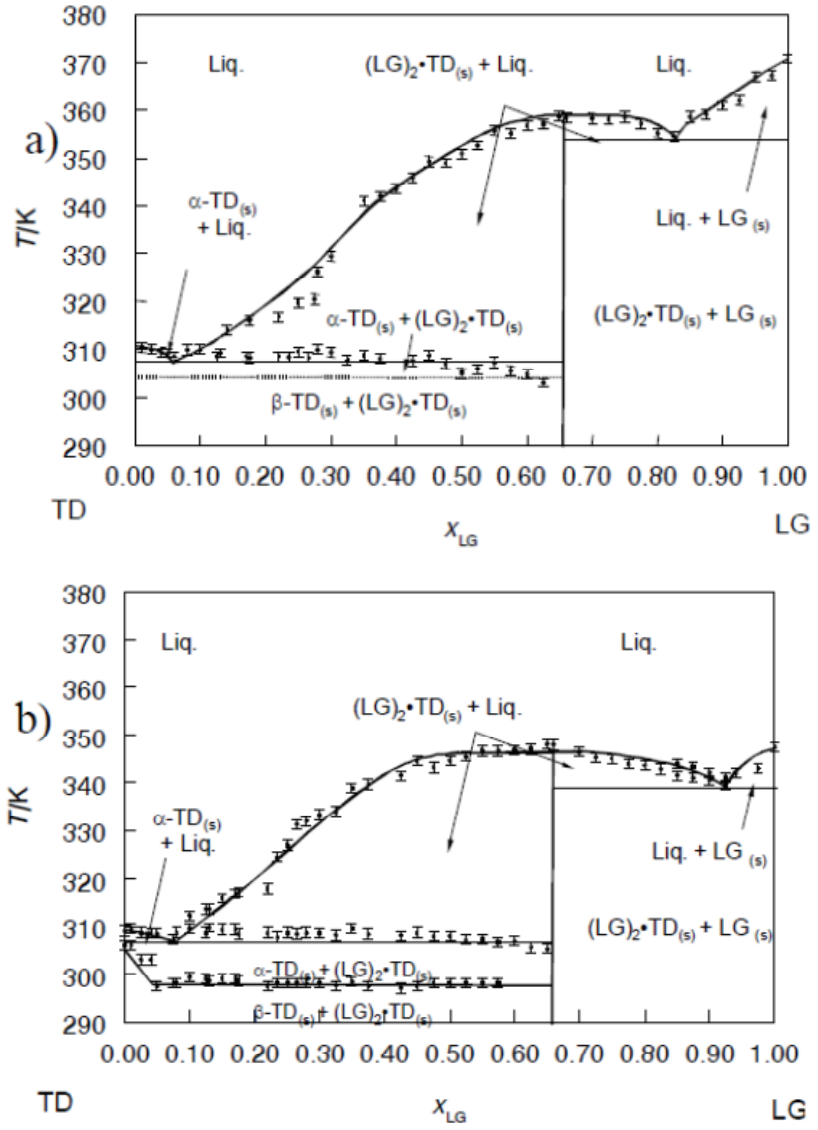

Figure 2.16. Binary phase diagrams determined on (a) heating and on (b) cooling for 1-tetradecanol (TD) and dodecyl gallate (DDG, also known as lauryl gallate, LG) mixtures. Note the formation of a binary compound, $(LG)_2$•TD (= 2DDG:TD-OH), at x_{LG} = 0.67. Reproduced with permission from reference 110 (D. C. MacLaren, *PhD Thesis*, Dalhousie University, 2003).

Binary mixtures of propyl gallate and octyl gallate with TD-OH, HD-OH and OD-OH did not demonstrate the formation of such a compound.[110] Figure 2.17 shows the phase diagram of the PG:HD-OH binary system, which is representative of all of the PG:alcohol and OG:alcohol mixtures. The phase diagram is characterized by a single eutectic observed at $x_{PG} = 0.15 \pm 0.05$, $T = 318 \pm 1$ K.[110] Freezing-point depression caused

the steady decrease in liquidus temperature and little deviation from the theoretical freezing-point was observed for this mixture, indicating weak interactions between the alcohol and gallate.[110,143] The lack of attractive interactions between these two components could have substantial implications on the colouring behaviour in three component systems containing PG and OG as the developer, and long-chain primary alcohols as the solvent.[110]

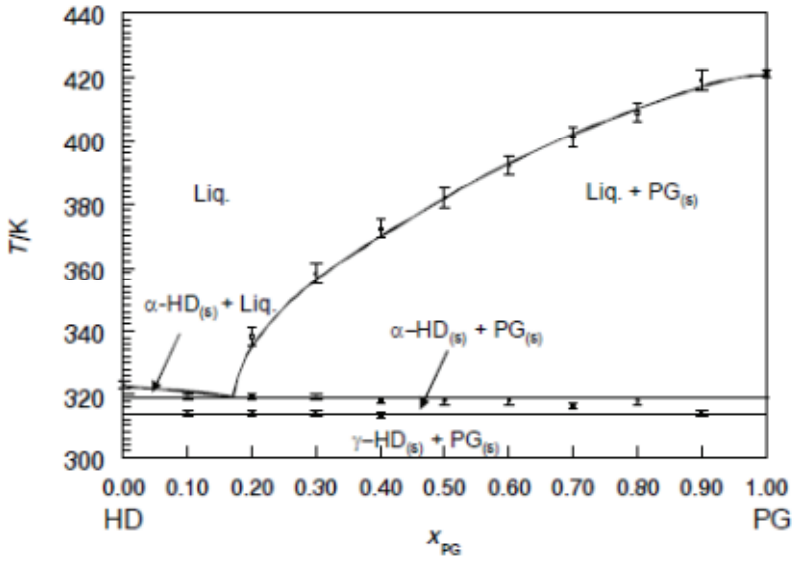

Figure 2.17. The binary phase diagram determined on heating for 1-hexadecanol (HD) and propyl gallate (PG) mixtures. Boundaries are added as a guide to the eye. The system is characterized by a eutectic at x_{LG} = 0.15 ± 0.05, 318 ± 1 K. No compound formation was observed for this binary system. Reproduced with permission from reference 110 (D. C. MacLaren, *PhD Thesis*, Dalhousie University, 2003).

Table 2.8 summarizes the features of the literature results concerning binary phase diagrams obtained for gallate:alcohol mixtures.[110] Compounds were formed in each of the binary mixtures containing DDG as the developer, whereas no compound formation was observed in binary mixtures containing PG and OG.[110,143] Eutectic points were the major feature observed in the PG and OG phase diagrams, with little deviation from ideal freezing point depression occurring in each of the mixtures.[110]

Table 2.8. Compound formation and eutectic data for binary mixtures of PG, OG, and DDG with TD-OH, HD-OH, and OD-OH; all data were obtained from DSC studies during heating runs at 5 K min^{-1}.[110]

Developer	Solvent	Compound Formed	Eutectic Point
DDG	TD-OH	2DDG:TD-OH	$x_{DDG} = 0.05 \pm 0.05$, $T = 307 \pm 1$ K
DDG	HD-OH	2DDG:HD-OH	$x_{DDG} = 0.10 \pm 0.05$, $T = 316 \pm 1$ K
DDG	OD-OH	2DDG:OD-OH	$x_{DDG} = 0.20 \pm 0.05$, $T = 325 \pm 1$ K
OG	TD-OH	None	$x_{OG} = 0.20 \pm 0.05$, $T = 302 \pm 1$ K
OG	HD-OH	None	$x_{OG} = 0.25 \pm 0.05$, $T = 315 \pm 1$ K
OG	OD-OH	None	$x_{OG} = 0.30 \pm 0.05$, $T = 324 \pm 1$ K
PG	TD-OH	None	$x_{PG} = 0.20 \pm 0.05$, $T = 308 \pm 1$ K
PG	HD-OH	None	$x_{PG} = 0.15 \pm 0.05$, $T = 318 \pm 1$ K
PG	OD-OH	None	$x_{PG} = 0.10 \pm 0.05$, $T = 328 \pm 1$ K

Some general conclusions can be drawn from these prior studies concerning the nature of the binary developer:solvent interaction in gallate:alcohol systems. First, propyl gallate and the primary alcohols do not undergo any significant attractive interactions.[110] Octyl gallate was observed to undergo some weak attractive interactions with the primary alcohols, likely van der Waals interactions, but these interactions were not strong enough to cause compound formation in the solid state.[110] Dodecyl gallate, on the other hand, interacts strongly with the alcohol solvents and compound formation was observed in each of the three binary mixtures containing DDG.[110,143] It is clear from these studies that the lengths of the alkyl chains play an important role in defining the degree of interaction between the gallate and the alcohol. It had been found that when the alkyl chains attached to the developer and the solvent, respectively, were well-matched in length, the two components were observed to undergo strong attractive interactions, allowing for the formation of a stable compound in the solid state.[110,143] Conversely, when the alkyl chain

lengths of the developer and solvent were poorly matched, little to no attractive interactions were observed in the solid state, and the solid behaved as a solid solution.[110]

Tang, MacLaren, and White also examined the thermochromic properties of three-component mixtures by using ink-jet printing (IJP) as the sample preparation method by depositing the three components onto a paper substrate, followed by heating and cooling steps.[102] The authors studied similar systems to those examined by MacLaren, using CVL as the dye, DDG as the developer, and primary alkyl alcohols (dodecyl to octadecyl alcohols, C_{12} to C_{18} chains) as the solid solvent. Mixtures containing tetradecanol were shown to be thermochromic over a wider range of compositions, than mixtures containing dodecanol, hexadecanol, and octadecanol solvent.[102]

Of particular importance to the present work, Tang *et al.* demonstrated that employing the shorter chain solvents (dodecanol and tetradecanol) could generate mixtures that were colourless in the solid state.[102] This was attributed to the lack of a rotator phase in dodecanol, and the reduced stability range of the rotator phase in tetradecanol. Increasing the chain length to hexadecanol and octadecanol resulted in mixtures that demonstrated colour in the solid state, an observation attributed to the enhanced stability of the rotator phase.[102] Tang *et al.* concluded that, in the concentration range they examined, conversion of the melt to the rotator enhanced colour formation upon cooling, and conversion to the LO-phase led to colour loss. Since the rotator phase of tetradecanol had a smaller range of stability than in hexadecanol and octadecanol, tetradecanol mixtures decoloured more quickly.[102]

In addition to the observations made about the nature of colour formation in the solid state, Tang *et al*. noted that hexadecanol containing mixtures did not demonstrate colour formation in the melt for the method used in that study (small samples on paper) in that concentration range.[102] This was attributed to the increased chain length of the alcohol yielding increased solvating strength of dissolving the developer, thereby preventing the developer from interacting with the dye in the melt.[102] Work presented in this thesis shows different results for bulk samples. Indeed, thermochromic mixtures comprised of CVL:DDG:HD-OH and CVL:DDG:OD-OH can become strongly coloured in the melt when the developer (*i.e.*, DDG) concentration is sufficiently large. In fact, close examination of the high solvent loading region shows that CVL:DDG:HD-OH systems can display both melt-darkened thermochromism (when the melt is darker than the equilibrium solid) and melt-lightened thermochromism (when the melt is less strongly coloured than the equilibrium solid), depending on the relative concentrations of the developer and solvent.

2.3 A Look Ahead

The primary focus of the present research is to gain a better understanding of the mechanisms of colour formation and colour erasure in reversible, three-component thermochromic mixtures containing CVL as the dye, alkyl gallates as the developer, and long-chain primary alcohols as the solvent. Previous research showed that competition between dye:developer and developer:solvent interactions controlled thermochromic behaviour in these mixtures.[101,102,110]

The current work aims at advancing the understanding of the chemical processes that occur in thermochromic mixtures, in particular the processes leading to colour formation in the solid state and, more importantly, the processes leading to the destruction of the coloured complex both on transition from solid to liquid, and *vice versa*. To this end, the influence of the alkyl chain length of the solvent and of the developer, respectively, on the thermochromic properties of three-component mixtures have been examined in great detail.

In CVL:DDG:alcohol mixtures, the developer and solvent components were previously shown to demonstrate strong attractive interactions due to the similar lengths of the alkyl chains, whereas in propyl gallate (PG) mixtures the mismatch in alkyl chain lengths prevented strong developer:solvent interactions.[101,110] The consequence was that the equilibrium solid state of PG-containing mixtures was coloured due to competing dye:developer interactions, whereas in DDG-containing mixtures the solid state was often colourless due to the preferential formation of developer:solvent interactions.[101,110]

Chapter 4 of the present work focuses on the influence of changing the alkyl chain length of the solvent in DDG mixtures, with a focus on examining the change in solid-state colour density. Chapter 5 examines the influence of changing the alkyl chain length of the developer (alkyl gallate) in three-component mixtures, with the same focus: how does the difference in alkyl chain length influence the thermochromic behaviour of such mixtures?

Chapter 6 further explores the impact of weak developer and solvent interactions in the solid state. Other phenolic developers lack structural similarities with the alkyl alcohol solvents, and therefore represent an archetypal example of developer and solvent

components that interact weakly in the solid state. To study the impact of changing the end-group of the solvent, octadecanethiol was used an alternative solvent component for selected mixtures.

Chapter 7 summarizes how sample composition influences the colouring behaviour of three-component mixtures through ternary thermochromic phase diagrams. Insights gained are useful in the preparation of thermochromic mixtures with optimal properties, by selecting mixtures composition based on the observed behaviour in specific compositional regimes.

Chapter 8 explores the properties of thermally erasable ink-jet printer (IJP) inks. Commercialization of thermochromic inks has long been a goal of industrial research in this area; however, many technical problems have prohibited widespread use. The preparation and optimization of some thermally erasable IJP inks is discussed herein.

Chapter 3 Experimental Methods

3.1 Materials

3.1.1 Research at Dalhousie University

All chemicals were obtained commercially, as detailed below, and used without further purification. The leuco dye, crystal violet lactone, 3,3-*bis*(*p*-*N,N*-dimethylaminophenyl)-6-*N,N*-dimethylaminophthalide, **CVL**, 97% CAS [1552-42-7] was obtained from Sigma-Aldrich.

The following developers were obtained from Sigma-Aldrich: 2,2-*bis*(4-hydroxyphenyl)propane, bisphenol A, **BPA**, 97%, CAS [80-05-7]; 2,4-dihydroxybenzophenone, **DHB**, 99%, CAS [131-56-6]; gallic acid, 3,4,5-trihydroxybenzoic acid, **GA**, 95-97%, CAS [149-91-7]; octyl gallate, 3,4,5-trihydroxybenzoic acid octyl ester, **OG**, 98%, CAS [1034-01-1] and dodecyl gallate, 3,4,5-trihydroxybenzoic acid dodecyl ester, **DDG**, 97%, CAS [1166-52-5]. Propyl gallate, 3,4,5-trihydroxybenzoic acid propyl ester, **PG**, ~90% tech., CAS [121-79-9] was obtained from Fisher-Eastman Scientific. Octadecyl gallate, 3,4,5-trihydroxybenzoic acid octadecyl ester, **ODG**, 97%, CAS [10361-12-3] was obtained from TCI America. The decyl (**DG**), tetradecyl (**TDG**) and hexadecyl (**HDG**) esters of gallic acid were synthesized in-house; the procedure is described in section 3.2.3.

The following solid solvents were obtained from Sigma-Aldrich: 1-tetradecanol, **TD-OH**, 96%, CAS [112-72-1]; 1-hexadecanol, **HD-OH**, 97%, CAS [36653-82-4]; 1-octadecanol, **OD-OH**, 99%, CAS [112-92-5]; 1-dodecanethiol, **DD-SH**, 98%, CAS [112-55-0]; 1-octadecanetiol, **OD-SH**, 98%, CAS [2885-00-9]; 1-dodecanoic acid, **DD-COOH**, 98%, CAS [143-07-7]; 1-tetradecanoic acid, **TD-COOH**, 95%, CAS [544-63-8];

1-dodecylamine, **DD-NH_2**, 98%, CAS [124-22-1]; 1-tridecylamine, **TrD-NH_2**, 98%, CAS [2869-34-3]; 1-hexadecylamine, **HD-NH_2**, 75% tech., CAS [143-27-1]; 1-octadecylamine, **OD-NH_2**, 90% tech., CAS [124-30-1]. The solid solvent 1-hexadecanoic acid, **HD-COOH**, 95%, CAS [57-10-3] was obtained from MCB chemicals and 1-octadecanoic acid, **OD-COOH**, 90% tech., CAS [57-11-4] was obtained from Shawinigan Chemicals.

The following reagents were obtained from Sigma-Aldrich: potassium thiocyanate, 98%, CAS [10387-40-3]; 1,12-dibromodecane, 98%, CAS [17,486-6]; *para*-toluenesulfonic acid monohydrate, ***p*-TsOH**, 98.5%, CAS [6192-52-5]; sodium chloride, 99%, CAS [7647-14-5]; sodium carbonate, 99% [497-19-8]; magnesium sulfate, ≥97%, [7487-88-9]. Silica gel for column chromatography, 60 μm mesh, CAS [112926-00-8] was obtained from Fluka. TLC plates containing a fluorescent dye impregnated into 60 μm mesh silica gel on aluminium plates were obtained from Silicycle.

Solvents including acetone, acetonitrile, 1-butanol, chloroform, dichloromethane, dimethyl formamide, ethanol, ethyl acetate, hexanes, methanol, and toluene were obtained from Chemical Stores and used without further purification. Compressed gases, helium and nitrogen for DSC experiments, were obtained from Praxair.

3.1.2 Research Internship at Toshiba Co. Research and Development Centre (RDC)

A research internship was carried out at Toshiba Co., Research and Development Centre (RDC), in Kawasaki, Japan, in 2010. During this time, the composition and properties of thermally erasable ink-jet printer (IJP) inks were studied. All materials used

at Toshiba Co. RDC were obtained commercially and used without purification. Many leuco dyes were examined in this work; many of these dyes were proprietary chemicals and as such few structures/chemical names are presented herein. The structures of the most important chemicals used in this work will be given when those chemicals are referenced in the body of the text. Most of the dyes studied were obtained from Yamada Chem. Co., Nippon Soda Co. Ltd., Hogoyoda Chem. Co. and Yamamoto Chem. Inc. Most of the phenolic developers were obtained from Yamada Chem. Co. Solvents were obtained through in-house chemical stores.

The following solvent modifiers were obtained from Sigma-Aldrich: propylene glycol monomethyl ether, **PGMME**, 99%, CAS [9005-25-8]; poly(vinyl alcohol), MW = 900-1100, **PVA**, 98%, CAS [9002-89-5]; glycerol, 1,2,3-propanetriol, 99%, CAS [56-81-5]. The cationic surfactant, Sanizole, was obtained from Kao Corporation and used as 2.5% by mass solution in distilled water. Paper samples for printing were obtained from a local Japanese office supply store and varied in quality from low-grade "economy" paper to high-grade, glossy photo-printing paper.

3.2 Sample Preparation

3.2.1 Three-Component Mixture Preparation

3.2.1.1 Gram-Scale (Bulk) Mixture Preparation

Gram-scale (bulk) mixtures were prepared by weighing appropriate amounts of the three components (dye, developer, and solvent) into glass sample vials (large vial = 16 mL, small vial = 4 mL) followed by heating to fusion. Allowing the mixtures to slowly cool to room temperature generally produced homogeneous mixtures; an example

of this is shown in Figure 3.1. In the case of CVL:DDG:OD-SH mixtures, dodecyl gallate precipitation from molten OD-SH and inhomogeneous crystallization of the OD-SH solvent caused significant phase separation. Phase separation after rapid cooling of CVL:DDG:OD-SH mixtures generally occurred after sitting for more than 24 hours at room temperature, whereas phase separation in CVL:DHB:HD-OH mixtures began only after two weeks at room temperature.

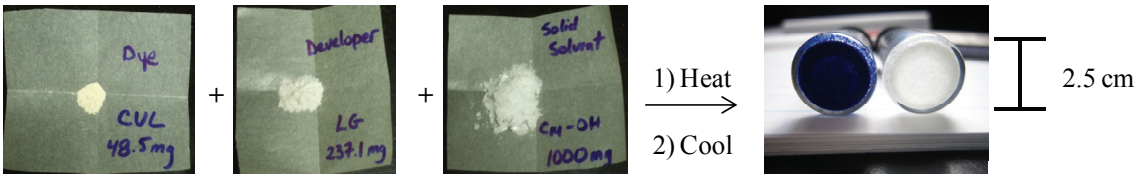

Figure 3.1. The method of preparation of bulk samples. Far right: both samples contain CVL as the dye and DDG as the developer. The blue sample contains HD-OH as the solvent while the white sample contains TD-OH as the solvent, demonstrating how the colour of the solid state depends on choice of solvent.

Approximately 500 samples in total were prepared and analyzed during the present work. The results reported herein were selected to best demonstrate the thermochromic behaviour of specific ternary systems. In some instances no colour was formed in either the solid state or the melt, or there was no difference in colour density between the solid and melt. Results determined but not reported in detail in Chapters 4 to 6 in colour density versus temperature plots are incorporated into the ternary thermochromic phase diagrams presented in Chapter 7.

It is useful at this point to describe the labelling system employed in this work to denote the composition of three-component thermochromic mixtures; the CVL:DDG:TD-OH system will be used as an example. The molar ratios for all samples discussed herein are normalized to the number of moles of CVL present in a sample. For this reason the molar ratios for any sample are reported as $[1:y:z]$, where the square brackets indicate

that sample composition is being reported. The *y* value corresponds to the number of moles of developer per mole of CVL. The *z* value is the number of moles of solvent per mole of CVL. For example, a sample prepared at a mixing ratio of [1:6:40] has a developer:dye molar ratio of 6:1, a solvent:dye molar ratio of 40:1 and a solvent:developer molar ratio of 40:6.

3.2.1.2 Microgram-Scale Sample Preparation

Microgram-scale samples were made by first preparing stock solutions of CVL in acetone, DDG in acetone or dichloromethane, and OD-SH in dichloromethane. The concentrations of these solutions were on the order of 1.0×10^{-5} mol L^{-1} for CVL and DDG, and on the order of 5.0×10^{-3} mol L^{-1} for OD-SH. Microlitre volumes of the three stock solutions were mixed in Teflon sample vial caps: an example is shown in Figure 3.2. The stock solutions were dispensed *via* micropipette. The mixtures were then allowed to dry overnight in the fumehood until the volatile solvent evaporated. Samples were produced in a combinatorial fashion in this way. Compositions examined using this method ranged from CVL:DDG ratios of 1:0.25 up to 1:10 and CVL:OD-SH ratios of 1:1 up to 1:1000.

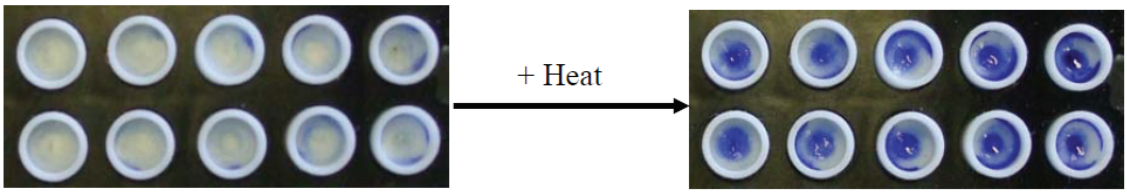

Figure 3.2. Microgram samples of CVL:DDG:OD-SH prepared in Teflon vial caps. Heating of the samples produced inhomogeneous blue colouration. The diameter of the vial caps is 8 mm.

3.2.1.3 Milligram-Scale Sample Preparation

Milligram-scale samples were also prepared in small sample vials (4 mL) in a similar fashion to the microgram samples. Larger volumes of the stock solutions were introduced into the sample vials, and the volatile solvent was allowed to evaporate overnight under a flow of compressed air. Milligram-scale samples were prepared due to the difficulties encountered with samples prepared in the Teflon vial caps, including difficulty with controlled heating and cooling and the smell produced by the OD-SH solvent. The microgram and milligram-scale samples suffered from inhomogeneous mixing in both the liquid and solid states and as a result demonstrated inhomogeneous colouration. Due to this complication, all of the results presented in this work were obtained for gram-scale mixtures.

3.2.2 Binary Sample Preparation

Binary samples comprising developer:solvent mixtures were also prepared for differential scanning calorimetry (DSC) experiments. Binary samples were prepared by mixing powders of the individual components in the appropriate amounts and heating to melt the mixture. For DSC experiments, the molten binary mixtures were transferred *via* Pasteur pipette into pre-weighed aluminium DSC pans and quickly cooled to obtain nearly homogeneous solid phases.

3.2.3 Synthesis of Intermediate Chain Length Alkyl Gallates

The gallic acid esters of decanol (DG), tetradecanol (TDG) and hexadecanol (HDG) were prepared by a Fischer esterification reaction using gallic acid (GA) as the

gallate source.[180] An example of this reaction, using tetradecanol and gallic acid as starting materials, is shown in Figure 3.3. In a typical reaction, to a round-bottomed flask was added 1-tetradecanol (1.30 g, 6.05 mmol), gallic acid monohydrate (1.00 g, 5.90 mmol) and catalytic *p*-toluenesulfonic acid (0.11 g, 0.59 mmol), along with a stirring bar. The mixture was heated to ~150 °C for 2 hours and kept under constant vacuum to aid in the removal of water, which is a reaction by-product. The reaction was monitored via thin layer chromatography (TLC) and cooled after the reaction was complete. The cooled reaction mixture was poured into an aqueous sodium carbonate solution and extracted with ethyl acetate. The ethyl acetate extract was then washed with a saturated sodium chloride solution and dried over magnesium sulfate. The ethyl acetate was removed *via* rotary evaporation and the crude reaction product was collected as an off-white solid. Purification by column chromatography (chloroform/methanol, 100/1) on silica gel (60 μm mesh, Fluka) yielded tetradecyl gallate (TDG, 0.71 g, 33% yield, M.P. = 95 to 98 °C, ESI-MS, *m/z* 389.2 (M+), ^{1}H NMR (300 MHz, *d*-DMSO) δ 6.93 (2H, s), 1.98 (2H, t), 1.2 - 1.1 (27H, m), 0.85 (3H, t)).

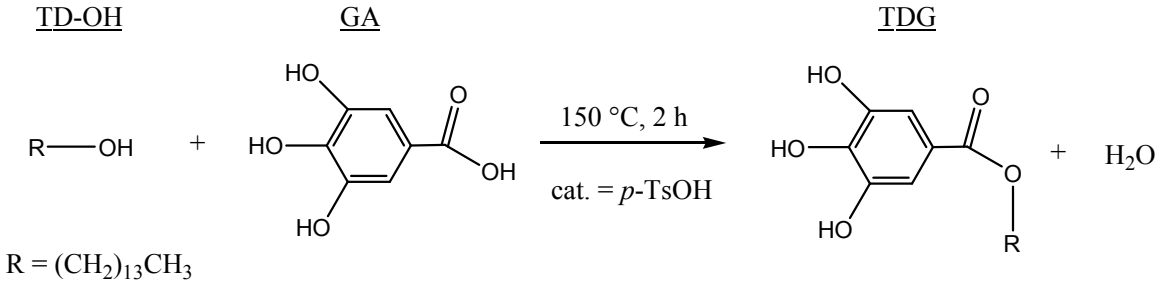

Figure 3.3. The *trans*-esterification reaction of tetradecanol (TD-OH) with gallic acid (GA) produces tetradecyl gallate (TDG).

3.2.4 Ink-Jet Printer (IJP) Ink Preparation – Toshiba Co. RDC

During an internship at Toshiba Co. RDC in 2011, the chemical and physical properties of thermochromic (*i.e.,* thermally erasable) ink-jet printer (**IJP**) inks were studied. All IJP inks studied in this work were prepared *via* the following method. Leuco dye (~50-75 mg) and phenolic colour developer (~500 mg) were added to a sample vial containing ~10 g of solvent. The solvent was composed mainly of ethanol (50-70%), with varying amounts of distilled water (15-30%), *iso*-propanol (10-15%) and/or PGMME (10%) to modify the viscosity, evaporation rate, and toxicity of the solvent. Additional additives to the ink included an aqueous surfactant solution (Sanizole), which was added to prevent clogging of the printer heads (the nozzles where the ink is sprayed out in "jets") and an aqueous PVA solution, which was added to modify the viscosity of the ink.

The resultant mixture was vigorously stirred for 10-15 minutes to ensure complete dissolution of the components and afterwards was gravity filtered through a 4 μm filter paper to remove any insoluble components remaining in the mixture. The internal diameter of the printer heads was on the order of 10 μm meaning that filtration of particles larger than 4 μm would reduce clogging of the printer heads. The freshly filtered ink was then promptly injected into empty printer cartridges, sealed, and stored away from light until printing.

3.3 Experimental Techniques

3.3.1 Colour Determination

Previous research in this laboratory used UV-Vis reflectance spectroscopy to analyze the colouring behaviour in three-component thermochromic mixtures.[101,102,110,181]

That approach employed an Ocean Optics reflectance spectrometer to measure the UV-Vis spectrum of a single sample as a function of temperature or as a function of time after quenching with liquid nitrogen. The setup presented numerous drawbacks including slow analysis speed due to single sample analysis, poor temperature control of the samples during heating and cooling, exposure of the mixtures to the atmosphere presenting problems with smell (*e.g.*, when using OD-SH as the solvent component), requirements for shielding of stray light from ambient lighting, and out-dated program software. As a result, new approaches to colour analysis were examined to increase analysis speed, to ensure samples remained sealed during heat/cool cycling, and to produce a more reproducible experimental setup.

3.3.1.1 Experimental Setup of Heat/Cool Cycling Experiments

The following experimental setup of heat/cool cycling experiments for colour determination was used for both methods of colour determination employed in this work (*vide infra*, sections 3.3.1.2 and 3.3.1.3). Bulk samples were prepared as described above (*vide supra*, section 3.2.1.1) in both large (16 mL) and small (4 mL) sample vials. To heat and cool these samples, a water bath was used. The temperature of the water bath was controlled by a hotplate (on heating) and the addition of ice (on cooling). Samples were held in the water bath by an aluminium plate into which 10 holes (large vials) or 32 holes (small vials) had been punched. This experimental setup is shown in Figure 3.4.

Figure 3.4. The experimental setup used during heat/cool cycling experiments. The heating rate was controlled by the hot plate and the cooling rate was controlled by the addition of ice to the water bath. The temperature was recorded by a mercury thermometer held in the water bath and the samples were held in the bath by a sheet of aluminium.

The temperature was recorded by a mercury thermometer held in the water bath, and the heating and cooling rates were ~1 to 2 K min^{-1} to ensure that thermal equilibrium between the thermally insulating samples and the surrounding water had been reached. The samples were removed from the water bath at regular intervals (usually every 5 °C), and the colour was analyzed in one of two ways, as described in the following sections. The temperature decrease upon removal from the water bath was measured using an IR thermometer and was observed to be less than 2 K min^{-1}. This results indicates that temperature loss upon removal from the water bath was a negligible source of error as the measurement time (*i.e.*, the time samples spent out of the water bath) was approximately 15 to 30 seconds.

This experimental approach to heat/cool cycling has numerous benefits over previous methods including dramatically increased analysis rates, consistent heating profiles between samples, isolation of foul-smelling samples from the atmosphere, and

more homogeneous mixing in both the solid and molten states due to the large sample masses.

3.3.1.2 Observational Spectroscopy

Observational spectroscopy experiments were used for preliminary studies on three-component systems; the observational spectroscopy results presented in Chapter 4 are qualitative in nature and are considered to be a launching point for the more quantitative results obtained from colour photo analysis experiments, which is described in section 3.3.1.3. Nevertheless, the observational spectroscopy results presented herein provide important information regarding the general trends of colouring behaviour in three-component systems with matched and mismatched alkyl chain lengths.

The colour density values reported for observational spectroscopy experiments were obtained by visually comparing the colour of each sample at a given temperature to the colour scale shown in Figure 3.5. The colour density of each block was determined by measuring the colour of each block in the *Lab** colour space and converting the L* coordinate to colour density, following the procedure described later in this chapter (section 3.3.1.4). Experimental data are presented as colour density versus temperature plots, where the numerical value of the ordinate corresponds to the colour density listed on the colour scale shown in Figure 3.5, and the abscissa corresponds to the temperature at which a specific colour value was recorded.

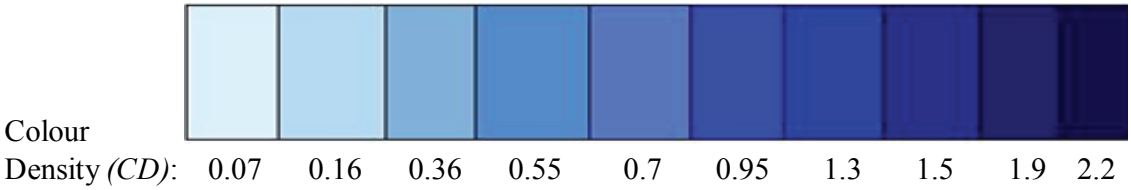

Figure 3.5. The colour scale used throughout this work to define the colour intensity of bulk three-component thermochromic mixtures. The values on the figure indicate the colour density (*CD*) of each colour as measured in the *Lab colour space.**

3.3.1.3 Colour Photo Analysis

To achieve a more quantitative analysis of colour, samples were imaged using a digital camera (Canon Powershot A3200 IS, 14.1 MPx), and the images were transferred to a PC. The images were then analyzed using the image analysis software programs GIMP 2.0 and ImageJ.[182,183] GIMP 2.0 was used to isolate images for each sample and to prepare publication-quality images of each sample at various temperatures. ImageJ was used to measure the colour of each sample at a variety of spots on the sample. The output colour values from ImageJ were in the RGB colour space; these values were then converted to the CIE *XYZ* and CIE *Lab** colour spaces before being converted into a colour density (*CD*) value.[184,185] The colour contrast, ΔCD, was calculated by taking the difference in colour density between two states (*e.g.*, the solid state and melt) of a given sample. The colour density values were plotted as a function of temperature (the heating and cooling runs are plotted on the same graphs) to demonstrate the colour behaviour of each sample. An example of a colour density versus temperature plot is shown in Figure 3.6.

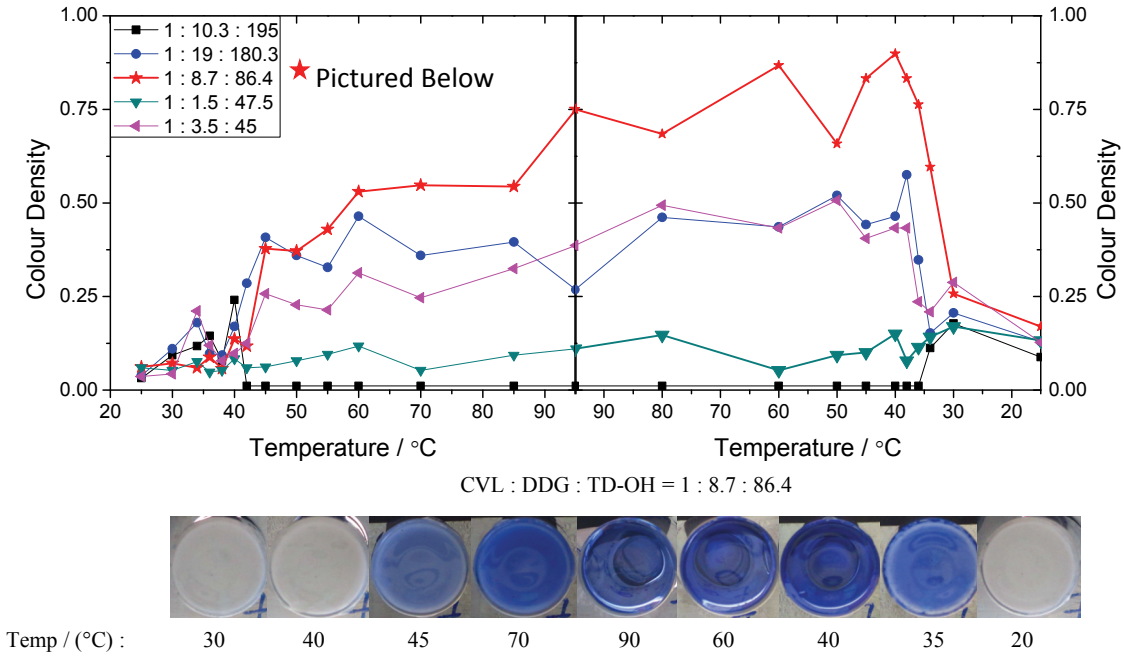

Figure 3.6. Top: a colour density versus temperature plot showing the colour change behaviour in the CVL:DDG:TD-OH ternary system at various concentrations. Lines are added as a guide to the eye. Bottom: colour photographs of the sample at a composition of [1:8.7:86.4] (mole ratios are normalized to CVL content) showing the change in observed colour. At room temperature, the colour density is very low and the sample is white/colourless. As the sample melts, the colour changes to blue and there is an increase in the colour density.

Samples studied using colour photo analysis were subjected to the heat treatment described in section 3.3.1.1. At a desired temperature, the aluminium plate was removed from the water bath, dried with paper towel and mounted on a sample holder roughly 30 cm above the digital camera. The samples were then immediately imaged (usually 4 samples per image) with a white reference material (Spectrolon disc) present in each photo to normalize the brightness of the image. This normalization approach removed some of the issues with stray light from ambient lighting sources, small changes in the height of the sample holder, and any variations in the settings of the camera. The degree of variation of the white background from "pure white" was then used to normalize the

colour of the same samples recorded in different images (*i.e.*, at different temperatures). This approach to image analysis is shown in Figure 3.7.

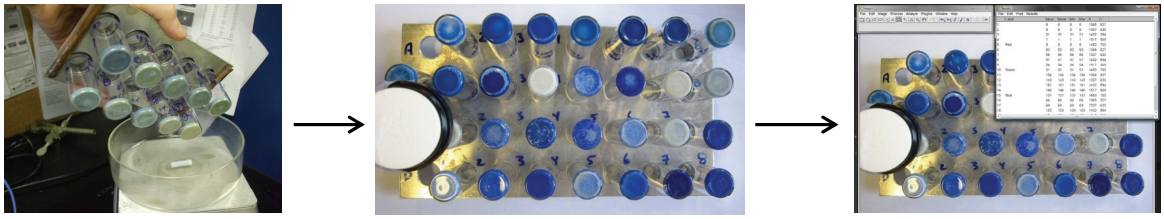

Figure 3.7. Samples were removed from the water bath, imaged with a digital camera, and analyzed with the image analysis software ImageJ.

3.3.1.4 Colour Space Conversions

The colour values from ImageJ were output in the *RGB* colour space, which is generally used for describing the colour of light emitting objects (*e.g.* TV screens, computer monitors, etc.). The *RGB* values were then converted to the CIE *XYZ* colour space, followed by a conversion to the CIE *Lab** colour space which provides a better representation of the observed colour of objects (*e.g.*, printed images, paints, etc.).[186] The CIE *Lab** colour space is shown schematically in Figure 3.8. There are three axes in this colour space; the a^* axis spans from red ($a^* > 0$) to green ($a^* < 0$), the b^* axis spans from yellow ($b^* > 0$) to blue ($b^* < 0$) and the L^* axis relates the lightness of the sample ($L^* = 100$ indicates a pure white sample, $L^* = 0$ indicates a pure black sample).

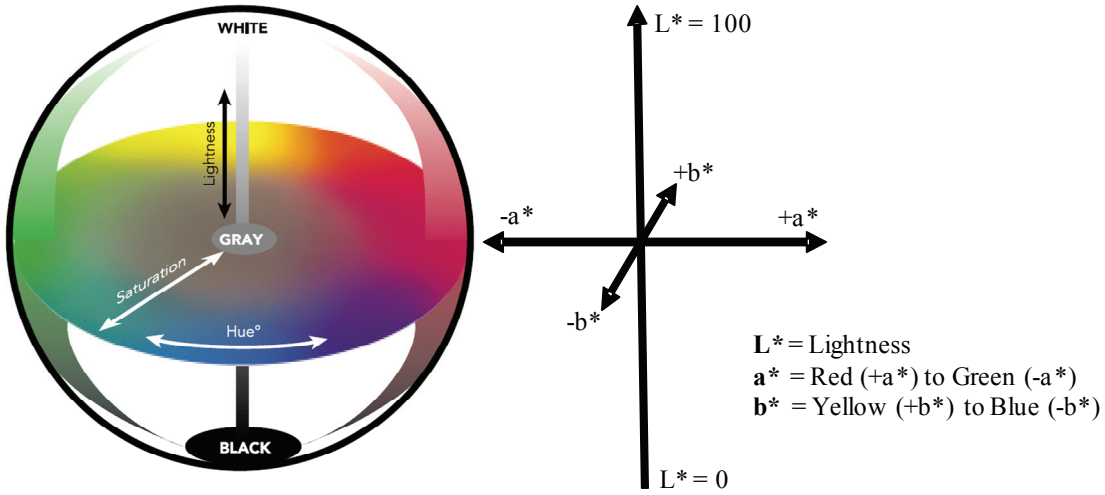

Figure 3.8. The CIE *Lab colour space. The *a** axis spans red to green, the *b** axis spans yellow to blue and the *L** axis, referred to as the lightness, spans *L** = 0 which is black to *L** = 100 which is white.[185,187]**

Since the output colour space of the ImageJ software is the *RGB* colour space, the colour coordinate values must be converted to the CIE *XYZ* colour space prior to conversion to colour density values.[183] The conversion was done in a multi-step procedure that is described below.

The first step in the transformation is the calculation of the variance, which is shortened to *var*, for each of the R, G, and B (red, green, and blue, respectively) coordinates. The *var* values for *R*, *G,* and *B* are:[183-187]

$$\text{var\_}R = 100 * ((R/255 + 0.55)/1.055)^{2.4} \quad (3.1)$$

$$\text{var\_G} = 100 * ((G/255 + 0.55)/1.055)^{2.4} \quad (3.2)$$

$$\text{var\_}B = 100 * ((B/255 + 0.55)/1.055)^{2.4} \quad (3.3)$$

The final CIE *XYZ* co-ordinates were then calculated from the variances values:[183-187]

$$X = \text{var\_}R*0.4124 + \text{var\_}G*0.3576 + \text{var\_}B*0.1805 \quad (3.4)$$

$$Y = \text{var\_}R*0.2126 + \text{var\_}G*0.7152 + \text{var\_}B*0.0722 \quad (3.5)$$

$$Z = \text{var\_}R*0.0193 + \text{var\_}G*0.1192 + \text{var\_}B*0.9505 \quad (3.6)$$

where *X*, *Y,* and *Z* represent coordinates in the CIE *XYZ* colour space. Conversion to the CIE *Lab** colour system followed a similar approach:[183-187]

$$\text{var\_}X = (X / 95.047)^{(1/3)} \quad (3.7)$$

$$\text{var\_}Y = (Y / 100.00)^{(1/3)} \quad (3.8)$$

$$\text{var\_}Z = (Z / 108.883)^{(1/3)} \quad (3.9)$$

where *X*, *Y,* and *Z* are the coordinates in the CIE *XYZ* colour space and *var_X* is the variance of the *X* coordinate, and so on. The conversion to CIE *Lab** co-ordinates followed: [183-187]

$$L* = (116 * \text{var\_}Y) - 16 \quad (3.10)$$

$$a* = 500 * (\text{var\_}X - \text{var\_}Y) \quad (3.11)$$

$$b* = 200 * (\text{var\_}Y - \text{var\_}Z) \quad (3.12)$$

where *L** is the lightness value, *a** runs the gamut from red to green, and *b** runs the gamut from yellow to blue.

Conversion to colour density, *CD*, can be done from either CIE *XYZ* or CIE *Lab** colour space, although it is simpler to convert from CIE *XYZ*.[188] The colour density value will be quite different for different colours (a dark yellow might have a higher *L** value than a dark blue) so it is important to be aware of the colour coordinates to ensure that the colour densities are in fact comparable. In this research project (both at Dalhousie and at Toshiba), the reported results are for leuco dyes that range from white to very dark blue. As such the CIE *Lab** co-ordinates are either very negative in the *b** value (very blue) or very near the origin. As a result, colour densities provide a suitable method for comparing the intensity of colour between many samples as the coloured form will usually be blue

and the decoloured form will always be white/colourless. With this in mind, the conversion from CIE *XYZ* to colour density was carried out as follows:[183-188]

$$CD = -\log (Y / 100) \tag{3.13}$$

where *CD* is the colour density and *Y* is the *Y* coordinate of the CIE *XYZ* colour space. The colour density values for the equilibrium solid state, CD_{Equil}, and the colour density of the melt, CD_{Melt}, are given in the body of the text for three-component mixtures, where appropriate. The colour contrast between the equilibrium solid state and the melt obtained on heating, ΔCD, was determined by taking the difference of colour density between the two states. Therefore, the colour contrast was determined by

$$\Delta CD = | CD_{Equil} - CD_{Melt} |. \tag{3.14}$$

A formal analysis of experimental error arising from this method of analysis was not carried out during the present work. Nevertheless, an estimate of the systematic errors associated with this experimental approach is presented. The variation in *CD* value for individual samples was observed to be 0.1 to 0.2. The maximum *CD* values obtained by colour photo analysis were usually 1.0 to 1.5. Therefore, the error associated with each individual measurement was on the order of 10 to 20 %.

3.3.2 Differential Scanning Calorimetry (DSC)

Differential scanning calorimetry was used to study the binary phase behaviour of developer-solvent mixtures, and the results of those studies were used to generate binary phase diagrams. DSC was first introduced in the 1960s by Perkin-Elmer™ and is currently the most widely used method of thermal analysis.[189,190,191] The technique measures the differential calorimetric properties of a sample material and compares it

with the thermal properties of a reference material. DSC can be used to determine useful thermal properties of materials including enthalpy and entropy changes and the temperature of thermal events with a reasonable degree of accuracy and precision. The precision of onset temperatures can be within 0.2% when slow heating rates are used, and the uncertainty in the enthalpy of transition can vary from a few percent (for thermal events of large enthalpy) to 10 % (for thermal events of low enthalpy).[192] DSC is a fast, reliable, commercially available thermal analysis technique that can be applied to small samples (~1 to 100 mg). The small sample size facilitates rapid scanning rates, typically of 5 to 10 K min^{-1} but as high as 500 K min^{-1}, and wide temperature ranges are available extending from 100 K to 1500 K.[189]

3.3.2.1 DSC Apparatus

The basic apparatus for power-compensated DSC is shown schematically in Figure 3.9. It consists of two individual calorimeter chambers (sample and reference, *S* and *R*) made from Pt/Rh and Pt/Ir alloys.[191] An aluminium, gold, stainless steel, or platinum pan containing the sample of interest is placed in the sample chamber. The reference chamber is generally occupied by an empty pan of the same type as the sample pan. It is important that the reference pan does not display any anomalous thermal effects in the temperature range to be used in the experiment.[189] Each of the chambers has its own resistance heater and platinum thermometer, which are linked to one another through a feedback circuit that is designed to minimize the temperature differential, ΔT_{SR}, between the sample and reference pans as both are heated through a set temperature

program. S and R are both in contact with a heat sink that is cooled with liquid nitrogen.[189-191]

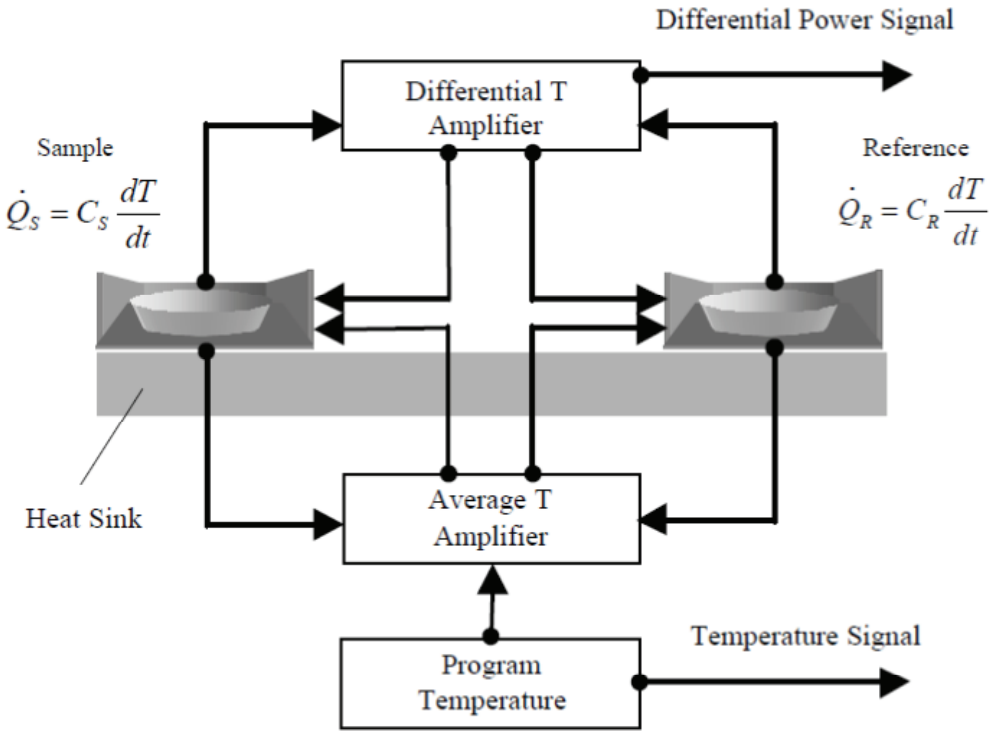

Figure 3.9. Schematic diagram of a power-compensated DSC apparatus. The separated sample (S) and reference (R) chambers have their own heaters and thermometers, which are linked through a feedback circuit that minimizes the temperature differential between S and R (ΔT_{SR}). If $\Delta T_{SR} = 0$, the average temperature amplifier controls the heating profile. If $\Delta T_{SR} \neq 0$, at which point a thermal event is occurring, both the differential temperature amplifier and the average temperature amplifier will heat S and R to minimize ΔT_{SR}. Adapted from references 189 and 191.

The temperature program is set by the average temperature amplifier which heats S and R. The power required to heat S and R can be expressed as:

$$\dot{Q}_S = C_S \frac{dT}{dt} \tag{3.15}$$

$$\dot{Q}_R = C_R \frac{dT}{dt}, \tag{3.16}$$

where $\dot{Q}_S$ and $\dot{Q}_R$ are the sample and reference powers and C_S and C_R are the sample and reference heat capacities, respectively. If the sample and reference heat capacities are equal, then $\Delta T_{SR} = 0$ and the average temperature amplifier heats the chambers exclusively while the differential temperature amplifier feedback loop remains open.[189]

In the case of a thermal event in the sample material (*e.g.*, a first-order phase transition), C_S changes significantly.[189-191] As C_S increases, T_S lags behind T_R and, since only the average temperature is being controlled, the reference pan heats faster than the sample. When ΔT_{SR} reaches a set threshold, the differential temperature amplifier loop closes and adjusts the power supplied to the reference to minimize $|\Delta T_{SR}|$. In the case of an endothermic event ($C_S > C_R$), the differential temperature amplifier supplies greater power to the sample than the average temperature amplifier does. In contrast, an exothermic event ($C_S < C_R$) will have excess power applied to the reference. This differential power being supplied by the differential temperature amplifier is the power signal seen in the output data.[189-191] This observed power signal can be expressed as:[189]

$$Signal = \dot{Q}_S - \dot{Q}_R = C_S \frac{dT}{dt} - C_R \frac{dT}{dt} = (C_S - C_R)\frac{dT}{dt}. \tag{3.17}$$

It is impossible to perfectly match C_S and C_R throughout the temperature range of a DSC experiment. Most DSC thermograms show a linear change in differential power, called a baseline, with a slope proportional to (C_S - C_R). In the case of a thermal event, the peak appears on top of the baseline.[189] An approximated baseline needs to be subtracted from the peak during data analysis. Thermograms are plotted as differential power versus time or temperature (versus temperature in this work). The enthalpy of a thermal event

can be determined by integrating the area under a power/time peak, after calibration.[189-191]

3.3.2.2 DSC Calibration

The previous section describes an idealized system and does not consider the temperature lag between the actual sample temperature, T_S, and the temperature of the thermometer recording it, T_{ST}.[189] This temperature lag can be minimized experimentally by ensuring good thermal contact between the sample and pan bottom and between the pan bottom and the surface of the sample chamber. The sample usually is annealed in the sample pan prior to any DSC experiment to ensure good contact with the pan. In addition to contact effects, the scan rate of the experiment plays an important role in determining the temperature lag:[189]

$$\dot{Q}_S = \frac{1}{R_S}(T - T_{ST}), \tag{3.18}$$

where $\dot{Q}_S$ is the heat flow from the sample and R_S is the resistance of the thermometer. Combining Eq. 3.18 with Eq. 3.15 gives:

$$T_S - T_{ST} = R_S C_S \frac{dT}{dt}. \tag{3.19}$$

Since (T_S - T_{ST}) is directly proportional to the scan rate (dT/dt), it is important to calibrate the instrument using the scan rate to be used in the experiment.[189-191]

Calibration is performed by measuring the transition temperatures and enthalpy changes of highly pure reference materials.[189-191] Although organics (*e.g.*, benzoic acid) can be used as calibration materials, small amounts of impurity (as low as 0.1%) can

significantly lower the melting temperature. For this reason, metals such as In and Zn are usually preferred because they can be obtained in >99.9% purity and are more resistant to chemical decomposition. In a calibration experiment, T_{onset}, and enthalpy change due to a transition, $\Delta_{trs}H$, are measured. T_{onset} is defined as the intercept of the baseline with the inflection point of the peak.[189-191] T_{onset} is a more reliable measurement of transition temperature than the peak temperature because it is less sensitive to temperature scan rate.[189]

A TA Instruments™ Q2000 series DSC was used for all experiments reported here. The instrument was calibrated using the melting point and enthalpy of an indium standard (Aldrich, 99.99%) under an atmosphere of dry nitrogen (25 mL min^{-1}). For the cooling portions of the experiments, a liquid nitrogen Dewar was connected to the system and cooling rates were controlled by the temperature controller. Scan rates of 2 to 20 K min^{-1} were used for phase diagram determination over a temperature range of 298 to 438 K.

3.3.3 Technologies for Toshiba Co. RDC Internship

3.3.3.1 Ink-Jet Printer

Ink-jet printing was carried out using a Canon model 8600 printer which was modified to remove "auto-shutoff" safety features, to accept printer cartridges from a third party supplier, and to print in a "black only" mode allowing the colour cartridge slots to remain empty. The printer, before and after modification, is shown in Figure 3.10. Unless otherwise indicated, all inks studied contained blue leuco dyes and printing was done on "utility grade" office paper. Two printing modes, "Normal" and "Bold", were

used throughout this work. Normal printing mode is similar to what would be used in an office setting whereas bold printing mode deposits a large amount of ink on the page making images much darker, as one might find in high-quality picture printing.

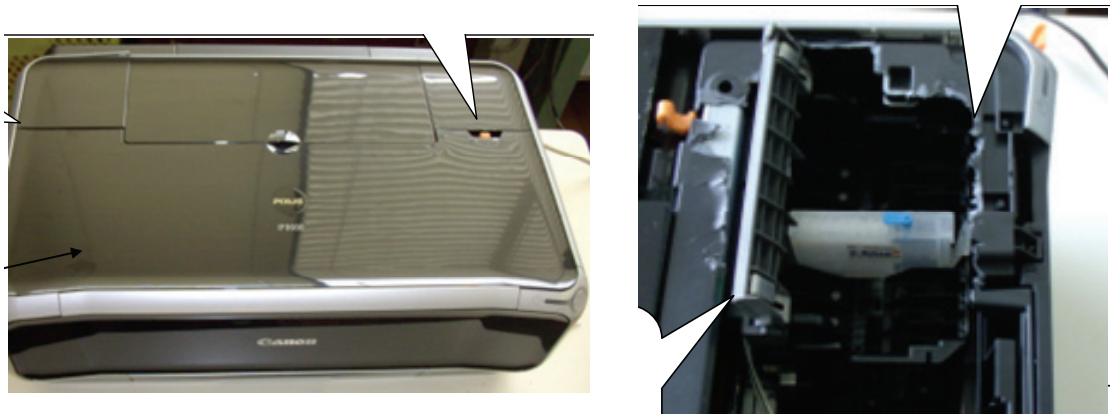

Figure 3.10. Left: the modified Canon 8600 printer that was used to print thermally erasable IJP inks. Right: the cartridge holder showing substantial modification to prevent auto shut-off features from functioning.

3.3.3.2 Colour Erasers

To erase the colour images formed on printing, two erasing devices were employed. The first eraser was an electric clothing iron. This iron did not have specific thermal controls and in general was not effective at completely removing images. Images that were erased with the clothing iron are referred to as “iron-erased” images in this work.

The more effective type of erasing was carried out with a programmable oven, which will be referred to as the “oven” in this work. The oven was essentially a slow heating and slow cooling furnace designed to evenly heat roughly 500 sheets (one ream) of paper. The heating profile was designed to prevent browning of sheets located near the edge of the ream, which could be exposed to much higher temperatures than those at the

interior of the ream if a fast heating rate was used. The heating profile began by slowly heating to ~130 °C over the course of one hour, maintaining this temperature for 2 to 3 hours, followed by slow cooling to room temperature over the course of one hour. "Oven-erased" samples typically were more thoroughly erased and maintained the loss of colour for much longer periods than the "iron-erased" samples.

3.3.3.3 Colour Analyzer

To measure the colour of printed and erased samples, a Konica Minolta "Chroma Meter" *CR-300* was used.[185] The colour analyzer is pictured in Figure 3.11. The colour analyzer irradiates a printed image with white light in a single intense pulse, and records the reflected visible light spectrum after absorption of specific wavelengths of light by the image on the page. The measured colour was reported in the CIE *Lab** colour space and was converted to a colour density using the method as described in section 3.3.1.4.[185,188]

Figure 3.11. The Konica Minolta Chroma Meter CR300 used to analyze the colour of printed images.

3.3.3.4 Print Test Sheet and Over-Write Testing

To ensure that the printed images from different inks were as consistent as possible, a "print test sheet" was created. The print test sheet contains four solid rectangles that were larger than the diameter of the lens of the image analyzer. In this way, only the colour of the printed image was recorded by the image analyzer. In addition to the solid rectangles, there were lines of text in English and Japanese (kangi and kana) that were used to visually examine the sharpness of the printed images.[188] While not explicitly measured and quantified, the sharpness of the printed text gave an indication about the viscosity of the printed inks and how quickly the solvent evaporated. An example of the "print test sheet" is shown in Figure 3.12 (a).

Figure 3.12 (b) shows the "print test sheet" for what is referred to here as "over-write" print testing. In over-write printing, a page that had been previously printed on and erased was re-used for subsequent printings. The dye and developer remaining on the page from the first printing can develop colour in a freshly printed sample. This is detrimental to the quality of the future printings as the new images can have varying colour density, non-uniform colour (*e.g.*, if the erased image contained a different colour ink), and can be more difficult to erase. Issues with over-write printing continue to plague the field of thermochromic inks as the dye and developer from previous printings almost always remain near the surface of the page.

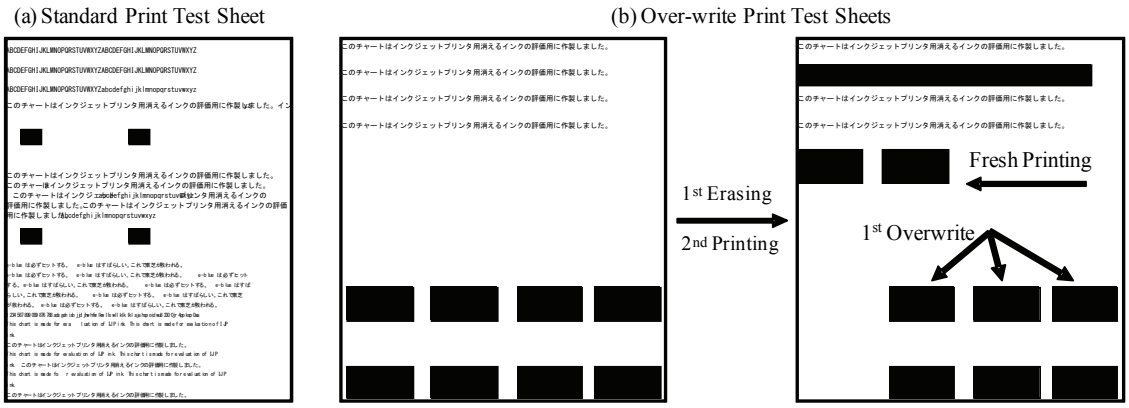

Figure 3.12. (a) The standard “print test sheet” showing image analysis rectangles and printed text. (b) "Over-write” print test sheets showing the first printed image and the location of the overwrite images. Note that there is a new “fresh printing” rectangle on this page for comparison with the over-write printed image.

Chapter 4 Influence of the Solid Solvent on the Thermochromic Behaviour of DDG-Containing Mixtures

4.1 Introduction and Background

Previous studies on three-component thermochromic mixtures comprising a leuco dye, phenolic developer, and long-chain alcoholic solvent demonstrated that changes in the length of the alkyl chain of the alcohol can modify the colouring behaviour of three-component mixtures.[101,102,110,181] Increasing the degree of mismatch of alkyl chain length for the alkyl chains attached to the gallate developer and the alcohol solvent caused increases to the both the colour density in the solid state and decolourization times after thermal quenching into a metastable solid state. However, those studies were focussed on the rate of colour dissipation from the metastable solid state and did not thoroughly examine how colouring behaviour (*i.e.*, which state, the solid or the melt, is the coloured state) could be varied by changing the alkyl chain lengths on the developer and the solvent.[101,102,110,181]

The CVL:DDG:TD-OH system was deemed to have the best thermochromic properties of the mixtures studied in MacLaren's work.[101,110] These mixtures could be converted from a colourless equilibrium solid to a dark blue molten state, and the latter could be "frozen" into the solid state by rapidly cooling with liquid nitrogen (LN_2). Dissipation of the coloured state occurred within a few minutes as the metastable solid returned to the colourless equilibrium solid state. Many mixtures employing different gallate developers (propyl, octyl, and dodecyl gallates) and alcoholic solvents (tetradecanol, hexadecanol, and octadecanol) were investigated using the same experimental approach, described above.[110]

As will be described further, during the preliminary stages of the research presented in this thesis, and by virtue of a serendipitous mixing error, it was discovered that by vastly increasing the amount of solvent present in mixtures containing poorly matched alkyl chain lengths (*i.e.*, very different lengths of the alkyl chains attached to the developer and solvent, respectively), colouring behaviour opposite to that observed in MacLaren's optimal CVL:DDG:TD-OH system[101] could be obtained. Samples containing mismatched alkyl chain lengths (*e.g.*, DDG with OD-OH) were strongly coloured in the solid state and lost their colour upon melting. This type of thermochromic behaviour will be referred to in this document as "melt-lightened" behaviour. Conversely, if the alkyl chains were similar in length (*e.g.*, DDG with TD-OH), the thermochromic mixtures were strongly coloured in the melt and weakly coloured in the equilibrium solid. This type of thermochromic behaviour will be referred to as "melt-darkened" behaviour.

This chapter explores the role of the solvent in the thermochromic behaviour of CVL:dodecyl gallate:alcohol mixtures, with a particular focus on controlling the colouring behaviour by changing the relative concentrations of each of the three components. The developer used in the studies presented in this chapter was dodecyl gallate (DDG, also known as lauryl gallate). Three alkyl alcohols were used (TD-OH, HD-OH, and OD-OH) as the solid solvent component. Table 2.1 lists the melting points and alkyl chain lengths of the alkyl gallate developers used throughout this work, and Figure 4.1 shows the structure of gallic acid and its associated esters. Table 4.1 lists the melting points, solid-solid phase transition temperatures, and alkyl chain lengths for the alkyl alcohol solvents used in this work. The experimental techniques used to study the colorimetric properties of these mixtures were observational spectroscopy and colour

photo analysis. See section 3.2.1 and section 3.3.1 for details on sample preparation and colour analysis techniques, respectively.

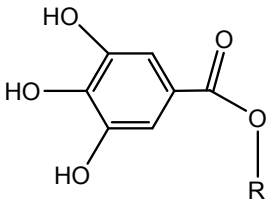

Gallic Acid: R = H
Gallic Acid Esters: R = C_nH_{2n+1}

Figure 4.1. The structure of gallic acid (R = H) and associated gallic acid esters (R = alkyl chain) used in this work.

Table 4.1. Melting points, solid-solid phase transition temperatures, and alkyl chain lengths of various alkyl alcohol solvents.

Name	Abbreviation (used here)	Alkyl Chain	Melting Point / (°C)[144-147]	Solid-Solid Phase Transition Temperature / (°C)[144-147]
1-Tetradecanol	TD-OH	$C_{14}H_{29}$	36 – 38	33 – 36
1-Hexadecanol	HD-OH	$C_{16}H_{33}$	48 – 50	43 – 46
1-Octadecanol	OD-OH	$C_{18}H_{37}$	56 – 59	52 – 55

4.1.1 Gross and Fine Features of Thermochromic Behaviour

In this and the two following chapters, the thermochromic behaviour of numerous dye:developer:solvent mixtures is presented. To better identify specific features of the thermochromic behaviour, and in particular to couple observed behaviour with known phenomena identified in other thermochromic systems, the analysis of experimental data is separated into two categories. These two categories, called the “gross” and “fine” features, are defined below.

4.1.1.1 Gross Features of Thermochromic Behaviour

The "gross features" define the general characteristics of a thermochromism system. These characteristics include the colour density of the coloured and decoloured states, as well as the degree of colour contrast observed upon phase transition from the equilibrium solid to the melt. The gross features are rather easily identified and are highly reliant on two factors: the degree of alkyl chain length matching between the developer and the solvent (which controls the strength of the developer:solvent interaction),[181] and the relative concentrations of each of the three components.[58,101,193] Most literature reports in the field of reversible thermochromism in multi-component mixtures have been focussed on optimizing, and attempting to explain the origins of, the gross features of thermochromic systems.[58,71,100,101,102,140,175,193]

4.1.1.2 Fine Features of Thermochromic Behaviour

The "fine features" identify more subtle changes in colouring behaviour that do not necessarily match the overall thermochromic behaviour observed in the gross features of a particular system. It is known that the colouring behaviour of a thermochromic system is sensitive to subtle chemical changes in the system which include variations in the polarity and H-bonding strength of the reaction medium,[71,101,102] changes in the solubility of the dye and developer during heating and cooling,[175,176] phase separation of the dye and developer from the solvent upon transition from the melt to the solid state,[100] and changes to the reaction environment due to polymorphic solid-solid phase transitions of the long-chain solid solvent.[194] The most commonly observed fine features in the present work were associated with LO-to-R phase transitions of the solvent

(polymorphism), poor dye and developer solubility in the molten solvent, and inhomogeneous phase separation of the dye and developer causing mixture decolouration.

The fine features of a thermochromic mixture are much less predictable than the gross features, and the assignment of their origins can be difficult. Using a knowledge of the physical properties of the chemicals involved, in conjunction with the reported behaviour in other thermochromic systems, the origins of some of the fine features observed in some thermochromic mixtures have been examined here. In many cases, the properties of the solid solvent play a crucial role in understanding the origin of the fine features of thermochromic systems.

4.2 Results and Discussion

To gain a better understanding of how changing the length of the alkyl chain attached to the solid solvent influences the colouring behaviour in three-component thermochromic mixtures, numerous dye:developer:solvent combinations were studied. The alcohol solvent alkyl chain length was varied from 14 to 18 carbon atoms, excluding alcohols with odd-numbered chain lengths, and dodecyl gallate (DDG, 12 carbon atom long alkyl chain) was used as the developer for all studies presented in this chapter. In all experiments reported in this chapter, the dye component was crystal violet lactone (CVL). Chapter 7 provides a summary of the results obtained in this chapter by presenting ternary thermochromic phase diagrams, which aid in the identification of compositional regions that display different thermochromic behaviour.

4.2.1 CVL:DDG:TD-OH Mixtures

4.2.1.1 Introduction to Studies on CVL:DDG:TD-OH Mixtures

A useful starting point in the comparison of thermochromic systems containing matched and mismatched alkyl chain lengths is the study of mixtures containing DDG and TD-OH, as they were found to demonstrate strong colouration in the melt and little to no colour in the equilibrium solid (*i.e.*, melt-darkened behaviour).[101] CVL:DDG:TD-OH mixtures have also been shown to demonstrate excellent colour contrast (*e.g.*, at a mixing ratio of $[1:6:40]$).[101,102]

The compositional ranges studied here for the CVL:DDG:TD-OH system differed between observational spectroscopy and colour photo analysis experiments. In the observational spectroscopy experiments, the compositional ranges varied from $[1:y:60]$ to $[1:y:90]$, where y, the molar ratio of DDG to CVL, varied from $y = 0.5$ to 10. For the colour photo analysis experiments, the developer molar ratios were in the range of $1.5 \leq y \leq 19$ and the solvent molar ratios were in the range of $45.5 \leq z \leq 190$. Rather than presenting an exhaustive list of all of the results obtained in this work, representative examples (*i.e.*, samples that best demonstrate the observed trends in colouring behaviour) obtained *via* observational spectroscopy and colour photo analysis are presented and discussed to provide general conclusions about the colouring behaviour in this thermochromic system.

4.2.1.2 Observational Spectroscopy Results

4.2.1.2.1 Gross Features of CVL:DDG:TD-OH Mixtures

Figure 4.2 shows the colour density plots for a selection of the samples in the $[1:y:60]$ and $[1:y:90]$ compositional ranges (where y varied from 0.5 to 10). The colour density (CD) values for the equilibrium solids (at the initial starting temperature, T = 25 °C) were $CD_{Equil} = 0$. This indicates that all of the samples were colourless at room temperature, in agreement with values reported in the literature.[101,110] Upon melting ($T_{fus,TD\text{-}OH}$ = 36 to 38 °C), most of the samples became coloured. From the data shown in Figure 4.2, it is apparent that the colour density of the coloured state was dependent on the concentration of developer present in the sample. Samples with DDG molar ratios of $y \leq 3$ did not become substantially coloured in the melt ($CD_{Melt} < 0.3$), whereas as samples with high DDG molar ratios became strongly coloured in the melt (*e.g.*, when y = 10, CD_{Melt} = 1.0 to 1.8).

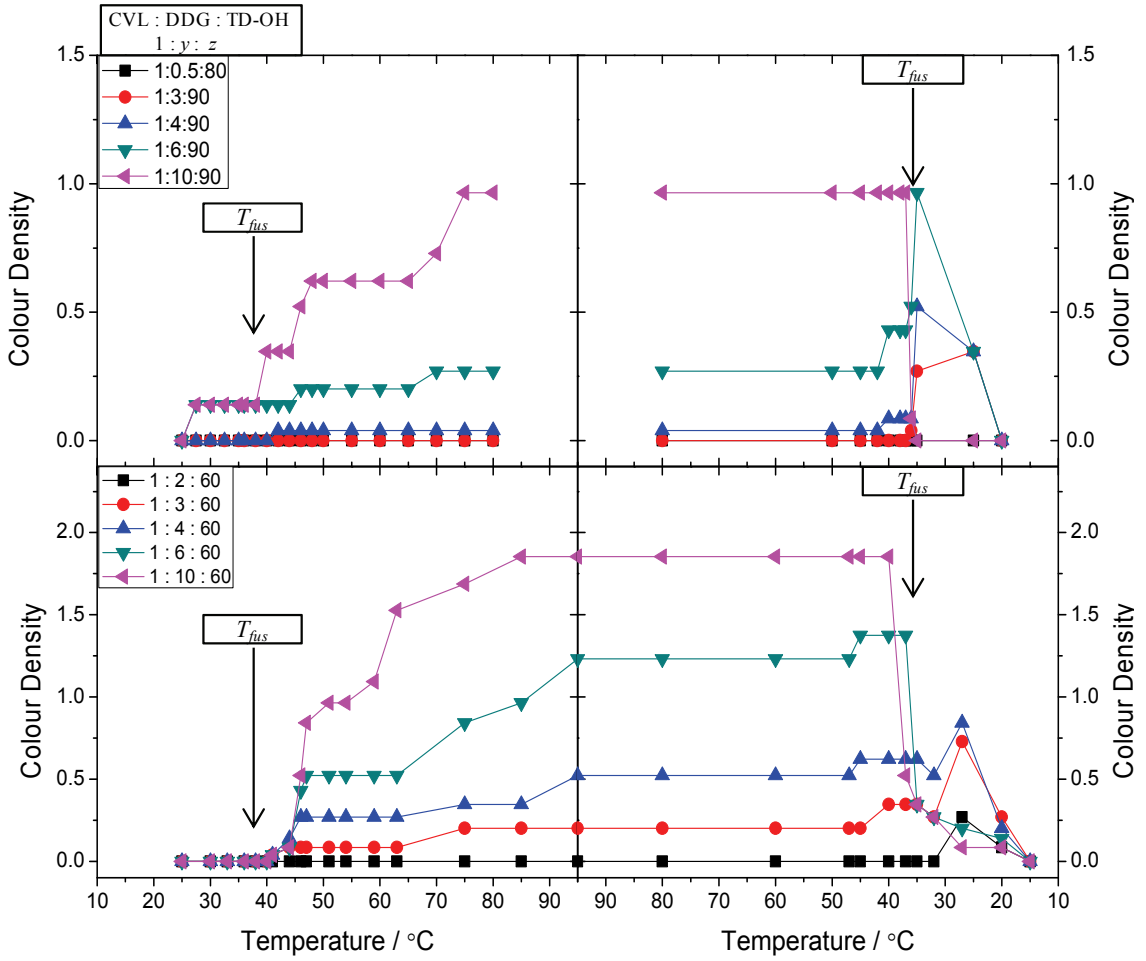

Figure 4.2. Colour density versus temperature plots obtained *via* observational spectroscopy for CVL:DDG:TD-OH samples in the [1 : *y* : 90] (top) and [1 : *y* : 60] (bottom) compositional ranges. The molar ratios of the three components are given on the figure. Heating rates during these experiments were d*T*/d*t* = 1 K min^{-1}. T_{fus} represents the melting point of the pure solvent. Lines are added as a guide to the eye. Error in *CD* was estimated to be +/-0.15. Note: data were only collected to 80 °C for the [1 : y : 90] samples.

Upon cooling to the solid state, the colour density in some samples did not immediately return to that of the equilibrium solid. This retention of colour is indicative of a metastable state forming after solvent cooling, in agreement with reports from the literature.[101] This metastable state was not kinetically stable, however, and the decoloured equilibrium state returned within a matter of minutes.

Many of the samples in the CVL:DDG:TD-OH system demonstrated high colour contrast between the coloured melt and decoloured equilibrium solid, with the colour of the molten state being highly dependent on the developer concentration. In particular, the [1:10:60] sample demonstrated excellent colour contrast (ΔCD_{Max} = 1.8), resulting from the formation of an intensely coloured melt (CD_{Melt} = 1.8) from a colourless equilibrium solid (CD_{Equil} = 0).

4.2.1.2.2 Fine Features of CVL:DDG:TD-OH Mixtures

The fine features observed in CVL:DDG:TD-OH samples can be split into two categories: features observed during heating (*i.e.*, changes associated with solvent melting and developer dissolution into the molten solvent) and features observed on cooling (*i.e.*, solvent solidification-induced colour changes), with the latter playing a more important role in this particular three-component system.

Referring to the initial heating portion of the curves in Figure 4.2, it is clear that the colour density of these samples rose as the solvent began to melt. This indicated that the developer, which is required to develop the colour of the dye, was segregated by the solvent while in the solid state, and as soon as the solvent began to melt the chemical interactions holding the developer and solvent together were disrupted. The disruption of the developer:solvent interaction liberated the developer, allowing for the formation of the strongly coloured dye:developer complex in the melt of samples that contained developer concentrations sufficiently high to initiate colour formation (*e.g.*, $y \geq 3$ for [1:y:60] samples).

Also for Figure 4.2, the largest and most rapid increases in colour density were observed immediately after the melting point of the solvent was exceeded, but the maximum colour density seen here for most samples was not reached until the mixture was heated to the highest temperature available on the water bath ($T_{max} \approx 80$ or 95 °C). The continued increase in colour density on heating is attributed to the relatively poor solubility of the developer. As the temperature of the solvent was increased, more of the developer dissolved in the molten solvent, promoting dye:developer interactions and, subsequently, the formation of more strongly coloured mixtures.

Enhanced developer dissolution in the high-temperature solvent (*i.e.*, > 70 °C) is the result of a couple of factors. The melting points of long-chain alkyl gallates fall within a fairly narrow range when the alkyl chain length is between 8 and 18 carbon atoms (*vide supra*, Table 2.1). Dodecyl gallate has a melting point of 96 to 99 °C,[128,130] therefore it stands to reason that the developer component should become more soluble as the temperature of the solvent approaches the melting point of the gallate developer. Furthermore, increased developer solubility was coupled with enhanced molecular mobility of the developer as the melting point of the developer was approached, which further aids in the mixing of components in the molten phase of the solvent.

The maximum colour density of the melt was achieved at or near the maximum temperature of the heat-cool cycle and was maintained until solvent solidification. The maintenance of the maximum colour density during cooling further supports the concept of enhanced developer solubility since molten, but poorly soluble, developer would precipitate inhomogeneously from the solvent on cooling prior to solvent solidification. Inhomogeneous precipitation of the developer would result in inconsistent colour density

during cooling and increased opacity of the mixture above the solvent freezing temperature; this behaviour was noted for samples containing mismatched alkyl chain lengths and will be discussed in subsequent chapters.

The colouring behaviour of TD-OH mixtures during cooling varied substantially from sample-to-sample, with a strong dependence on the developer concentration. Referring to Figure 4.2, in particular to the cooling portion of the graph in the region of $45°C > T > 20°C$, it is clear that the colouring behaviour of the [1:3:60] and [1:4:60] samples was very different from that of the samples with higher developer concentrations, such as the [1:6:60] and [1:10:60] samples.

Looking first at the curves for the [1:6:60] and [1:10:60] samples on cooling, there was a slight increase in colour density just prior to solvent solidification (observed in $y = 3$, 4, and 6 samples, but not when $y = 10$ due to colour density saturation), which occurred at $T \approx 45$ °C. As the solvent began to solidify into its R-phase in the [1:6:60] and [1:10:60] samples, the developer quickly precipitated from solution, thereby disrupting the colour-forming dye:developer complex and giving rise to rapid decolourization of the mixture. Further cooling caused additional colour density decreases after a few minutes, due to conversion to the equilibrium solid state and the formation of the 2DDG:TD-OH compound described in section 2.2.2.2.[101,110,164]

The [1:2:60], [1:3:60], and [1:4:60] samples demonstrated rather different fine features during cooling compared to the [1:6:60] and [1:10:60] samples. At a temperature just above the melting point of the solvent (T_{fus} = 36 to 38 °C),[144] there was a slight increase in the colour density of the mixtures, as described above. As the samples were further cooled, and the solvent solidified in the R-phase, the colour density

decreased slightly. This decrease in colour density for the $y = 3$, 4 samples was substantially less sharp than the colour density drops observed in the samples with $y = 6$, 10. This indicates that the precipitation of the developer from the solid solvent was not as complete in $y = 3$, 4 samples as it was for samples with larger developer concentrations (*e.g.*, samples with $y = 6$, 10).

A consequence of incomplete developer precipitation from the solvent was the maintenance of moderate colouration into the solid state for samples with $y = 3$, 4. The solvent immediately solidified into the R-phase prior to undergoing a solid-solid phase transition to the low-temperature ordered phase (LO-phase). While in the R-phase, the heightened orientational disorder of the solvent phase likely promoted dissociation of the coloured complex, which accounts for the immediate, however small, drop in colour density as the freezing point of the solvent was reached (for $y = 3$ and 4 samples). Further cooling caused the solvent to transition from the R-phase to the LO-phase, at which point a moderate spike ($\Delta CD = 0.5$) in the colour density was observed. This spike is attributed to a "freezing-in" of the coloured complex, as had been observed in rapidly quenched thermochromic mixtures.[101,102] The proposed mechanism explaining the colouring behaviour after solvent solidification in this system, which involves a solid-solid phase transition from the R-phase to the LO-phase and the creation of a metastable solid state, is supported by the fact that the metastable state was short-lived and returned to the colourless equilibrium state within a matter of minutes.[101]

The fine features of the $[1:y:90]$ samples were similar to those observed in the $[1:y:60]$ samples. The $y = 10$ sample underwent rapid decolourization upon

solidification of the solvent due to the near-complete, inhomogeneous precipitation of the developer from the solvent causing the coloured dye:developer complex to be destroyed.

The $[1:y:90]$ samples with y = 3, 4, or 6 demonstrated behaviour similar to the $[1:y:60]$ samples with similar developer concentrations. There was a brief spike in colour density of the mixtures prior to solvent solidification, coupled with an additional increase in colour density just after solvent solidification. No reduction in colour density was observed between the two aforementioned increases in colour density in $[1:y:90]$ samples, in contrast to what had been observed for $[1:y:60]$ samples. Once again, the spike in colour density that occurred after solvent solidification was likely the result of transition through the R-phase to the LO-phase of the solvent, whereby transition to the LO-phase briefly froze the coloured complex into the solid state of the solvent, yielding a metastable coloured solid, which returned to the decoloured equilibrium state after a few minutes.

4.2.1.3 Colour Photo Analysis of CVL:DDG:TD-OH Mixtures

4.2.1.3.1 Gross Features of CVL:DDG:TD-OH Mixtures

The results obtained *via* colour photo analysis are presented separately from those obtained *via* observational spectroscopy. The colour photo analysis experiments employed a white reference material (Spectrolon), composed of a highly reflective Teflon block, to normalize the measured brightness of each sample. This allows for colour density comparisons between mixtures containing different chemical components (*e.g.*, different developers and solvents) at different concentrations, and under different lighting conditions.

Figure 4.3 shows the colour photo analysis colour density versus temperature plots for selected samples in the CVL:DDG:TD-OH system. The gross features of this system are in accord with those presented in section 4.2.1.2.1 and those reported in the literature.[101,102,110] Melt-darkened behaviour was observed for most samples, with the equilibrium solid state being decoloured at all compositions, while the melt became coloured in samples that contained sufficiently high developer concentrations.

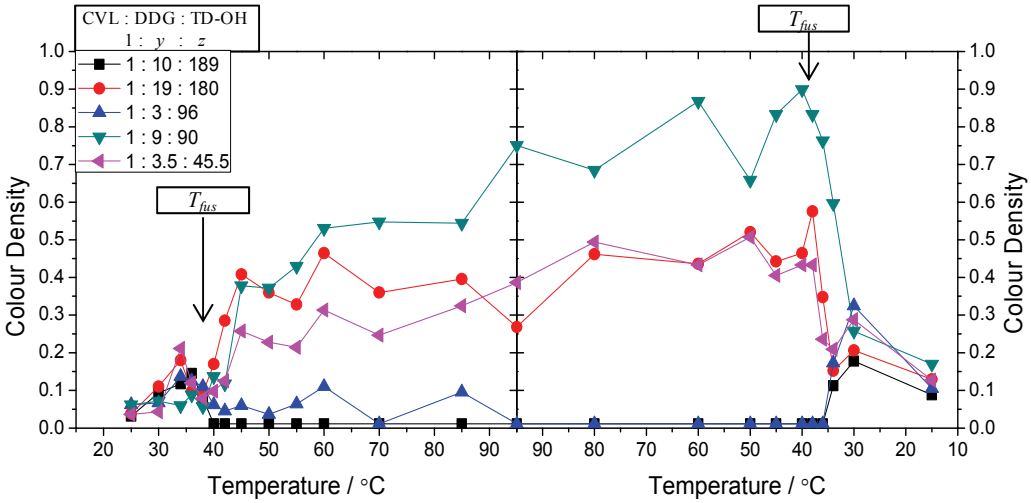

Figure 4.3. Colour density versus temperature plots obtained *via* colour photo analysis for samples in the CVL:DDG:TD-OH system. The molar ratios of the three components are given on the figure. Heating rates during these experiments were d*T*/d*t* = 1 K min^{-1}. T_{fus} represents the melting point of the pure solvent. Lines are added as a guide to the eye. Error in *CD* was estimated to be +/-0.15.

Some samples lacked colour in both the equilibrium solid and the melt owing to the fact that the developer concentration was too low (*e.g.*, [1:3:96] sample) or the solvent concentration was too high (*e.g.*, [1:10:189] sample). In the intermediate cases where the developer concentration was high (*e.g.*, [1:19:180] sample) or the solvent concentration was low (*e.g.*, [1:3.5:45.5] sample), the equilibrium solid was colourless and the melt became coloured. In all of the samples, the solid initially formed on cooling from the melt was more strongly coloured than the pre-melt equilibrium solid indicating

the formation of a metastable solid. After a few minutes at room temperature ($T \sim 15$ °C), however, the metastable solid was converted to the equilibrium solid and colour was lost.

The colour contrast between the coloured and decoloured states, ΔCD, which is arguably the most important characteristic of any thermochromic system, was observed to be very tuneable in the CVL:DDG:TD-OH system by modifying the developer and solvent concentrations. The colour contrast of the [1:9:90] sample (Figure 4.3) was very good ($\Delta CD_{Max} = 0.7$), once the developer completely dissolved in the molten solvent, and could potentially be increased further since the equilibrium solid remained virtually colourless over the entire compositional range studied.

4.2.1.3.2 Fine Features of CVL:DDG:TD-OH Mixtures

To give the reader a better appreciation for what a specific colour density value looks like in the solid and molten states, colour images are presented for selected dye:developer:solvent combinations studied *via* colour photo analysis. Figure 4.4 shows the colour photos obtained for the [1:9:90] sample. The equilibrium solid was completely colourless, with colour development occurring above the melting point of the solvent (T_{fus} = 36 to 38 °C)[144] was exceeded. The colour density of the [1:9:90] sample began to rise sharply above 42 °C, before attaining moderate colouration at 45 °C.

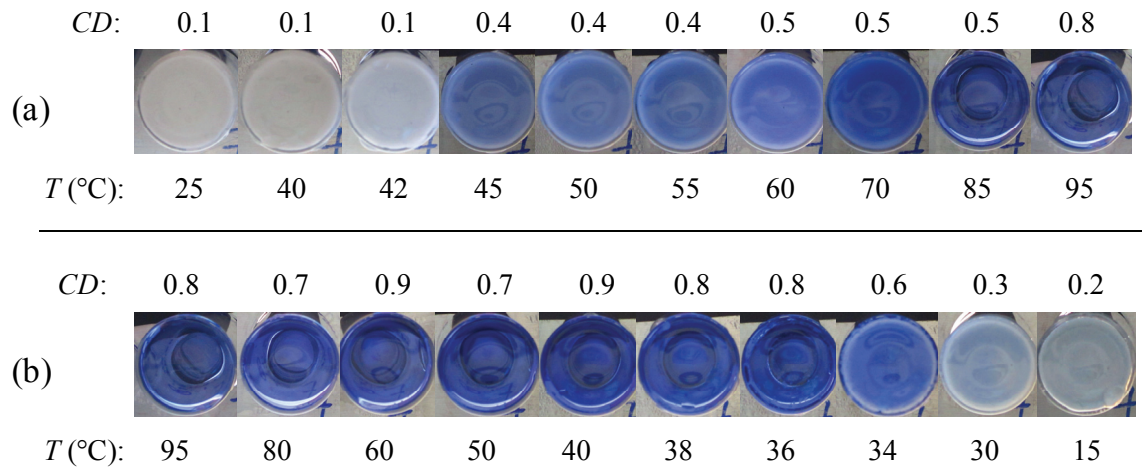

Figure 4.4. Colour photographs (a) on heating and (b) on cooling of the CVL:DDG:TD-OH sample at a composition of [1:9:90]. Note the formation of colour upon melting (T > 42 °C) and reduction in colour density upon solidification (T < 36 °C).

As described in section 4.2.1.2.2, the developer component does not always fully dissolve as soon as the solvent melts. This phenomenon resulted in a gradual increase in the observed colour density of a given mixture as the melting point of the gallate developer was approached. This effect was also observed in three-component mixtures containing HD-OH and OD-OH as the solvent, and will be further discussed in subsequent sections of this chapter (sections 4.2.2 and 4.2.3).

The effect of insoluble developer on the colorimetric properties of thermochromic mixtures is seen in Figure 4.4 (a). As the temperature exceeded the melting point of the solvent ($T_{fus,TD\text{-}OH}$ = 36 to 38 °C), the mixture gained a light blue hue. The mixture remained opaque throughout much of the temperature range, indicating the presence of insoluble developer. At 85 °C, the developer became fully dissolved in the solvent, producing a completely transparent melt. At this elevated temperature the maximum colour density of the melt was reached, indicating that the developer had fully dissolved

in the solvent since, for melt-darkened thermochromic mixtures, dye:developer complex formation would be strongest when the developer is fully dissolved.

As the sample in Figure 4.4 was cooled from 95 °C, there was effectively no change in colour density or opacity throughout the entire temperature range until the solvent solidified just below its literature melting point.[144] The lack of crystallization of the developer on cooling indicates that the developer had become dissolved in the solvent. If the solvent and developer were both molten and immiscible, the developer would begin to crystallize well before the solvent crystallized due to their substantially different melting points (see Table 2.1 and Table 4.1). Crystallization of the developer did not occur independently of the solvent crystallization and therefore the developer must have been dissolved in the solvent.

Developer solubility in the solvent, and subsequently the colouring behaviour of the melt, is intimately coupled with the developer:solvent mixing ratio. Figure 4.5 shows colour images of the [1:10:189] sample on heating and cooling. This sample contained substantially increased solvent loading compared to the [1:9:90] sample (Figure 4.4) while maintaining nearly the same dye:developer ratio. The increased solvent loading in the [1:10:189] sample allowed for a higher concentration of developer in the molten mixture, reducing opacity in the melt.

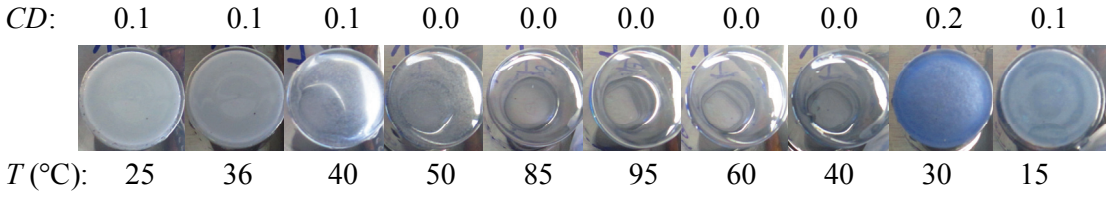

Figure 4.5. Colour photographs of the CVL:DDG:TD-OH sample at a composition of [1:10:189]. Note the high transparency of the molten phase of the mixture, as well as the lack of colour formation on solvent melting ($T \geq 40$ °C) and the appearance of colour upon solidification ($T \leq 30$ °C).

Coupled with reduced opacity was the reduction in melt colour density observed in mixtures with high solvent loading and/or low developer concentrations. The aforementioned [1:10:189] sample was completely colourless in the melt as a result of the substantially increased solvent loading. While in the melt, the developer concentration must be sufficiently large to allow the developer to interact with the dye and thereby produce colour. If the developer concentration was too low, the likelihood of an interaction between the dye and developer was substantially reduced and no colour was formed in the melt.

Figure 4.6 shows digital photos of the [1:3.5:45.5] sample during heating and cooling. The dye:developer ratio in this mixture was much lower than that of the [1:10:189] sample, however, the solvent concentration also was substantially reduced. As a result of the decreased solvent concentration, the opacity effects resulting from insoluble developer were observed throughout the entire temperature range. The decreased solvent concentration also resulted in an increase in the colour density of the melt, giving rise to a faint blue molten phase.

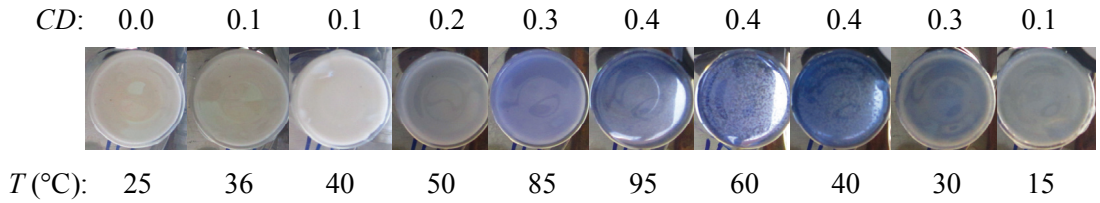

Figure 4.6. Colour photographs of the CVL:DDG:TD-OH sample at a composition of [1:3.5:45.5]. Note the formation of colour upon melting ($T \geq 50$ °C) and loss of colour upon solidification ($T \leq 30$ °C).

The fine features discussed in section 4.2.1.2.2, based on observational spectroscopy results for the same CVL:DDG:TD-OH ternary system, were also observed

during the colour photo analysis experiments. Samples which formed very deeply coloured molten phases, as a result of their high developer and low solvent concentrations, underwent rapid colour loss upon solidification of the solvent and did not show a brief spike in colour density on further cooling. Referring back to Figure 4.3 (colour density versus temperature plots) and Figure 4.4 (colour photos of the [1:9:90] sample on cooling), it is clear that the colour density drops rapidly upon solidification of the solvent, with the retention of moderate colour as the sample passes through the R-phase of the solvent (T = 34 °C, glossy appearance indicates R-phase formation).

Some samples, particularly those which did not form colour in the melt, demonstrated colour formation upon solidification of the solvent. All of the samples shown in Figure 4.3, with the exception of the [1:9:90] sample, showed a brief spike in colour density after solidification of the molten solid. In samples demonstrating colour in the melt, there was a sharp decrease in colour density as solidification began (*i.e.*, due to R-phase formation) followed by a brief spike in colour density upon transition from the solvent R-phase to the LO-phase. The transition to the LO-phase effectively froze the solid into a metastable state which was darker than the equilibrium solid, and was lost after some time when the equilibrium solid was achieved.

Figure 4.5 provides a good visual representation of the brief spike in colour density that occurs just after solvent freezing in CVL:DDG:TD-OH system. There was no colour formation observed in the sample on heating from the equilibrium solid, even at the highest temperature attained on the water bath. During cooling, no developer precipitation or colour formation was observed until the solvent began to solidify ($T \approx 34$ °C), at which point weak colouration was observed upon transition to the R-phase. The

transition to the LO-phase created a short-lived metastable state with slightly enhanced colour density compared to the pre-melt equilibrium solid, but the increased colour density was quickly lost as the equilibrium solid phase was achieved.

4.2.1.4 Conclusions Concerning CVL:DDG:TD-OH Mixtures

The gross features of thermochromic behaviour in the CVL:DDG:TD-OH system obtained *via* observational spectroscopy demonstrated that the equilibrium solid is the decoloured state, the melt is the coloured state, and that colour contrast can be high but depends largely on the developer concentration. The equilibrium solid was observed to be colourless in virtually all mixtures, and the colour density of the melt was dependent on the relative developer and solvent concentrations. There was a developer loading threshold value above which a coloured melt was formed and below which the melt always lacked colour formation. This developer loading threshold also was dependent on the solvent concentration, increasing from $y \approx 2$ when $z = 60$ to $y \approx 3$ when $z = 90$, due to the relative decrease in dye and developer concentrations caused by the increased solvent concentration.

The results obtained *via* colour photo analysis were largely in agreement with those obtained *via* observational spectroscopy for the CVL:DDG:TD-OH system. CVL:DDG:TD-OH mixtures were characterized by very good colour contrast ($\Delta CD_{max} = 0.7$) between completely decoloured equilibrium solids and coloured melts. The colour density of the melt was enhanced by increasing the developer concentration, while changing the solvent concentration usually had larger implications on the solubility of the developer and opacity of the melt.

The fine features of thermochromic behaviour, identified during the heating portion of the experiment, include the initial development of colour upon solvent melting coupled with continued increases in melt colour density as the mixture was heated to $T \approx$ 95 °C. Increased solvent temperatures promoted enhanced dissolution of the developer into the solvent, which produced an increasingly dark melt, until the maximum temperature of the water bath was reached and the colour density levelled off.

On cooling, samples with low and intermediate developer concentrations (*e.g.*, when $y \leq 5$ to 6) usually darkened slightly just prior to solvent solidification, and darkened much more as the solvent transitioned from the R-phase to the LO-phase, producing a darker metastable solid. The metastable solid was kinetically unstable and converted to the equilibrium solid in a matter of minutes. Samples containing large developer concentrations (*e.g.*, when $y = 10$), on the other hand, underwent rapid and nearly complete colour loss upon solvent solidification due to the rapid precipitation of the developer. Due to the rapid colour loss, the equilibrium solid state colour density was returned almost immediately after solvent solidification.

In samples with intermediate developer concentrations and relatively high solvent concentrations, conversion to the solid state caused increased colour density. The initial increase on solidification of the solvent was associated with formation of the R-phase of the solvent, and subsequent conversion of the R-phase to the LO-phase caused a "freezing-in" of the colour in the form of a short-lived metastable solid state.

4.2.2 CVL:DDG:HD-OH Mixtures

4.2.2.1 Introduction to Studies on CVL:DDG:HD-OH Mixtures

Previous research on three-component thermochromic mixtures containing HD-OH as the solvent indicated that this system behaves in a fashion similar to the related TD-OH system.[101,143] The equilibrium solid was observed to have a lighter colour than the melt and the quenched metastable solid was found to be darker than the equilibrium solid, but the decolourisation rates of the metastable state were found to be substantially longer (t_d > 30 min) than for the TD-OH system.[101,143] The observed behaviour was seen over a wide compositional range, $1 \leq y \leq 12$ and $25 \leq z \leq 85$.[101,143]

In an effort to confirm what had been reported previously, many samples in the aforementioned compositional ranges were prepared and studied. In a surprising turn of events, it was observed that samples outside this compositional range, containing a large concentration of solvent (*e.g.,* when z = 90 to 100) and small concentration of developer (*e.g.*, when $0.5 \leq y \leq 5$), actually demonstrated behaviour opposite to that reported by both MacLaren and Tang for lower solvent concentrations.[101,102,110,181]

In the higher solvent concentration samples, the equilibrium solid demonstrated moderate colouration that often was lost upon solvent melting, indicating that the solid was the coloured state and that the melt was the decoloured state. The quenched metastable solid usually was the darkest state, before converting to the equilibrium solid over a period of 30 to 60 minutes. As was the case with TD-OH mixtures, the colour density of the samples with a large concentration of solvent (*e.g.*, when z = 90 to 100) was highly dependent on the developer concentration.

The CVL:DDG:HD-OH system is an example of a mismatched system, containing solvent and developer alkyl chains that differ in length by four carbon atoms. This mismatch in alkyl chain length causes the interaction of the developer and solvent in the solid state to be weaker than in "matched" systems (*e.g.*, CVL:DDG:TD-OH mixtures, where the alkyl chains vary in length by two carbon atoms) and as a result, the equilibrium solid is usually observed to be coloured. Strong developer:solvent interactions, as seen in matched systems, reduce colour formation in the solid state because the developer is sequestered by the solvent, preventing dye:developer interactions and colour formation.

4.2.2.2 Observational Spectroscopy Results for CVL:DDG:HD-OH Mixtures

4.2.2.2.1 Gross Features of CVL:DDG:HD-OH Mixtures

Figure 4.7 shows colour density versus temperature plots for selected samples in the CVL:DDG:HD-OH ternary system at a variety of solvent concentrations (*e.g.,* where $z = 90$, 60, and 30). At high developer concentrations, the colouring behaviour was somewhat similar to that observed for the TD-OH system (*i.e.*, melt-darkened). The [1:10:90], [1:5:60], and [1:4:30] samples all were coloured in the equilibrium solid and became more intensely coloured upon solvent melting. The metastable solid formed after solvent solidification (T_{fus} = 48 to 50 °C)[144] was the most intensely coloured state, before losing colour density as the mixture returned to the equilibrium solid state. The darkening of the sample ([1:10:90]) on melting was reminiscent of the behaviour observed in TD-OH mixtures (section 4.2.1), but with reduced colour contrast for the HD-OH sample.

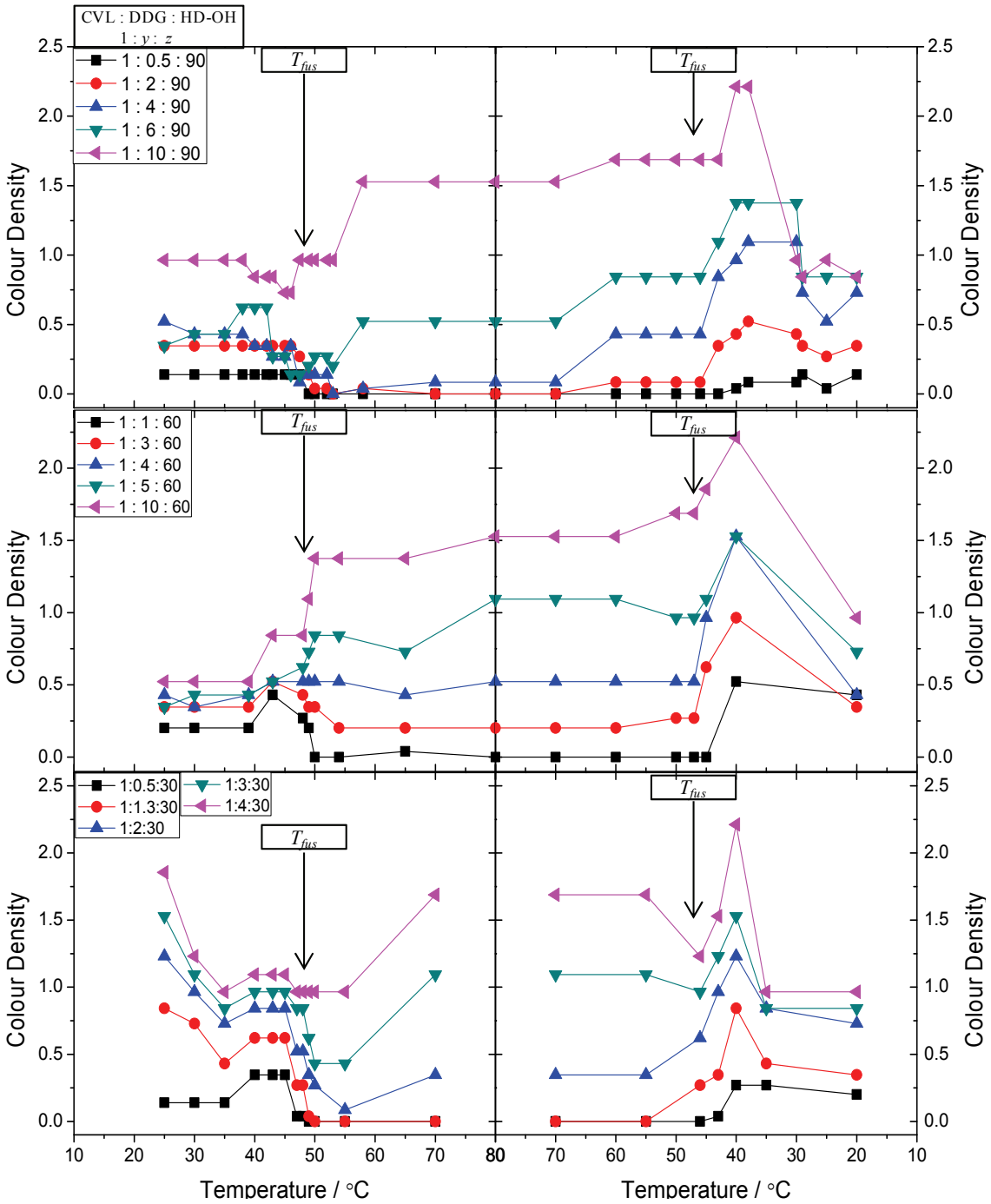

Figure 4.7. Colour density versus temperature plots obtained *via* observational spectroscopy for CVL:DDG:HD-OH samples in the [1:*y*:90] (top), [1:*y*:60] (middle), and [1:*y*:30] (bottom) compositional ranges. The molar ratios of the three components are given on the figure. Heating rates during these experiments were d*T*/d*t* = 1 K min^{-1}. T_{fus} represents the melting point of the pure solvent. Lines are added as a guide to the eye. Error in *CD* was estimated to be +/-0.15. Note: data were only collected to 70 °C for the [1:*y*:30] samples.

As the developer concentration was decreased, the colour density in both the solid state and the melt was reduced. The colour density of the melt exhibited strong developer concentration dependence, particularly after the developer more completely dissolved in the molten solvent (*e.g.*, when $T > 60$ °C). As the developer concentration was further decreased ($y \leq 4$ for $z = 90$ samples), the colour density in the equilibrium solid became higher than the colour density in the melt. Therefore, the less coloured state in these samples was the melt and the more coloured state was the equilibrium solid, in contrast to the behaviour observed in TD-OH samples.

Furthermore, this behaviour was in contrast to that described by MacLaren and Tang, who treated the equilibrium solids as the decoloured state and the melt as the coloured state in each of the three-component thermochromic systems studied in their work.[101,102] Additionally, there was a developer concentration threshold below which the colouring behaviour changed from melt-darkened to melt-lightened thermochromism. In samples with $z = 90$, this threshold developer concentration was observed to be $y \approx 6$.

Colouring behaviour very similar to the $z = 90$ samples was observed for the $z = 60$ samples, which are also shown in Figure 4.7 (middle). Once again, at high developer concentrations (*e.g.*, when $y \geq 5$), the melt was more strongly coloured than the equilibrium solid, indicating melt-darkened behaviour. Samples that contained less developer ($y < 4$) were more strongly coloured in the equilibrium solid than in the melt, indicating melt-lightened behaviour. The decreased solvent concentration (*e.g.*, when $z = 60$) caused a relative increase in the concentrations of CVL and DDG, allowing for the inversion of colouring behaviour to occur at lower developer concentrations. For samples with $z = 60$, the developer concentration threshold dropped to $y \approx 4$.

Figure 4.7 (bottom) shows colour density versus temperature plots for selected samples with z = 30. These samples demonstrated behaviour similar to the previously discussed HD-OH mixtures and, as expected, the developer concentration threshold for inversion of colouring behaviour fell to an even lower value ($y \approx 3$). It must be noted that the initial colour densities during the heating portion of the heat-cool cycle (at $T = 25$ °C) shown in Figure 4.7 (bottom) are non-equilibrium values due to the fact that the samples had not reached thermal equilibrium (after sample preparation) prior to the start of the slow heat-cool cycle experiment. The colour densities reported at $T = 20$ °C during the cooling portion of the experiment are equilibrium values, which were obtained by allowing the samples to sit at room temperature overnight. Therefore, the assignment of $y \approx 3$ as the developer concentration threshold was based on the post-solidification colour density, which represented the equilibrium colour density.

An important difference between the samples with $z = 30$ and the previously examined samples ($z = 60$ or $z = 90$) was that even at low developer concentrations (*e.g.*, $y = 2$ to 4) the equilibrium colour density (observed at $T = 20$ °C on cooling) was rather high. In particular, the [1:2:30] sample (Figure 4.7 (bottom), blue triangles) demonstrated an equilibrium colour density of $CD_{\text{Equil}} \approx 0.7$, which was substantially higher than that of the [1:3:60] sample ($CD_{\text{Equil}} \approx 0.3$) and the [1:2:90] sample ($CD_{\text{Equil}} \approx 0.3$). The higher equilibrium colour densities observed for $y = 30$ samples were attributed to the low solvent concentration, which caused the relative dye and developer concentrations to increase.

Also due to the low solvent concentration, fully decoloured melts were difficult to obtain. The best colour contrast observed for melt-lightened $y = 30$ samples was seen for

the [1:1.3:30] sample, which became fully decoloured in the melt (CD_{Melt} = 0.0), but showed only light colouration in the solid state (CD_{Equil} = 0.3), yielding poor colour contrast (ΔCD_{Max} = 0.3).

A final set of samples in this series was prepared with low solvent concentrations (*e.g.*, with $z < 30$) to determine if the loss of colour in the melt could be maintained while substantially increasing the relative concentrations of CVL and DDG (by virtue of the decreased solvent concentration). Figure 4.8 shows the colour density versus temperature plots for selected samples with $z < 30$. These samples showed low colour density in the pre-melt equilibrium solid as a result of the low developer loading ($y \leq 1$) and all except for one, [1:0.7:26.9], exhibited complete colour loss upon melting. The latter did show some colour loss. Due to the increase in the concentration of the colour-forming components, it was difficult to obtain good colour contrast between the coloured and decoloured states in this compositional range.

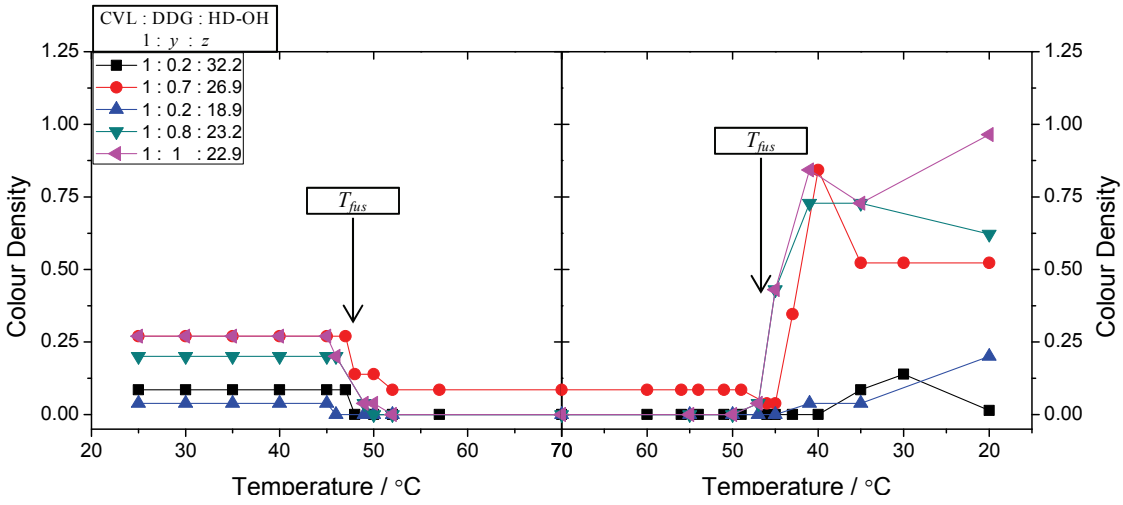

Figure 4.8. Colour density versus temperature plots obtained *via* observational spectroscopy for samples in the CVL:DDG:HD-OH system (where $z < 30$). The molar ratios of the three components are given on the figure. Heating rates during these experiments were dT/dt = 1 K min^{-1}. T_{fus} represents the melting point of the pure solvent. Lines are added as a guide to the eye. Error in *CD* was estimated to be +/-0.15.

4.2.2.2.2 Fine Features of CVL:DDG:HD-OH Mixtures

The fine features associated with the heating portion of the heat-cool cycle were more difficult to resolve in this ternary system than in the CVL:DDG:TD-OH system. In general, the most common feature was a moderate darkening ($\Delta CD \approx 0.3$) of samples prior to solvent melting. This feature was seen most prominently for samples with $z = 30$, where a broad spike in colour density was observed between 40 °C $\leq T \leq$ 48 °C on heating, before the colour density dropped near the melting point of the pure solvent. Although this feature was not observed in every sample, its presence in numerous samples (*e.g.*, [1:6:90], [1:1:60], and [1:y:30]) indicated that transition into the solvent R-phase has significant implications on the colouring behaviour of thermochromic mixtures.

The spike in colour density observed on heating often was observed to occur at temperatures below the LO-to-R transition temperature range of the pure solvent ($T_{trs,HD\text{-}OH}$ = 43 to 46 °C).[148] The source of this spike in colour density was likely due to transition into the R-phase; however, the fact that it was an increase in colour density and not a decrease in colour density was counter-intuitive. In the majority of samples studied in this work (most of which demonstrated melt-lightened behaviour), transition into the R-phase of the solvent caused decolouration of the mixtures. In fact, decolouration of CVL:DDG:HD-OH mixtures upon transition to the solvent R-phase was observed in numerous colour photos shown in the section 4.2.2.3, which presents colour photo analysis of CVL:DDG:HD-OH mixtures. This raised an interesting question: why did the colour density of CVL:DDG:HD-OH mixtures observed by observational spectroscopy increase near the LO-to-R phase transition?

As the solvent transitions into the R-phase from the equilibrium LO-phase, the developer becomes more mobile due to the increased molecular mobility of the solvent molecules in the R-phase. When this occurs, the dye:developer interaction is temporarily weakened, and some mild colour loss occurs. At temperatures just above T_{trs}, the solvent transitions from the R-phase back into the LO-phase when the sample is removed from the water bath. As has been noted in previous sections of this thesis, conversion from the melt and/or R-phase to the LO-phase of the solvent causes the colour density to spike due to the formation of a metastable solid state. Therefore, the spike in colour density observed during heating, and prior to solvent melting, for CVL:DDG:HD-OH mixtures was due to the formation of a more intensely coloured metastable mixture in which the solvent is temporarily in the LO-phase. In the samples that showed colour density increases prior to the LO-to-R phase transition temperature range for the pure solvent, the colour density was also noted to decrease immediately prior to solvent melting. This behaviour is characteristic of transition into the R-phase, in which decolouration of the mixture is caused by dissociation of the dye:developer complex due to enhanced molecular mobility in the dynamically disordered rotator phase.

An important consideration in the study of three-component thermochromic mixtures is the solubility of the dye and developer in both the solid and liquid phases of the solvent. As previously discussed, a proposed mechanism for colour formation in these systems suggested that phase separation, and the solubility of the dye and developer, play a crucial role in the colouring behaviour of reversible thermochromic mixtures.[100]

In the CVL:DDG:HD-OH system, both the dye and developer have relatively low solubility in molten HD-OH. While it is not directly evident from the data presented in

Figure 4.7 and Figure 4.8, both CVL and DDG have such low solubility in HD-OH that the melt is often opaque due to the presence of insoluble DDG and/or CVL. This behaviour is evidenced in Figure 4.9 by the visual observation of insoluble CVL[‡] in the decoloured melt of the CVL:DDG:HD-OH mixture, at a composition of [1:0.5:23].

T (°C):	20	40	45	50	85	50	46	44	30	20

Figure 4.9. Colour photographs of the CVL:DDG:HD-OH sample at a composition of [1:0.5:23]. The yellow colour of the melt is due to insoluble *leuco*-CVL.

Returning to Figure 4.7, it can be observed that the colour density of $z = 90$ samples at 80 °C was lower than the colour density of the melt during the cooling phase (60 to 50 °C). This behaviour was the result of increased dissolution of the developer in the molten solvent as the samples spent more time in the melt. This effect was greatest at moderate developer concentrations (*e.g.*, when $y \approx 4$ to 6). At low developer concentrations (*e.g.*, $y \leq 2$), there simply was not enough developer present to obtain strong colouration in the melt, regardless of dye and developer solubility.

In the [1:10:60] sample, the colour of the melt quickly became saturated as the solvent melted and further dissolution of DDG and/or CVL had little influence on the colour density of the mixture. The high developer concentration likely means that the developer solubility limit is reached quickly, preventing the increase in colour density observed in samples containing lower developer concentrations (*e.g.*, the $y = 3$, 4

[‡] *Leuco*-CVL is often yellow due to the presence of small amounts of impurities.

samples), which continue to become more strongly coloured in the melt during the cooling phase as more developer dissolved in the molten solvent.

A similar effect of increasing colour density with time in the melt was seen in z = 30 samples, where the colour density continued to increase during heating of the melt up to 70 °C. The increase in melt colour density would likely have been greater if the samples were heated to 95 °C as the melting point of the gallate was approached. Increased colour density with temperature and time spent in the melt was not observed in $z < 30$ samples (Figure 4.8), presumably due to the low solvent concentration reducing the amount of developer which could become dissolved in the melt.

Another important fine feature observed in CVL:DDG:HD-OH mixtures was the colouring behaviour upon solvent solidification. Samples in the [1:y:90] compositional range (Figure 4.7, top) demonstrated two types of solidification-induced colouring behaviour. At high developer loading (*e.g.*, [1:10:90]), the colour density did not increase immediately upon solidification of the solvent into the R-phase (T = 48 to 45 °C), and spiked upon transition from the R-phase to the LO-phase (T = 43 to 40 °C). The colour density of the [1:10:90] sample then dropped precipitously as the solvent was further cooled, likely due to inhomogeneous phase separation of the developer from the solvent, thereby returning the equilibrium colour density at 30 °C.

A similarly intense colour density decrease was observed for the [1:4:30] sample as a result of the relatively large developer concentration. Upon solidification of the solvent into the R-phase, little change in the colour density was observed (T = 46 to 43 °C). Conversion of the R-phase solid to the LO-phase caused an immediate spike in the colour density, which was followed by a significant decrease in colour density on

cooling to $T = 35$ °C. The large decrease in colour density observed after LO-phase formation was attributed to rapid and inhomogeneous precipitation of the poorly soluble developer, a mechanism suggested previously in section 4.2.1.2 to explain the dramatic colour density decreases observed in CVL:DDG:TD-OH mixtures containing large developer concentrations (*e.g.*, the [1:10:60] and [1:10:90] samples).

Most CVL:DDG:HD-OH samples at low developer concentrations ($y < 5$) displayed slightly different colouring behaviour on cooling compared with the high developer concentration samples. This was mostly due to the relatively low developer concentrations, which prevented the rapid, inhomogeneous precipitation of the developer that occurred in samples containing large developer concentrations (*e.g.*, [1:10:90] in Figure 4.7). Referring to Figure 4.7, the colour density of most samples spiked slightly after solvent solidification. This spike in colour density, observed around T ≈ 45 to 40 °C, corresponded to the transition from the R-phase to the LO-phase of the solvent. The colour density in the low developer concentration samples was maintained across a wider temperature range than in high developer concentrations samples, since the developer did not rapidly phase-separate from the solid solvent. This slow decrease in colour density, occurring around 30 °C, was similar to the results obtained by MacLaren, Tang, and White for CVL:DDG:HD-OH mixtures, , which decoloured more slowly than similar CVL:DDG:TD-OH compositions.[101,102]

4.2.2.3 Colour Photo Analysis of CVL:DDG:HD-OH Mixtures

Colour photo analysis was also carried out on samples in the CVL:DDG:HD-OH system. It must be noted that, although colour photo analysis is generally more

quantitative than observational spectroscopy, the measurements reported here for the CVL:DDG:HD-OH system were carried out during preliminary stages of colour photo analysis and were not referenced against a pure white reference material. As a result, the reported colour density values in Figure 4.10 and Figure 4.11 are artificially high. Although the colour density values of these samples cannot be directly compared with other systems reported in this work, the trends in colouring behaviour remain important.

4.2.2.3.1 Gross Features of CVL:DDG:HD-OH Mixtures

The gross features of thermochromic behaviour in the CVL:DDG:HD-OH system, observed by means of colour photo analysis, correspond well with those observed *via* observational spectroscopy (*vide supra*, section 4.2.2.2.1). Figure 4.10 shows the colour density versus temperature plots for selected samples in the CVL:DDG:HD-OH ternary system. Most of the samples in this system demonstrated moderate colouration in the solid state, with the colour intensity reduced or lost entirely upon melting. This confirmed that the equilibrium solid was the coloured state and that the molten phase was the decoloured state; the opposite behaviour was observed in CVL:DDG:TD-OH mixtures, which had decoloured equilibrium solids and coloured melts.

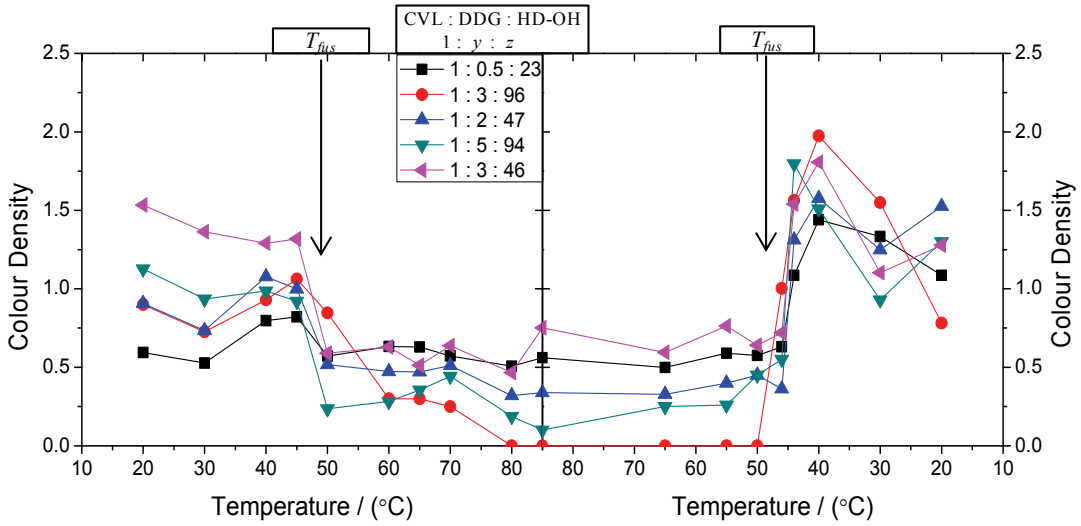

Figure 4.10. Colour density versus temperature plots obtained *via* colour photo analysis for samples in the CVL:DDG:HD-OH system. Note that these data were not normalized with a reflective white standard material. The molar ratios of the three components are given on the figure. Heating rates during these experiments were d*T*/d*t* = 1 K min^{-1}. T_{fus} represents the melting point of the pure solvent. Lines are added as a guide to the eye. Error in *CD* was estimated to be +/-0.15.

Subsequent cooling of the molten mixtures produced very strongly coloured metastable solid states upon transition to the LO-phase of the solvent. The metastable solid states were relatively short-lived, and the colour density decreased as the mixtures returned to the equilibrium solid state. The partial decolourization of the metastable solid occurred over the course of roughly 30 minutes, similar to the decolourization rates observed in previous studies on CVL:DDG:HD-OH mixtures.[101,102]

Colour contrast between the coloured and decoloured states of CVL:DDG:HD-OH mixtures was shown to be dependent on both the developer concentration and the solvent concentration. This is visualized in Figure 4.11, which shows colour images CVL:DDG:HD-OH samples at a variety of compositions.

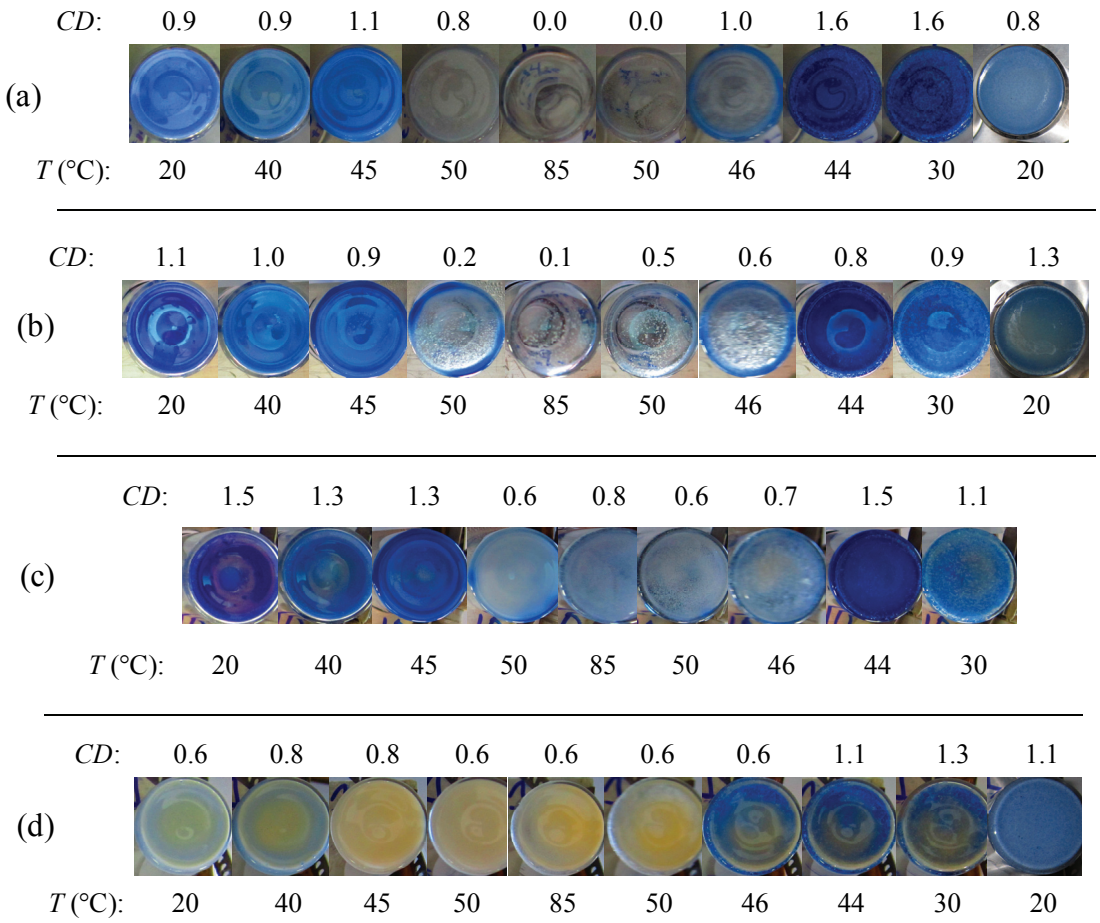

Figure 4.11. Colour photographs of CVL:DDG:HD-OH samples at a variety of compositions; (a) [1:3:96], (b) [1:5:94], (c) [1:3:46], and (d) [1:0.5:23].

The [1:3:96] sample (Figure 4.11(a)) and the [1:5:94] sample (Figure 4.11(b)) demonstrated the best thermochromic properties observed in the CVL:DDG:HD-OH system. In both, the melt was transparent and nearly completely colourless (CD_{Melt} = 0.0 to 0.1), the equilibrium solid was dark blue in colour (CD_{Equil} = 0.9 to 1.1), and the colour contrast (ΔCD = 0.9 to 1.0) was excellent. The ideal thermochromic behaviour of these samples indicates that CVL:DDG:HD-OH mixtures have potential utility in commercial applications, as the colour change observed upon switching between the coloured and decoloured states is dramatic. The behaviour observed in these samples is comparable to

that observed in the materials used in the Coors Light® beer bottle labels,[195,196] although the transition temperatures are shifted from ~ 5 to 10 °C to ~ 46 to 50 °C as a result of the different melting points of the solid solvents employed.[144]

Samples containing increased developer concentrations and/or decreased solvent concentrations (*e.g.*, [1:3:46]) were found to be darker in both the equilibrium solid state (CD_{Equil} = 1.5) and in the melt (CD_{Melt} = 0.7) when compared with fully decoloured samples (*e.g.*, [1:3:96]). The darkening of both the melt and solid state caused the overall colour contrast (ΔCD = 0.8) to remain similar to that of the [1:3:96] sample, but the increased colour density of the "decoloured state" reduced the overall thermochromic effect.

4.2.2.3.2 Fine Features of CVL:DDG:HD-OH Mixtures

Returning to Figure 4.10, which shows the colour density versus temperature plots, there was a broad spike in colour density for most samples just prior to solvent melting. This spike in colour density was also observed in the digital photographs, as seen in Figure 4.11 (a) at 45 °C. The increase in colour density here was a consequence of the solvent transitioning to the R-phase while in the water bath, and then back into the LO-phase upon removal from the bath. This caused the formation of a more intensely coloured, metastable solid state associated with LO-phase formation. A similar feature was noted in the discussion of the fine features of CVL:DDG:HD-OH mixtures studied *via* observational spectroscopy (*vide supra*, section 4.2.2.2.2), and is most prominent in the pre-melting behaviour of mixtures in the [1:*y*:30] compositional range (see Figure 4.7, bottom).

As the solvent melted (T_{fus} = 48 to 50 °C),[144] most samples immediately lost colour density, in agreement with the type of behaviour expected for this type of thermochromic system containing mismatched alkyl chain lengths. Samples which contained low developer concentrations (*e.g.*, the [1:0.5:23] and [1:2:47] samples in Figure 4.10) did not demonstrate high contrast between the equilibrium solid and the molten phase. This was attributed to the fact that the low developer concentration prevented strong colouration in the equilibrium solid and, therefore, the colour loss on melting was relatively small compared to samples with more intensely coloured solid states.

Conversely, the colour density of the [1:3:46] sample in Figure 4.11 (c), which contained a relatively high developer concentration, was found to increase slightly across the temperature range 60 °C ≤ T ≤ 85 °C before reaching a plateau at 85 °C. This behaviour was attributed to the enhanced solubility of the developer as the temperature of the mixture was raised, following the incomplete dissolution of the developer in the molten solvent upon initial solvent melting. Similar to the fine features observed in the TD-OH system, the [1:3:46] sample demonstrated high melt opacity despite solvent melting, indicating the presence of insoluble developer. This is evidenced by the white/blue colour of the melt of the [1:3:46] sample shown in Figure 4.11 (c).

Figure 4.11 (d) shows the colour images of the [1:0.5:23] sample. The most important feature to note here is the yellow colour of the melt. The yellow colour arose from the presence of insoluble CVL, which resulted from the low solvent concentration. In previous samples, the low solvent concentration resulted in poor developer dissolution in the melt. It is likely that some DDG also was insoluble in molten [1:0.5:23],

although it was difficult to identify the presence of the colourless developer due to the yellow colour of *leuco*-CVL. Furthermore, the developer concentration here is much lower than in the [1:3:46] sample, which showed opacity due solely to insoluble DDG as evidenced by the lack of yellow colouration (see Figure 4.11 (c)).

It is important to note that the colour density of samples which contain insoluble products does not fall to zero in the melt, even if no colour is observed due to the ring-opening reaction. Fortunately, the yellow colour associated with leuco-CVL and the white colour associated with insoluble gallates does not contribute significantly to the overall colour density. Even in these "non-white-adjusted" samples, the colour density of yellow coloured melts was below $CD_{\text{Melt}} = 0.6$, and would be much lower with white reference adjustment.

On cooling, the colour density of most samples was essentially invariant until the solvent solidified. Solidification of the solvent into the R-phase was not observed to cause immediate increases in colour density in most samples, as evidenced by the lack of colour formation in the centre of the samples at 46 °C, as shown in Figure 4.11. Colour formation at the exterior of the sample vials was indicative of transition from the solvent R-phase (which is glossy and weakly coloured) to the LO-phase (which is waxy/opaque and strongly coloured). The colour density of all samples shown in Figure 4.10 rapidly increased upon conversion from the R-phase to the LO-phase of the solvent. This increase in colour density matched the colour enhancement observed by MacLaren and Tang during thermal quenching experiments,[101,102] and conversion to the LO-phase of the solvent has been shown to promote enhanced colour formation in the ternary systems studied in this work.

4.2.2.4 Conclusions Concerning CVL:DDG:HD-OH Mixtures

The results presented in this section provide evidence that modifying the degree of alkyl chain length matching between the developer and solvent in CVL:gallate:alcohol systems can be used to control the colouring behaviour. In the CVL:DDG:HD-OH system, the equilibrium solid was almost always coloured, in stark contrast with the CVL:DDG:TD-OH system which demonstrated colourless equilibrium solids at virtually all compositions. In the case of CVL:DDG:HD-OH mixtures, the alkyl chain lengths differed by four carbon atoms, which appears to be near the threshold for inversion of colouring behaviour (*i.e.,* switching between melt-darkened and melt-lightened thermochromism).

The gross features observed in CVL:DDG:HD-OH mixtures include the observation that the equilibrium solid was coloured, that the melt can be fully decoloured or deeply coloured (depending on developer concentration), and that the metastable solid created by cooling the melt (or R-phase) to the LO-phase was the most highly coloured state observed, having a moderately long lifetime (decolourization times were on the order of 30 minutes). The best colour contrast (ΔCD_{Max} = 0.9 to 1.0) was obtained for mixtures with strongly coloured equilibrium solids and fully decoloured melts. In some cases, low developer concentrations prevented strong colouration in the solid state which reduced the overall thermochromic colour contrast. Conversely, high developer concentrations caused both the equilibrium solid and the melt to become more strongly coloured, which resulted in detrimental reductions in the overall thermochromic colour contrast.

Numerous fine features were observed for CVL:DDG:HD-OH mixtures. Moderate increases in colour density prior to solvent melting were observed due to conversion of the pre-melt R-phase to the LO-phase of the solvent when the samples were removed from the water bath, which generated a dark, metastable solid state. A steady increase in the melt colour density was observed for most samples as the melt was further heated due to increased developer solubility with increased solvent temperature. An increase in colour density was observed on transition from the R-phase to the LO-phase of the solvent during cooling due to the formation of a deeply coloured, metastable solid state. And lastly, rapid precipitation of the developer upon solvent solidification caused immediate decolourization in samples containing high developer concentrations (*e.g.*, [1:10:90] and [1:4:30]).

The developer concentration threshold, above which the melt is darker than the equilibrium solid and below which the melt is lighter than the equilibrium solid, is highly dependent on the solvent concentration. In $z = 90$ mixtures, the developer concentration threshold was $y \approx 6$. Decreasing the solvent concentration to $z = 60$, and thereby increasing the relative developer concentration, caused the threshold to fall to $y \approx 4$. Further decreasing the solvent concentration to $z = 30$ caused the threshold to drop to $y \approx 3$.

These results also indicate that the direction of colouring behaviour (*i.e.*, melt-lightened versus melt-darkened) in mixtures containing poorly matched alkyl chain lengths is critically dependent on the solvent concentration. Samples which contained higher solvent concentrations (*e.g.*, when $z = 90$ to 100) became decoloured in the melt more easily than samples with low solvent concentrations (*e.g.*, when $z \leq 30$).

Furthermore, due to the poor solubility of the dye and/or developer, at low solvent concentrations (*e.g.*, $z < 60$) the molten phase was much more likely to be opaque.

4.2.3 CVL:DDG:OD-OH Mixtures

4.2.3.1 Introduction to Studies on CVL:DDG:OD-OH Mixtures

Studies on the thermochromic properties of three-component mixtures containing OD-OH as the solvent have also been reported in the literature.[102,110] The behaviour of these mixtures, in the compositional range bound by $1 \leq y \leq 12$ and $25 \leq z \leq 76$, was very similar to that of the HD-OH mixtures[110]; the equilibrium solid was always coloured and the quenched metastable solid was more strongly coloured than the equilibrium solid. The decolourization times of OD-OH mixtures were substantially longer than those of HD-OH samples ($t_d > 24$ h) and the observed colour contrast between the equilibrium and metastable solids was very low. For this reason, thermochromic mixtures containing OD-OH, in the compositional range bound by $1 \leq y \leq 12$ and $25 \leq z \leq 76$, were considered to be of very poor quality.[101,102,110]

The previous studies on this system, however, were mainly concerned with the thermochromic colour changes associated with formation of an intensely coloured metastable solid from the melt, and the degree of colour contrast between the equilibrium solid and the quenched metastable solid. As a result, high colour contrast mixtures demonstrating coloured equilibrium solids and decoloured melts were not specifically identified for this ternary system.[101,102]

As was the case with HD-OH mixtures (section 4.2.2), the lengths of the solvent and developer alkyl chains are poorly matched in the CVL:DDG:OD-OH system (six

carbon atom difference). Therefore, the hypothesized colouring behaviour for the CVL:DDG:OD-OH system was that at sufficiently high solvent concentrations and sufficiently low developer concentrations, the equilibrium solid would be coloured and the melt would be decoloured. Increasing the developer concentration would increase the colour density of both states, until the developer concentration threshold was surpassed, causing the melt to become darker than the equilibrium solid, as had been observed in the CVL:DDG:HD-OH system.

4.2.3.2 Gross Features of CVL:DDG:OD-OH Mixtures

The results presented in this section were obtained *via* observational spectroscopy. Figure 4.12 shows colour density versus temperature plots for CVL:DDG:OD-OH samples with $z = 100$ (top), $z = 90$ (middle), and $z = 80$ (bottom). Based on the results discussed above for HD-OH mixtures, these samples demonstrated the behaviour hypothesized for mixtures containing poorly matched alkyl chain lengths.

For $z = 100$ samples, at low developer concentrations (*e.g.*, when $y \leq 5$), the melt became colourless and the colour density of the pre-melt equilibrium solid state was dependent on the developer concentration. Large developer concentrations (*e.g.*, when $y > 5$) caused the mixtures to retain some colour upon melting ($T_{\text{fus,OD-OH}} = 56$ to 59 °C),[144] thereby reducing colour contrast. The [1:10:100] sample was moderately coloured in the melt, particularly after the sample was heated to 70 °C, with the melt colour density ($CD_{\text{Melt}} = 0.5$ slightly lower than the equilibrium solid (where $CD_{\text{Equil}} = 0.9$). The behaviour of the [1:10:100] sample indicates that the developer concentration threshold, above which the melt is darker than the equilibrium solid, is near $y \approx 10$. The colour

contrast of the [1:10:100] sample (ΔCD = 0.4) was poor due to its proximity to the developer concentration threshold value.

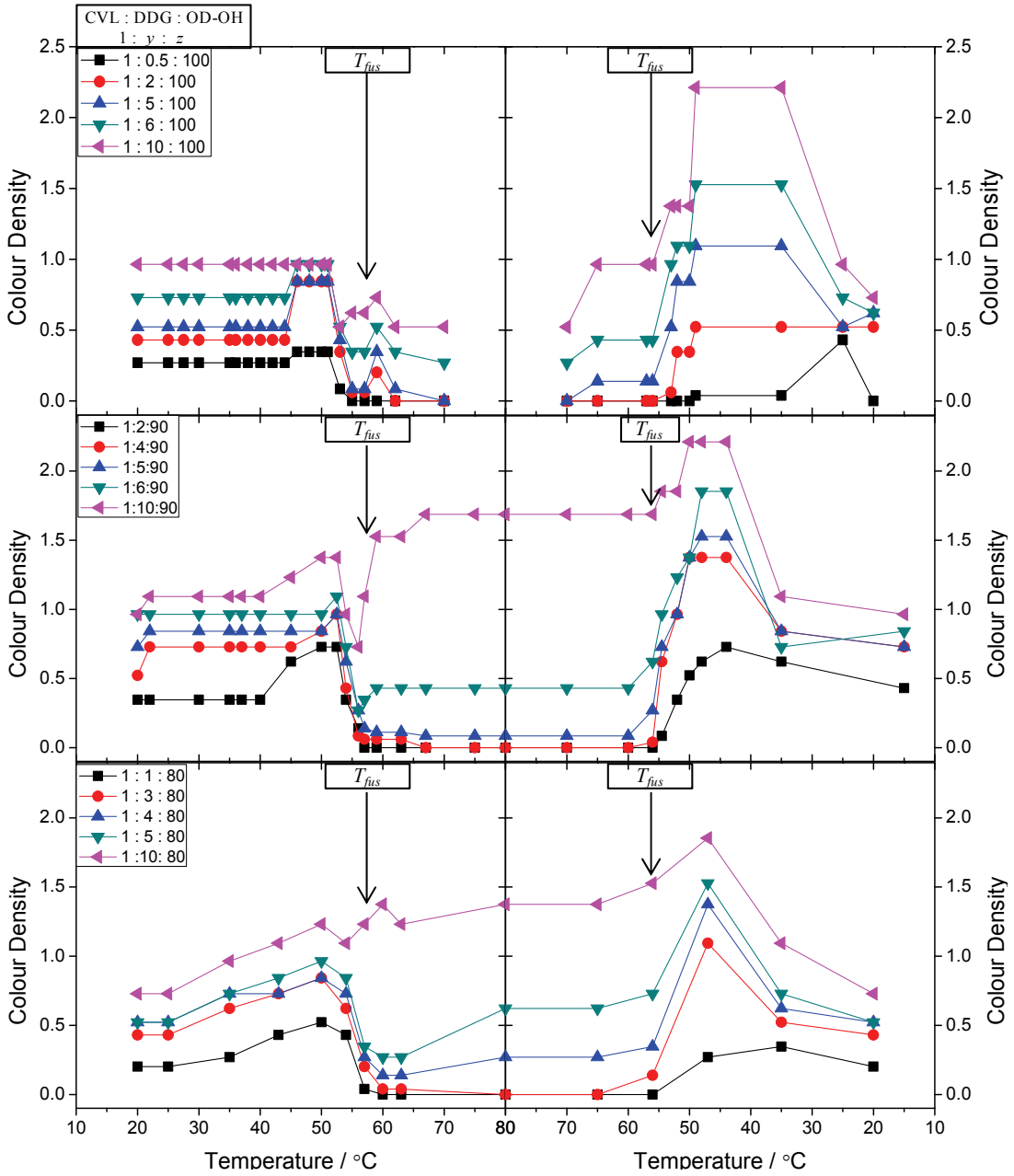

Figure 4.12. Colour density versus temperature plots obtained *via* observational spectroscopy for CVL:DDG:OD-OH samples in the [1:*y*:100] (top), [1:*y*:90] (middle), and [1:*y*:80] (bottom) compositional ranges. The molar ratios of the three components are given on the figure. Heating rates during these experiments were d*T*/d*t* = 1 K min^{-1}. T_{fus} represents the melting point of the pure solvent. Lines are added as a guide to the eye. Note: data were only collected to 70 °C for the [1:*y*:100] samples. Error in *CD* was estimated to be +/-0.15.

For samples with $z = 90$, behaviour similar to that of the $z = 100$ samples was observed, with increased colour densities of both the solid state and melt due to the decreased solvent concentration. The melt became completely colourless ($CD_{\text{Melt}} = 0$) when $y \leq 4$, which is slightly lower than was observed in samples with $z = 100$. Although not identified by the results shown in Figure 4.12 (middle), the developer concentration threshold, above which the melt is darker than the equilibrium solid, falls somewhere in the range of $6 \leq y \leq 10$. The colour density of the $[1:10:90]$ sample increased upon solvent melting (*i.e.*, melt-darkened), whereas melt of the $[1:6:90]$ sample was less strongly coloured than the equilibrium solid (*i.e.*, melt-lightened), indicating that the developer concentration threshold should fall in the $6 \leq y \leq 10$ range.

Figure 4.12 (bottom) shows the colour density versus temperature plots for samples with $z = 80$. The decreased solvent concentration had a number of influences including an increase in melt colour density at intermediate developer concentrations (*e.g.*, when $y = 4$ and 5), a decrease in the developer concentration threshold above which the melt was darker than the equilibrium solid (now at $y = 5$), and a decrease in the developer concentration required for a fully decoloured melt (reduced to $y \leq 3$).

Solidification of the solvent into the LO-phase caused large increases in the colour density of the majority of the samples. Upon transition from the melt to the R-phase ($T \approx 57$ to 55 °C), little change in the colour density was observed. Further cooling to $T < 55$ °C resulted in colour density increases, and was indicative of the formation of a deeply coloured, metastable solid state in which the solvent was in the LO-phase. Conversion to the equilibrium solid occurred overnight at 20 °C.

Good colour contrast between the coloured equilibrium solid and decoloured melt was observed in a number of samples. In particular, the [1:5:100] sample demonstrated decent colour contrast (ΔCD = 0.6) between the moderately coloured equilibrium solid (CD_{Equil} = 0.6) and the decoloured melt (CD_{Melt} = 0). The [1:5:90] sample also demonstrated good colour contrast (ΔCD_{Max} = 0.7) between a dark solid state (CD_{Equil} = 0.8) and a weakly coloured melt (CD_{Melt} = 0.1).

4.2.3.3 Fine Features of CVL:DDG:OD-OH Mixtures

On heating, many samples that contained intermediate developer concentrations (*e.g.*, y = 1 to 5) demonstrated spikes in colour density near the transition temperature of the LO-to-R phase transition. This behaviour was explained previously for the CVL:DDG:HD-OH system, and is due to the conversion of the R-phase of the solvent back to the LO-phase on removal from the water bath. A dark, metastable state containing the solvent in the LO-phase is responsible for the colour formation, and the colour was lost on subsequent R-phase reformation with increased temperature, particularly at temperatures just below the melting point of the pure solvent (T_{fus} = 56 to 59 °C).[144]

Returning to Figure 4.12 (top), which shows the colour density versus temperature plots for samples in the [1:y:100] compositional range, and focussing on the cooling portion of the figure, it is clear that the colour density of the molten mixtures increased across the 70 °C to 60 °C temperature range. This behaviour was explained for CVL:DDG:HD-OH mixtures as being a result of enhanced developer dissolution in the molten solvent, which caused increased colour density in the melt. This behaviour was

also shown to a lesser extent for [1:y:80] mixtures (Figure 4.11 (bottom)), but curiously for [1:y:90] mixtures (Figure 4.11 (middle)). Nevertheless, increased solvent temperatures caused increased dissolution of the colour forming components, promoting colour formation in the melt.

Looking at the data for [1:y:100] samples with y = 2, 5, and 6 samples, it is clear that there was a levelling off in post-solidification colour density after the immediate colour density increase. This plateau is indicative of the formation of the LO-phase from the R-phase, and the colour density decrease which occurs just after the plateau was attributed to precipitation of the developer and a move towards the equilibrium solid state. Similar behaviour was shown for [1:y:90] samples, where the initial spike in colour density was followed by a brief plateau, before reduction of colour density to near equilibrium values.

4.2.3.4 Conclusions Concerning CVL:DDG:OD-OH Mixtures

The results presented in this section provide further evidence that mixtures containing substantially mismatched developer and solvent alkyl chain lengths can be coloured in the equilibrium solid and decoloured in the melt. As was the case with the HD-OH system, the developer concentration is the defining factor in determining if the melt will be darker than the equilibrium solid. There is a developer concentration threshold above which the melt is darker than the equilibrium solid. In the case of z = 100 mixtures, this threshold value was y > 10. As the solvent concentration was decreased to z = 90, the developer concentration threshold decreased to a value between y = 6 and y = 10. At z = 80, the developer concentration threshold dropped to $y \approx 5$. The decrease in the

developer concentration threshold was therefore shown to be solvent concentration dependent, which is understandable since decreasing the solvent concentration causes relative increases in both the developer and dye concentrations.

In the CVL:DDG:OD-OH system, the solid state was almost always coloured, in stark contrast with the CVL:DDG:TD-OH system which demonstrated colourless equilibrium solids at virtually all compositions. In the case of CVL:DDG:OD-OH mixtures, the alkyl chain lengths differ by six carbon atoms, which is above the threshold for inversion of colouring behaviour (*i.e.,* switching from melt-darkened to melt-lightened thermochromism).

The gross features demonstrated by samples in the CVL:DDG:OD-OH system include the observation that the equilibrium solid was coloured, the melt can be fully decoloured or deeply coloured (depending on the developer concentration), and the metastable solid created by cooling to the LO-phase of the solvent was the most strongly coloured form of the mixture and had a much longer lifetime than those observed in TD-OH or HD-OH mixtures. Decolourization times were on the order of 12 hours.

The fine features observed for CVL:DDG:OD-OH mixtures include increased colour density upon transition to the LO-phase from the melt, the rapid precipitation of developer and/or dye upon solvent solidification in samples with high developer concentration (e.g. the [1:10:90] and [1:10:100] samples), and the steady increase in colour density of most samples as the melt was further heated due to increasing developer and dye dissolution with increased solvent temperature.

In the CVL:DDG:OD-OH system, it was possible to obtain a decoloured melt and coloured equilibrium solid (*i.e.*, melt-lightened behaviour) if the concentrations of the

three components fell within the appropriate ranges. When the developer concentration was sufficiently low and the solvent concentration sufficiently high, the equilibrium solid was the coloured state and the melt was completely decoloured. If the developer concentration was very high, the melt became darker than the equilibrium solid. In both of these cases, the overall colour density of the coloured state was controlled by the amount of developer present, and the colour contrast between the two states was highly dependent on the solvent concentration. Moderate colour contrast ($\Delta CD_{Max} = 0.7$) was obtained (for the [1:5:90] sample) for CVL:DDG:OD-OH mixtures, a value which likely could be optimized further with careful selection of the concentration of each component of the thermochromic mixture.

4.3 Summary of the Influence of Solvent Alkyl Chain Length

The results presented in this chapter provide useful insights into the colouring behaviour of three-component thermochromic mixtures in CVL:DDG:alcohol systems. Based on the experimental results presented here, it is apparent that the colouring behaviour, *i.e.*, melt-lightened vs. melt-darkened thermochromism, can be controlled by modifying the degree of alkyl chain length matching in dye:developer:solvent systems.

In the TD-OH system, the alkyl chains attached to the gallate and alcohol varied in length by only two carbon atoms, producing a system with well-matched alkyl chain lengths. In the case of well-matched alkyl chain lengths, the equilibrium solid was always observed to be the decoloured state. The colour of the melt was controlled by the developer concentration. Low developer concentrations produced mixtures with little to no colour in the melt coupled with colourless equilibrium solids. Increasing the developer

concentration caused the melt to become coloured, yielding melt-darkened thermochromism. Further increases in the developer concentration caused the decoloured equilibrium solid to gain colour, thereby reducing the overall colour contrast observed in the mixture, a decidedly detrimental effect for a thermochromic material.

Increasing the chain length of the alkyl alcohol increased the degree of alkyl chain length mismatch in both the HD-OH (four carbon atom difference) and OD-OH (six carbon atom difference) systems, which resulted in an inversion of the colouring behaviour at compositions. In mixtures containing mismatched alkyl chain lengths, the equilibrium solid usually was observed to be the coloured state and the melt was the decoloured state, yielding melt-lightened thermochromism. Since the colour density of both states was highly dependent on the developer concentration, and the equilibrium solid was almost always coloured, no mixture demonstrating a coloured melt and colourless equilibrium solid was observed in HD-OH or OD-OH systems with DDG as the developer.

In all of the studied HD-OH and OD-OH systems, there was a developer concentration threshold above which the melt was darker than the equilibrium solid, resulting in behaviour similar to that observed in the TD-OH system (*i.e.*, melt-darkened thermochromism). Below this developer concentration threshold, the melt was less strongly coloured than the equilibrium solid (*i.e.*, melt-lightened thermochromism).

The developer threshold value was shown to decrease with decreasing solvent concentration. In the CVL:DDG:HD-OH system, at $z = 90$ the threshold value was $y \approx 6$. At $z = 60$, the threshold value dropped to $y \approx 4$, and in $z = 30$ samples, the threshold value had dropped to $y \approx 3$. The steady decrease in developer concentration threshold with

decreasing solvent concentration provides an experimental key to obtaining good control of colouring behaviour in these types of reversibly thermochromic systems.

The threshold values obtained for OD-OH mixtures were similar to those obtained for HD-OH mixtures. In the OD-OH system, at $z = 100$ the threshold value was $y > 10$. At $z = 90$, the threshold value had dropped to $6 \leq y \leq 10$, and at $z = 80$, the threshold value dropped further to $y \approx 5$.

In the CVL:DDG:TD-OH system, the equilibrium solid was colourless at most compositions, therefore the developer concentration threshold of interest involved colour formation in the melt. In mixtures with $z = 60$, the developer:dye molar ratio was required to be above $y = 2$ for the development of colour in the melt. Increasing the solvent concentration to $z = 90$ caused the developer threshold value to increase to $y = 4$, although the colour density of the melt at the developer concentration threshold was very low ($CD_{\text{Melt}} = 0.1$).

The fine features associated with mixtures in the TD-OH, HD-OH, or OD-OH systems were fairly consistent across the three solvents. While in the molten phase, the colour density of coloured melts generally increased as the temperature of the heating bath was further increased due to a combination of increased developer dissolution into the solvent and also enhanced melting of the developer as the melting point of the long-chain gallate was approached.

In general, transition to the R-phase of the solvent from the LO-phase (on heating) caused a slight decrease in the colour density of the mixtures. It was noted, however, that when the temperature of the mixture was near to the LO-to-R phase transition temperature, removing the sample from the water bath caused the solvent to transition

from the R-phase back into the LO-phase. This generated a metastable solid state that was strongly coloured, before additional heating caused the R-phase to return and the colour density to be reduced, prior to solvent melting. Alternatively, transition to the R-phase of the solvent from the melt (on cooling) had little impact on the colour density and usually the colour density of the melt was maintained.

On cooling, conversion of the R-phase to the LO-phase promoted colour density increases in most samples. The conversion to the LO-phase caused a "freezing-in" of the coloured complex, akin to the effect of thermal quenching with liquid nitrogen studied by MacLaren, Tang, and White, which was shown to cause large increases in the colour density of similar mixtures.[101,102] At high developer concentrations, the transition from the R-phase to the LO-phase on cooling caused the rapid precipitation of developer, yielding dramatic decreases in colour density immediately upon transition to the LO-phase. Nevertheless, decolourization rates of the metastable solid produced by conversion to the LO-phase were strongly dependent on the solvent used, with the decolourization rates dramatically decreasing as the solvent alkyl chain length was increased.

The results presented in this chapter lead to an interesting question: if changing the length of the alkyl chain attached to the alcohol solvent can play such a substantial role in controlling the colouring behaviour of three-component thermochromic mixtures, does modifying the length of the alkyl chain attached to the alkyl gallate have a similarly significant impact on the colouring behaviour? Chapter 5 explores the influence of changing the length of the alkyl chain attached to the alkyl gallate on the colouring behaviour of such reversible three-component thermochromic mixtures.

Chapter 5 Influence of Developer Chain Length on Thermochromic Behaviour

5.1 Introduction

Chapter 4 discussed the influence of changing the length of the solvent alkyl chain on the thermochromic behaviour of three-component systems by comparing mixtures containing TD-OH (section 4.2.1) with mixtures containing HD-OH (section 4.2.2) and OD-OH (section 4.2.3). Using DDG as the developer, it was observed that increasing the alkyl chain length of the solvent from 14 carbon atoms (TD-OH) to 16 or 18 carbon atoms (HD-OH and OD-OH, respectively) caused the thermochromic behaviour to change dramatically.

When the alkyl chain lengths were well-matched (*e.g.*, DDG with TD-OH), melt-darkened thermochromic behaviour was observed. In these samples, the equilibrium solid state was decoloured with the mixture gaining colour as the solvent melted. Conversely, when the lengths of the alkyl chains were poorly matched (*e.g.*, DDG with HD-OH and OD-OH), the type of thermochromic behaviour observed was dependent on the relative concentrations of the developer and solvent, with a developer concentration threshold separating the melt-lightened regime (at low developer loading) from the melt-darkened regime (at high developer loading). In both instances, the equilibrium solid state usually was coloured and the colour of the melt was dependent on the relative concentration of the developer.

To study the influence of modifying the developer alkyl chain length, alkyl gallates of varying chain length were employed as developers. Table 5.1 lists the alkyl gallate developers used in these experiments, where the alkyl chain lengths vary from 18

carbon atoms (ODG) to zero carbon atoms (GA). The three alcoholic solvents used were TD-OH, HD-OH, and OD-OH (see Table 4.1), and CVL was used as the dye component, as before.

Table 5.1. Melting points and alkyl chain lengths of various alkyl gallate developers.

Name	Abbreviation	Alkyl Chain	Melting Point / (°C) Literature[128-131]	Melting Point / (°C) Present Result
Gallic Acid	GA	H	251 – 252	254 – 260 (decomp)
Propyl Gallate	PG	C_3H_7	146 – 149	149 – 151
Octyl Gallate	OG	C_8H_{17}	101 – 104	95 – 98
Dodecyl Gallate	DDG	$C_{12}H_{25}$	96 – 97	97 – 99
Octadecyl Gallate	ODG	$C_{18}H_{37}$	102 – 104	102 – 104

In instances of well-matched alkyl chain lengths (*e.g.*, ODG with OD-OH), melt-darkened behaviour is hypothesized. In the solid state, the alkyl chains attached to the developer and solvent undergo van der Waals interactions allowing for tight packing of the alkyl chains. The close-packed arrangement of the alkyl chains, coupled with hydrogen-bonding interactions between the phenolic protons of the gallate and the hydroxyl protons of the alcohol, causes the formation of a strongly interacting developer:solvent complex, which sequesters the developer from the dye while in the solid state, thereby preventing colour formation. The formation of these developer:solvent complexes was confirmed by MacLaren and White, who used DSC to elucidate the binary phase behaviour of developer:solvent mixtures composed of alkyl gallates and alkyl alcohols.[101,110,143] Melting of the solid mixture liberated the developer and, when the developer concentration was sufficiently high, colour was formed in the melt.

In instances of poorly matched alkyl chain lengths (*e.g.*, PG with TD-OH, OG with OD-OH, *etc.*), the hypothesized thermochromic behaviour is that at high developer and low solvent concentrations, melt-darkened behaviour will be observed. Conversely, at low developer and high solvent concentrations, melt-lightened behaviour could be observed. Additionally, at a given solvent concentration, a developer concentration threshold would separate the melt-lightened and melt-darkened thermochromic regimes. This type of behaviour was observed for both the CVL:DDG:HD-OH and CVL:DDG:OD-OH systems.

In the solid state, the dissimilar lengths of alkyl chain attached to the developer and solvent prevent attractive alkyl chain packing interactions, thereby inhibiting the formation of a developer:solvent complex.[101,110] As a result, the developer is not sequestered by the solvent and is free to develop the dye (*i.e.*, generate colour) in the solid state. As the solvent melts, the developer can either dissolve into the solvent and diffuse away from the dye (yielding melt-lightened behaviour) or, or in the case of high developer concentration, can cause further darkening of the mixture (melt-darkened behaviour) by reacting with free *leuco*-CVL.

5.2 Experimental Results and Discussion

5.2.1 Octadecyl Gallate (ODG) Mixtures

Although no previous investigations into the thermochromic behaviour of CVL:ODG:alcohol systems have been reported in the literature, some predictions about the colouring behaviour of ODG-containing systems can be made based on the studies of CVL:DDG:alcohol systems.[101,102,110,143]

In the case of CVL:ODG:OD-OH mixtures, the lengths of the alkyl chains are perfectly matched (there is no difference in chain length) indicating that these mixtures would demonstrate melt-darkened thermochromism. This type of behaviour is also likely to be observed in the CVL:ODG:HD-OH system, due to the good alkyl chain length matching (two carbon atom difference) in this system. The CVL:DDG:TD-OH system (section 4.2.1) had alkyl chains which differed in length by only two carbon atoms and demonstrated melt-darkened thermochromic behaviour, so this behaviour is also hypothesized for the CVL:ODG:HD-OH system.

Colouring behaviour in the CVL:ODG:TD-OH system cannot so easily be predicted based solely on alkyl chain length difference (four carbon atom difference). Although the chain lengths are similar, previous studies on the CVL:DDG:HD-OH system (section 4.2.2) showed that when the alkyl chain lengths differed by four carbon atoms, the observed thermochromic behaviour (*i.e.* melt-lightened vs. melt-darkened) was strongly dependent on the developer concentration. Due to the difference in alkyl chain length (four carbon atom difference), this type of developer concentration-dependent thermochromic behaviour was anticipated for CVL:ODG:TD-OH mixtures.

5.2.1.1 CVL:ODG:TD-OH Mixtures

5.2.1.1.1 Gross Features of CVL:ODG:TD-OH Mixtures

Figure 5.1 shows the colour density versus temperature plots for samples in the CVL:ODG:TD-OH ternary system. Contrary to expectations, melt-darkened thermochromic behaviour was observed for this system. Nearly of the samples in the CVL:ODG:TD-OH system were completely colourless in the solid state, and when the

developer concentration was sufficiently high (*e.g.*, when $y \approx 6$), the melt became strongly coloured.

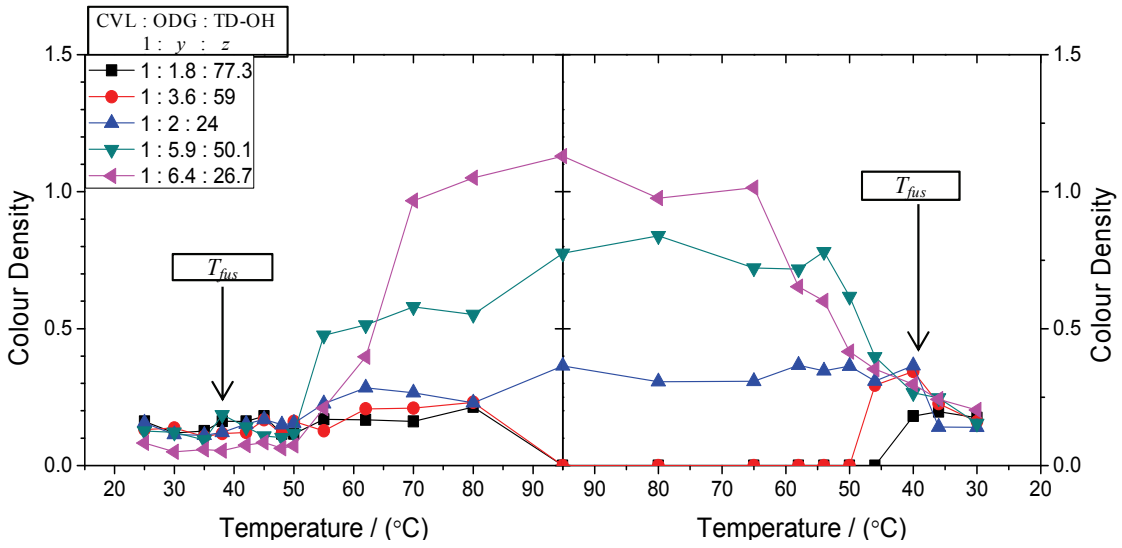

Figure 5.1. Colour density versus temperature plots obtained via colour photo analysis for samples in the CVL:ODG:TD-OH system. The molar ratios of the three components are given on the figure. Heating rates during these experiments were dT/dt = 1 K min^{-1}. T_{fus} represents the melting point of the pure solvent. Lines are added as a guide to the eye. Error in *CD* was estimated to be +/-0.15.

The colour density of samples which demonstrated colouration in the melt was observed to increase gradually as the temperature of the mixtures was increased, reaching a maximum colour density at the maximum temperature of the heating bath (T_{max} = 95 °C). The colour density was maintained during cooling in most samples (not all data are shown here), until the freezing point of the solvent was reached, at which point the colour density dropped, returning the colour density of the equilibrium solid.

Due to the lack of colour in the solid state, and the strong colouration of some samples in the melt, very high colour contrast was obtained. In particular, the [1:6.4:26.7] sample demonstrated very good colour contrast, with a large colour density difference (ΔCD = 1.1) between the coloured melt (CD_{Melt} = 1.2) and decoloured

equilibrium solid (CD_{Equil} = 0.1). This level of contrast was higher than that observed in a similar compositional range in the CVL:DDG:TD-OH system (ΔCD_{max} = 0.7). The high degree of colour contrast is visualized by the colour photos shown in Figure 5.2 (a).

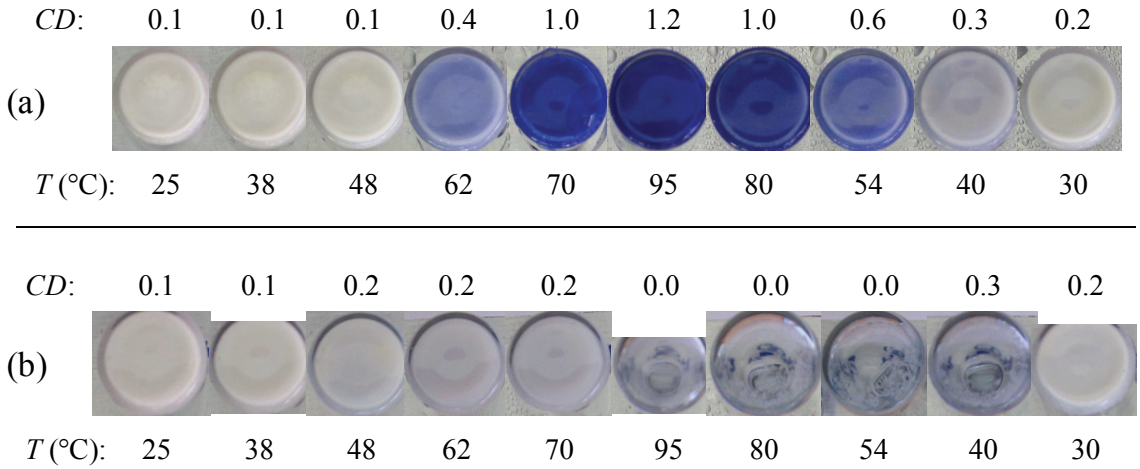

Figure 5.2. Colour photographs of CVL:ODG:TD-OH samples at compositions of (a) [1:6.4:26.7] and (b) [1:3.6:59].

5.2.1.1.2 Fine Features of CVL:ODG:TD-OH Mixtures

Figure 5.2 shows colour images of two samples in the CVL:ODG:TD-OH system. The sample shown in Figure 5.2 (b), at a composition of [1:3.6:59], was colourless in both the melt and the solid state. This is a result of the low developer concentration and relatively high solvent concentration. This sample can be compared with the sample in Figure 4.6 in the CVL:DDG:TD-OH system (section 4.2.1.3.2), which had a similar composition of [1:3.5:45.5]; the colouring behaviour is quite different. The CVL:DDG:TD-OH sample demonstrated light colouration in the melt, whereas the CVL:ODG:TD-OH sample was not coloured at any temperature. Both of the samples,

however, demonstrated the high melt opacity associated with poor developer solubility in the molten solvent.

For the sample shown in Figure 5.2 (a), at a composition of [1:6.4:26.7], the strongest colour observed in the melt was obtained at the highest temperature accessible on the water bath, T = 95 °C, indicating enhanced developer solubility at this elevated temperature. Additionally, increased developer solubility could be coupled with enhanced melting of the developer as the melting point of the developer ($T_{fus,ODG}$ = 104 to 105 °C)[128] was approached.

Inhomogeneous precipitation of the developer from the molten solvent at near-solidification temperatures caused the significant colour density decreases observed on cooling for the [1:6.4:26.7] and [1:5.9:50.1] samples. Figure 5.2 (a) showed that ODG did not fully dissolve in the molten TD-OH, due largely to the low solvent concentrations (*e.g.*, when $z \approx 25$). As the temperature of the solvent decreased, dissolved ODG began to inhomogeneously precipitate from solution well above the solvent freezing point (colour loss due to developer precipitation occurred at $T \approx$ 60 to 50 °C). Similar decolourization due to developer precipitation was noted for the [1:5.9:50.1] sample at $T \approx$ 50 to 45 °C.

The R-phase of the solvent did not play a significant role in the fine features of thermochromic behaviour in this system, which was not surprising given that R-phase transitions also had little impact on the colouring behaviour in the CVL:DDG:TD-OH system.

5.2.1.1.3 Conclusions Concerning CVL:ODG:TD-OH Mixtures

Thermochromic behaviour in this system followed the general trends observed for melt-lightened thermochromic mixtures as a result of attractive developer:solvent interactions in the solid state. The equilibrium solid was always decoloured, the melt could become coloured at high developer concentrations, and excellent colour contrast ($\Delta CD_{max} = 1.1$) was obtained at high developer and low solvent concentrations. The developer was only partially soluble in the molten solvent at near-melting temperatures, as evidenced by the high opacity of freshly molten mixtures, although heating to temperatures near the melting point of the gallate promoted developer dissolution and deepening of the colour of the melt.

Developer precipitation prior to solvent solidification was observed in samples containing low solvent concentrations, due to the poor solubility of the developer. This resulted in colour density decreases in samples with $z \approx 25$ prior to solvent solidification. This decrease was not observed in samples with $z > 50$, due to the complete dissolution of the developer in the molten solvent. The pre-solidification decrease in colour density was attributed to inhomogeneous precipitation of the developer from the molten solvent.

In this system, unlike those previously studied (*e.g.*, the CVL:DDG:alcohol systems), transition of the solvent to its R-phase had little impact on the fine features of the thermochromic behaviour. The reason for the lack of R-phase influence in this system is not yet understood, but could be related to the packing structure of the developer:solvent complex in the solid state. A tightly bound developer:solvent complex, with alkyl chains packed tightly in the solid state, could prevent the developer from

becoming more mobile in the temperature regime of the R-phase, precluding colour enhancement in the solid state.

5.2.1.2 CVL:ODG:HD-OH Mixtures

5.2.1.2.1 Gross Features of CVL:ODG:HD-OH Mixtures

The colouring behaviour observed in the CVL:ODG:HD-OH ternary system agreed with the hypothesized behaviour, as most of these samples demonstrated the melt-darkened thermochromic behaviour. Figure 5.3 shows the colour density versus temperatures plots for selected samples in the CVL:ODG:HD-OH system. The equilibrium solid colour densities were very near to zero ($CD_{Equil} < 0.2$), indicating that the solid states were essentially colourless at most compositions. High melt colour densities were achieved at high developer and low solvent concentrations.

Colourless melts were also observed in this system as a result of high solvent concentration (*e.g.* the [1:5.1:82.4] sample) and low developer concentration (*e.g.*, the [1:1.9:47.5] sample). In these mixtures, the developer became completely dissolved in the solvent, preventing the formation of the coloured dye:developer complex in the melt.

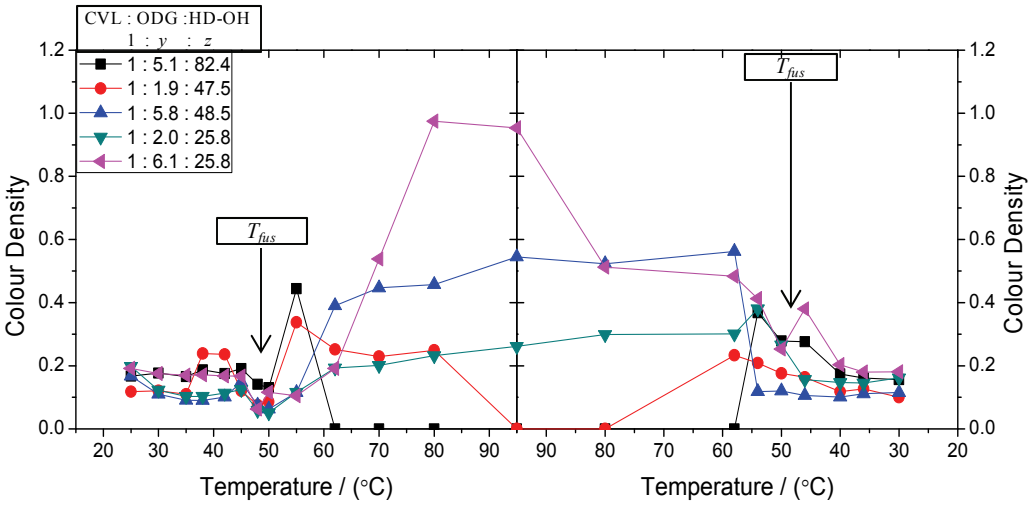

Figure 5.3. Colour density versus temperature plots obtained *via* colour photo analysis for samples in the CVL:ODG:HD-OH system. The molar ratios of the three components are given on the figure. Heating rates during these experiments were d*T*/d*t* = 1 K min^{-1}. T_{fus} represents the melting point of the pure solvent. Lines are added as a guide to the eye. Error in *CD* was estimated to be +/-0.15.

High colour contrast mixtures were easily accessible in this system due to the nearly colourless equilibrium solids. The [1:6.1:25.8] sample displayed the best colour contrast (ΔCD = 0.8), as a result of a weakly coloured equilibrium solid (CD_{Equil} = 0.2) and a strongly coloured melt (CD_{Melt} = 1.0). However, the maximum colour density of this sample was not maintained across the entire temperature range and was only achieved between 80 and 95 °C. The reason for this is the poor solubility of the developer in the molten solvent, which caused inhomogeneous precipitation of the developer from the melt prior to solvent solidification. Other mixtures containing much less developer, or more solvent, demonstrated more consistent colour density across the entire temperature due to the complete dissolution of the developer in the molten solvent.

5.2.1.2.2 Fine Features of CVL:ODG:HD-OH Mixtures

Figure 5.4 shows colour images of the [1:5.8:48.5] and [1:6.1:25.8] samples. These samples demonstrated very light colouration in the solid state, the formation of a coloured state upon melting, and the subsequent loss of colour prior to solidification of the solvent due to precipitation of the developer from the molten mixture. The colour density of the melt increased as the samples were further heated to 95 °C, which was coupled with reduced opacity for the [1:5.8:48.5] sample. As discussed in Chapter 4, the latter feature is a result of both enhanced developer solubility in the melt and melting of the developer as the melting point of the developer was approached.

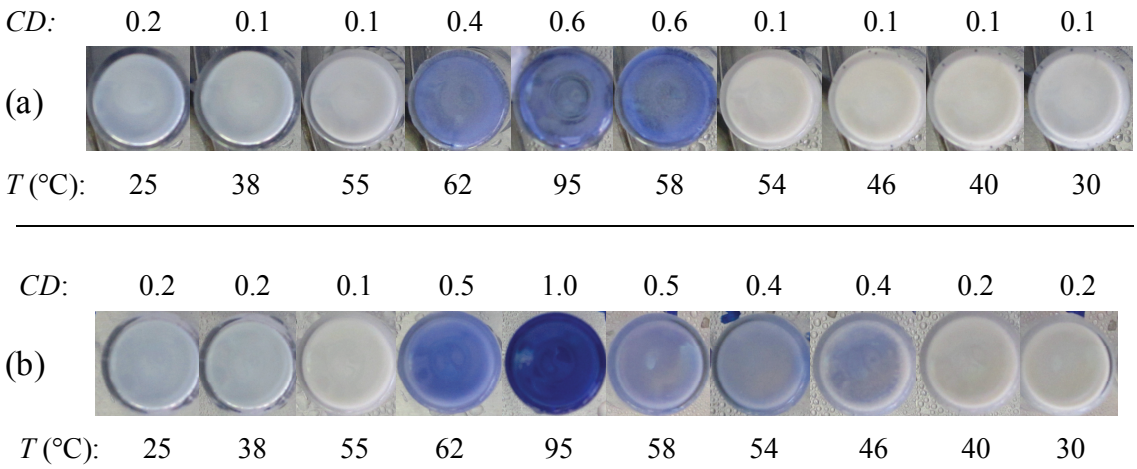

Figure 5.4. Colour photographs of the CVL:ODG:HD-OH samples at compositions of (a) [1:5.8:48.5] and (b) [1:6.1:25.8].

The samples shown in Figure 5.4 both underwent colour density decreases prior to the solidification of the solvent ($T_{fus,HD\text{-}OH}$ = 48 to 50 °C).[144] This was the result of the precipitation of the developer from the molten solvent during cooling due to the low solvent concentrations (*e.g.*, z = 25 to 50) and high developer concentrations (*e.g.*, $y \approx 6$). Similar behaviour was observed in the CVL:ODG:TD-OH system (section 5.2.1.1, Figure

5.2) for samples containing low solvent concentrations (*e.g.*, the [1:6.4:26.7] sample). It is evident that high solvent concentrations (*e.g.*, $z > 60$) coupled with high developer concentrations (*e.g.,* $y > 6$) are required to generate strong colour formation in the melt and to obtain good developer solubility to ensure consistent colouration across the entire temperature range of the molten mixture.

The solvent R-phase generally played a small role in the fine features of colouring behaviour in this system. During the initial heating portion of the heat-cool cycle, little change in the colour density upon transition from the solvent LO-phase to the R-phase was observed for most samples. Colour was only formed after melting of the solvent and dissolution of the developer. Prior to melting, the developer was sequestered by the solvent due to the presence of developer:solvent complexes.

Thermal analysis of HDG:HD-OH binary mixtures[§] demonstrated the existence of a developer R-phase in the developer rich region (x_{HDG} = 0.9 to 1) of the binary phase diagram, but only the freezing transition was observed at the compositions used in three-component mixtures (x_{DEV} = 0.05 to 0.20), therefore the developer R-phase was not considered to have a significant impact on the colouring behaviour in ODG mixtures.

On cooling from 95 °C, the colour density of most samples remained nearly invariant until the freezing point of the solvent was reached. At this temperature, samples containing relatively low developer concentrations (*e.g.*, [1:5.1:82.4] and [1:1.9:47.5]) experienced a spike in colour density associated with partial precipitation

[§] Thermal analysis *via* DSC was carried out in the present work, but is not reported here as HDG was not used as a developer in thermochromic mixtures.

of the developer. This spike in colour density was maintained through the R-phase and into the LO-phase of the solvent, before being lost as the equilibrium state of the mixture was returned on further cooling. Conversely, ODG rapidly precipitated from samples containing high developer concentrations (*e.g.*, [1:5.8:48.5]) prior to solvent solidification, as evidenced by the decrease in colour density of these samples at temperatures above the literature freezing point of the solvent ($T_{fus,HD\text{-}OH}$ = 48 to 50 °C).

5.2.1.2.3 Conclusions Concerning CVL:ODG:HD-OH Mixtures

The thermochromic behaviour in this ternary system agreed with the hypothesized behaviour. As a result of the well-matched alkyl chain lengths attached to ODG and HD-OH, these mixtures demonstrated melt-darkened thermochromism, and high colour contrast (ΔCD_{max} = 0.8) could be obtained due to the low colour density of the solid state.

The developer had poor solubility in the molten solvent, which gave rise to high melt opacity at temperatures near the melting point of the solvent. Increasing the temperature of the solvent caused the developer to become more dissolved in the solvent, which generally reduced the opacity and increased the colour density of the molten mixture. Also, in accord with behaviour observed in the CVL:ODG:TD-OH system, the solvent R-phase in these samples had little influence on the colouring behaviour of the solid state, with negligible changes in colour density observed upon transition to the R-phase on heating, and little change in the colour density upon transition from the melt (*i.e.*, on cooling).

5.2.1.3 CVL:ODG:OD-OH Mixtures

5.2.1.3.1 Gross Features of CVL:ODG:OD-OH Mixtures

Figure 5.5 shows the colour density versus temperature plots for samples in the CVL:ODG:OD-OH system. The equilibrium solids were very weakly coloured and darkened upon solvent melting, with the colour density of the melt dependent on the developer and solvent concentrations. Very good colour contrast was obtained in samples containing high developer and low solvent concentrations. In particular, the [1:5.9:25.2] sample demonstrated high colour contrast (ΔCD = 0.8) between the coloured state (CD_{Melt} = 0.9) and the decoloured state (CD_{Equil} = 0.1).

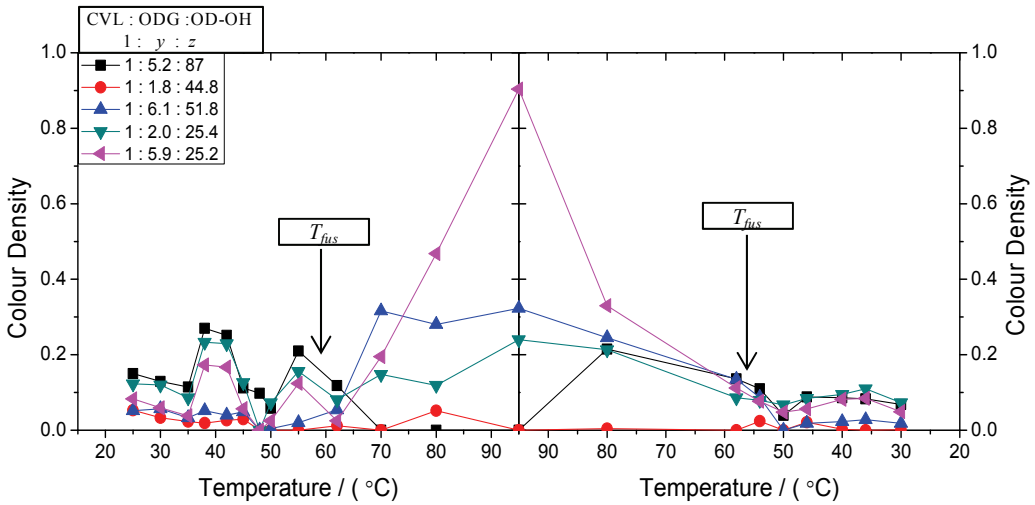

Figure 5.5. Colour density versus temperature plots obtained *via* colour photo analysis for samples in the CVL:ODG:OD-OH system. The molar ratios of the three components are given on the figure. Heating rates during these experiments were d*T*/d*t* = 1 K min^{-1}. T_{fus} represents the melting point of the pure solvent. Lines are added as a guide to the eye. Error in *CD* was estimated to be +/-0.15.

5.2.1.3.2 Fine Features of CVL:ODG:OD-OH Mixtures

The colouring behaviour of the CVL:ODG:OD-OH sample at a composition of [1:5.9:25.2] was nearly identical to that of the CVL:ODG:HD-OH sample at a

composition of [1:6.1:25.8]. Both samples demonstrated high colour contrast ($\Delta CD_{\max}$ = 0.8 for both) and deep colouration at the highest temperature of the heat-cool cycle (T_{max} = 95 °C), and in both cases the colour was not maintained across the entire temperature range of the melt due to inhomogeneous precipitation of the developer as the melt was cooled.

A difference between this system and the CVL:ODG:HD-OH system, was that virtually all CVL:ODG:OD-OH samples that were coloured in the melt demonstrated colour loss prior to solvent solidification. CVL:ODG:HD-OH mixtures underwent decolourization of the melt only in samples with high developer concentration (*e.g.*, when $y \approx 6$) and fairly low solvent concentrations (*e.g.*, when $y \leq 50$). Pre-solidification colour loss is indicative of inhomogeneous precipitation of the developer from the molten solvent, suggesting that ODG has lower solubility in OD-OH than in HD-OH.

Figure 5.6 shows colour photos of the [1:5.2:87] and [1:5.9:25.2] samples. In the [1:5.2:87] sample, the dye:developer ratio in this mixture was large enough that colour could have developed in the melt, but the high solvent concentration prevented colour formation. The equilibrium solid in this mixture was weakly coloured, although not so much as to define the equilibrium solid as the "coloured state" for these mixtures. Nevertheless, the melt was colourless and this sample was effectively always decoloured.

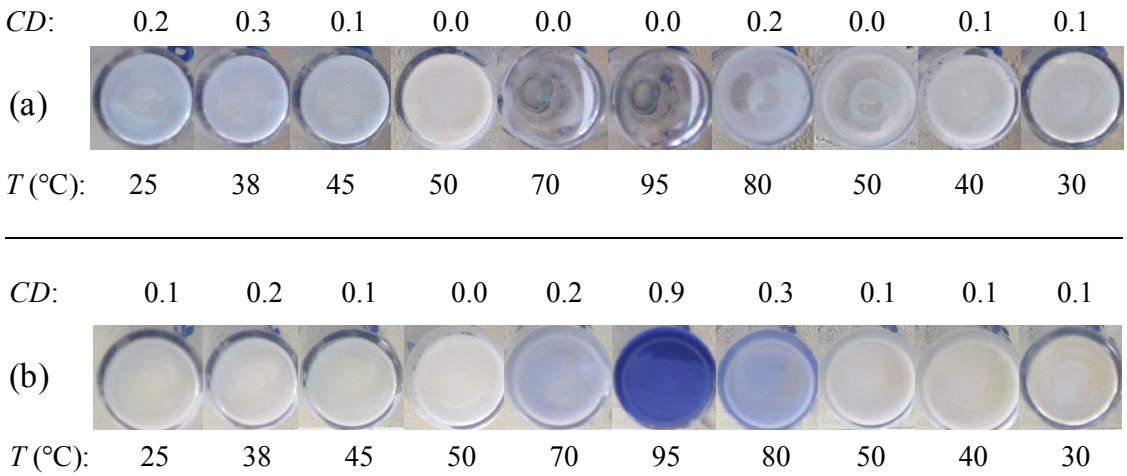

Figure 5.6. Colour photographs of the CVL:ODG:OD-OH samples at compositions of (a) [1:5.2:87] and (b) [1:5.9:25.2].

A sharp decrease in the solvent loading resulted in a large relative increase in both the CVL and developer concentrations, which resulted in the formation of a coloured melt. Figure 5.6 (b) shows colour images of the [1:5.9:25.2] sample. In this sample, the equilibrium solid was colourless and the melt became strongly coloured at the highest temperature reached by the water bath due to enhanced developer dissolution. Furthermore, approaching the melting point of the developer likely increased the miscibility of previously insoluble developer with the molten solvent, which further increased colour density in the melt.

Once again, the solvent R-phase played little role in the colouring behaviour of the CVL:ODG:OD-OH system, mirroring the behaviour observed in the other ODG systems. Little change in the colour density was observed in the LO-to-R phase transition temperature range of pure OD-OH ($T_{trs,OD\text{-}OH}$ = 52 to 55 °C),[144,148] with only a minor spike of ΔCD = 0.1 to 0.2 occurring for some of the samples presented in Figure 5.5. This spike in colour density at T = 40 °C was attributed to the conversion of the solvent R-

phase back into the LO-phase upon removal from the water bath, which caused the formation of a weakly coloured metastable solid state, as had been observed in the CVL:DDG:HD-OH system (section 4.2.2). After solidification of the solvent, little change in the colour density of the mixtures was observed since the inhomogeneous precipitation of the developer from the melt caused the colour density to drop significantly prior to solvent solidification. Cooling to the LO-phase of the solvent returned the pre-melt colour density without the formation of a coloured, metastable solid state.

5.2.1.3.3 Conclusions Concerning CVL:ODG:OD-OH Mixtures

The thermochromic behaviour in this ternary system agreed with predictions. Melt-darkened thermochromism and very good colour contrast ($\Delta CD_{max} = 0.8$) was obtained in mixtures containing appropriate developer and solvent concentrations.

ODG demonstrated poor solubility in molten OD-OH, which resulted in high opacity of the melt during heating. At the highest temperature obtained on heating, $T =$ 95 °C, the developer became fully dissolved in the molten solvent for most of the samples examined. On cooling, inhomogeneous precipitation of the developer caused the colour density of the melt to substantially decrease prior to solvent solidification. This behaviour is further indicative of poor developer solubility in the molten solvent.

The solvent R-phase played a minor role in the colouring behaviour. Prior to solvent melting, a small increase in the colour density of the solid state was observed. This feature was attributed to transition of the solvent from the R-phase back into the LO-phase at near LO-to-R transitions temperatures, which caused formation of a weakly

coloured metastable solid state. Further heating regenerated the R-phase, and the weak colouration of the metastable state was lost. As a result of the inhomogeneous precipitation of the developer during the cooling, the R-phase of the solvent did not play a role in the post-melt colouring behaviour of CVL:ODG:OD-OH mixtures. After solvent solidification, the colour of the solid state did not vary upon further cooling, indicating that the slow cooling rate and developer precipitation from the melt rapidly generated the equilibrium solid state of these mixtures on solvent solidification.

5.2.1.4 Summary of Thermochromic Behaviour in CVL:ODG:Alcohol Mixtures

Melt-darkened thermochromic behaviour was observed in each of the ODG-containing systems. This type of behaviour is characteristic of dye:developer:solvent systems in which the alkyl chains attached to the developer and the solvent are well-matched in terms of length. In such mixtures, the equilibrium solid is the decoloured state, the melt is the coloured state, and good colour contrast can be obtained when the developer and solvent concentrations are chosen appropriately. In general, high developer concentrations (*e.g.*, when $y > 5$) and relatively low solvent concentrations (*e.g.*, when $z \approx$ 25 to 30) were required to generate a sufficiently coloured melt. The equilibrium solid was observed to be colourless, or very nearly colourless, in all of the mixtures studied, indicating that the most important factor in obtaining optimal thermochromic behaviour in ODG-containing mixtures is the generation of a sufficiently coloured molten state.

As had been observed in DDG-containing systems, ODG often had poor solubility in the molten solvent. This gave rise to high opacity in the molten mixtures at

temperatures near the melting point of the solvent. Increasing the temperature of the solvent caused enhanced dissolution of the developer, which decreased the opacity of the mixture and contributed to the darkening of the melt at elevated temperatures (in mixtures that formed coloured melts).

The poor solubility of ODG in each of the molten solvents also resulted in the inhomogeneous precipitation of ODG during cooling of the mixtures. This caused the colour density of the melt to drop significantly prior to solvent freezing in mixtures that contained high developer and low solvent concentrations. Unfortunately, it was these mixtures that demonstrated the highest melt colour density and best colour contrast. It is clear from this behaviour that optimal thermochromic properties can be difficult to achieve. Increasing the developer concentration to enhance colour density in the coloured state and the overall colour contrast caused detrimental effects such as high opacity on heating, inhomogeneous precipitation on cooling, and colour loss at temperatures higher than melting point of the solvent, whereas the melting point has been traditionally used to control the colour change temperature.[100]

The solvent R-phase did not play an important role in the colouring behaviour of CVL:ODG:alcohol mixtures, although some pre-melt colour changes associated with formation of the R-phase were observed. Prior to solvent melting during the heating portion of the heat-cool cycle, the solvent R-phase was noted to cause a small increase in the colour density of the CVL:ODG:OD-OH mixtures, but not in the CVL:ODG:TD-OH and CVL:ODG:OD-OH mixtures. This resulted from conversion of the solvent R-phase back to the LO-phase upon removal from the heating bath, creating a weakly coloured metastable solid state, which became decoloured upon further heating.

The solvent R-phase had little influence on the post-melt solid state colouration of CVL:ODG:alcohol mixtures as a result of the inhomogeneous precipitation of the developer during cooling. Since most of the developer had precipitated prior to solidification of the solid, the equilibrium state of the solid mixture was formed almost immediately upon solvent solidification and the solvent R-phase had little impact on the post-solidification colouring behaviour.

The influence of the solvent R-phase on the colouring behaviour in CVL:DDG:alcohols was also noted to be stronger in the HD-OH and OD-OH mixtures compared with the TD-OH mixtures. The reason for this behaviour is not fully understood, although it appears that the solvent R-phase has a wider range of stability in alcohols with longer chain lengths since the inter-chain interactions (*i.e.* van der Waals interactions) are more important to defining the solid state structure than the hydrogen-bonding framework that forms at the end of the chains as the alkyl chain length increases.[144,148,156]

Additionally, it is likely that the hydrogen-bonding network that forms between the hydroxyl groups at the end of the chains plays a more important role in defining the structure of short chain alcohols, as no R-phase is observed in alcohols with carbon chains of 12 carbon atoms or less.[144,148,156] In effect, in alcohols containing longer alkyl chains, the rotator phase has a wider temperature range of stability, and it is this feature that results in the stronger influence of the rotator phase on the solid state properties of thermochromic mixtures in samples containing HD-OH and OD-OH compared with those containing TD-OH.

5.2.2 Octyl Gallate (OG) Mixtures

The thermochromic behaviour of the three systems containing octyl gallate as the developer were hypothesized to follow the trends observed for mixtures containing poorly matched alkyl chain lengths since the alkyl chain attached to octyl gallate is only eight carbon atoms long, and the shortest alcohol solvent is 14 carbon atoms long. These features include coloured equilibrium solids, molten phases that can be coloured or decoloured depending on the developer and solvent concentrations, and optimal melt-lightened thermochromism below a developer concentration threshold. Above the developer concentration threshold, melt-darkened thermochromism would be anticipated.

Some preliminary investigations into the colouring behaviour and crystallization phenomena of CVL:OG:alcohols mixtures have been reported in the literature.[101,110] MacLaren and White demonstrated that in CVL:OG:alcohol mixtures, the equilibrium solid was very strongly coloured over a wide range of developer concentrations, where $3 \leq y \leq 24$ and $z = 40$, and that the thermally quenched solid maintained virtually the same degree of colouration after one week on the bench at room temperature.[101,110] Samples in OG-containing systems were deemed to be essentially non-thermochromic due to the lack of colour density change between the equilibrium and quenched solid states.[101,110]

5.2.2.1 CVL:OG:TD-OH Mixtures

5.2.2.1.1 Gross Features of CVL:OG:TD-OH Mixtures

Figure 5.7 shows the colour density versus temperature plots for selected samples in the CVL:OG:TD-OH system. The hypothesized colouring behaviour was indeed observed in these samples. The equilibrium solid state was coloured in many of the

samples, and the colour was lost upon melting for most samples. The [1:5.7:23.6] sample (containing high developer and low solvent concentrations) demonstrated melt-darkened behaviour, indicating the existence of a developer concentration threshold above which the melt is darker than the equilibrium solid.

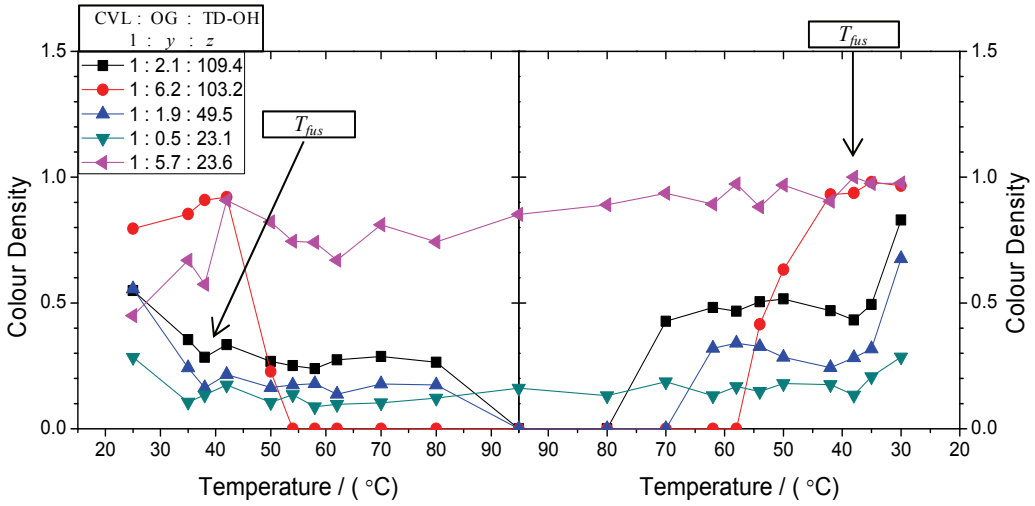

Figure 5.7. Colour density versus temperature plots obtained *via* colour photo analysis for samples in the CVL:OG:TD-OH system. The molar ratios of the three components are given on the figure. Heating rates during these experiments were d*T*/d*t* = 1 K min^{-1}. T_{fus} represents the melting point of the pure solvent. Lines are added as a guide to the eye. Error in *CD* was estimated to be +/-0.15.

Many of the samples presented in Figure 5.7 have sufficiently low developer concentrations that most became fully decoloured in the melt, particularly after the heating bath reached T = 95 °C. Figure 5.8 (a) shows colour photos of the [1:6.2:103.2] sample, which displayed very good colour contrast (ΔCD = 0.8), resulting from the formation of a strongly coloured equilibrium solid (CD_{Equil} = 0.8) and a fully decoloured melt (CD_{Melt} = 0).

The large solvent concentration promoted dissolution of the developer in the molten solvent, thereby reducing the amount of ring-opened CVL present in the molten mixture. This sample displayed deep colouration in the solid, no colour in the melt, and

very good contrast between the coloured and decoloured states, satisfying a number of the criteria required of useful thermochromic materials.[101,110]

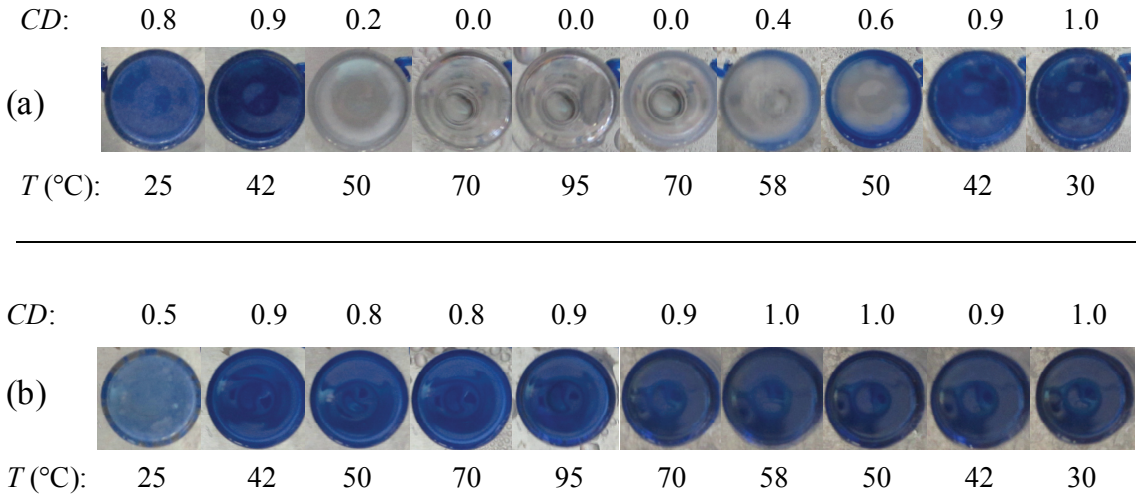

Figure 5.8. Colour photographs of CVL:OG:TD-OH samples at a composition of (a) [1:6.2:103.2] and (b) [1:5.7:23.6].

Figure 5.8 (b) shows colour photos of the sample at a composition of [1:5.7:23.6]. This sample contained substantially less solvent than the [1:6.2:103.2] sample and, as a result, the sample did not lose colour on heating. This resulted in a mixture that had effectively no colour contrast between the two states. This type of colouring behaviour was observed by MacLaren and led to the labelling of systems which demonstrated this type of behaviour as having "very poor" thermochromic properties.[101,110] Comparing the two samples in Figure 5.8 shows that the most important factor in determining the degree of contrast in these systems is the relative proportions of the three components, and in the case of CVL:OG:TD-OH mixtures, a large amount of solvent was required to properly adjust the colour contrast between the equilibrium solid (*i.e.*, the coloured state) and the melt (*i.e.*, the decoloured state).

Comparing the colouring behaviour of the CVL:OG:TD-OH sample at a composition of [1:5.7:23.6] (Figure 5.8 (b)) with the CVL:ODG:TD-OH sample at a composition of [1:6.4:26.7] (see Figure 5.2 (a)) and the CVL:ODG:OD-OH sample at a composition of [1:5.9:25.2] (see Figure 5.6 (b)), it is clear that the melt colour densities are remarkably similar. The CVL:ODG:TD-OH sample had a melt colour density of CD_{Melt} = 1.2, the CVL:ODG:OD-OH sample had a melt colour density of CD_{Melt} = 0.9, and the CVL:OG:TD-OH sample had a melt colour density of CD_{Melt} = 0.9. The similarity in melt colour density across these three mixture compositions, which demonstrate different optimal thermochromic behaviour (melt-darkened thermochromism for the ODG-containing mixtures versus melt-lightened thermochromism for the OG-containing mixtures), provides evidence that the type of thermochromism observed is largely determined by the degree of interaction of the developer and solvent in the solid state.

MacLaren's studies on the binary phase diagrams of alkyl gallate:alkyl alcohol mixtures can be used to demonstrate that when two components showed compound formation in the solid state (*e.g.*, the DDG:TD-OH system, see Figure 2.16), archetypal melt-darkened thermochromism can be expected for three-component mixtures.[101,110,143] Conversely, if the compounds lacked compound formation in solid state, such as in the OG:TD-OH binary phase diagram shown in Figure 5.9, then three-component thermochromic mixtures will tend to demonstrate melt-lightened behaviour at high solvent concentrations, resulting from the dye:developer complexes that dominate in the solid state due to the lack of competition from developer:solvent interactions.[110]

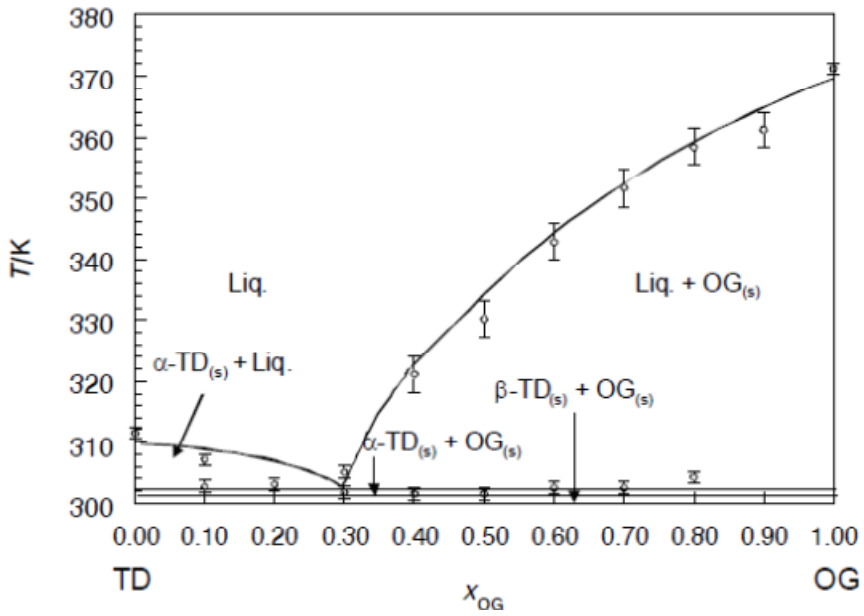

Figure 5.9. Binary phase diagram determined on heating for tetradecanol (TD) and octyl gallate (OG) mixtures. Note the lack of compound formation and the formation of a single eutectic. Reproduced with permission from reference 110 (D. C. MacLaren, *PhD Thesis*, Dalhousie University, 2003).

High solvent concentrations are sufficient to decolourize the melt of many mixtures, as was observed in the CVL:ODG:OD-OH system, particularly for the sample at a composition of [1:5.2:87] (see Figure 5.6 (a)), which was not substantially coloured at any point in the heat-cool cycle. The CVL:OG:TD-OH sample at a similar composition of [1:6.2:103.2] (see Figure 5.8), was likewise decoloured in the melt, and this gave rise to high contrast, melt-lightened thermochromism.

5.2.2.1.2 Fine Features of CVL:OG:TD-OH Mixtures

OG showed rather poor solubility in molten TD-OH. This behaviour can be observed from Figure 5.8. Looking first at Figure 5.8 (a), in particular at the T = 50 °C photo during heating, a ring of insoluble developer is observed at the exterior of the sample vial. The insoluble developer did become fully dissolved in the solvent as the

temperature was increased past 70 °C, mainly due to the high solvent concentration. The high developer concentration, coupled with the poor solubility of the developer in the molten solvent, caused the developer to begin to precipitate from the molten mixture as the mixture was cooled to $T \approx 60$°C. This is evidenced in Figure 5.8 (a) as a blue ring forming at the exterior of the sample vial. This increase in colour density prior to solidification of the solvent is detrimental to the overall thermochromic effect since the melting point of the solvent should ideally control the thermochromic transition temperature,[100,173] and colour formation was observed well above the melting point of TD-OH ($T_{fus,TD\text{-}OH}$ = 36 to 38 °C).[144]

The sample shown in Figure 5.8 (b) remained opaque throughout the entire temperature range due to the low solvent concentration, which prevented the developer from becoming fully dissolved in the molten solvent. The low solvent concentration was also responsible for the maintenance of strong colouration in this sample throughout the entire heat-cool cycle. This type of behaviour, the lack of colour loss on melting, was a factor in the labelling of such systems as "very poor" thermochromic materials in previous research.[101,110]

The colour density of most of the samples presented in Figure 5.7 increased on cooling prior to solvent solidification due to the precipitation of the developer. Due to the fact that the developer precipitated from the melt prior to solvent solidification in CVL:OG:TD-OH mixtures, near equilibrium colour density values were obtained well before the transition to the solvent R-phase. For this reason, the solvent R-phase had little impact on the colouring behaviour of mixtures in the CVL:OG:TD-OH system.

5.2.2.1.3 Conclusions Concerning CVL:OG:TD-OH Mixtures

Thermochromic behaviour in the CVL:OG:TD-OH system agreed with the anticipated behaviour: melt-lightened behaviour was observed for most samples. The equilibrium solid state was coloured in most cases and the melt became decoloured when the appropriate developer and solvent concentrations were chosen. High colour contrast ($\Delta CD_{max} = 0.8$) between the equilibrium solid and the melt was obtained in samples with high developer and solvent concentrations (*e.g.*, for the [1:6.2:103.2] sample). Otherwise, at developer concentrations that exceeded the developer concentration threshold, the melt became darker than the equilibrium solid (*i.e.*, melt-darkened behaviour was observed).

The developer demonstrated rather poor solubility in the molten solvent which caused the melt to remain opaque until the highest temperature of the heating bath was reached, particularly in mixtures which contained low solvent concentrations (*e.g.*, when $z < 100$). Poor developer solubility also resulted in precipitation of the developer prior to solidification of the solvent during cooling, precluding the influence of solid-solid phase transitions on the colouring behaviour in the solid state. Therefore, the solvent R-phase had virtually no influence on the colouring behaviour of these mixtures.

5.2.2.2 CVL:OG:HD-OH Mixtures

5.2.2.2.1 Gross Features of CVL:OG:HD-OH Mixtures

Figure 5.10 shows the colour density versus temperature plots for selected samples in the CVL:OG:HD-OH system. The colouring behaviour observed in this system mirrored that observed for the CVL:OG:TD-OH system. As a result of the poorly

matched alkyl chain lengths of OG and HD-OH, most of the mixtures studied demonstrated melt-lightened behaviour. At high developer concentrations and low solvent concentrations (*e.g.*, in the [1:5.6:23.9] sample), the colour density of the melt was the same as that of the equilibrium solid, again indicating the existence of a developer concentration threshold above which melt-darkened behaviour is observed.

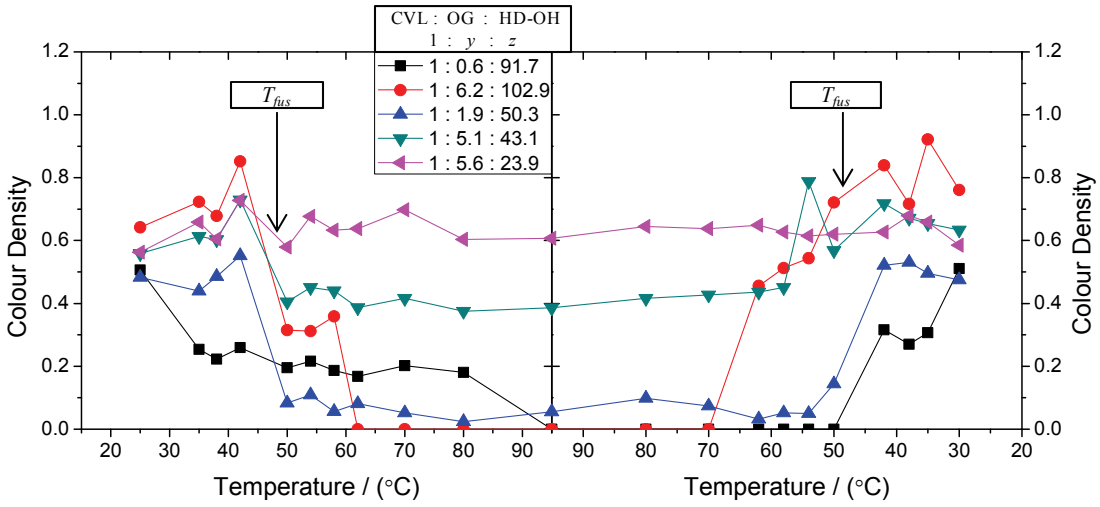

Figure 5.10. Colour density versus temperature plots obtained *via* colour photo analysis for samples in the CVL:OG:HD-OH system. The molar ratios of the three components are given on the figure. Heating rates during these experiments were d*T*/d*t* = 1 K min^{-1}. T_{fus} represents the melting point of the pure solvent. Lines are added as a guide to the eye. Error in *CD* was estimated to be +/-0.15.

At high solvent concentrations (*e.g.*, when $z \approx 100$), the coloured equilibrium solid melted to form a colourless molten state, giving rise to mixtures that demonstrated good colour contrast. In the case of the [1:6.2:102.9] sample, the equilibrium solid was moderately coloured ($CD_{Equil} = 0.6$) and the melt was completely colourless ($CD_{Melt} = 0.0$), yielding a colour contrast of $\Delta CD = 0.6$. Although this value is lower than had been observed in the CVL:OG:TD-OH samples (where $\Delta CD_{max} = 0.8$), the fact that the melt was essentially completely colourless indicates that higher contrast might yet be attainable by increasing the developer concentration.

When the solvent concentration was reduced, and the relative CVL and developer concentrations were increased (*e.g.*, in the [1:5.6:23.9] sample), the colour contrast between the equilibrium solid state and the melt was lost, and the colour density of the sample remained high across the entire temperature range. Additionally, samples containing less developer (*e.g.*, the [1:0.6:91.7] sample) demonstrated lower equilibrium colour density (CD_{Equil} = 0.5), which caused the overall colour contrast to be reduced.

5.2.2.2.2 Fine Features of CVL:OG:HD-OH Mixtures

Samples in the CVL:OG:HD-OH ternary system demonstrated many of the same fine features that were observed in the CVL:OG:TD-OH system. Once again, the developer had rather poor solubility in the molten solvent, which caused the molten mixture to remain opaque until the melt temperature exceeded 80 °C. This feature is seen in Figure 5.10 as a small reduction in the colour density of the melt in the [1:5.6:23.9] and [1:0.6:91.7] samples around $T \approx 70 - 80$ °C, which resulted from reduced melt opacity associated with increased developer dissolution.

The colour density of samples containing relatively high developer concentrations (*e.g.*, when y = 5 to 6) was observed to spike prior to solvent solidification; this was attributed to the precipitation of the developer from the molten solvent. In samples containing low developer concentrations (*e.g.*, the [1:1.9:50.3] sample), the spike in colour density occurred after solvent solidification (T < 50 °C). This type of behaviour is required of useful thermochromic materials since the melting point of the solvent should be the sole determining factor in defining the thermochromic transition temperature.

As a result of the inhomogeneous precipitation of the developer from the molten solvent in samples containing high developer concentrations, the solvent R-phase often had little effect on the thermochromic behaviour of these mixtures in the solid state. In samples containing low developer concentrations (*e.g.*, the [1:1.9:50.3] sample), the developer remained dissolved until solvent solidification occurred. As a result, the solvent R-phase did play a role in the colouring behaviour of the solid state in such samples.

Looking at the cooling portion of the heat-cool cycle in Figure 5.10, there were small but noticeable spikes in the colour density of the low developer concentration samples (*e.g.*, [1:1.9:50.3]) after the initial solvent-solidification induced colour density increase. This spike was attributed to conversion from the solvent R-phase to the LO-phase which acts as a type of thermal "quenching". Also, prior to solvent melting during the heating portion of the experiments, spikes in colour density associated with solvent conversion from the pre-melt solvent R-phase to the LO-phase were noted. As discussed previously, at bath temperatures just above the LO-to-R phase transition, the solvent is in the R-phase. Upon removal from the bath, conversion of the solvent from the R-phase to the LO-phase generates a coloured metastable state, which causes colour density enhancement in the pre-melt solid state. Further heating to near-melt temperatures returns the R-phase of the solvent with concomitant decreases in colour density. The solvent R-phase provides a more dynamic medium in the solid state, which allows for disruption of the dye:developer complex; this behaviour is akin to the decolourization observed in the melt due to dissociation of the colour-forming components.

5.2.2.2.3 Conclusions Concerning CVL:OG:HD-OH Mixtures

The gross features of thermochromic behaviour in the CVL:OG:HD-OH ternary system agreed with the hypothesized results. Melt-lightened behaviour was obtained in samples containing low developer concentrations and/or high solvent concentrations. The high solvent concentration allowed for enhanced developer dissolution in the molten solvent which disrupted the formation of ring-opened CVL, thereby removing colour. At low solvent concentrations, the melt retained strong colouration indicating that the melt could be made darker than the equilibrium solid (*i.e.*, melt-darkened behaviour) by exceeding the developer concentration threshold. Good colour contrast ($\Delta CD_{max} = 0.6$) was obtained by choosing appropriate developer and solvent concentrations.

The fine features observed in this ternary system were also consistent with those observed previously in the CVL:OG:TD-OH system. The low solubility of the developer caused the molten mixture to remain opaque throughout the majority of the heat-cool cycle. Samples that contained high developer concentrations and/or low solvent concentrations were characterized by inhomogeneous precipitation of the developer prior to solvent solidification, which caused the melt colour density to spike prematurely. This behaviour is detrimental to the overall thermochromic effect as the desired thermochromic transition temperature should be controlled solely by the melting point of the solvent.[100]

The solvent R-phase played a slightly larger role in this system than in CVL:OG:TD-OH mixtures, as evidenced by the small increases in colour density observed prior to solvent melting in a majority of the samples studied, due to conversion from the pre-melt R-phase back to the LO-phase upon removal from the water bath. On

cooling, transition from the melt to the R-phase of the solvent did not significantly impact the colour density of the mixtures, whereas transition from the R-phase to the LO-phase of the solvent caused substantial increases in solid state colour density in mixtures that did not suffer from inhomogeneous precipitation of the developer from the molten solvent during cooling (*e.g.*, when $y < 2$).

5.2.2.3 CVL:OG:OD-OH Mixtures

5.2.2.3.1 Gross Features of CVL:OG:OD-OH Mixtures

Figure 5.11 shows the colour density versus temperatures plots for samples in the CVL:OG:OD-OH system. Melting of the coloured equilibrium solid gave rise to a decoloured melt at sufficiently high solvent concentrations (*e.g.*, when $y \approx 85$ to 90). Decreasing the solvent concentration caused the melt to become strongly coloured in samples that also contained high developer concentrations, leading to the observation of a developer concentration threshold above which melt-darkened behaviour was observed (*e.g.*, in the [1:5.9:24.4] sample).

High colour contrast ($\Delta CD = 0.8$) for the [1:5.2:86.5] sample was observed between the coloured equilibrium solid ($CD_{Equil} = 0.8$) and the fully decoloured melt ($CD_{Melt} = 0$), although this high colour contrast was only observed over a small portion of the heat-cool cycle, as inhomogeneous developer precipitation during cooling caused the melt colour density to spike well before solvent solidification.

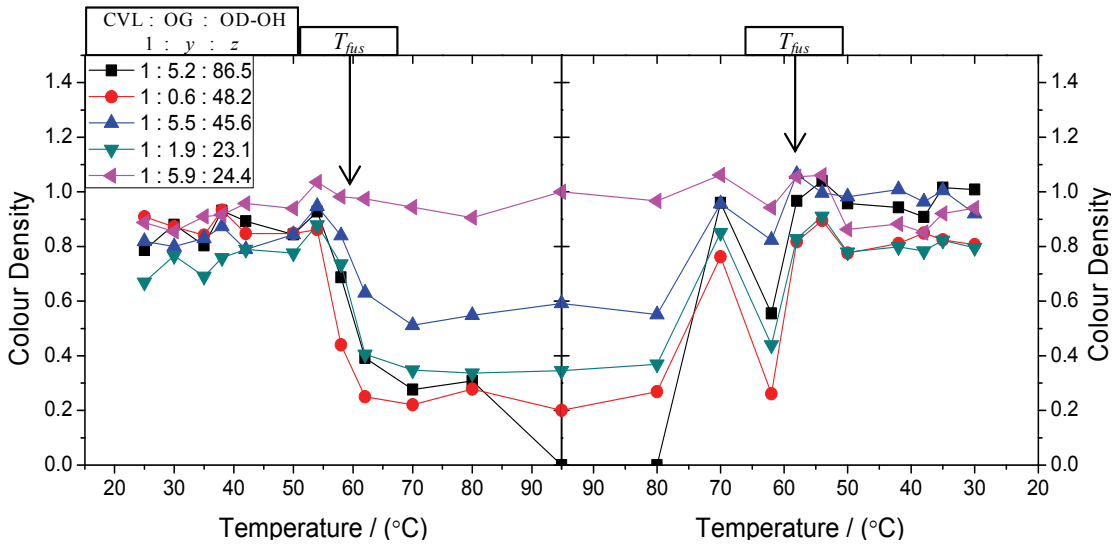

Figure 5.11. Colour density versus temperature plots obtained *via* colour photo analysis for samples in the CVL:OG:OD-OH system. The molar ratios of the three components are given on the figure. Heating rates during these experiments were d*T*/d*t* = 1 K min^{-1}. T_{fus} represents the melting point of the pure solvent. Lines are added as a guide to the eye. Error in *CD* was estimated to be +/-0.15.

5.2.2.3.2 Fine Features of CVL:OG:OD-OH Mixtures

While the solid state demonstrated darker colouration than was observed in the same compositional ranges in TD-OH and HD-OH mixtures, fully decoloured mixtures could only be obtained by heating to 95 °C. This behaviour is indicative of poor OG solubility in the molten solvent. The low solubility of OG in the molten solvent is evidenced by the dramatic spike in colour density at $T \approx 70$ °C (on cooling) for the majority of samples, which was caused by inhomogeneous developer precipitation Furthermore, the [1:5.2:86.5] sample demonstrated reduced melt colour density over the 60 to 95 °C temperature range, indicating that OG continued to dissolve in this mixture, implying poor solubility in the molten solvent at lower temperatures.

The R-phase of the solvent played an important role in the colouring behaviour obtained both on heating and cooling in this ternary system. Figure 5.12 shows colour

photos of the [1:1.9:23.1] sample, which demonstrates the important role of the R-phase in this ternary system. On heating, the colour density of the solid state was observed to initially increase at 50 to 54 °C, which is near the low end of the LO-to-R phase transition temperature range for the pure solvent (T_{trs} = 52 to 55 °C).[144,148] As before, conversion from the R-phase back to the LO-phase upon removal from the water bath generated a dark, metastable solid state (due to LO-phase formation). Further heating of the sample caused near-complete decolouration of the mixture between 58 and 62 °C, which is at the high end of the melting temperature range of the pure solvent ($T_{fus,OD\text{-}OH}$ = 56 to 59 °C).[144]

On subsequent cooling from 95 °C, the developer precipitated from the molten solvent at 70 °C. This behaviour was observed for most of the samples shown in Figure 5.11. Cooling to 62 °C caused the molten solvent to solidify into the R-phase resulting in brief decolourization of the mixtures, as evidenced in Figure 5.12 by the large decrease in colour density at 62 °C. Further cooling of the mixtures caused the solvent to transition into the LO-phase (at 58 °C), thereby returning the high colour density of the pre-melt, equilibrium solid, which was maintained on cooling to 30 °C.

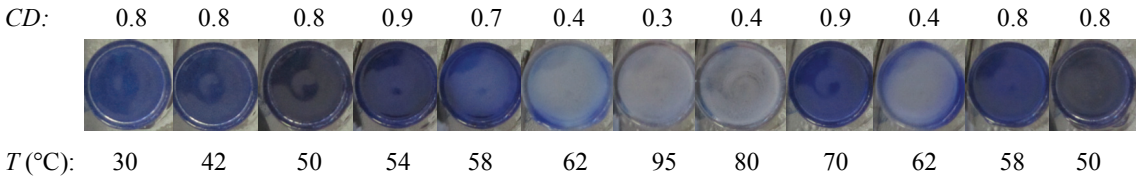

Figure 5.12. Colour photographs of the CVL:OG:OD-OH sample at a composition of [1:1.9:23.1].

5.2.2.3.3 Conclusions Concerning CVL:OG:OD-OH Mixtures

Thermochromic behaviour in the CVL:OG:OD-OH system agreed with the behaviour hypothesized for mixtures containing poorly matched alkyl chain lengths. The equilibrium solid was shown to be strongly coloured at most compositions, the molten phase could be decoloured when appropriately large solvent concentrations were used, and good colour contrast ($\Delta CD_{max} = 0.8$) could be achieved through proper selection of the concentrations of each of the three components. Unfortunately, the poor solubility of the developer in the molten solvent caused these samples to suffer detrimental effects including high opacity in the melt after solvent melting and prior to solvent solidification, and inhomogeneous precipitation of the developer that resulted in unwanted colour formation in the melt.

In contrast to what had been observed in CVL:OG:TD-OH and CVL:OG:HD-OH mixtures, the R-phase of the solvent played a more significant role in the colouring behaviour in this system. On heating, the colour density of most mixtures increased near the LO-to-R phase transition temperature of the pure solvent due to the conversion of the solvent R-phase back to the LO-phase upon removal from the water bath. On cooling, solidification of the solvent into the R-phase caused a substantial decrease in the colour that formed due to inhomogeneous precipitation of the developer from the molten solvent prior to solvent solidification, and subsequent conversion of the solvent to the LO-phase returned the strong colouration of the equilibrium solid state.

While this system did not display ideal thermochromic behaviour over a wide compositional range, changing the relative compositions of the three components lead to the identification of a few mixtures with very good colour contrast. Detrimental effects

such as high melt opacity and thermochromic transition temperatures that were not solely controlled by the solvent melting point, however, were observed for most of the samples studied in this work, indicating that CVL:OG:OD-OH mixtures may not be suitable for application as thermochromic materials.

5.2.2.4 Summary of Thermochromic Behaviour in CVL:OG:Alcohol Mixtures

Octyl gallate containing mixtures demonstrated thermochromic behaviour characteristic of three-component systems in which the developer and solvent alkyl chain lengths are poorly matched. In such mixtures, the equilibrium solid state usually is strongly coloured and the molten phase can become fully decoloured if the solvent concentration is sufficiently high. When a strongly coloured solid melts to form a decoloured melt, melt-lightened thermochromism with high colour contrast can be achieved. This optimal thermochromic behaviour was observed in all three OG-containing systems, in particular when the developer concentration was relatively large (*e.g.*, $5 \leq y \leq 6$) and the solvent concentration was large enough to cause decolourization of the melt (*e.g.*, $z \approx 90$ to 100). The high developer concentration promotes colour formation in the solid state and the high solvent concentration promotes dissolution of the developer in the molten solvent, which results in colour loss in the melt.

In mixtures containing high developer concentrations and low solvent concentrations (*e.g.*, when $5 \leq y \leq 6$ and $z \approx 25$), low colour contrast was observed upon melting of the mixtures, since the solid and molten states demonstrated similar colour densities. Melt-darkened thermochromism was observed for the CVL:OG:TD-OH system

when the developer concentration exceeded a threshold value that was dependent on the relative solvent concentration in a given mixture. Although the colour intensified on melting, the strong colouration of the solid state prevented high colour contrast between the two states, indicating that mixtures at such compositions are indeed poor thermochromic materials.

Octyl gallate demonstrated poor solubility in each of the three solvents employed here. This behaviour was not unexpected as solubility issues were noted in DDG- and ODG-containing mixtures as well. There are two major consequences of the poor solubility of the developer. First, the molten mixture remains opaque at near-melting temperatures during the heating phase until the developer is able to fully dissolve in the solvent. Second, the developer can inhomogeneously precipitate during cooling, prior to the solidification of the solvent, causing an increase in colour density at temperatures greater than the anticipated transition temperature of the mixture. The transition temperature of thermochromic materials is usually defined by the melting point of the solvent; therefore such instances, in which colour forms above the solvent transition temperature, are inherently detrimental to the overall thermochromic effect in melt-lightened thermochromic materials.

5.2.3 Propyl Gallate (PG) Mixtures

In three-component thermochromic mixtures containing propyl gallate as the colour developer, the developer and solvent alkyl chains are very poorly matched in terms of length. The alkyl chain of propyl gallate (three carbon atoms in length) is substantially shorter than even the shortest alcohol used in this work (TD-OH, 14 carbon

atoms). As a result, the thermochromic behaviour in all of the CVL:PG:solvent systems examined here was hypothesized to follow the same general trends observed for mixtures with poorly matched alkyl chain lengths. PG-containing mixtures were hypothesized to demonstrate melt-lightened thermochromism at high solvent concentrations, the formation of coloured equilibrium solids at most compositions, and, when the developer concentration is high and the solvent concentration is low, such that the developer concentration threshold is exceeded, melt-darkened behaviour was expected.

The colouring behaviour hypothesized for propyl gallate mixtures has been observed in numerous other systems (*e.g.*, OG-containing mixtures, DDG with HD-OH, *etc.*), therefore colour images are not presented in the following subsections. Due to the similarity of the thermochromic behaviour in all three ternary systems containing PG as the developer, the results from studies on TD-OH, HD-OH, and OD-OH mixtures are discussed collectively.

5.2.3.1 Introduction to Studies of PG-Containing Mixtures

Previous work in the field of rewritable thermochromic mixtures examined the colouring behaviour of CVL:PG:alcohol ternary systems.[101,110] MacLaren and White focussed on the change in colour density between the equilibrium solid and the quenched metastable solid states in this concentration range and did not consider high solvent concentrations. For this reason, PG-containing mixtures were deemed of "very poor" quality as thermochromic materials.[101,110] As noted in the preceding sections of this chapter, samples containing poorly matched alkyl chain lengths can become completely decoloured in the molten phase and, therefore, can demonstrate very good colour

contrast, making these types of mixtures attractive thermochromic materials. Unsurprisingly, this type of behaviour was indeed observed in the PG-containing ternary systems.

5.2.3.2 Gross Features of PG-Containing Mixtures

Figure 5.13 shows the colour density versus temperature plots for the CVL:PG:TD-OH system. The equilibrium solid was strongly coloured in most cases, and the colour density was dependent on the developer and solvent concentrations. When the solvent concentration was sufficiently low, the melt also became coloured. The [1:6:25.9] sample demonstrated higher colour density in the melt (at $T = 95$ °C) than was observed in the solid state, indicating the existence of a developer concentration threshold above which melt-darkened behaviour is observed and below which melt-lightened behaviour is observed.

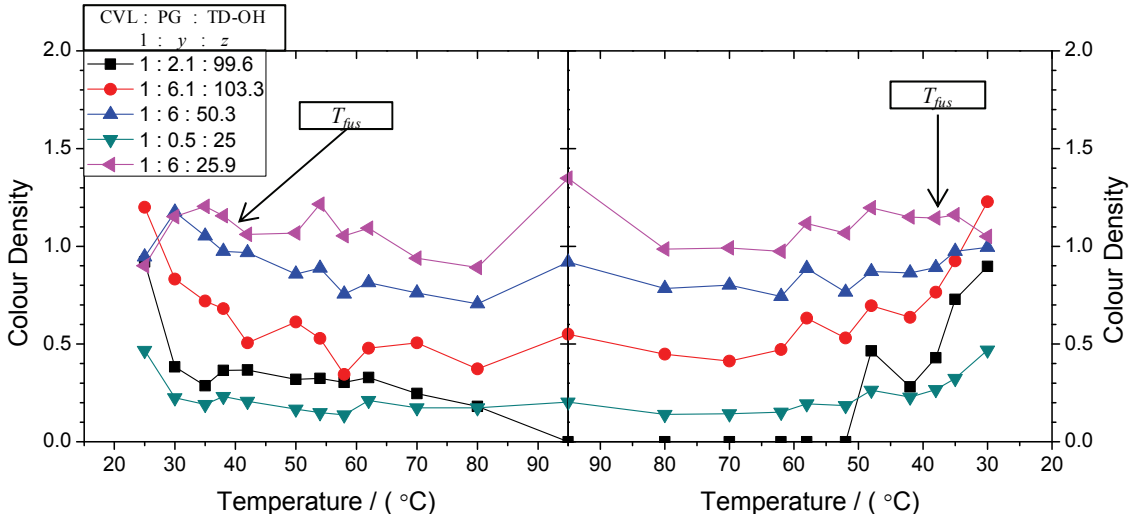

Figure 5.13. Colour density versus temperature plots obtained *via* colour photo analysis for samples in the CVL:PG:TD-OH system. The molar ratios of the three components are given on the figure. Heating rates during these experiments were $dT/dt = 1$ K min^{-1}. T_{fus} represents the melting point of the pure solvent. Lines are added as a guide to the eye. Error in *CD* was estimated to be +/-0.15.

Few samples in the CVL:PG:TD-OH system demonstrated good colour contrast between the solid and molten phases, although the sample at a composition of [1:2.1:99.6] demonstrated particularly good contrast. In this sample, the strongly coloured equilibrium solid ($CD_{\text{Equil}} = 0.9$) melted to give a completely decoloured melt ($CD_{\text{Melt}} = 0$, at $T = 95$ °C), yielding high colour contrast ($\Delta CD = 0.9$). From these data, it is apparent that most of the samples do not form completely decoloured melts, which reduces the overall colour contrast, creating mixtures demonstrating less than ideal thermochromic properties.

Figure 5.14 shows the colour density versus temperature plots for samples in the CVL:PG:HD-OH system. The equilibrium solid was the coloured state demonstrating high colour density in most samples, and the melt was decoloured when the solvent concentration was high (*e.g.*, when $z \approx 100$).

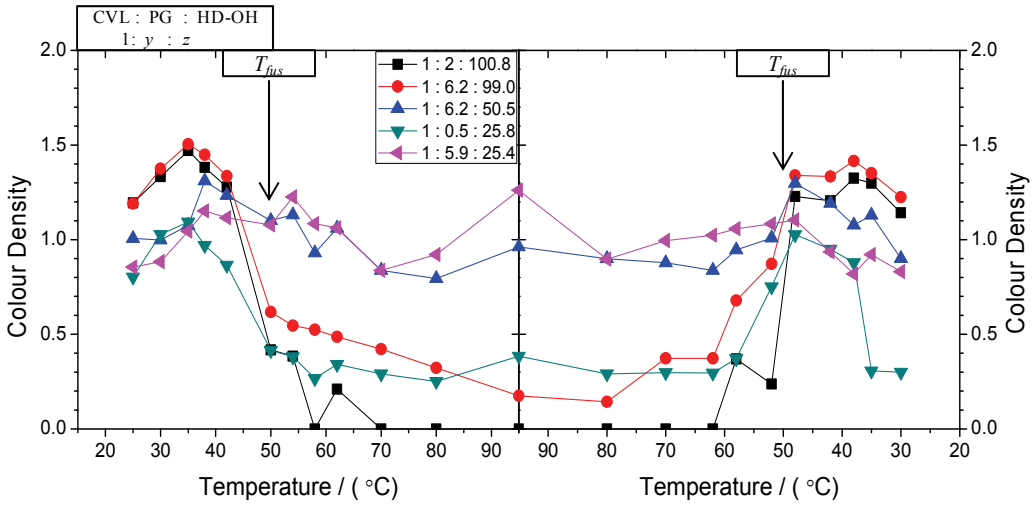

Figure 5.14. Colour density versus temperature plots obtained *via* colour photo analysis for samples in the CVL:PG:HD-OH system. The molar ratios of the three components are given in the figure. Heating rates during these experiments were $dT/dt = 1$ K min^{-1}. T_{fus} represents the melting point of the pure solvent. Lines are added as a guide to the eye. Error in *CD* was estimated to be +/-0.15.

A wider concentration range of samples in the CVL:PG:HD-OH system became fully decoloured in the melt compared with the CVL:PG:TD-OH system (note: not all data are shown), which could be a result of different solvent strengths of the two solvents. It was shown for the CVL:DDG:solvent systems that CVL has lower solubility in HD-OH than in TD-OH (*vide supra*, section 4.2.2), so it is possible that this decrease in solubility gave rise to less colour formation in the melt in HD-OH mixtures. Nevertheless, the [1:6.2:99.0] sample, shown in Figure 5.15, demonstrated high colour contrast due to a strongly coloured equilibrium solid (CD_{Equil} = 1.2) that melted to form a nearly colourless melt (CD_{Melt} = 0.2), affording the high colour contrast (ΔCD = 1.0).

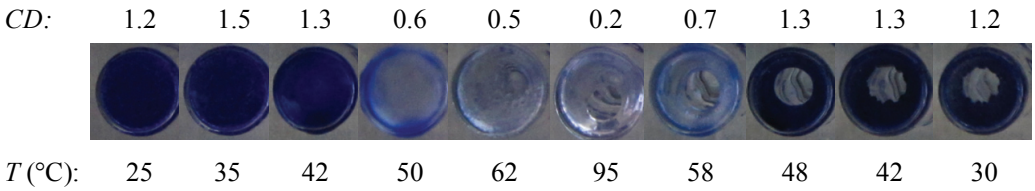

Figure 5.15. Colour photographs of the CVL:PG:HD-OH sample at a composition of [1:6.2:99.0]. Note the loss of colour on melting ($T \geq 50$ °C), the reappearance of colour upon solidification of the developer ($T < 58$ °C), and further intensification of the colour on solidification of the solvent ($T = 48$ °C).

Figure 5.16 shows the colour density versus temperature plots for samples in the CVL:PG:OD-OH system. The equilibrium solids were strongly coloured, and mixtures containing high solvent concentrations (*e.g.*, when $z \approx 100$) melted to form a decoloured melt. The colour of the melt was dependent on the developer and solvent concentrations, and samples that contained high developer and low solvent concentrations demonstrated more intensely coloured molten phases, indicating the existence of a developer concentration threshold.

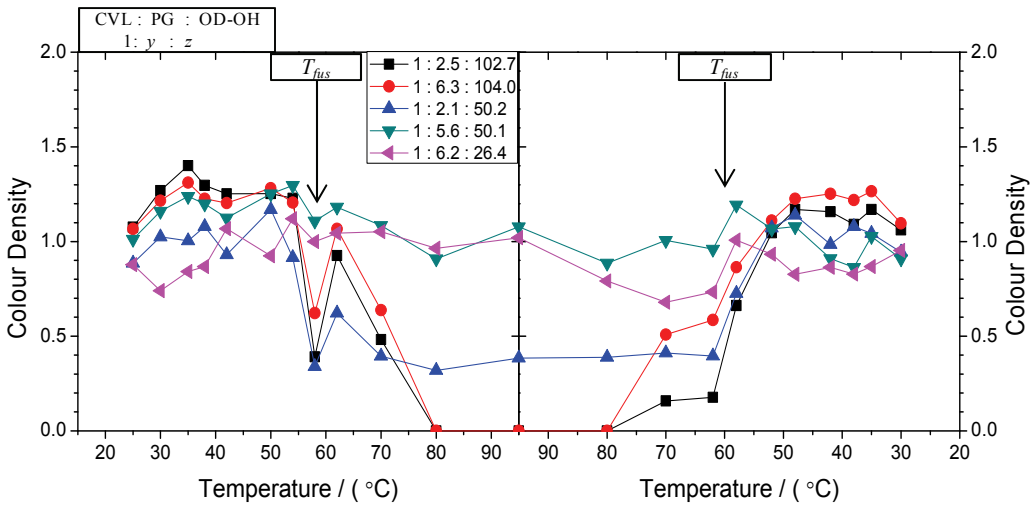

Figure 5.16. Colour density versus temperature plots obtained *via* colour photo analysis for samples in the CVL:PG:OD-OH system. The molar ratios of the three components are given on the figure. Heating rates during these experiments were d*T*/d*t* = 1 K min^{-1}. T_{fus} represents the melting point of the pure solvent. Lines are added as a guide to the eye. Error in *CD* was estimated to be +/-0.15.

The increase in colour density of the melt for mixtures with lower solvent concentrations (*e.g.*, when $z \leq 50$) resulted in a reduction of the colour contrast in these samples, thereby reducing the quality of the thermochromic effect. However, samples containing a large amount of solvent demonstrated very good colour contrast owing to their completely colourless molten phases. In particular, the [1:2.5:102.7] sample demonstrated high colour density in the solid state ($CD_{Equil} = 1.0$) and a completely colourless melt ($CD_{Melt} = 0$), yielding excellent colour contrast ($\Delta CD = 1.0$).

5.2.4.3 Fine Features of PG-Containing Mixtures

The fine features observed in the PG-containing systems were relatively consistent across the three solvents used. Propyl gallate has a much higher melting point (T_{fus} = 146 to 149 °C)[128] than the longer chain gallates (typically $T_{fus} \approx$ 95 to 105 °C)[128,131] which means that increasing the temperature of the heating bath is unlikely to

promote developer melting and therefore any effects associated with reduced opacity in the melt, enhanced melt colour density in high developer concentration samples, or reduced colour density in high solvent concentration samples, must be due to enhanced developer dissolution in the molten solvent.

In the TD-OH system, very little colour density change was observed across the heat-cool cycle for the majority of the samples studied here. This indicated that the developer had particularly low solubility in the molten solvent and heating the mixture to 95 °C did little to disrupt colour formation, except at high solvent concentrations (*e.g.*, when $z \approx 100$). In the HD-OH system, the colour density of the melt-lightened mixtures fell off rapidly as the solvent reached its melting point, providing evidence that the developer was more soluble in HD-OH than in TD-OH, whereby melting of the solvent promoted developer dissolution and destruction of the coloured complex. The solvent concentration range for decolourization of the melt was similar in the OD-OH and HD-OH systems, and was wider than that observed for TD-OH mixtures, again indicating that the developer is more easily dissolved into the melt of HD-OH and OD-OH mixtures than in TD-OH mixtures.

The solvent R-phase did not play a significant role in the TD-OH mixtures, as no colour changes associated with transition from either the LO-phase (on heating) or the melt (on cooling) were observed. The spikes in colour density on cooling in these samples were only related to transition of the solvent into the LO-phase and the return to the coloured equilibrium solid, which was the hypothesized behaviour based on the poor matching of the alkyl chain lengths in these mixtures.

Conversely, the solvent R-phase was observed to play a more integral role in the colouring behaviour in the solid state of the HD-OH and OD-OH mixtures. Figure 5.14 shows moderate spikes in the colour density of HD-OH mixtures prior to solvent melting (at $T \approx 40$ °C), which was attributed to transition from the pre-melt R-phase back to the LO-phase of the solvent, coupled with formation of a coloured, metastable solid state. This behaviour was also noted in Figure 5.16 ($T \approx 50$ °C), which shows the colouring behaviour of OD-OH mixtures, and in the CVL:DDG:HD-OH system discussed in Chapter 4 (section 4.2.2).

After solidification of the melt in both HD-OH and OD-OH mixtures, the expected spike in colour density associated with solidification of the solvent was observed. Shortly after this spike in colour density, many of the high solvent concentration (*i.e.*, $z \approx 100$) samples showed an additional gradual increase in colour density associated with the completion of solvent LO-phase formation, which returned the colour of the equilibrium solid.

5.2.3.4 Conclusions Concerning PG-Containing Mixtures

As hypothesized, the gross features of thermochromic behaviour in CVL:PG:solvent mixtures followed the trends for systems containing poorly matched alkyl chain lengths. The equilibrium solid states were almost always coloured, and the best colour contrast in these systems was obtained when the melt was fully decoloured, yielding melt-lightened thermochromism. High solvent concentrations (*e.g.*, when $z \approx 100$) were required for decolourization of the melt. High colour contrast samples were

obtained in all three solvent systems, with the HD-OH and OD-OH systems having the highest contrast (ΔCD_{max} = 1.0) followed closely by the TD-OH system (ΔCD_{max} = 0.9).

Poor developer solubility in the molten solvent caused detrimental effects including high opacity in the melt immediately upon solvent melting and prior to solvent solidification, and inhomogeneous precipitation of the developer which resulted in unwanted colour formation in the melt. The influence of the R-phase of the solvent was not seen in TD-OH mixtures, and was relatively weak for HD-OH and OD-OH mixtures compared to the results obtained for DDG-containing mixtures.

5.2.4 Gallic Acid (GA) Mixtures

5.2.4.1 Introduction to Studies of GA-Containing Mixtures

The study of mixtures containing gallic acid (GA, Figure 5.17) as the colour developer presented two important technical challenges. First, gallic acid has exceptionally low solubility in the alcoholic solvents used in this work. Gallic acid contains three phenolic protons and a carboxylic acid moiety, and lacks the solubility-enhancing aliphatic chain of the other developers, which essentially renders GA insoluble in the molten mixture. Secondly, the melting point of GA is very high ($T_{fus,GA}$ = 250 to 252 °C)[131] compared to the long-chain alkyl gallates due to the strong intermolecular hydrogen bonding network formed by the hydroxyl and carboxylic acid moieties, and the absence of the long alkyl chain. The long alkyl chain serves to lower the melting point of alkyl gallates; the melting points for long-chain alkyl gallates level off around T_{fus} ~ 95 to 105 °C, beginning with octyl gallate.[128-131] The gallate developers with long alkyl chains tend to begin to melt at the temperature of the water bath in the present experiments

(95 °C), thereby increasing miscibility with the solvent; this was not possible with gallic acid. Nevertheless, gallic acid mixtures were examined using the same colour photo analysis techniques used to study the colouring behaviour in mixtures containing long-chain gallate developers.

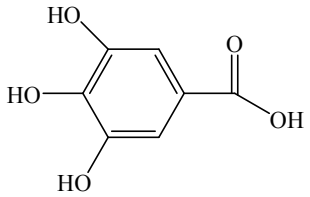

Figure 5.17. The structure of gallic acid (GA).

Due to the large difference in chain length between GA (zero carbon atoms) and the alcoholic solvents (14 to 18 carbon atoms), thermochromic behaviour characteristic of systems containing poorly matched alkyl chain lengths was hypothesized. Due to the similar alkyl chain length mismatch between GA and the three solvents, the thermochromic behaviour of GA-containing mixtures was hypothesized to be consistent across all three solvents used, so the three systems are discussed collectively.

5.2.4.2 Gross Features of Behaviour in GA-Containing Mixtures

Figure 5.18 shows the colour density versus temperature plots for samples in the CVL:GA:TD-OH system. The observed colouring behaviour was rather different from any of the previously examined systems. In CVL:GA:TD-OH mixtures, the initial solid state was very weakly coloured, which likely was a result of poor mixing of the three components during sample preparation. Upon melting of the solvent, samples containing large amounts of developer (*e.g.*, $y \approx 6$) became coloured, while samples containing much less developer showed only very weak colouration.

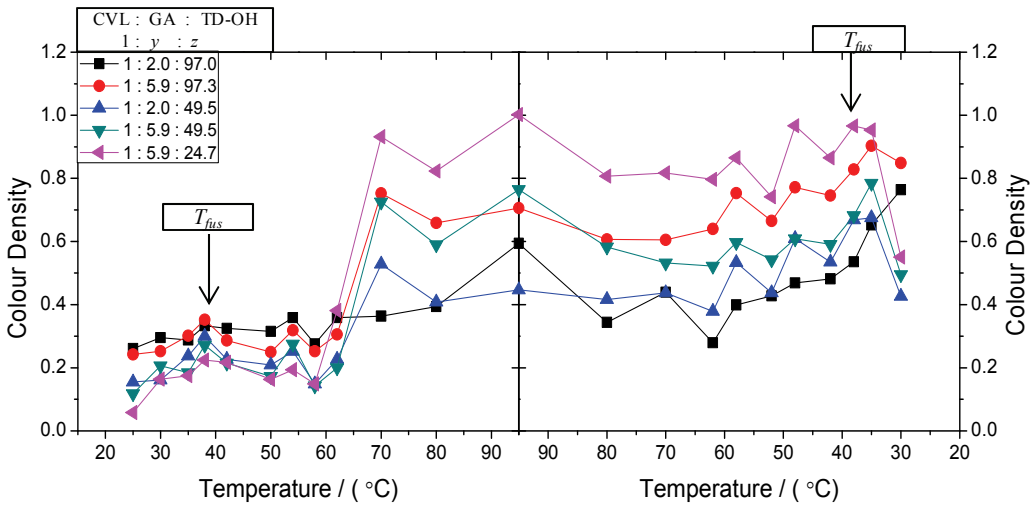

Figure 5.18. Colour density versus temperature plots obtained *via* colour photo analysis for samples in the CVL:GA:TD-OH system. The molar ratios of the three components are given on the figure. Heating rates during these experiments were d*T*/d*t* = 1 K min^{-1}. T_{fus} represents the melting point of the pure solvent. Lines are added as a guide to the eye. Error in *CD* was estimated to be +/-0.15.

The major difference between the CVL:GA:TD-OH mixtures and the OG- and PG-containing mixtures is that the molten phase of CVL:GA:TD-OH mixtures tended to be opaque at all temperatures as a result of the poor solubility and high melting point of GA. For this reason, the colour density of the melt was generally higher than anticipated, even at concentrations where a decoloured melt was hypothesized (*i.e.*, when $z \approx 100$). Upon solidification, the solids became strongly coloured regardless of the colour density of either the pre-melt solid or the melt, indicating that, in fact, the solid truly was the coloured state.

A complication associated with the poor miscibility/solubility of GA with the long-chain alcohol solvent was observed in Figure 5.18. The colour density of samples containing large developer concentrations (*e.g.*, $y \approx 6$) decreased substantially after solvent solidification (around $T = 30$ °C). This was due to inhomogeneous phase

separation of the GA developer from the solid solvent, which caused rapid decolouration of these mixtures in the solid state.

Figure 5.19 shows the colour density versus temperature plots for samples in the CVL:GA:HD-OH system. The colouring behaviour in the HD-OH system was in good agreement with the behaviour hypothesized for GA-containing mixtures. The solid phases were coloured, with the colour being lost upon melting in samples with $z \geq \sim 50$. Samples with high developer concentrations maintained some blue colour into the melt, with the colour of the melt due in part to the formation of the coloured form of CVL by the insoluble gallic acid. Upon solvent solidification, the strongly coloured solid state returned, with a more intensely coloured metastable state eventually converting to a less strongly coloured equilibrium solid state. The behaviour observed here closely matches that observed in the CVL:OG:HD-OH and CVL:PG:HD-OH systems, indicating again that mismatched alkyl chain lengths can give rise to predictable behaviour.

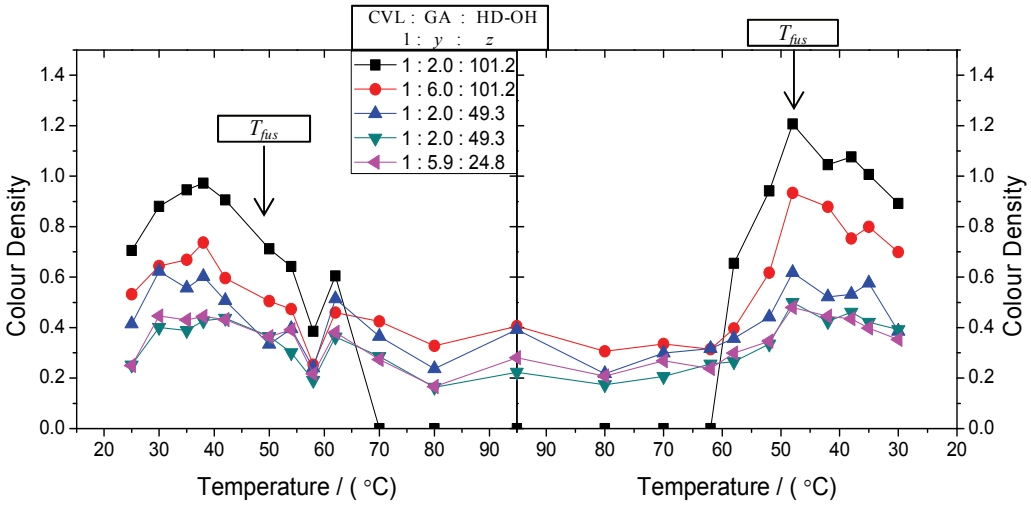

Figure 5.19. Colour density versus temperature plots obtained *via* colour photo analysis for samples in the CVL:GA:HD-OH system. The molar ratios of the three components are given on the figure. Heating rates during these experiments were $dT/dt = 1$ K min^{-1}. T_{fus} represents the melting point of the pure solvent. Lines are added as a guide to the eye. Error in *CD* was estimated to be +/-0.15.

Figure 5.20 shows the colour density versus temperature plots for samples in the CVL:GA:OD-OH system. This system showed anomalous behaviour not seen in the CVL:GA:TD-OH or CVL:GA:HD-OH systems. The colour density of the equilibrium solid was once again very low, owing to poor mixing of the three components in the solid state. Heating to just below the melting point of OD-OH ($T_{fus,OD\text{-}OH}$ = 56 to 59 °C)[144] caused no change in the colour density of the solid. As the melting point of the solvent was exceeded, the mixtures became strongly coloured and then quickly lost colour density on further heating. Colour was almost completely lost at 95 °C, but began to reform during cooling at 70 °C due to inhomogeneous precipitation of the developer, followed by further colour formation on solidification of the solvent. After cooling further past the freezing point of the solvent, colour was lost again as the equilibrium solid state was returned. Figure 5.21 shows colour photos of the sample at a composition of [1:6.2:102.8] to demonstrate this strange colouring behaviour.

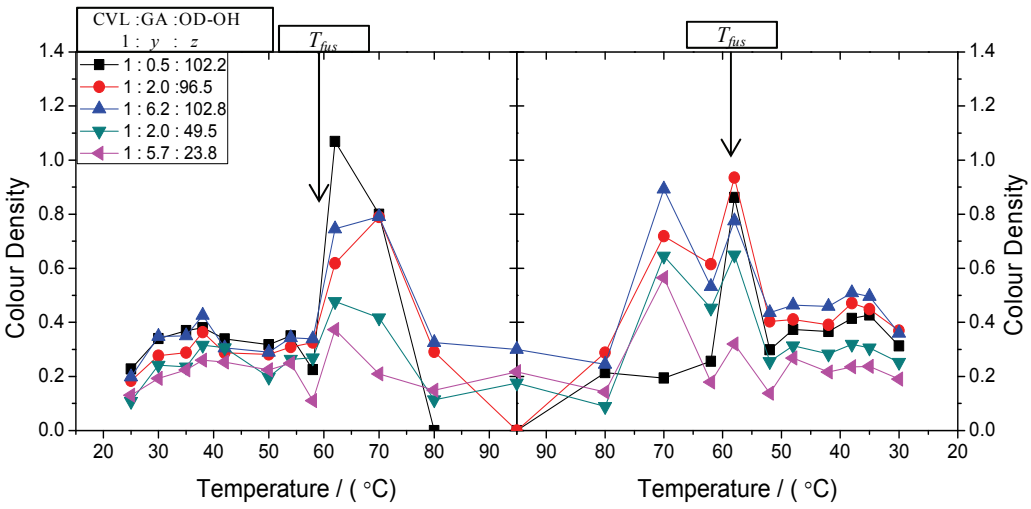

Figure 5.20. Colour density versus temperature plots obtained *via* colour photo analysis for samples in the CVL:GA:OD-OH system. The molar ratios of the three components are given on the figure. Heating rates during these experiments were d*T*/d*t* = 1 K min^{-1}. T_{fus} represents the melting point of the pure solvent. Lines are added as a guide to the eye. Error in *CD* was estimated to be +/-0.15.

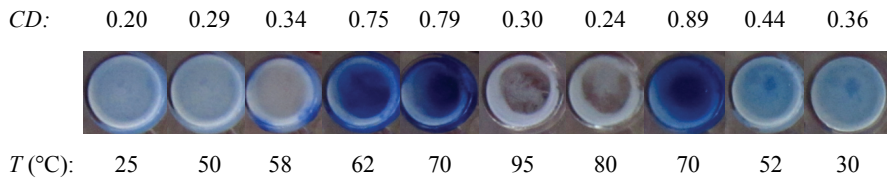

Figure 5.21. Colour photographs of the CVL:GA:OD-OH sample at a composition of [1:6.2:102.8].

5.2.4.4 Summary of Thermochromic Behaviour in CVL:GA:Alcohol Mixtures

Thermochromic mixtures containing gallic acid presented an interesting scenario in which the poor solubility of the developer in the molten solvent played an important role in defining the colouring behaviour. The low developer solubility made complete colour erasure in the molten state nearly impossible, even at mixing ratios which were shown to form fully decoloured melts in OG- and PG-containing mixtures.

The thermochromic behaviour of GA-containing mixtures was quite different across the three solvents studied here. In the CVL:GA:TD-OH mixtures, the equilibrium solid state was initially decoloured and the melt became more strongly coloured, indicating melt-darkened behaviour. However, the post-solidification colour density remained very high, which suggested that the lack of pre-melt colour was due to poor mixing of the three components immediately after sample preparation.

CVL:GA:HD-OH mixtures demonstrated the melt-lightened behaviour characteristic of mixtures containing mismatched alkyl chain lengths. These mixtures were coloured in the solid state and became less strongly coloured in the melt. The major detrimental factor observed in such mixtures was the high opacity of the melt due to poor GA solubility.

CVL:GA:OD-OH mixtures demonstrated the most interesting features as the equilibrium solids were generally weakly coloured, likely due to poor mixing of the three components, and became intensely coloured near the melting point of the pure solvent (both on heating and cooling). The R-phase may be responsible for this generation of colour as the heightened degree of rotational freedom of the solvent likely caused increased molecular mobility in the solid state, promoting the interaction of the dye and developer and giving rise to colour formation.

Unfortunately, the high opacity of the melt and unpredictable nature of the colouring behaviour in GA-containing mixtures precludes their utility in thermochromic applications.

5.3 Summary of the Influence of Developer Chain Length

The results presented in this chapter provide valuable insights into the thermochromic behaviour of three-component, reversible thermochromic systems containing alkyl gallate developers and alkyl alcohol solvents, allowing for the prediction of thermochromic behaviour in such systems.

When the alkyl chains attached to the gallate and alcohol, respectively, are well-matched in terms of chain length, thermochromic behaviour adhering to the following trends was observed: (1) at sufficient solvent concentration, the equilibrium solid was decoloured, (2) the melt was coloured when the developer concentration was relatively high (*e.g.*, when $y > 2$) and the solvent concentration was relatively low (*e.g.*, when $z < 60$), (3) the mixture was effectively never coloured when the developer concentration was very low (*e.g.*, when $y < 2$) and the solvent concentration was high (*e.g.*, when $z > 60$),

and (4) at very low solvent concentrations (*e.g.*, when $z \leq 25$), the equilibrium solid could become coloured, thereby reducing colour contrast. In general, melt-darkened thermochromism was observed for mixtures containing well-matched alkyl chain lengths.

To obtain mixtures with sufficiently high colour contrast, a relatively large amount of solvent is required in the mixture (*e.g.*, $z \geq 50$) to ensure completely colourless equilibrium solids. To ensure that the colour of the melt is sufficiently high, the developer concentration must be substantially higher than that of the dye (*e.g.*, $y \geq 5$). The three octadecyl gallate (ODG) containing mixtures, in which the alkyl chain lengths are well-matched, all demonstrated this type of melt-darkened behaviour.

Alternatively, melt-lightened thermochromic behaviour can be obtained if the lengths of the alkyl chains attached to the gallate and the alcohol, respectively, are poorly matched, and the solvent concentration is high (*e.g.*, when $z \approx 100$). In three-component mixtures demonstrating this type of alkyl chain length mismatch, such as the OG-, PG- and GA-containing systems, melt-lightened thermochromism adhering to the following trends was observed: (1) the equilibrium solid usually was strongly coloured, (2) the melt could be completely decoloured if the solvent concentration was high (*e.g.*, when $z \approx 100$), (3) the colour density of the coloured state was strongly dependent on the developer concentration, and (4) the degree of colour loss upon transition to the melt was dependent on the solvent concentration.

In certain cases, the developer and solvent components can demonstrate substantial structural dissimilarities which caused other types of problems. For example, with the developers propyl gallate and gallic acid, the length of the alkyl chain is so short that these developers were very poorly soluble in the molten phase of the solvent. This

caused high opacity in what should ideally be a completely colourless, transparent melt. This behaviour was observed to a lesser extent in other mixtures containing poorly matched alkyl chain lengths such as the CVL:OG:OD-OH and CVL:DDG:OD-OH mixtures. When the alkyl chains were well-matched, the developer often demonstrated better solubility in the molten solvent, reducing melt opacity.

Other issues associated with poor solubility of the developer in the solvent further complicated the thermochromic behaviour in the molten state. For example, during sample preparation, and upon freezing of the molten phase, the three components of the mixture can become phase-separated, thereby preventing homogenous colouration in solid state. In some instances where the colour of the solid phase was expected to be very high, as in mismatched systems such as the PG and GA systems, poor mixing in the solid phase artificially lowered the colour density of the coloured solid phase. This issue could potentially be avoided by adding additional components to the mixtures, such as emulsifiers or surfactants to aid in solid state phase mixing, but unfortunately it is highly likely that these additives would disrupt the expected thermochromic behaviour in such systems.

The R-phase of the solvent was shown to play a role in the colouring behaviour of the solid state of these mixtures. Transition to the R-phase from the LO-phase (on heating) provided a more mobile medium for the dye and developer due to the heightened dynamical disorder of the R-phase. In most samples on heating, conversion to the R-phase caused the colour density of the mixture to decrease as the temperature approached the melting point of the pure solvent. Conversely, near the LO-to-R phase transition temperature, the R-phase of the solvent converted into the LO-phase on removal from the

water bath due to localized cooling at the surface of the sample vial. The conversion to the LO-phase caused the formation of a coloured, metastable solid state (akin to the increase in colour observed on cooling for R-to-LO phase transitions), which caused the apparent colour density of the pre-melt solid to increase. Further heating of the mixture returned the R-phase, which resulted in decreased solid state colour density at temperatures just below the melting point of the mixture.

On cooling, conversion from the melt to the R-phase generally maintained the colour density of the melt, or in the event of an increase in colour density due to inhomogeneous precipitation of the developer from the molten solvent, promoted colour density decreases on solvent solidification. Conversion of the R-phase to the LO-phase caused large increases in the colour density of the solid state coupled with a "freezing-in" effect, akin to the effect of thermal quenching with liquid nitrogen that was used by MacLaren, Tang, and White to maintain a long-lived metastable solid state in similar mixtures.[101,102,110,181] Decolourization rates of the metastable solid produced by conversion to the LO-phase were strongly dependent on the solvent used, with the decolourization rates dramatically decreasing as the solvent alkyl chain length was increased.

The results presented in this chapter lead to an interesting question: if the phenolic developer comes from another chemical family (*e.g.*, benzophenones, bisphenols, *etc.*) and demonstrates a high degree of structural dissimilarity with the solvent (*i.e.*, a poorly matched developer:solvent system), would the thermochromic behaviour of the new system match that observed in OG-, PG-, and GA-containing mixtures, which have poorly matched alkyl chain lengths? Chapter 6 is focussed on answering this question.

Chapter 6 Thermochromic Behaviour in Mixtures Containing Other Developers and Solvents

6.1 Introduction and Background

6.1.1 Summary of Variable Alkyl Chain Length Experiments

The experiments described in Chapter 4, which examined the influence of the solvent alkyl chain length on thermochromic behaviour in three-component mixtures, and Chapter 5, which examined the influence of the developer alkyl chain length, demonstrated that the type of thermochromic behaviour observed in such systems is largely dependent on the difference in length of the alkyl chains attached to the developer and solvent and on the relative concentrations of the developer and solvent.

In mixtures containing well-matched alkyl chain lengths (chain length difference of zero to four carbon atoms), the equilibrium solid state was almost always decoloured and the melt could become coloured if the developer concentration was sufficiently large. This type of thermochromism is referred to as melt-darkened thermochromism in this thesis.

If the alkyl chain lengths were poorly matched (chain length difference of four carbon atoms or higher) the observed thermochromic behaviour was strongly influenced by the developer concentration. At low developer concentrations, little colour was observed in these mixtures, regardless of the solvent concentration. At high developer and high solvent concentrations, the solid states were intensely coloured and the molten phases became decoloured. This type of thermochromism is referred to as melt-lightened thermochromism in this thesis.

The degree of colour contrast between the coloured and decoloured states is an integral characteristic of thermochromic behaviour. Both the melt-lightened and melt-darkened mixtures examined in this thesis have been shown to demonstrate good colour contrast. In the case of melt-darkened mixtures, high developer concentrations were required to generate a dark molten phase and good colour contrast. In melt-lightened mixtures, high solvent concentrations were required to disrupt colour formation in the melt and yield good contrast.

In this chapter, the thermochromic properties of mixtures containing CVL as the dye, HD-OH as the solvent, and two new phenolic developers that do not belong to the gallate family, are examined. In addition to changing the type of developer used, the thermochromic properties of a CVL:DDG:solvent mixture containing an alkyl thiol as the solvent component are examined.

6.1.2 Other Phenolic Developers

Based on the results discussed in section 6.1.1, it was hypothesized that three-component thermochromic mixtures containing phenolic developers and alkyl alcohol solvents that displayed substantially different chemical structures would behave in a manner similar to the previously discussed three-component mixtures that contained poorly matched alkyl chain lengths. To this end, two phenolic developers commonly used in thermochromic applications, bisphenol A and 2,4-dihydroxybenzophenone, were selected for investigation of such 'chemically dissimilar' mixtures.

6.1.2.1 Bisphenol A (BPA)

Figure 6.1 shows the structure of 2,2-*bis*(4-hydroxyphenyl)propane, also known as bisphenol A (BPA). BPA is one of the most industrially relevant phenolic compounds in the world. BPA is a primary component in the common thermoplastic polycarbonate (found in plastic bottles, greenhouse panelling, DVDs, *etc.*),[197,198,199] is used in the production of epoxy resins,[200] and is used as the acidic developer component in thermal receipt paper, in which BPA generates the coloured form of a leuco dye that is embedded in the receipt paper.[33-36,41,42,105,123,124,201] However, it must be noted that BPA is a known toxic compound that disrupts endocrine function in humans, and as such its usage in consumer end-products has been reduced substantially in recent years.[202,203,204,205]

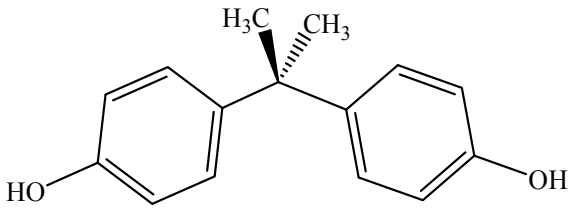

Figure 6.1. Structure of bisphenol A.

6.1.2.2 2,4-Dihydroxybenzophenone (DHB)

Figure 6.2 shows the structure of 2,4-dihydroxybenzophenone (DHB), which has also been employed as a developer in thermochromic applications.[105,123,124,201] In particular, DHB was tested during preliminary development of the thermochromic laser-jet toner e-blue™, which is currently marketed in Japan by Toshiba Co.[41,42,206,207,208] As an extension of their work on thermochromic laser jet toners, Toshiba Co. has also developed thermochromic ink-jet printing technologies which incorporate DHB as a phenolic developer.[201,209]

Chapter 8 of this thesis describes work carried out by the present author during an internship with Toshiba Co. During this internship, it was observed that DHB can be a very effective developer component in thermally erasable ink-jet printer inks. Based on the work carried out during the internship, DHB was selected for study as a developer for use in rewritable three-component thermochromic mixtures (see Chapter 8 for details).

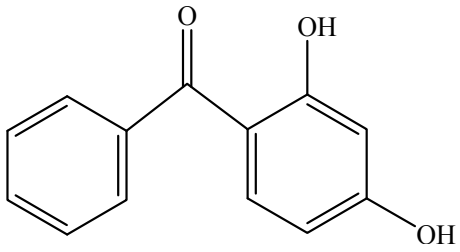

Figure 6.2. Structure of 2,4-dihydroxybenzophenone.

6.1.3 Other Solvent – Octadecanethiol

Early in the studies presented in this thesis, octadecanethiol (OD-SH) was chosen for use as a solvent component due to the inherent structural similarities it shares with the long-chain alkyl alcohols.[210] In a surprising turn of events, and due to a serendipitous calculation error, it was found that three-component thermochromic mixtures containing octadecanethiol as the solvent component exhibited thermochromic behaviour similar to mixtures containing poorly matched alkyl chain lengths. Details of the thermochromic behaviour of octadecanethiol-containing mixtures are presented in section 6.2.3.

6.2 Experimental Results and Discussion

6.2.1 CVL:BPA:HD-OH Mixtures

6.2.1.1 Introduction to Studies on CVL:BPA:HD-OH Mixtures

As discussed in section 6.1.2, BPA has previously been employed as a phenolic developer in studies on three-component, reversible thermochromic mixtures.[100,175] In such systems, the solid state generally displays strong colouration and the molten phase can become decoloured if the concentration of the solvent is sufficiently large.[100,175] This type of melt-darkened behaviour, observed previously in the present work for system with poorly matched alkyl chain lengths, was hypothesized for the CVL:BPA:HD-OH system.

6.2.1.2 Gross Features of CVL:BPA:HD-OH Mixtures

To study the thermochromic behaviour of CVL:BPA:HD-OH mixtures, two broad concentration regimes were tested: (1) the low solvent concentration regime (where z = 20 to 100), and (2) the high solvent concentration regime (where z = 300 to 2000). At all of the compositions tested, the solid state was the coloured state and the melt became decoloured. This type of melt-lightened behaviour had been hypothesized for the CVL:BPA:HD-OH system, due to the lack of structural similarity between BPA and HD-OH.

Figure 6.3 shows the colour density versus temperature plots for samples in the CVL:BPA:HD-OH system at low solvent concentration (top, z = 20 to 100) and at high solvent concentration (bottom, z = 300 to 2000). In the low solvent concentration regime, the colour density of the solid state was very high. It is clear from the colour density

values that these samples were strongly coloured in the solid states (CD_{Equil} = 1.0 to 1.4) and nearly fully decoloured in the melt (CD_{melt} = 0.0 to 0.1). The colour contrast obtained in this compositional range was the highest observed in this work, with ΔCD_{max} = 1.1 to 1.4 for the [1:8:91] and [1:4:95.4] samples.

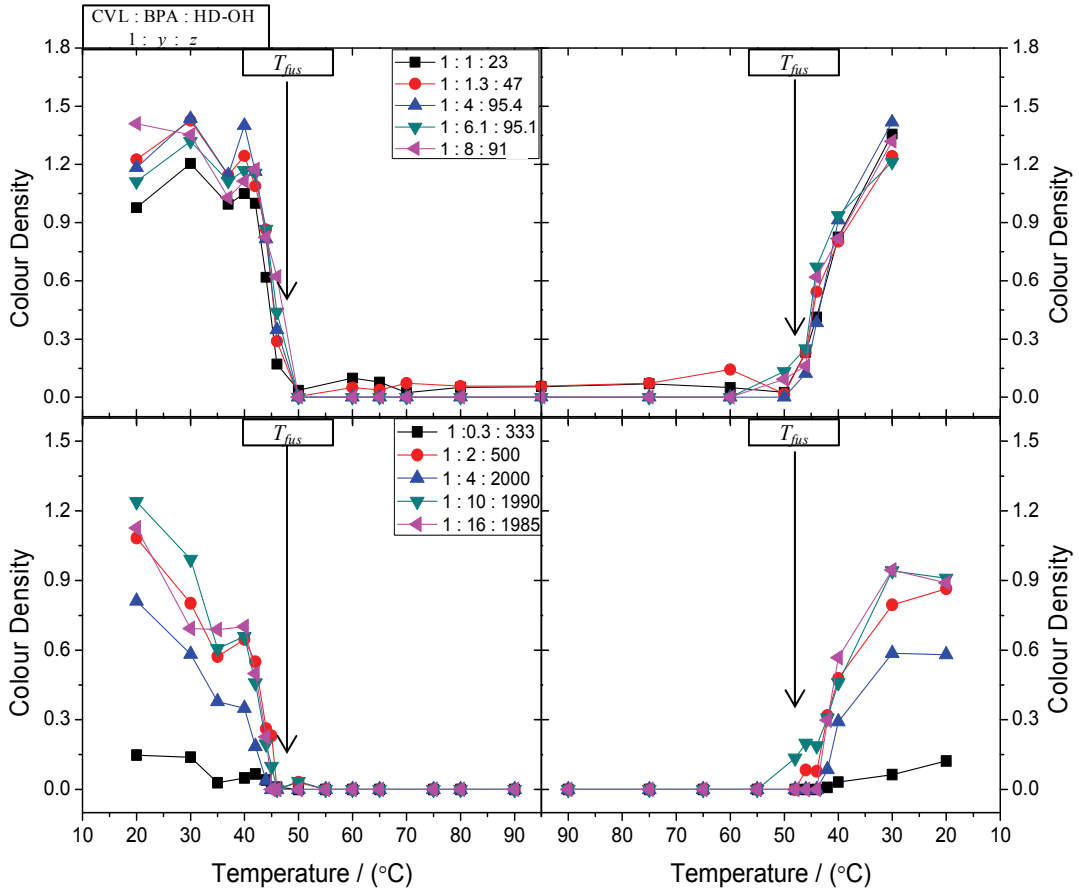

Figure 6.3. Colour density versus temperature plots obtained *via* colour photo analysis for CVL:BPA:HD-OH samples in the (top) low solvent concentration regime and (bottom) high solvent concentration regime. The molar ratios of the three components are given on the figure. Heating rates during these experiments were d*T*/d*t* = 1 K min^{-1}. T_{fus} represents the melting point of the pure solvent. Lines are added as a guide to the eye. Error in *CD* was estimated to be +/-0.15. Note that data for the high concentration regime were only collected to 90 °C.

The best colour contrast obtained for samples in the low solvent concentration regime was obtained when the melt became fully decoloured and was completely transparent. Figure 6.4 (a) shows such an example, the [1:8:91] sample, which was

deeply coloured in the solid state (CD_{Equil} = 1.4) and was completely transparent and colourless in the melt (CD_{Melt} = 0.0), giving rise to excellent colour contrast (ΔCD = 1.4).

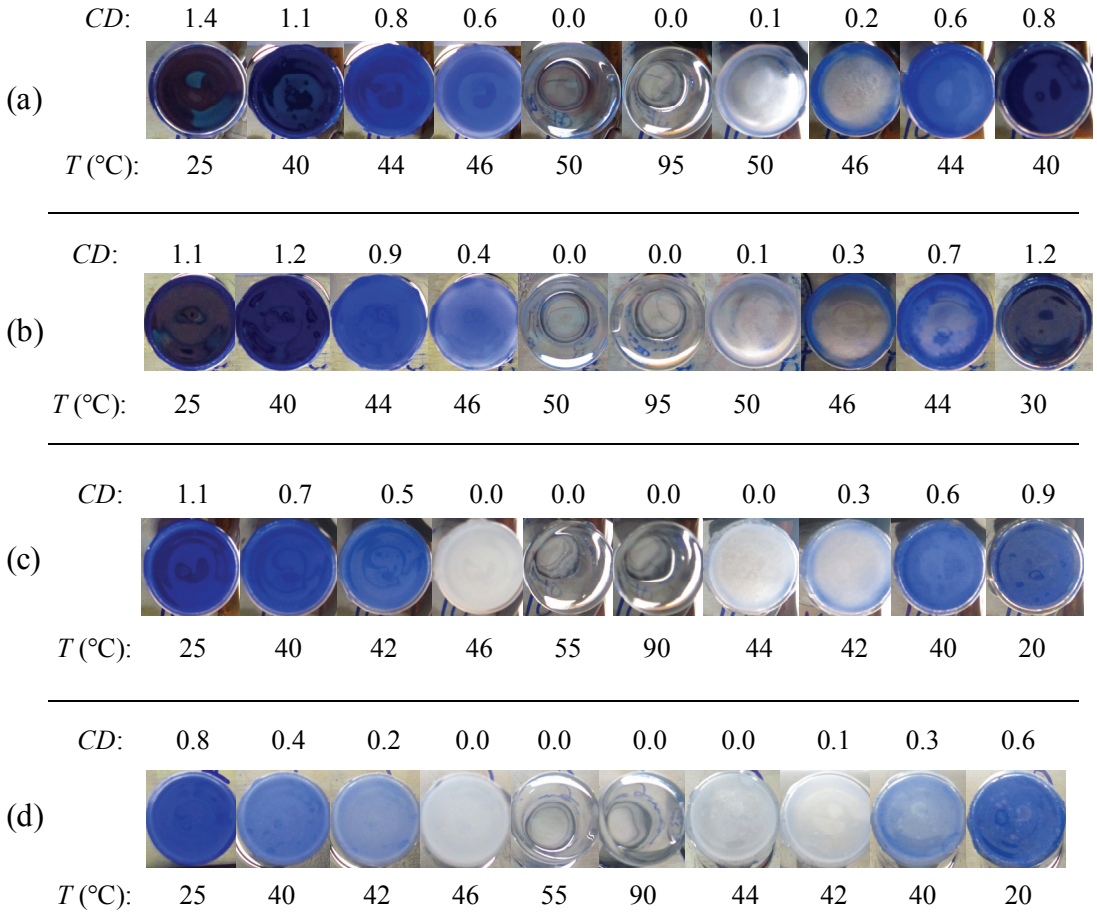

Figure 6.4. Colour photographs of CVL:BPA:HD-OH samples at various compositions; (a) [1:8:91], (b) [1:6.1:95.4], (c) [1:16:1985], and (d) [1:4:2000].

The same colouring features were observed in many samples in this concentration regime, particularly in samples with solvent concentrations near z = 100. The [1:6.1:95.4] sample, shown in Figure 6.4 (b), also demonstrated high colour contrast (ΔCD = 1.1) and a fully decoloured molten state, indicating that this compositional range is ideal for melt-lightened thermochromic behaviour.

The gross features of colouring behaviour in the high solvent concentration regime (where z = 300 to 2000) were not substantially different from the gross features observed in the low solvent concentration regime (where z = 20 to 100). Figure 6.3 (bottom) shows the colour density versus temperature plots for a series of samples in the high solvent concentration regime. In samples containing high solvent concentrations, the equilibrium solid states were coloured, although less strongly coloured than those in the low solvent concentration regime, and all of the samples analyzed melted to form completely decoloured, transparent melts.

The solid state colour densities in the high solvent concentration regime were generally lower than those observed in the low solvent concentration regime, and covered a much broader range (CD_{Equil} = 0.1 to 1.2). Although the equilibrium colour densities were lower, the molten phase of every sample in this regime was fully decoloured and completely transparent, yielding very good colour contrast (ΔCD_{max} = 1.1) in samples containing high developer concentrations (*e.g.*, [1:16:1985]).

The samples shown in Figure 6.4 (c) ([1:16:1985]) and Figure 6.4 (d) ([1:4:2000]) demonstrated very similar thermochromic behaviour. The colour density of the [1:16:1985] sample was slightly higher than that of the [1:4:2000] sample across the entire temperature range and the overall colour contrast also was greater for the y = 16 sample, however the transition temperatures for complete colour loss on heating ($T \geq 46$ °C) and colour reformation on cooling ($T \leq 40$ °C) were the same for both samples. Additionally, the colour density of the solid states of the y = 10 and 16 samples were virtually identical (see Figure 6.3), indicating that a saturation developer concentration was reached at large y values.

6.2.1.3 Fine Features of CVL:BPA:HD-OH Mixtures

The most apparent fine features observed for CVL:BPA:HD-OH mixtures were seen in mixtures containing low solvent concentrations (*e.g.*, when $z = 20$ to 50). In most samples with $z < 50$, the molten phase was observed to contain insoluble dye and/or developer, which caused high opacity in the melt. Insoluble CVL was easily observed in the molten solvent at $z \approx 20$ to 30 as a yellow solid, as evidenced in Figure 6.5 (a), which shows the [1:1:23] sample. In this sample, the deeply coloured solid state decoloured on heating as the solvent melting point was approached ($T = 44$ to 46 °C), yielding an opaque, yellow-coloured melt. It was likely that insoluble developer was also present in the molten phase due to the low solvent concentration, but, due to the yellow colour of CVL, the white BPA solids were obscured.

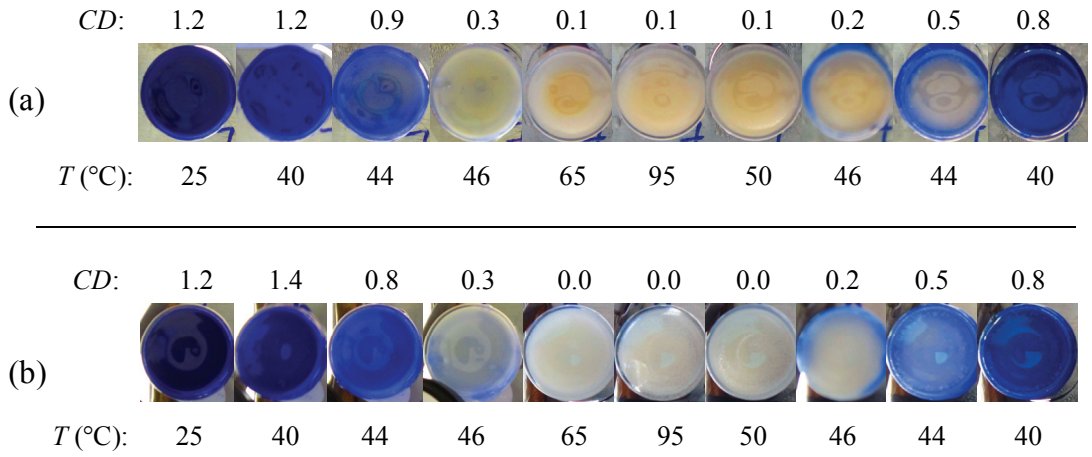

Figure 6.5. Colour photographs of CVL:BPA:HD-OH samples at low solvent concentrations (a) [1:1:23] and (b) [1:1.3:47].

Insoluble BPA was also observed in samples containing low solvent concentrations. When $z \approx 50$, the opaque melt was white in colour, indicating that only the developer was insoluble at these compositions (BPA is a white solid). For example,

the [1:1.3:47] sample shown in Figure 6.5 (b) demonstrated this type of behaviour. Nevertheless, the samples shown in Figure 6.5 demonstrated very good melt-lightened thermochromism, in which the strongly coloured solid state melted to form a decoloured melt with excellent contrast between the solid and molten states (ΔCD_{max} = 1.1 to 1.2).

The colouring behaviour of all of the CVL:BPA:HD-OH samples presented here followed the same general trends: a deeply coloured solid state melted to form a decoloured melt with very high colour contrast between the two states; at low solvent concentrations the melt became opaque due to poor dye and/or developer solubility with strong colouration returned upon solidification of the solvent.

The change in colour density from the low-temperature solid state to the melt was, however, remarkably gradual. Figure 6.6 shows this gradual change in colour density across the heat-cool cycle. The low-temperature solid state (25 to 40 °C) began to decolour around 42 to 44 °C and continually lost colour density until the solvent became fully molten ($T_{fus,HD\text{-}OH}$ = 48 to 50 °C).[144] The reduction in colour density prior to solvent melting (42 to 46 °C), and the reformation of colour upon solidification of solvent (50 to 44 °C), indicated that the R-phase of the solvent (T_{trs} = 43 to 46 °C)[144,148] plays an important role in the colouring behaviour of such mixtures.

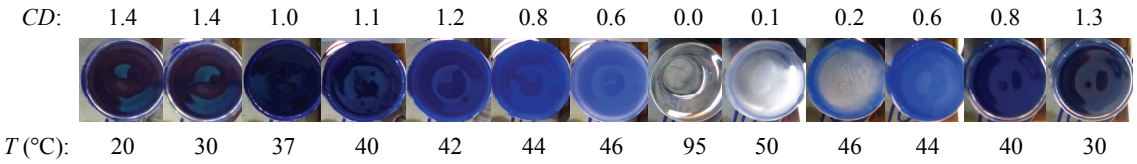

Figure 6.6. Colour photographs of the CVL:BPA:HD-OH sample at a composition of [1:8:91]. Note the gradual loss of colour on heating beginning around 40 to 42 °C before colour is completely lost upon solvent melting. On cooling, colour did not reappear with solvent solidification (T < 50 °C), instead requiring conversion to the LO-phase of the solvent (46 to 40 °C) for the full reappearance of colour.

In particular, the increased degree of rotational freedom and heightened dynamical disorder of the solvent while in the R-phase enhanced the mobility of the developer, allowing it to dissociate from the dye:developer complex and thereby disrupt the colour-forming interaction, mimicking the loss of colour that was observed in the melt. On subsequent cooling, the solvent solidification into the R-phase was insufficient to cause colour formation in solid state for the same reason (*i.e.*, enhanced developer mobility in the solid state). As the solvent solidified into the R-phase, colour was only observed on the exterior of the sample vial because the exterior of the vial is cooler than in the centre, promoting the formation of the LO-phase near the exterior of the vial, whereas colour cannot reform near the centre of the vial since the solvent remains in the R-phase. Further cooling of the mixture generated the LO-phase throughout the sample, and the pre-melt colouration returned.

6.2.1.4 Conclusions Concerning CVL:BPA:HD-OH Mixtures

The thermochromic behaviour observed for CVL:BPA:HD-OH mixtures demonstrated features consistent with the behaviour hypothesized for mixtures containing structurally dissimilar developer and solvent components. The low-temperature solid states were observed to be strongly coloured at virtually all compositions, indicating that CVL and BPA undergo stronger attractive interactions in the solid state than BPA with HD-OH. As the solid was gradually heated, the colour density gradually decreased. This behaviour is intimately coupled with the transition of the solvent from the low-temperature ordered phase (LO-phase) to the rotator phase (R-phase), as the colour density decreases were observed to occur within the LO-to-R-phase transition

temperature range for HD-OH (T_{trs} = 43 to 46).[144,148] In some instances, the colour density was almost entirely lost prior to complete melting of the solvent, indicating that the high degree of molecular mobility in the R-phase was sufficient to disrupt the CVL:BPA interaction.

Melting of the mixture caused the colour to be completely lost in most samples; when the solvent concentration was low (*e.g.*, when $z < 50$) the melt did retain some colour due primarily to insoluble BPA, and also due to insoluble CVL at very low solvent concentrations (*e.g.*, when $z < 30$). High opacity in the melt is generally regarded as problematic for the purposes of application of thermochromic materials, and as such it is apparent that the solvent concentration should be kept relatively high (*e.g.*, $z > 100$) as this allows for complete dissolution of both CVL and BPA in the molten solvent.

Colour formation on cooling mirrored the behaviour observed during the heating portion of the heat-cool cycle. Immediately upon solvent solidification, the solvent was in the R-phase. This phase was shown to promote dissociation of the CVL:BPA complex on heating, therefore freezing into the solvent R-phase prevented colour reformation during cooling. Some samples showed blue-coloured rings at the exterior of the sample vial while the centre of the vial lacked colouration. This colouration was due primarily to the fact that the exterior of the vial cools more quickly than the interior when removed from the water bath, promoting transition of the solvent to the LO-phase concomitant with colour reformation. As the samples were further cooled, the solvent was converted to the LO-phase and the deep colouration of the pre-melt, LO-phase solid state was returned.

The pre-melt R-phase behaviour seen here for CVL:BPA:HD-OH mixtures also was noted for CVL:DDG:HD-OH mixtures discussed in Chapter 4, in which the pre-melt

colour density was shown to increase near the start of the LO-to-R phase transition temperature range. In that system, conversion of the pre-melt R-phase back to the LO-phase caused the formation of a more deeply coloured, metastable solid state, and therefore it appeared that the R-phase was causing colour density increases.

All of the samples in the CVL:BPA:HD-OH system formed strongly coloured low-temperature solid states, melted to form decoloured melts (*i.e.*, decoloured in the sense that no *blue*-CVL was present), and demonstrated a wide range of colour contrast values varying from good (ΔCD_{max} = 0.7 to 0.8) to exceptionally high (ΔCD_{max} = 1.1 to 1.4). The melt-lightened behaviour seen in these samples was in excellent accord with the hypothesized behaviour for such mixtures containing structurally dissimilar developer and solvent components, and represents the best thermochromic behaviour observed in the present work.

6.2.2 CVL:DHB:HD-OH Mixtures

6.2.2.1 Introduction to Studies on CVL:DHB:HD-OH Mixtures

Although DHB has been identified as a suitable developer for thermochromic systems in the patent literature,[105,123,124,206-209] to date there are no studies in the academic literature regarding its potential use as a developer in three-component, reversible thermochromic mixtures. To this end, and to further test the hypothesis that mixtures containing structurally dissimilar developer and solvent components would demonstrate high-contrast melt-lightened thermochromism, DHB was employed as the developer component in CVL:developer:HD-OH mixtures.

6.2.2.2 Gross Features of CVL:DHB:HD-OH Mixtures

CVL:DHB:HD-OH samples were prepared in two concentration regimes: the low solvent concentration regime (where $z \approx 15$ to 100) and the high solvent concentration regime (where $z \approx 235$ to 2125). Figure 6.7 shows the colour density versus temperatures plots for samples containing low solvent concentrations (Figure 6.7 (top), $z = 15$ to 100) and high solvent concentrations (Figure 6.7 (bottom), $z = 235$ to 2125).

In the low concentration regime, the colour density of the solid state was very high in all samples studied, with *CD* values ranging from ~ 1.0 to 1.5. The colour density of these mixtures was observed to decrease precipitously as the solvent began to melt ($T_{fus,HD\text{-}OH} = 48$ to 50 °C).[144] Most of these mixtures did not become completely transparent in the molten phase due to the presence of insoluble CVL and/or DHB. Nevertheless, the blue colour associated with ring-opened CVL was in fact lost in most samples as the solvent melted, and was returned upon solidification of the solid during the cooling phase of the heat-cool cycle.

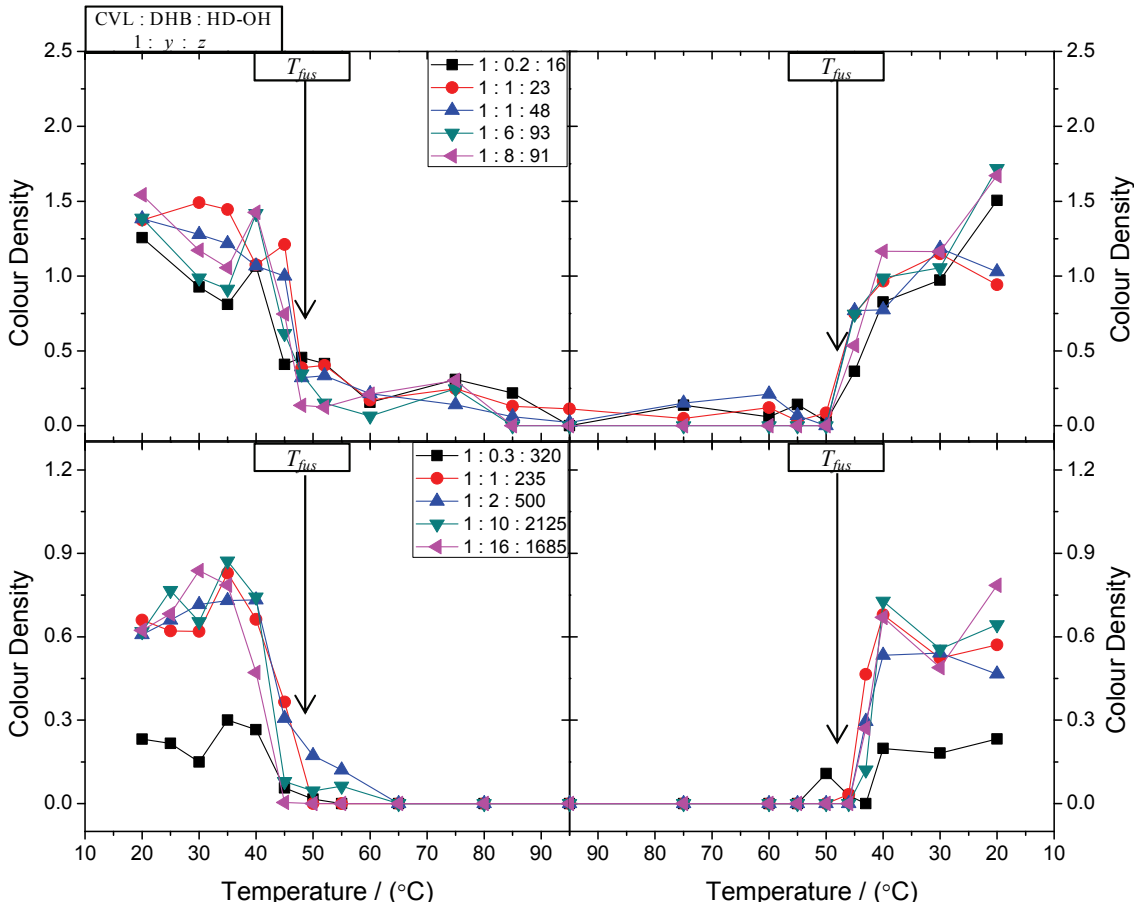

Figure 6.7. Colour density versus temperature plots obtained *via* colour photo analysis for samples in the CVL:DHB:HD-OH system in the low solvent concentration (top) and high solvent concentration (bottom) regimes. The molar ratios of the three components are given on the figure. Heating rates during these experiments were d*T*/d*t* = 1 K min^{-1}. T_{fus} represents the melting point of the pure solvent. Lines are added as a guide to the eye. Error in *CD* was estimated to be +/-0.15.

The largest colour contrast was observed in the [1:8:91] and [1:6:93] samples, which were the samples that contained the highest ratio of developer to dye. Additionally, of the five samples reported in Figure 6.7 (top), only these two melted to form fully transparent melts, due to the high solvent concentration (*e.g.*, $z \approx 90$).

Figure 6.8 (a) shows colour photos of the [1:8:91] sample. The colour density was very high in the equilibrium solid state (*CD* = 1.5) and the blue colour due to ring-opened CVL gradually weakened as the temperature was increased, first beginning to

decolour in the range 40 to 45 °C, then rapidly decolouring around 48 °C (the start of the melting range of the pure solvent), before becoming nearly completely decoloured above 50 °C. The melt became completely transparent at 52 °C but retained weak blue/green colouration until 95 °C, at which point the blue colouration was completely lost, indicating that all of the DHB had become dissolved in the molten solvent.

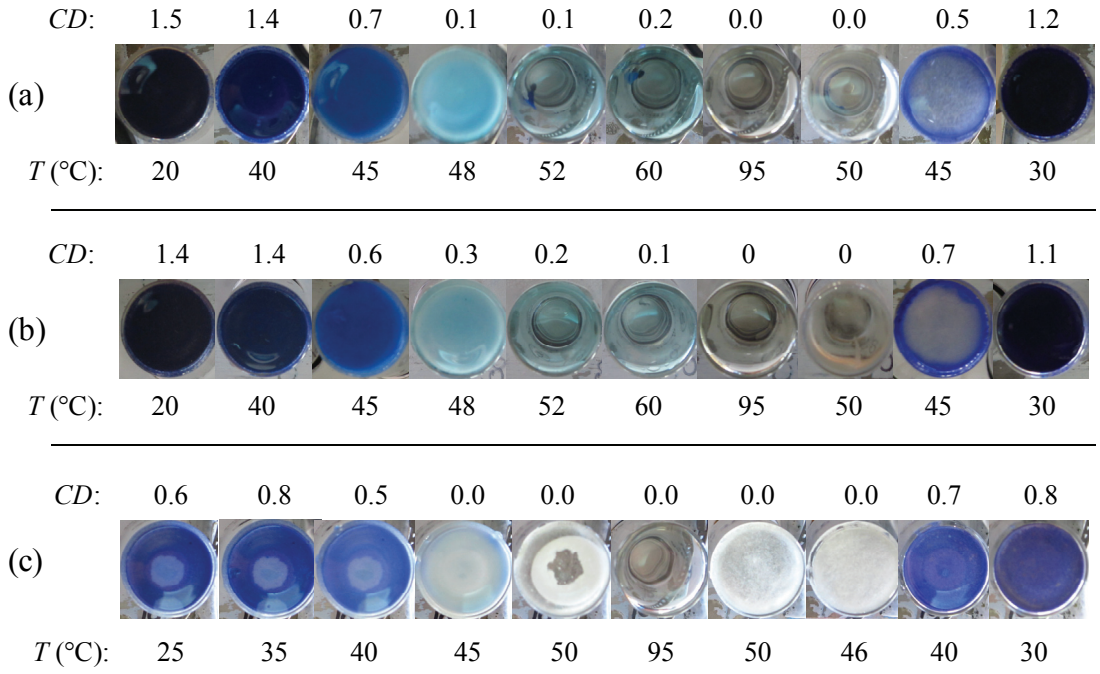

Figure 6.8. Colour photographs of CVL:DHB:HD-OH samples at various compositions: (a) [1:8:91], (b) [1:6:93], and (c) [1:16:1685].

Upon cooling, the solvent began to solidify below 50 °C and colour began to return at roughly 45 °C, intensifying rapidly as the mixture was further cooled, and by 30 °C the pre-melt colour density had returned. The high colour density of the solid state, negligible colour in the melt, and the large colour contrast between the solid and melt (ΔCD_{Max} = 1.5) make such mixtures extremely attractive for use in thermochromic materials.

The [1:6:93] sample, shown in Figure 6.8 (b), demonstrated thermochromic behaviour very similar to that of [1:8:91]. The colour contrast of [1:6:93] was very high (ΔCD = 1.4) resulting from the conversion of an intensely coloured solid state to a colourless melt, indicating that high solvent concentrations (*e.g.*, $z \approx 100$) are required for transparent, decoloured molten phases.

Vastly increasing the solvent concentration had two major effects: (1) the colour density in the solid state was substantially reduced and (2) the molten phases for all of the samples studied became completely transparent due to the improved solubility of the dye and developer in the solvent. The consequences of these effects were that the overall colour contrast in samples with high solvent concentrations were generally much lower than in low solvent concentration samples, but the improved solubility of the dye and developer in the molten solvent prevented the formation of high opacity melts, which are detrimental to the overall thermochromic effect.

Figure 6.7 (bottom) shows the colour density versus temperature plots for a series of samples in the high solvent concentration regime. The solid-state colour densities were much lower than those of the low solvent concentration samples (see Figure 6.7 (top)) and fell within a range of CD_{Equil} = 0.2 to 0.8, with most samples in the 0.6 to 0.8 range. Since all of the samples melted to form completely colourless molten phases, the colour contrast in these samples was moderate (ΔCD_{max} = 0.6 to 0.8), with negligible differences in colour contrast between samples with high and low dye:developer ratios, except for the [1:0.3:320] sample, which was weakly coloured in the solid state.

Figure 6.8 (c) shows colour photos of the [1:16:1685] sample to demonstrate the general features of the high solvent concentration samples. In the solid state, the sample was blue with moderate colour density (CD_{Equil} = 0.6). Upon heating, the colour density decreased gradually. At 35 °C, the colour density was similar to the equilibrium colour density. By 40 °C, the colour began to fade and was almost completely lost by 45 °C, indicating transition to the solvent R-phase (T_{trs} = 43 to 46 °C).[144,148] It is important to note here that 45 °C is below the melting point of pure HD-OH (T_{fus} = 48 to 50 °C).[144] At 50 °C, the sample was completely decoloured, with a small amount of solid solvent remaining in the mixture (note: the solid must be the solvent as DHB is yellow in colour). Further heating produced a completely transparent mixture.

On cooling, the solvent began to solidify prior to colour regeneration; between 50 and 46 °C a substantial amount of solvent had solidified without colour generation. By 40 °C, most of the colour had returned to the sample and by 30 °C the colour intensity reached a maximum value (CD = 0.8). This sample demonstrated good colour contrast (ΔCD = 0.6), similar to that of the CVL:gallate:alcohol mixtures discussed in Chapters 4 and 5.

6.2.2.3 Fine Features in CVL:DHB:HD-OH Mixtures

The fine features of thermochromic behaviour in the CVL:DHB:HD-OH ternary system were reminiscent of those seen in the related CVL:BPA:HD-OH ternary system. For example, when the solvent concentration was low (*e.g.*, when z = 15 to 50), the molten phase was usually opaque due to the presence of insoluble dye and/or developer.

This is evidenced in Figure 6.9 which shows colour photos of the [1:0.2:16] and [1:1:48] samples. In the [1:0.2:16] sample, the low solvent concentration prevented dissolution of the dye in the molten solvent, resulting in the retention of yellow colouration (sometimes cyan) throughout the entire heat-cool cycle. The green colour formed in the melt was a result of the mixing of the blue colour from residual ring-opened CVL with the yellow colour of the dye and developer, both of which were not completely soluble in the molten solvent at this composition.

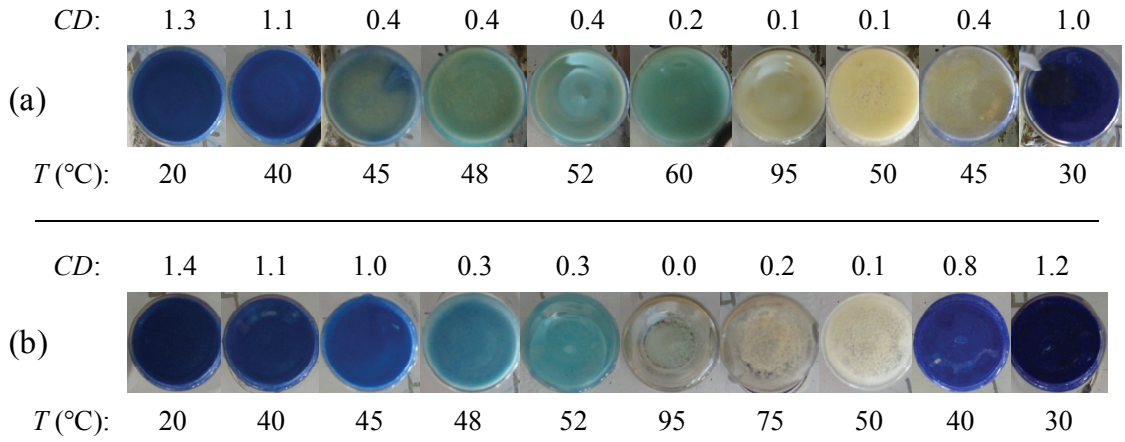

Figure 6.9. Colour photographs of CVL:DHB:HD-OH samples at compositions of (a) [1:0.2:16] and (b) [1:1:48]. Both samples demonstrate high melt opacity due to low solvent concentrations.

Increasing the solvent concentration to $z \approx 50$ caused the dye to become fully dissolved in the molten solvent, but was not sufficient to allow for complete dissolution of the developer across the entire temperature range of the heat-cool cycle. Figure 6.9 (b) shows colour photos of the [1:1:48] sample in which the developer precipitated from the molten solvent prior to solidification of the solvent (at 75 °C during cooling). In this instance, the dye became fully dissolved in the molten solvent, as did the developer at 95 °C, briefly yielding a transparent melt, prior to inhomogeneous precipitation of the developer during the cooling portion of the experiment. In contrast to the colour

generation mechanism proposed by Burkinshaw *et al.*,[16,100] inhomogeneous precipitation (*i.e.*, phase separation) of the developer did not immediately generate colour in such mixtures.

All of the CVL:DHB:HD-OH samples shown here (in Figures 6.8 and 6.9) demonstrate very similar colour change behaviour. The most intensely coloured state obtained was the low-temperature solid state, which was observed when the solvent was in the low-temperature ordered phase (LO-phase). Heating the samples to ~ 40 to 45 °C caused a moderate degree of colour loss, indicating that conversion to the rotator phase (R-phase) of the solvent was responsible for the colour loss in this range (the transition temperature range of pure HD-OH on heating is 43 to 46 °C).[144,148] Further heating to 48 °C caused more dramatic colour loss as the solvent began to melt, and by 52 °C the intense blue colour due to ring-opened CVL was nearly entirely lost.

The colour changes on cooling in these samples also indicated that the R-phase plays an important role in the colouring behaviour of such mixtures. In particular, when the solvent was in the R-phase the samples usually behaved more like a molten mixture than a low-temperature solid mixture. Referring to Figure 6.8 (c) and Figure 6.9 (a), these samples did not display the blue colour associated with ring-opened CVL at ~45 °C on cooling. At this temperature, the solvent had begun to solidify, as evidenced by the high opacity of the mixtures. Although the solvent had solidified, no blue colour was formed in these mixtures, indicating that while in the R-phase the developer and dye were still sufficiently phase-separated to prevent colour generation.

Looking specifically at 45 °C on cooling, the samples shown in Figure 6.8 (a) and (b) show the formation of intense blue colouration at the exterior of the sample vials, but

not in the centre. In the centre of these vials, the solvent was visually observed to be in the R-phase by virtue of the high glossiness of the solid, which is characteristic of the R-phase of alkyl alcohols.[148] The central regions of these samples, in which the solvent remained in the R-phase, were essentially colourless and only conversion from the R-phase to the LO-phase of the solvent, by further cooling, returned the coloured state of the samples.

6.2.2.4 Conclusions Concerning CVL:DHB:HD-OH Mixtures

The CVL:DHB:HD-OH mixtures demonstrated features similar to the behaviour observed for the CVL:BPA:HD-OH mixtures, and in good accord with the behaviour hypothesized for mixtures containing structurally dissimilar developer and solvent components. The low-temperature solid states were observed to be strongly coloured at virtually all compositions, indicating that CVL and DHB experience stronger attractive interactions in the solid state than DHB and HD-OH.

The colour density of the intensely coloured solid state gradually decreased as the temperature was raised. This behaviour was intimately coupled with the transition of the solid from the low-temperature ordered phase (LO-phase) to the rotator phase (R-phase) since the decrease in colour density was observed to occur within the LO-to-R phase transition temperature range for pure HD-OH (T_{trs} = 43 to 46).[144,148] In CVL:DHB:HD-OH mixtures, the blue colouration was nearly entirely lost prior to solvent melting, indicating that the high degree of molecular mobility in the R-phase is sufficient to disrupt the CVL:DHB interaction.

In contrast to the CVL:BPA:HD-OH mixtures, CVL:DHB:HD-OH mixtures often retained weak cyan colouration into the molten state as a result of the yellow colour of insoluble DHB overlapping with residual *blue*-CVL. As the solvent was heated to 95 °C, and the DHB dissolved, this cyan colour was lost. When the solvent concentration was low (*e.g.*, when $z < 50$), the melt did retain some colour due primarily to insoluble DHB, but also due to insoluble *leuco*-CVL when the solvent concentration was very low (*e.g.*, when $z < 20$). High opacity in the melt is generally regarded as problematic for the purposes of application in thermochromic materials, and as such it is apparent that the solvent concentration should be kept relatively high (*e.g.*, $z > 100$) to allow for complete dissolution of both CVL and DHB in the molten solvent.

Colour formation on cooling matched the behaviour observed during the heating portion of the heat-cool cycle, with the exception of the lack of formation of the weak cyan colour near the freezing point of the solvent. Immediately upon solvent solidification, the solvent was in the R-phase and samples were not coloured. Some samples showed blue-coloured rings at the exterior of the sample vial while the centre remained colourless, due to the exterior ring of the sample vial being slightly cooler than the interior. As the samples were further cooled, the entire mixture converted to the LO-phase and the deep colouration of the pre-melt, LO-phase solid state was returned.

Most of the samples in the CVL:DHB:HD-OH system formed strongly coloured low-temperature solid states, melted to form largely decoloured melts, and demonstrated a wide range of colour contrasts varying from good ($\Delta CD_{max} = 0.7$ to 0.8) to excellent ($\Delta CD_{max} = 1.4$ to 1.5). The melt-lightened behaviour seen in these samples was similar to the results obtained from studies on CVL:BPA:HD-OH mixtures, and was in excellent

accord with the hypothesized behaviour for such mixtures containing structurally dissimilar developer and solvent components.

6.2.3 CVL:DDG:OD-SH Mixtures

6.2.3.1 Introduction to Studies on CVL:DDG:OD-SH Mixtures

MacLaren and White carried out extensive studies on CVL:developer:solvent mixtures with a focus on examining time-dependent colour changes after thermal quenching with liquid nitrogen.[101,110] To extend this work, the current author selected octadecanethiol (OD-SH) as a new solvent component to test the influence of the solvent end-group on thermochromic behaviour. During preliminary testing of CVL:DDG:OD-SH mixtures, it was observed that at conventional mixing ratios (*e.g.*, [1:6:40], [1:10:100], *etc.*), all of the samples prepared were very strongly coloured in the solid state (*e.g.*, CD_{Equil} = 1.0 to 1.5) and even more strongly coloured in the melt (*i.e.*, CD_{Melt} > 1.5). Although some thermochromism was identified (*i.e.*, $\Delta CD \neq 0$), the colour contrast was poor owing to the fact that both the solid state and the melt were strongly coloured.

During sample preparation of CVL:DDG:OD-SH mixtures meant to be in the [1:*y*:100] compositional range, a mixing error yielded thermochromic mixtures demonstrating excellent melt-lightened behaviour. As a result of the accidental 10-fold increase in solvent concentration, it was observed that strongly coloured solid states could be melted to form colourless melts. At this point it was realized that this behaviour could also be possible in systems demonstrating poor colour contrast (*e.g.*,

CVL:DDG:OD-OH, CVL:PG:solvent, *etc.*) which had been deemed of poor thermochromic quality in previous studies.[110]

This serendipitous mixing error paved the way for the studies presented in Chapters 4, 5, and 6. Regardless of the importance of this discovery to the present work, mixtures containing OD-SH will likely never find any practical use due to the overwhelming stench produced by thiol-containing compounds. Nevertheless, the study of CVL:gallate:OD-SH mixtures is of importance to the present study, and as such the results of examination of thermochromic behaviour in CVL:DDG:OD-SH mixtures are presented in the following sections.

6.2.3.2 Gross Features of CVL:DDG:OD-SH Mixtures

The thermochromic behaviour of CVL:DDG:OD-SH mixtures was studied using the observational spectroscopy technique described in section 3.3.1.2, and the colour scale shown in Figure 3.5 was used to determine the colour density of the solid and molten states.

To obtain good colour contrast between the coloured equilibrium solid state and the decoloured melt in CVL:DDG:OD-SH mixtures, very high solvent concentrations were required. Figure 6.10 shows the colour density versus temperature plots for CVL:DDG:OD-SH samples containing extremely high solvent concentrations ($z \approx 1900$ to 2100). Melt-lightened thermochromic behaviour was observed for most samples in this concentration regime, with moderately coloured pre-melt solid states ($CD_{\text{Equil}} \approx 0.5$ to 1.0) melting to form largely decoloured melts. Only the $y = 10$ sample demonstrated substantial colouration into the melt ($CD_{\text{Melt}} = 0.4$). This resulted in colour contrast

values on the order of $\Delta CD_{max} \approx 0.5$ to 0.8 for most samples. The sample with $y = 2$ was never coloured due to the very low dye and developer concentrations in this sample.

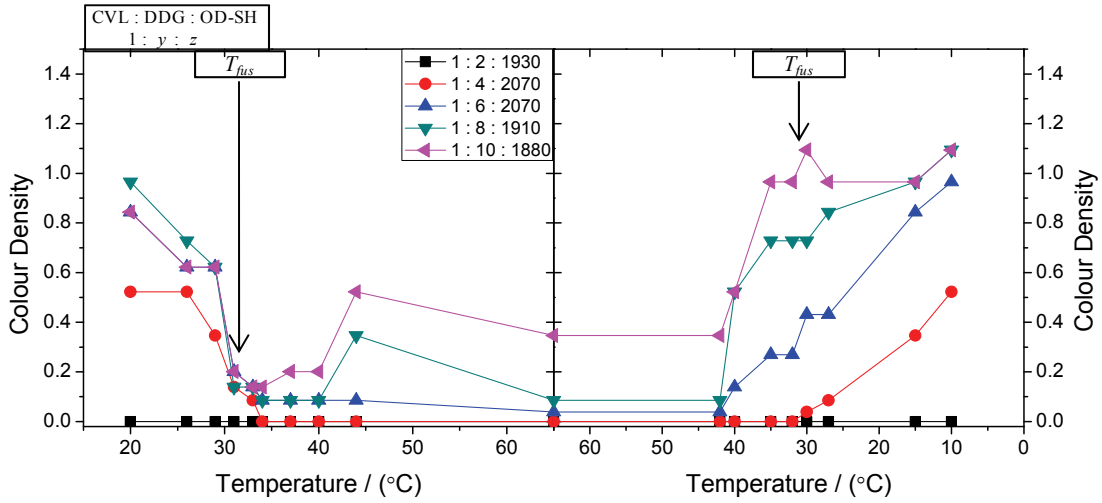

Figure 6.10. Colour density versus temperature plots obtained *via* observational spectroscopy for samples in the CVL:DDG:OD-SH system with $z \approx 1900$ to 2100. The molar ratios of the three components are given on the figure. Heating rates during these experiments were $dT/dt = 1$ K min^{-1}. T_{fus} represents the melting point of the pure solvent. Lines are added as a guide to the eye. Error in *CD* was estimated to be +/-0.15.

The colour density of these samples on cooling generally began to return prior to solvent solidification ($T_{fus,OD\text{-}SH}$ = 30 to 33 °C).[210] Similar behaviour was noted in the CVL:OG:TD-OH system (section 5.2.2.1) for the [1:6.2:103.2] sample (see Figure 5.8), in which precipitation of the developer from the molten solvent caused colour formation prior to solvent solidification. The increase in colour density observed for CVL:DDG:OD-SH samples with $z \approx 1900$ to 2100 and $y \geq 6$ was also due precipitation of the developer from the molten solvent resulting in the formation of the coloured dye:developer complex.

Decreasing the solvent concentration caused increases to the colour density in the solid state and in the melt. Figure 6.11 shows the colour density versus temperature plots

for samples with $z \approx 900$ to 1000. Melt-lightened behaviour was observed for most samples in this concentration regime. The colour densities of the solid state in the $z \approx 900$ to 1000 regime were generally higher than in the $z \approx 1900$ to 2100; in particular the [1:10:880] sample demonstrated strong colouration in the solid state ($CD_{\text{Equil}} \approx 1.2$). The colour density of the melt, however, was also substantially increased ($CD_{\text{melt}} \approx 1.0$), which reduced the overall colour contrast.

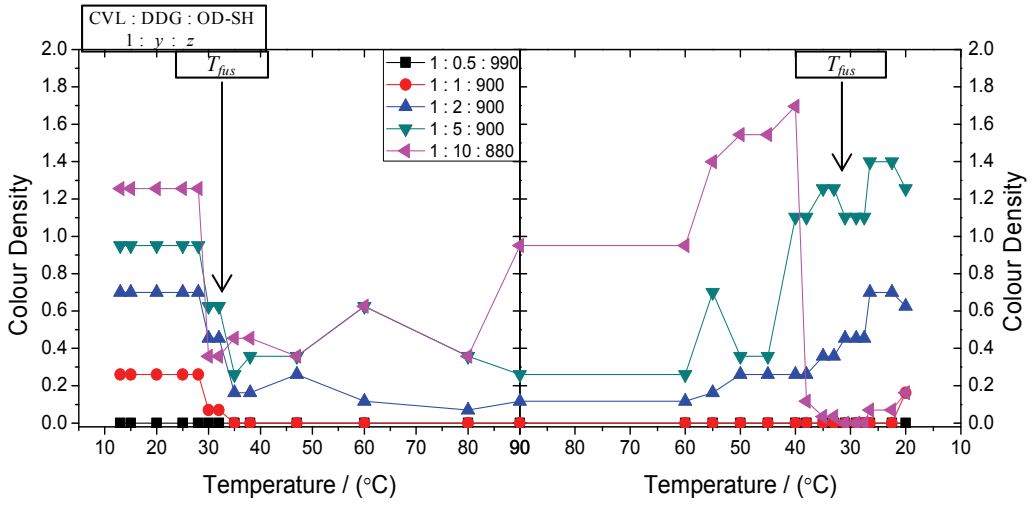

Figure 6.11. Colour density versus temperature plots obtained *via* observational spectroscopy for samples in the CVL:DDG:OD-SH system with $z \approx 900$ to 1000. The molar ratios of the three components are given on the figure. Heating rates during these experiments were $dT/dt = 1$ K min^{-1}. T_{fus} represents the melting point of the pure solvent. Lines are added as a guide to the eye. Error in *CD* was estimated to be +/-0.15.

The [1:2:900] sample formed a nearly colourless melt coupled with a moderately coloured solid state, yielding reasonable colour contrast ($\Delta CD \approx 0.5$) compared to the [1:2:1930] sample, which was not coloured at any temperature. The best colour contrast observed in the $z \approx 900$ to 1000 samples was obtained for the [1:5:900] sample, which formed a coloured solid ($CD_{\text{Equil}} \approx 0.9$) and melted to give a weakly coloured melt ($CD_{\text{Melt}} \approx 0.3$), yielding a colour contrast of $\Delta CD \approx 0.6$. As the solvent concentration was

decreased, the maximum colour contrast obtained in CVL:DDG:OD-SH mixtures was reduced.

Further deducing the solvent concentration resulted in the appearance of melt-darkened behaviour at high developer concentrations, although melt-lightened thermochromism was observed for some samples. Figure 6.12 shows the colour density versus temperature plots for samples in the $z \approx 650$ to 715 (top) and $z = 500$ (bottom) regimes. The [1:5:700] and [1:10:700] samples demonstrated melt-darkened behaviour, indicating the presence of a developer concentration threshold for inversion of colouring behaviour near $y = 5$ for the $z = 650$ to 715 regime.

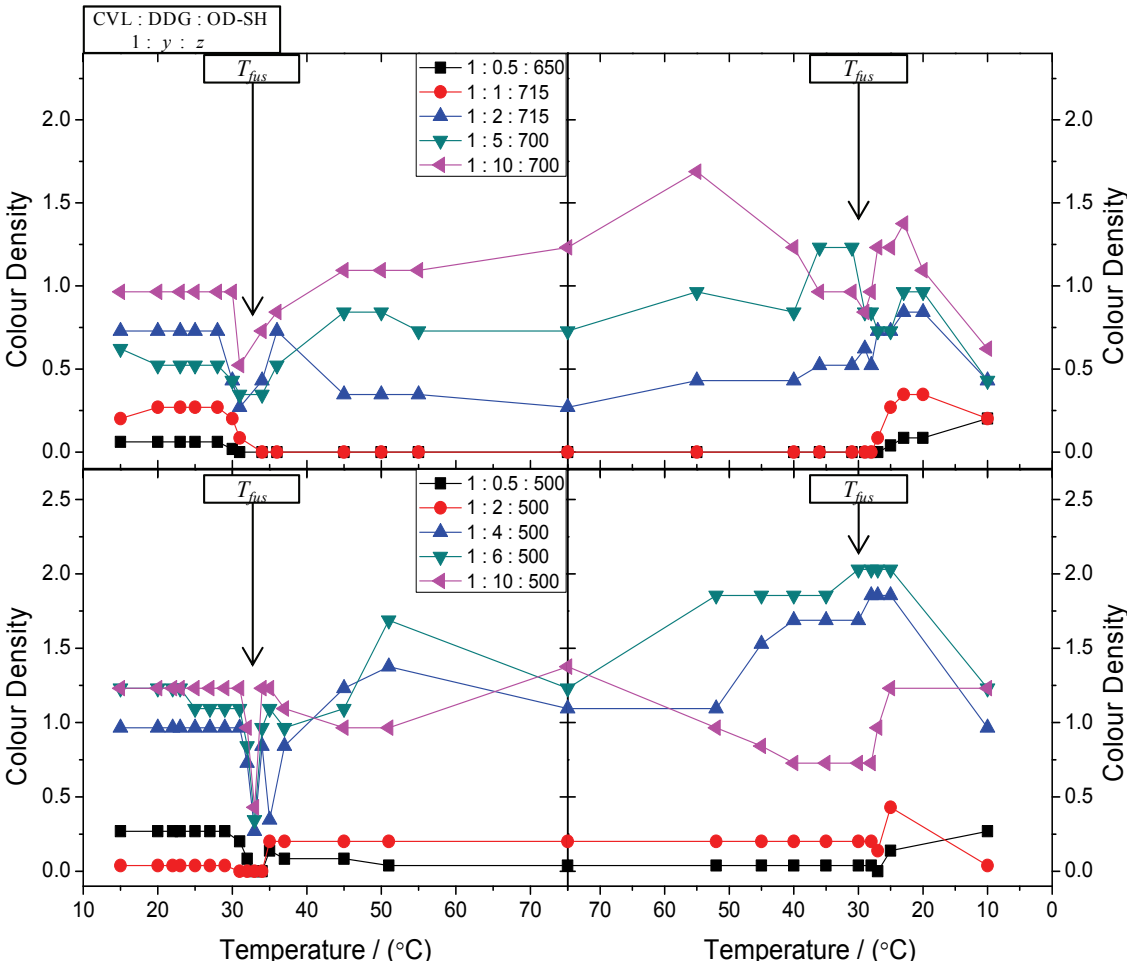

Figure 6.12. Colour density versus temperature plots obtained *via* observational spectroscopy for CVL:DDG:OD-SH samples in the (top) $z \approx 650$ to 715 and (bottom) $z = 500$ compositional ranges. The molar ratios of the three components are given on the figure. Heating rates during these experiments were $dT/dt = 1$ K min^{-1}. T_{fus} represents the melting point of the pure solvent. Lines are added as a guide to the eye. Error in *CD* was estimated to be +/-0.15.

The colour contrast in the $z = 650$ to 715 regime was poor for all samples studied due to the shift in thermochromic behaviour (melt-lightened versus melt-darkened) at intermediate ($y \approx 5$) developer concentrations. Below the threshold value the colour density of the solid state was low ($CD_{Equil} \leq 0.7$), and above the threshold value the colour density of the solid state was relatively high ($CD > 0.6$), resulting in thermochromic transformations of low colour contrast ($\Delta CD_{max} \approx 0.2$ to 0.6).

Further decreasing the solvent concentration (*e.g.*, samples with $z = 500$) had the predicted effect of reducing overall colour contrast even further, while increasing the colour density of the solid state. Figure 6.12 (bottom) shows the colour density versus temperature plots for $[1:y:500]$ samples. The $[1:4:500]$ sample demonstrated melt-darkened behaviour, indicating that the developer concentration threshold was below $y = 4$ for this series of samples. As with the $z \approx 700$ samples, colour contrast values were very poor in this solvent concentration regime ($\Delta CD_{max} \approx 0.3$), owing to the high colour of the solid state ($CD_{Equil} \approx 1.0$ to 1.2) and the similar colour density of the molten mixtures.

Two important features emerged from the study of CVL:DDG:OD-SH mixtures. First, the colour contrast of these mixtures depended strongly on the concentration of the solvent, with formation of high colour contrast samples relying on high dilution of the colour-forming components in the melt. Second, the developer concentration threshold also depended on the solvent concentration. The dye:developer ratio of the developer concentration threshold was observed to decrease from $y \leq 5$ at $z \approx 700$ to $y \leq 4$ at $z \approx 500$, although more data in these compositional regimes (where $500 \leq z \leq 715$) are required to confirm the exact value of the developer concentration thresholds.

6.2.3.3 Fine Features of CVL:DDG:OD-SH Mixtures

The fine features observed in the CVL:DDG:OD-SH system were very similar to those observed in the previously examined CVL:gallate:alcohol systems. The most important features were the decolouration of solid samples upon conversion to the R-phase of the solvent on heating, poor solubility of the developer in the melt at low solvent

concentrations, and the phase-separation of the developer from the low-temperature (LO) phase of solid solvent that caused large drops in the colour density in the solid state.

Looking first at the pre-melt solid state colour densities of the samples shown in Figure 6.10 (where $z \approx 1900$ to 2100), it is apparent that the decrease in colour density on heating was fairly gradual. The low-temperature solid state, which exists below 25 °C, slowly lost colour density as the mixture was heated to ~30 °C. The solvent was visually observed to transform to the R-phase over this temperature range by virtue of the change from a waxy, opaque solid to a glossy, translucent solid. The colour density increase on cooling from the decoloured melt was also observed to be a gradual process, whereby the colour began to reform around ~ 40 °C, gradually intensifying in the 40 to 30 °C region (corresponding to the liquid-to-R phase transition), before rapidly intensifying as the temperature dropped below 20 °C, at which point the solvent was completely in the LO-phase. Similar behaviour was observed for the $z \leq 1000$ samples, although the temperature range of gradual colour loss was substantially shorter due to the decreased solvent concentrations.

In samples containing relatively large developer concentrations (*e.g.*, when $y \geq 4$), insoluble developer was observed in the molten phase of the mixtures. The amount of insoluble developer increased as the developer concentration increased, as expected, and in most samples with $y = 10$, the melt was completely opaque. As before, increasing the temperature of the water bath to 95 °C was sufficient to cause complete dissolution of DDG, which reduced the opacity of the melt. Due to the low dye concentration, no insoluble CVL was observed in the molten phase of CVL:DDG:OD-SH mixtures (*i.e.* there was an absence of yellow colour in molten mixtures).

The poor solubility of DDG in the molten solvent caused inhomogeneous precipitation of DDG prior to solvent solidification in many of the samples containing high developer concentrations (*e.g.*, when $y > 4$). Although this behaviour can be difficult to identify in the colour density plots shown in this section, some of the mixtures exhibited increased colour density prior to solvent solidification associated with the observed precipitation of DDG. Referring to Figure 6.11, which shows samples in the $[1{:}y{:}900 \text{ to } 1000]$ regime, the colour density of most mixtures was observed to increase gradually on cooling prior to solvent solidification. This behaviour indicated that the precipitation of the developer promoted colour formation in the melt prior to solvent solidification.

The $[1{:}10{:}880]$ sample showed a fine feature that caused substantial difficulties in the study of low solvent concentration samples (*e.g.*, $z < 100$) in the CVL:DDG:OD-SH system: the colour density of the solid dropped to near-zero values near the freezing point of the solvent. The reason for this was the inhomogeneous precipitation of the developer from the solvent, without concomitant precipitation of the dye, which prevented colour formation in the solid state. A wide range of compositions in the $[1{:}y{:}20 \text{ to } 100]$ mixing range were prepared in milligram quantities during preliminary investigations into the thermochromic behaviour of CVL:DDG:OD-SH mixtures, but inhomogeneous phase separation of the developer from the dye and solvent caused irregular colouring behaviour (*i.e.*, regions of intense-blue colouration coupled with completely colourless regions within a single sample), which resulted in the need to carry out thermochromic analysis on bulk (*i.e.*, gram-scale sized) mixtures.

6.2.3.4 Conclusions Concerning CVL:DDG:OD-SH Mixtures

Thermochromic behaviour in the CVL:DDG:OD-SH system followed trends hypothesized for mixtures contained poorly matched developer and solvent components. The solid states generally were strongly coloured, and could melt to form either less strongly coloured liquid phases (*i.e.*, melt-lightened behaviour) or more strongly coloured liquid phases (*i.e.*, melt-darkened behaviour). The type of thermochromism observed was dependent on the concentrations of the developer and the solvent.

Melt-lightened behaviour could be obtained in samples containing very high solvent concentrations ($z > 1000$) due to the decolourization of the molten phase. In such mixtures, high developer concentrations were required to generate solids dark enough to yield good colour contrast ($\Delta CD_{max} = 0.5$ to 0.8). Reducing the solvent concentration caused increases in the colour density of both the solid state and the melt, thereby reducing the overall colour contrast ($\Delta CD_{max} \approx 0.3$ to 0.8) observed in samples with intermediate solvent concentration ($700 \leq z \leq 1000$).

Reduced solvent concentrations also resulted in the appearance of a developer concentration threshold above which melt-darkened behaviour was observed, and below which melt-lightened behaviour was observed. The developer concentration threshold was observed in $z \approx 700$ mixtures to be $y \leq \sim 5$, and in $z \approx 500$ mixtures to be $y \leq \sim 4$, although due to the small amount of data recorded in these compositional regimes it is possible that the developer threshold value was equal for both regimes. The value of the developer threshold likely continues to decrease with decreasing solvent concentration until melt-darkened behaviour is observed at all dye:developer molar ratios. Note: at very

low solvent concentrations, for example when $z \leq 100$, this is the case, as confirmed by experiments not presented in this thesis.

The R-phase also plays an important role in the colouring behaviour of CVL:DDG:OD-SH mixtures. Gradual colour loss was observed during the heating portion of the heat-cool cycle as the solvent transitioned through the R-phase. On solidification, colour slowly regenerated in the R-phase until the LO-phase of the solvent was formed, at which point the pre-melt colour density was returned. The low solubility of DDG in OD-SH caused the melt to become opaque in a number of mixtures containing intermediate solvent concentrations ($500 < z < 1000$). The low solubility of DDG also caused inhomogeneous precipitation of the developer on cooling, which presented problems such as increased melt colour density prior to solvent solidification and loss of colour in the solid state due to dye and developer phase separation (as seen in the [1:10:880] sample). The other pressing issue with using alkanethiols in thermochromic formulations is the terrible stench produced by such compounds, which limits their use to strictly academic pursuits.

6.2.4 Binary Phase Diagram Determination

6.2.4.1 Introduction to Binary Phase Diagram Determination

An important aspect in the study of the competition between dye:developer and developer:solvent interactions in three-component mixtures is the elucidation of the binary phase diagram for developer:solvent mixtures. The thermochromic behaviour observed for mixtures containing poorly matched alkyl chain lengths, as discussed in Chapters 4 and 5, was the result of weak interactions between the developer and solvent

in the solid state, which liberated the developer to interact with the dye and thereby generate colour in the solid state.

Thermochromic mixtures containing BPA and DHB as the developer were hypothesized to have even weaker interactions with the alcoholic solvent in the solid state due to the low degree of structural similarity between the mainly aromatic developer and the mainly aliphatic solvent. To this end, phase diagrams of binary mixtures of BPA with HD-OH and DHB with HD-OH were obtained *via* differential scanning calorimetry (DSC) to study the interactions between the developer and solvent in the solid state. The details of DSC methods are given in section 3.3.2.

The elucidation of phase diagrams for the alkyl gallate:alkyl alcohol binary systems was previously examined by MacLaren and White.[110,143] A summary of their results was presented previously in section 2.2.2.2 of this thesis. Briefly, the binary developer:solvent phase diagram of DDG:TD-OH (Figure 2.16) showed the formation of a compound, (DDG_2)•TD-OH, suggesting a strong attractive interaction between DDG and TD-OH in solid state.[110,143] As a result, the developer:solvent interaction dominates in the solid state of CVL:DDG:TD-OH mixtures, preventing the formation of dye:developer complexes and, therefore, colour in the equilibrium solid.[110,143]

Conversely, in alkyl gallate:alkyl alcohol mixtures that contained poorly matched alkyl chain lengths (*e.g.*, PG with HD-OH, Figure 2.17), no compound formation was observed, suggesting that in the solid state the two components interact very weakly.[110] Additionally, the absence of compound formation was also observed in PG:TD-OH, PG:OD-OH, OG:TD-OH, OG:HD-OH, and OG:OD-OH mixtures.[110] Three-component mixtures containing these binary developer:solvent combinations all behaved similarly

(see Chapter 5 of this thesis for thermochromic behaviour of CVL:PG/OG:alcohol mixtures), with the formation of a coloured solid state due to the dominant dye:developer interaction.

The low degree of structural similarity between the developer and solvent in the BPA:HD-OH and DHB:HD-OH systems suggests that the binary phase diagrams of such combinations should resemble the PG:HD-OH binary system (Figure 2.17). This expectation was reinforced by both the low degree of structural similarity between BPA/DHB and HD-OH and by the fact that three-component mixtures containing BPA and DHB demonstrated thermochromic behaviour similar to mixtures containing OG and PG as the developer component (see sections 5.2.2 and 5.2.3, respectively).

6.2.4.2 Binary Phase Diagram Determination for BPA:HD-OH Mixtures

The binary phase diagram for BPA:HD-OH mixtures, obtained from the heating portion of DSC experiments, is shown in Figure 6.13. No compound formation was observed between BPA and HD-OH and a single eutectic was identified in the region of $0.1 < x_{BPA} < 0.2$. The shape and features of the BPA:HD-OH phase diagram were very similar to those of the PG:HD-OH phase diagram shown in Figure 2.17. Both systems, which demonstrated strongly coloured solid states in three-component mixtures, lacked the formation of a compound in the solid state, further supporting the hypothesis that little interaction between the developer and solvent occurs in the solid state of mixtures that form coloured solid states and undergo melt-lightened thermochromism.

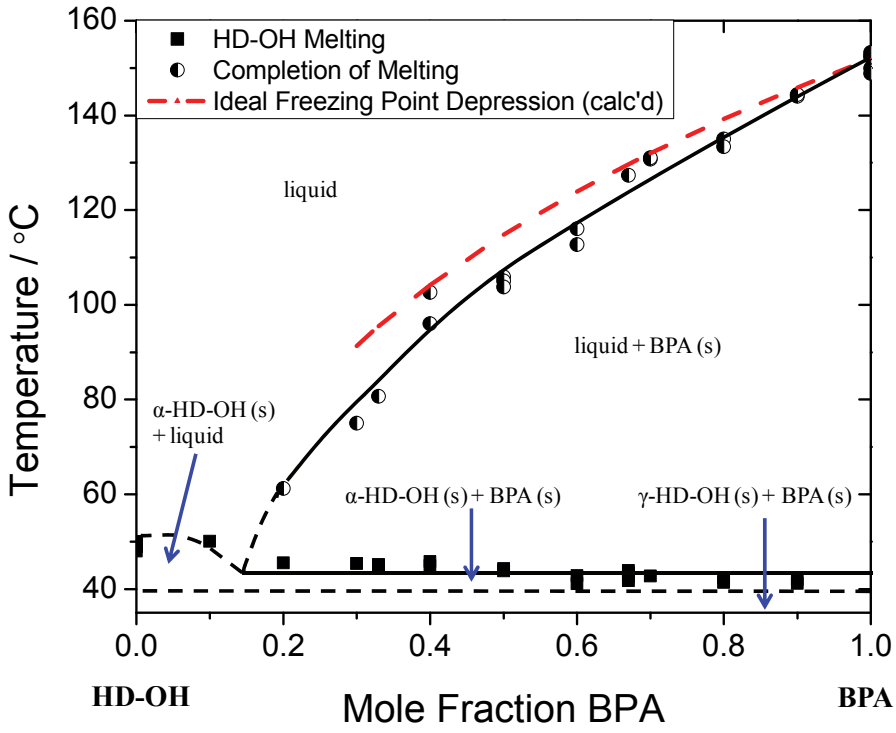

Figure 6.13. Binary phase diagram determined by DSC on heating for 1-hexadecanol (HD-OH) and bisphenol A (BPA) mixtures. Note the lack of compound formation.

The boundary curve between solid+liquid regions and liquid-only regions in a binary phase diagram (*i.e.*, the completion of melting of the mixture) is the liquidus curve. The boundary curve for the transition from a solid+liquid region to a solid-only region is the solidus curve. A eutectic is observed when two liquidus curves and a solidus curve intersect.[211,212,213] At the eutectic composition, all of the components in the solid state melt uniformly and completely at one temperature to form a liquid mixture containing the dissociated components, here called A and B. On either side of the eutectic point, the liquidus curves for component A and component B, respectively, vary as a function of composition. The liquidus curves for each pure component begin at the melting point of the pure component ($T°_{fus}$) and slope downward towards the eutectic point as the composition of the binary mixture is changed. The basic curvature of the

liquidus curve is governed by the ideal freezing point depression of component A by the addition of component B,[211-213]

$$\ln x_A = \frac{\Delta_{fus}H^{\circ}_A}{R}\left(\frac{1}{T^{\circ}_{fus,A}} - \frac{1}{T^{obs}_{fus}}\right) \quad (6.1)$$

where x_A is the mole fraction of component A, $\Delta_{fus}H^{\circ}_A$ is the enthalpy of fusion of pure A, R is the gas constant, $T^{\circ}_{fus,A}$ is the melting temperature of pure A, and T^{obs}_{fus} is the observed melting temperature of the mixture. Deviations from the ideal freezing point depression are indicative of interactions occurring between the two components of the mixture. To a simple approximation, a steeper downward slope than the ideal freezing point depression is indicative of attractive interactions between the two components.[211-213]

From Figure 6.13, the melting point of BPA decreased as a function of $x_{HD\text{-}OH}$, as expected from equation (6.1), and demonstrated a slight negative deviation from the calculated ideal freezing point depression. This behaviour is indicative of the formation of a solid solution in which the HD-OH and BPA molecules undergo an attractive interaction. The deviation from ideal freezing point depression is, however, small.

The observed phase behaviour of BPA:HD-OH mixtures provides additional evidence that in the solid state these two components do not undergo any substantial attractive interactions. Although a weak attractive interaction was observed, the strength of this interaction is quite small, and was insufficient to lead to compound formation. This behaviour causes the dye:developer complex to dominate in the solid state, allowing for the intense colouration of the solid state in ternary mixtures such as CVL:BPA:HD-

OH and CVL:PG:HD-OH, which contain structurally dissimilar developer and solvent components.

6.2.4.3 Binary Phase Diagram Determination for DHB:HD-OH Mixtures

Figure 6.14 shows the binary phase diagram for DHB:HD-OH mixtures as determined *via* DSC analysis. The phase diagram of the DHB:HD-OH binary system was very similar to that of BPA:HD-OH and PG:HD-OH mixtures. DHB was slightly more difficult to study than BPA due to vitrification of DHB during cooling, which sometimes prevented crystallization in HD-OH rich mixtures. In such instances, it was either impossible to resolve DHB melting during heating runs (particularly when $x_{DHB} < 0.2$) or the glassy DHB crystallized on heating, giving rise to exothermic transitions during the heating cycles (melting is endothermic, therefore exothermic DHB crystallization peaks distorted the shape of the HD-OH melting transition peaks). Nevertheless, sufficient data for DHB melting were obtained across a large portion of the binary phase diagram ($0.3 \leq x_{DHB} \leq 1$) to allow the elucidation of the binary phase diagram for DHB:HD-OH.

No compound formation was observed in the DHB:HD-OH phase diagram, and the freezing point depression of the DHB liquidus curve had a slightly negative deviation from ideality. These features are indicative of a weak attractive interaction between DHB and HD-OH that was not strong enough to cause compound formation in the solid state. The deviation from ideal freezing point depression was slightly larger for DHB than was observed for BPA, indicating a slightly stronger attraction in the DHB binary system. Nevertheless, neither system demonstrated particularly strong attraction between the two components, in accord with the hypothesized behaviour.

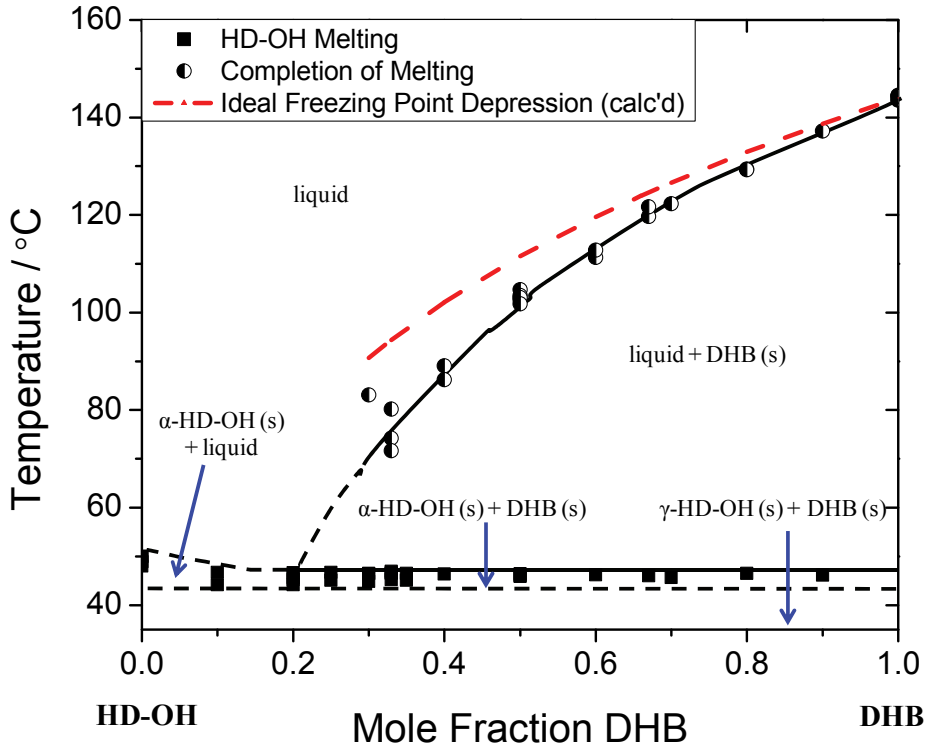

Figure 6.14. Binary phase diagram determined by DSC on heating for 1-hexadecanol (HD) and 2,4-dihydroxybenzophenone (DHB) mixtures. Note the lack of compound formation.

6.2.4.4 Binary Phase Diagram Determination for DDG:OD-SH Mixtures

The binary phase diagram for DDG:OD-SH mixtures was determined *via* DSC analysis to determine the degree of interaction between the two components in the solid state. A binary phase diagram similar to those obtained for BPA:HD-OH and DHB:HD-OH mixtures was hypothesized based on the similar thermochromic behaviour observed for the three-component system, although the possibility for compound formation was more likely in the DDG:OD-SH system due to the similarity in alkyl chain lengths. MacLaren and White observed compound formation in mixtures of DDG and OD-OH,[101,110,143] leading to the possibility of compound formation in DDG:OD-SH.

The binary phase diagram determined on heating *via* DSC experiments in shown in Figure 6.15. The results obtained were markedly different from previous results. The LO-to-R phase transition temperature and the melting temperature of OD-SH were essentially invariant across the entire temperature range. Furthermore, the melting transition of DDG was also essentially invariant across the entire temperature range after a brief decrease in melting temperature in the range of $0.9 \leq x_{DDG} \leq 1$. The melting behaviour observed in the DDG:OD-SH binary phase diagram indicates that these two components do not undergo any appreciable interactions in the solid state even though both components contain relatively long alkyl chains.

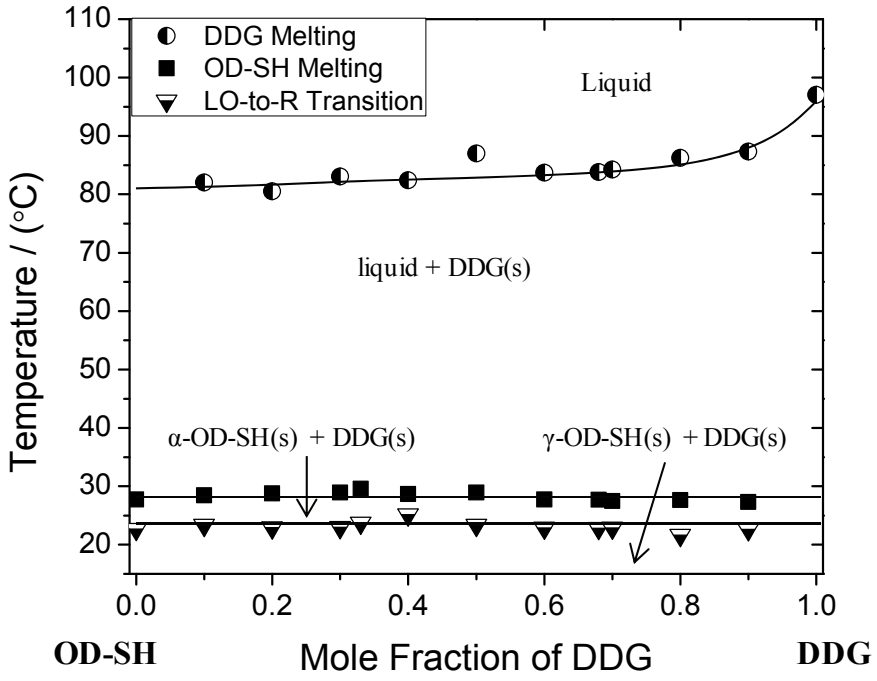

Figure 6.15. Binary phase diagram determined by DSC on heating for 1-octadecanethiol (OD-SH) and dodecyl gallate (DDG) mixtures. Note the invariance in the melting and solid-solid phase transition temperatures of OD-SH and the nearly invariant melting transition temperature of DDG.

Based on the thermochromic behaviour observed in the experiments discussed in section 6.2.3 (regarding CVL:DDG:OD-SH mixtures), the structure of the binary phase

diagram is not too surprising. DDG demonstrated poor solubility in the melt and was prone to inhomogeneous phase separation from the solid solvent (causing complete colour loss in the solid state in some ternary samples). Additionally, CVL:DDG:OD-SH mixtures demonstrated thermochromic behaviour characteristic of mixtures containing developer:solvent combinations lacking strong attractive interactions in the solid state (*i.e.*, melt-lightened thermochromism at high solvent concentrations). Therefore the binary phase diagram aids understanding of the observed thermochromic behaviour of CVL:DDG:OD-SH mixtures.

6.2.4.5 Summary of Binary Phase Diagram Determination

The binary phase diagrams for BPA:HD-OH and DHB:HD-OH mixtures were almost identical in structure, and demonstrated remarkable similarities to the phase diagrams of PG:alkyl alcohol and OG:alkyl alcohol mixtures previously reported by MacLaren.[110] In these binary systems, a single eutectic was observed in the solvent rich portion of the phase diagram, and slight negative deviation from ideal freezing point depression was observed for both systems, indicating weak attractive interactions between the developer and solvent components. For BPA:HD-OH mixtures, the eutectic was in the range $0.1 < x_{BPA} < 0.2$, while for DHB:HD-OH mixtures, the eutectic was in the range $0.15 < x_{DHB} < 0.3$. The strength of the attractive interaction of DHB:HD-OH appeared to be greater than the BPA:HD-OH interaction due to a slightly more negative deviation from ideal freezing point depression, although the difference was too small to draw any definitive conclusions about the relative strengths of the interactions.

Neither BPA:HD-OH nor DHB:HD-OH mixtures demonstrated compound formation in the solid state indicating that the developer:solvent interactions in CVL:BPA:HD-OH and CVL:DHB:HD-OH mixtures are weak, likely much weaker than the competing dye:developer interactions. This result is in accord with the thermochromic behaviour of three-component systems containing these developers, as described in sections 6.2.1 and 6.2.2, which showed that the solid state of these mixtures is strongly coloured due to the formation of coloured dye:developer complexes.

The DDG:OD-SH binary phase diagram was characterized by nearly invariant liquidus and solidus curves, indicating that little to no interaction occurs between DDG and OD-SH. In these mixtures, the LO-to-R phase transition and melting temperatures of OD-SH did not vary across the entire compositional range, and the melting temperature of DDG underwent only slight depression around x_{DDG} = 0.9 to 1. These results are in accord with the observed thermochromic behaviour of the CVL:DDG:OD-SH system in which the solid state of the mixture was strongly coloured at most solvent concentrations.

6.3 Conclusions Regarding Thermochromism in Mixtures Containing BPA, DHB, or OD-SH

The thermochromic behaviour observed for three-component mixtures containing chemically dissimilar developer and solvent components was in accord with the hypothesized behaviour, namely that these mixtures would not form strong developer:solvent interactions in the solid state and, as a result, the solid states of these mixtures would generally be strongly coloured, and decolouration of the melt would be reliant on high solvent concentrations.

CVL:BPA:HD-OH mixtures demonstrated melt-lightened behaviour across a wide compositional range. In the low solvent concentration regime (*e.g.*, when $z = 25$ to 100), all of the samples studied demonstrated highly coloured equilibrium solids ($CD_{\text{Equil}} = 0.9$ to 1.5) coupled with largely decoloured molten phases ($CD_{\text{Melt}} = 0.0$ to 0.2). This behaviour gave rise to the best colour contrast observed in this work, $\Delta CD_{\text{max}} \approx 1.4$, obtained for the [1:8:91] sample.

A complication associated with the weak interaction of BPA with HD-OH was that BPA demonstrated poor solubility in molten HD-OH, which resulted in high opacity of molten mixtures containing low solvent concentrations (*e.g.*, when $z \leq 50$). The binary phase diagram showed that when $x_{\text{BPA}} \geq 0.2$, BPA melted incongruently from HD-OH. This behaviour suggests that in three-component mixtures with $z \leq 50$, two inhomogeneous phases exist in which, (1) CVL and BPA are dissolved in molten HD-OH, and (2) solid BPA comprises a second phase. In the liquid region, the solubility limit of BPA in the molten HD-OH solvent is reached, and excess BPA remains solid.

Vastly increasing the solvent concentration (*e.g.*, where $z \geq 300$) resulted in the complete dissolution of the developer, reducing the opacity of the melt. However, the increase in solvent concentration (*e.g.*, $300 \leq z \leq 2000$) also generally caused the solid state colour density to decrease ($CD_{\text{Equil}} = 0.8$ to 1.2 for coloured samples), thereby reducing the overall colour contrast in mixtures containing high solvent concentrations ($\Delta CD_{\text{max}} = 1.2$). Nevertheless, the CVL:BPA:HD-OH ternary system represents the best example of high colour contrast, melt-lightened thermochromism observed in this thesis.

CVL:DHB:HD-OH mixtures demonstrated melt-lightened thermochromic behaviour that was largely the same as that observed for the CVL:BPA:HD-OH system.

At relatively low solvent concentrations (*e.g.*, when $z < 100$), the equilibrium solid states were strongly coloured (CD_{Equil} = 1.2 to 1.5) and generally melt to form largely decoloured molten states (CD_{Melt} = 0.0 to 0.2) that were often highly opaque due to the poor solubility of DHB in molten HD-OH. Similar to CVL:BPA:HD-OH mixtures, the CVL:DHB:HD-OH mixtures formed two phases upon solvent melting, a liquid phase which contained molten HD-OH with dissolved DHB, and a second solid phase which contained DHB. In this instance, the high opacity of the mixture after solvent melting resulted in the retention of blue colouration associated with *blue*-CVL that mixed with the yellow colour of insoluble DHB to generate weak cyan colouration of the opaque molten phase. This is in contrast to the opaque, molten BPA-containing mixtures, which were white.

To reduce the opacity of the melt, the solvent concentration could be vastly increased (*e.g.*, where $z > 250$). While this reduced the opacity of the melt and eliminated the cyan colouration associated with insoluble DHB, it also caused a reduction in the solid state colour density of these mixtures (CD_{Equil} = 0.6 to 0.9). As a result, the overall colour contrast varied significantly from mixtures containing low solvent concentrations (ΔCD_{max} = 1.2 to 1.4, when $z < 100$) to mixtures containing high solvent concentrations (ΔCD_{max} = 0.7 to 0.8, when $z > 250$).

The solvent R-phase was shown to play an increased role in the colouring behaviour of CVL:BPA:HD-OH and CVL:DHB:HD-OH mixtures, as the colour changes on transition through the R-phase were very gradual. On heating, the strongly coloured solid state gradually lost colour density through the LO-to-R transition, before colour was completely lost on solvent melting. On cooling, colour formation was noted near the R-

to-LO transition temperature at the exterior of the sample vials, which was attributed to conversion of the solvent from the R-phase to the LO-phase since the exterior of the vial was cooler than the interior, which had remained decoloured (and in the R-phase).

CVL:DDG:OD-SH mixtures also demonstrated similar behaviour, however decolouration of the melt required much higher solvent concentrations than the BPA and DHB mixtures. When $500 < z < 715$, melt-darkened behaviour was noted for $y \geq 4$ samples, indicating the presence of a developer concentration threshold for inversion of colouring behaviour.

Increasing the solvent concentration of CVL:DDG:OD-SH mixtures (*e.g.*, $z \approx 900$ to 1000) gave rise to mixtures that had coloured solid states ($CD_{\text{Equil}} = 0.7$) and decoloured melts. To obtain fully decoloured melts across a wide range of developer concentrations, very high solvent concentrations were required (*e.g.*, when $z \approx 2000$). At these high solvent concentrations, the solid states generally demonstrated moderate colour density ($CD_{\text{Equil}} = 0.5$ to 1.0) and largely decoloured melts ($CD_{\text{Melt}} = 0.0$ to 0.4), which resulted in moderate colour contrast between the coloured and decoloured states ($\Delta CD_{\text{max}} = 0.5$ to 0.9).

The binary phase diagrams for BPA:HD-OH and DHB:HD-OH mixtures were very similar showing the presence of a single eutectic and the lack of compound formation. Deviations from ideal freezing point depression indicated that these developers experience a weak attractive interaction with HD-OH, but the interaction was not strong enough to cause compound formation in the solid state. Conversely, DDG:OD-SH mixtures showed little modification of the transition temperatures associated with

solvent LO-to-R phase transition and OD-SH melting, indicating that little interaction between the developer and solvent occurs in this system.

The thermochromic behaviour of three-component mixtures, and the binary phase behaviour of two-component mixtures, for the systems described in this chapter were in accord with the behaviour hypothesized for systems that contain chemically dissimilar components. In general, the three-component mixtures demonstrated coloured equilibrium solid states that became decoloured on heating, with colour loss beginning upon transition to the solvent R-phase and intensifying upon melting of the solvent. On cooling, solidification of the solvent into the R-phase did not cause immediate regeneration of colour in these mixtures, and conversion of the solvent to its LO-phase was required to cause the colour to return. In the solid state of such mixtures, the dye:developer interaction dominates and strongly coloured solid states were obtained a most compositions. Due to the formation of decoloured melts obtained at high solvent concentrations, optimal melt-lightened thermochromism should be expected for three-component mixtures containing chemically dissimilar developer and solvent components.

Chapter 7 Ternary Thermochromic Phase Diagrams

7.1 Introduction and Background

Studies on the thermochromic properties of numerous dye:developer:solvent mixtures comprising a wide range of compositions were presented in Chapter 4 (CVL:DDG:alcohol mixtures), Chapter 5 (CVL:alkyl gallate:alcohol mixtures), and Chapter 6 (CVL with other developers and solvents). These studies showed that thermochromic mixtures containing well-matched developer and solvent alkyl chain lengths (*e.g.*, DDG:TD-OH, and the ODG-containing mixtures) generally demonstrated melt-darkened thermochromism, in which a decoloured equilibrium solid could be converted to a coloured molten phase at high developer concentrations. In mixtures containing dissimilar developer and solvent components (*e.g.*, BPA/DHB:HD-OH mixtures), all of the compositions studied were strongly coloured in the equilibrium solid and became decoloured upon melting, with varying amounts of insoluble material present in the molten phase, depending on the composition of the mixture.

In alkyl gallate:alcohol mixtures with poorly matched alkyl chain lengths (*e.g.*, PG- and OG-containing mixtures, DDG:OD-OH, *etc*.), the equilibrium solid state generally was coloured and the colour of the melt was highly dependent on the concentration of the developer and solvent. In these mixtures there was often a developer concentration threshold below which melt-lightened thermochromism was observed (*i.e.*, the melt was decoloured compared to the equilibrium solid) and above which the melt-darkened thermochromism was observed (*i.e.*, the melt was darker than the equilibrium solid). At the developer concentration threshold, the melt and equilibrium solid had effectively the same colour density.

To gain a better understanding of how the composition of thermochromic mixtures influences their colouring behaviour (*e.g.*, melt-darkened vs. melt-lightened thermochromism, changing colour density and colour contrast, *etc*.), ternary thermochromic phase diagrams can be used to map the type of colouring behaviour observed in different compositional regimes. An example of this approach, employed in the analysis of colour fade rates in thermally quenched (*i.e.*, frozen with liquid nitrogen) thermochromic (or potentially thermochromic) samples prepared by ink jet printing onto a paper substrate, is shown in Figure 7.1.[102,181]

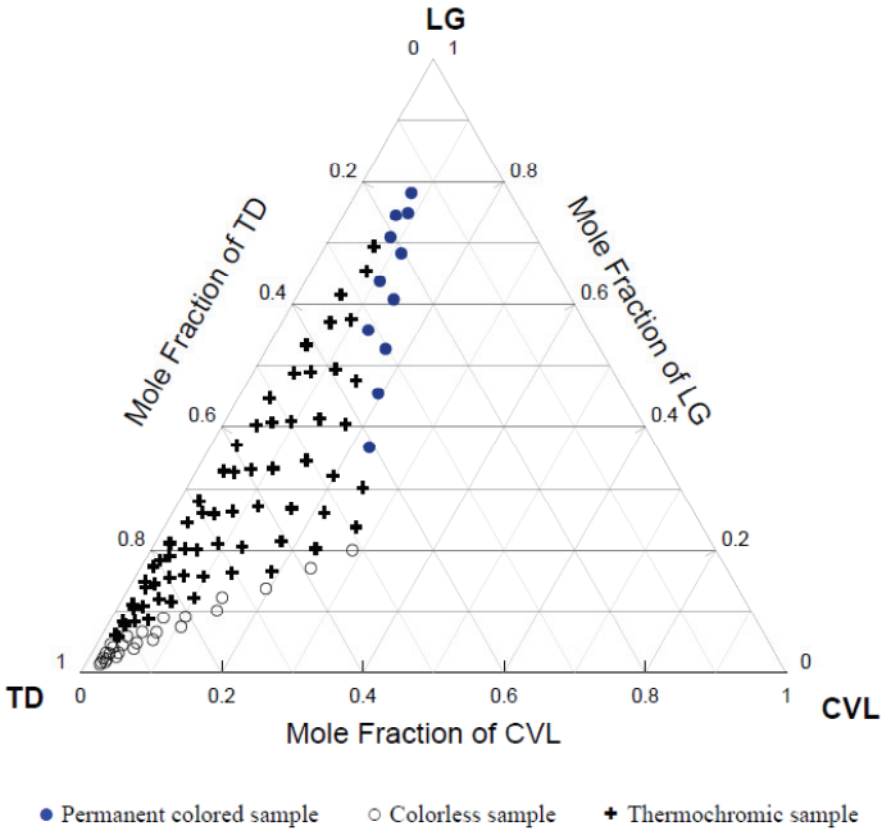

Figure 7.1. A ternary thermochromic phase diagram of the CVL:DDG:TD-OH system (note: LG ≡ DDG, TD ≡ TD-OH). The thermochromic behaviour of thermally quenched samples deposited onto paper *via* ink jet printing is mapped onto the ternary phase diagram to identify which type of behaviour occurs within specific compositional regions of the phase diagram. Here thermochromic samples became coloured after thermal quenching into a metastable solid state, and colour was lost after standing at room temperature, after which the decoloured equilibrium solid state was returned. Reproduced with permission from reference 181 (H. Tang, *MSc Thesis*, Dalhousie University, 2007).

Three regions of distinct colouring behaviour were observed for the CVL:DDG:TD-OH samples prepared by ink jet deposition. At high CVL mole fraction ($x_{CVL} > 0.15$ to 0.2) and high DDG mole fraction ($x_{LG} > 0.4$), most of the samples studied were permanently coloured. These samples did not decolour over time after thermal quenching and were therefore deemed non-thermochromic. At low CVL and LG mole fractions ($x_{CVL} \approx x_{LG} = 0.05$ to 0.15), the mixtures were not coloured at any stage of the thermal treatment and were labelled colourless. At intermediate values of x_{CVL} and x_{LG}, colour fade was observed after quenching, and therefore these samples were deemed to be thermochromic.[102,181]

Tang, MacLaren, and White also extended this method of analysis to the CVL:DDG:HD-OH and CVL:DDG:OD-OH ternary systems.[102,181] However, their studies were focussed on the colour fade rate after thermal quenching and did not explicitly compare the difference in colour density between the equilibrium solid state and the melt, in contrast to the analysis carried out in the present work. As a result of the different modes of analysis employed, and in particular due to the differences in sample sizes used[**], it is difficult to correlate the results of the ternary phase diagram analysis obtained by Tang *et al.* (*i.e.*, the phase diagram shown in Figure 7.1)[102,181] with the results presented in the present work. Nevertheless, ternary phase diagrams for the three-

[**] Sample sizes in ink jet printed samples were on the order of μg/mm^2. It was observed in the present work that low mass samples suffered from detrimental issues including phase separation, inhomogeneous colouration, and incomplete mixing, as noted in section 3.2.1.2.

component systems discussed in Chapters 4 through 6 have been compiled and are discussed in the subsequent sections of this chapter.

In the present analysis, the gross features of colouring behaviour were used to define different regions of the ternary phase diagrams. To this end, colour density values measured *via* observational spectroscopy and/or colour photo analysis were categorized into four ranges and given labels to relate the "observed colour" of each sample in the solid state and in the melt. The colour density ranges for the observed colour are given in Table 7.1.

Table 7.1. The colour designation of thermochromic samples as a function of colour density.

Colour Designation	Colour Density Values
Colourless	$CD \leq 0.1$
Light	$0.1 < CD < 0.5$
Medium	$0.5 \leq CD < 0.8$
Dark	$0.8 \leq CD$

The thermochromic colour changes of interest in the present work are between the equilibrium solid state and the melt, and therefore the labelling of each ternary thermochromic phase diagram relates the change in colour density upon transition from the equilibrated initial solid state to the melt.[††] The measured colour contrast values for every sample analyzed are not reported in this chapter; only the *maximum* values of colour density and colour contrast obtained for each ternary system are reported here. All

[††] In general, the colour density of most samples was highest immediately after cooling from the R-phase to solvent LO-phase. Therefore, immediate post-melt colour density values are not suitable for determination of colour contrast values.

molar ratios are reported in mole percent, expressed as x_n, for numerical convenience considering the low concentration of dye and developer relative to the amount of solvent present in each sample.

7.2 Ternary Thermochromic Phase Diagram Determination

7.2.1 Thermochromic Phase Diagrams of ODG-Containing Mixtures

7.2.1.1 CVL:ODG:TD-OH Thermochromic Phase Diagram

The thermochromic mixtures comprised of CVL, ODG, and alcohol solvent all demonstrated the type of colouring behaviour hypothesized for mixtures containing well-matched alkyl chain lengths. In the solid state, all of the samples were colourless, and when the developer concentration was sufficiently large the melt became coloured. Figure 7.2 shows a portion of the ternary phase diagram of the CVL:ODG:TD-OH system. The samples in the region of $x_{ODG} \approx 4$ to 8% showed light colouration in the melt, while samples that contained more developer ($x_{ODG} > 10\%$) became more intensely coloured in the melt, and samples with less developer ($x_{ODG} < 4\%$) were always colourless in the melt.

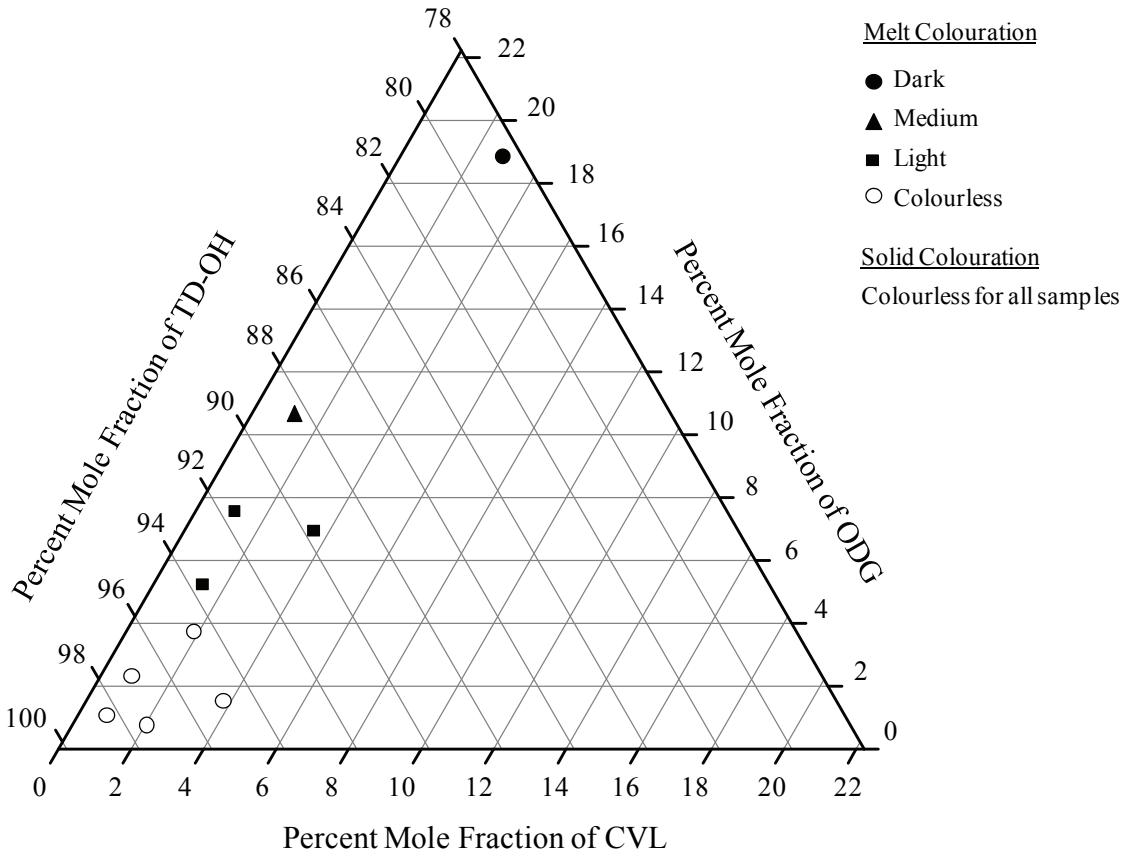

Figure 7.2. A portion of the ternary thermochromic phase diagram of the CVL:ODG:TD-OH system, showing the melt colouration. The equilibrium solids were all colourless.

7.2.1.2 CVL:ODG:HD-OH Thermochromic Phase Diagram

Figure 7.3 shows a portion of the ternary phase diagram of the CVL:ODG:HD-OH system. The general features of this phase diagram matched those observed for the CVL:ODG:TD-OH system. When $x_{CVL} < 4\%$ and $x_{ODG} < 4\%$, all of the samples were colourless. When $x_{ODG} \approx 6$ to 8%, the samples were lightly coloured in the melt, and substantially increasing the ODG concentration ($x_{ODG} > 10\%$) yielded mixtures with much higher melt colour densities.

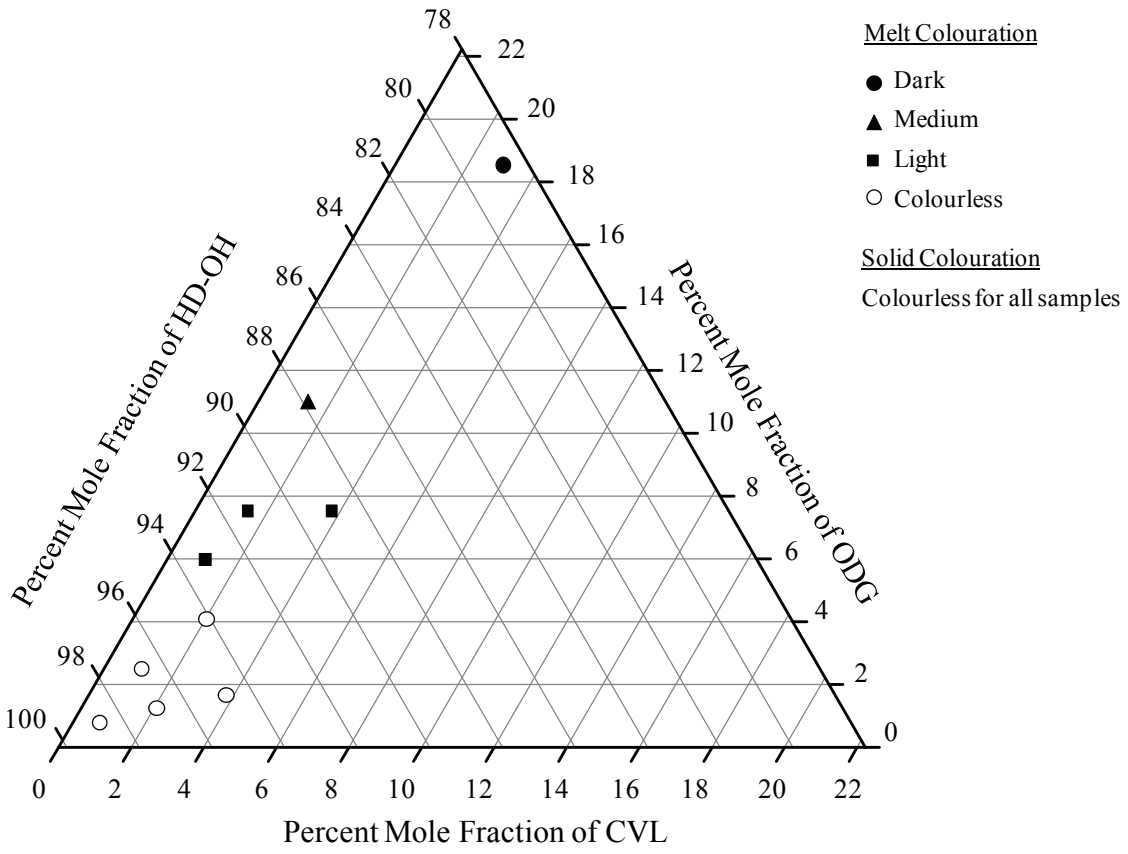

Figure 7.3. A portion of the ternary thermochromic phase diagram of the CVL:ODG:HD-OH system, showing the melt colouration. The equilibrium solids were all colourless.

7.2.1.3 CVL:ODG:OD-OH Thermochromic Phase Diagram

Similar colouring behaviour was observed for CVL:ODG:OD-OH mixtures, as shown in Figure 7.4. Once again, at low developer concentrations (*e.g.*, when $x_{ODG} < 4\%$) the mixtures were always colourless. Increasing the concentration of developer caused the melt to become coloured, although in this system only lightly coloured melts were observed in the range of $4\% < x_{ODG} < 11\%$. Vastly increasing the developer concentration to $x_{ODG} > 18\%$ resulted in the formation of a dark melt, mirroring the behaviour observed in the TD-OH and HD-OH systems.

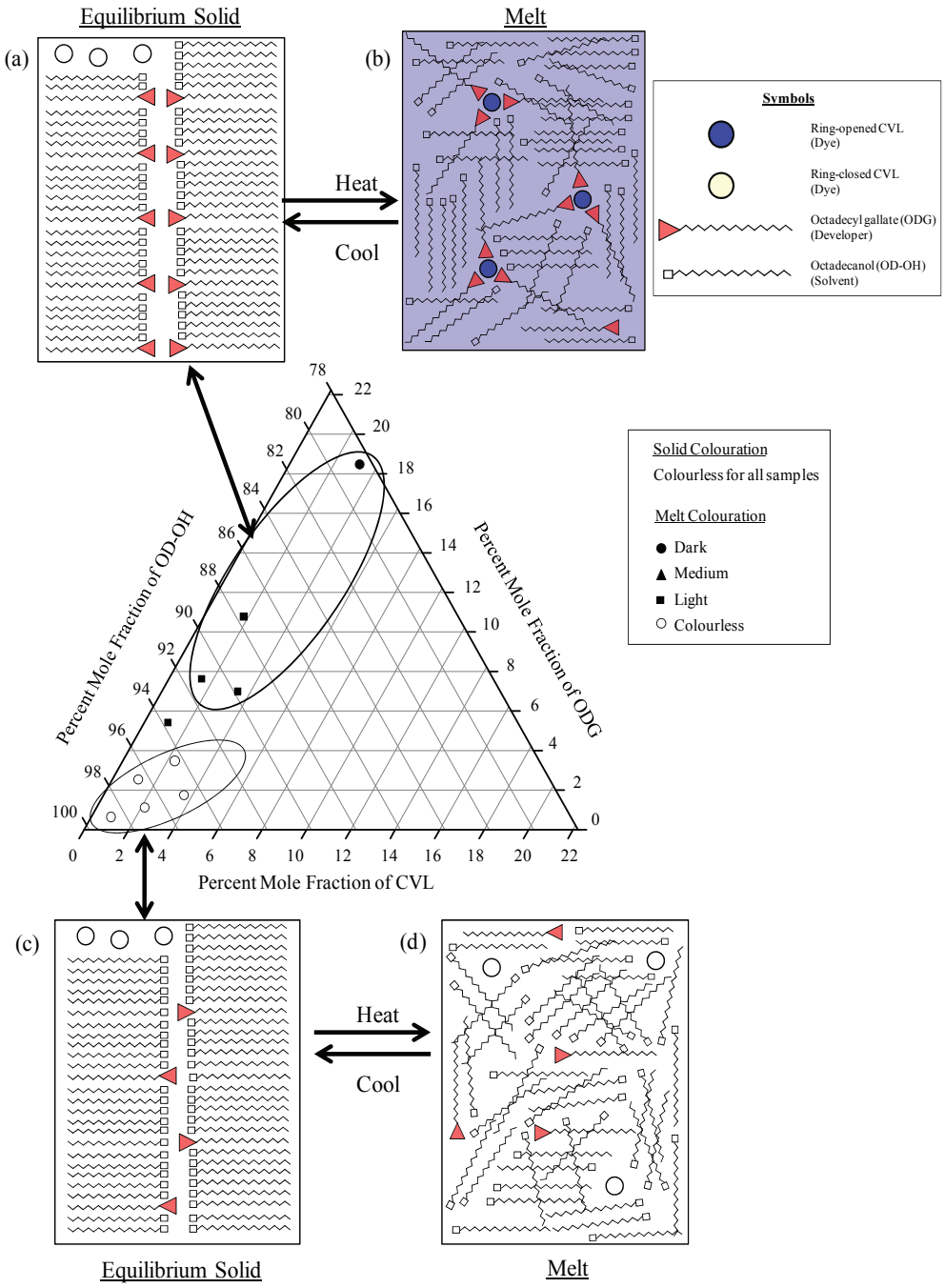

Figure 7.4. A portion of the ternary thermochromic phase diagram of the CVL:ODG:OD-OH system, showing the melt colouration. The equilibrium solids were all colourless. Samples with high developer concentrations (*e.g.*, when $x_{ODG} > 6\%$) demonstrated melt-darkened thermochromism in which (a) the solid state was colourless and (b) the melt was coloured. Samples with high solvent concentration and low developer concentrations (*e.g.*, when $x_{ODG} < 4\%$ and $x_{OD\text{-}OH} > 94\%$) were (c) colourless in the solid state and (d) colourless in the melt. In the schematic diagrams, the number of dye and developer molecules is shown as being the same for both the solid and melt but, for the ease of drawing, the number of solvent molecules is not conserved.

Included in Figure 7.4 are schematic representations of the hypothesized structural organization of the dye, developer, and solvent molecules in three-component systems demonstrating well-matched alkyl chain lengths and melt-darkened thermochromism. Figure 7.4 (a) and (c) show schematic representations of the equilibrium solid state. The solvent molecules form an ordered structure with the hydroxyl groups aligned and the alkyl chains forming a regular structure. The developer can become incorporated into the solvent structure due to the similarity in alkyl chain length. As a result, the dye is excluded from the developer-solvent complex and no colour is observed in the solid state.

On heating, two different cases are illustrated (Figure 7.4 (b) and (d)). When the developer concentration is low and the solvent concentration is high (*e.g.*, when $x_{ODG} <$ 4% and $x_{OD\text{-}OH} > 94\%$), no colour is formed in the melt due to the high dilution of the colour-forming components (Figure 7.4 (d)). Increasing the developer concentration results in the formation of a coloured molten state, with the colour density of the mixture dependent on the developer concentration (Figure 7.4 (b)).

7.2.1.4 Summary of CVL:ODG:Alcohol Thermochromic Phase Diagrams

All of the ODG-containing mixtures demonstrated colourless equilibrium solid states, and some melted to form coloured molten phases, giving rise to the melt-darkened thermochromic behaviour characteristic of thermochromic mixtures containing well-matched developer and solvent alkyl chain lengths. Due to the lack of colour formation observed in the equilibrium solid state of ODG-containing mixtures, the colour contrast observed in these mixtures was defined by the colour density of the melt. Table 7.2 lists

the maximum colour contrast values observed here, and the associated equilibrium solid and melt colour densities, for each of the three CVL:ODG:alcohol ternary systems examined in this work. The CVL:ODG:TD-OH sample showed the best colour contrast with $\Delta CD_{max} = 1.1$, which was among the highest values observed in the present work.

Table 7.2. The colour density and colour contrast values obtained *via* colour photo analysis for ODG-containing mixtures, showing data for the samples demonstrating the highest colour contrast for each ternary system.

Components	Composition	CD_{Equil}	CD_{Melt}	ΔCD_{Max}
CVL:ODG:TD-OH	[1:6.4:26.7] $x_{ODG} = 19\%$ $x_{TD\text{-}OH} = 78\%$	0.1	1.2	1.1
CVL:ODG:HD-OH	[1:6.1:25.8] $x_{ODG} = 19\%$ $x_{HD\text{-}OH} = 78\%$	0.1	1.0	0.9
CVL:ODG:OD-OH	[1:5.9:25.2] $x_{ODG} = 18\%$ $x_{OD\text{-}OH} = 79\%$	0.1	0.9	0.8

7.2.2 Thermochromic Phase Diagrams of DDG-Containing Mixtures

The DDG-containing mixtures demonstrated the widest variation in colouring behaviour observed in this work. Due to the similar length of the developer and solvent alkyl chains in the CVL:DDG:TD-OH system, mixtures of this type demonstrated melt-darkened thermochromism. Conversely, due to the significant mismatch in alkyl chain length between DDG and OD-OH, and to a lesser extent between DDG and HD-OH, these two systems demonstrated both melt-lightened and melt-darkened thermochromism, with complete decolourization occurring when melt-lightened

thermochromism was observed and higher colour contrast observed in melt-darkened mixtures.

7.2.2.1 CVL:DDG:TD-OH Thermochromic Phase Diagram

CVL:DDG:TD-OH mixtures were studied by both MacLaren et *al.*[101,110] and Tang *et al*.,[102,181] although different methods of sample preparation were used in the two studies. Both found that CVL:DDG:TD-OH mixtures formed colourless solid states, which could be melted to form strongly coloured molten phases. This behaviour was also observed in the present work, as evidenced by the data shown in Figure 7.5. At low developer concentrations (*e.g.*, when $x_{DDG} \leq 4\%$), the samples were always colourless. Moderate increases to the developer concentration ($x_{DDG} \approx 4$ to 6%), yielded samples that demonstrated light colouration in the melt, and further increases to the developer concentration ($x_{DDG} \approx 6$ to 7%) gave samples with medium melt colour density. To obtain high melt colour density, high developer concentrations were required ($x_{DDG} = 9$ to 14%). These developer concentrations were lower than was required for dark colour generation in CVL:ODG:alcohol mixtures.

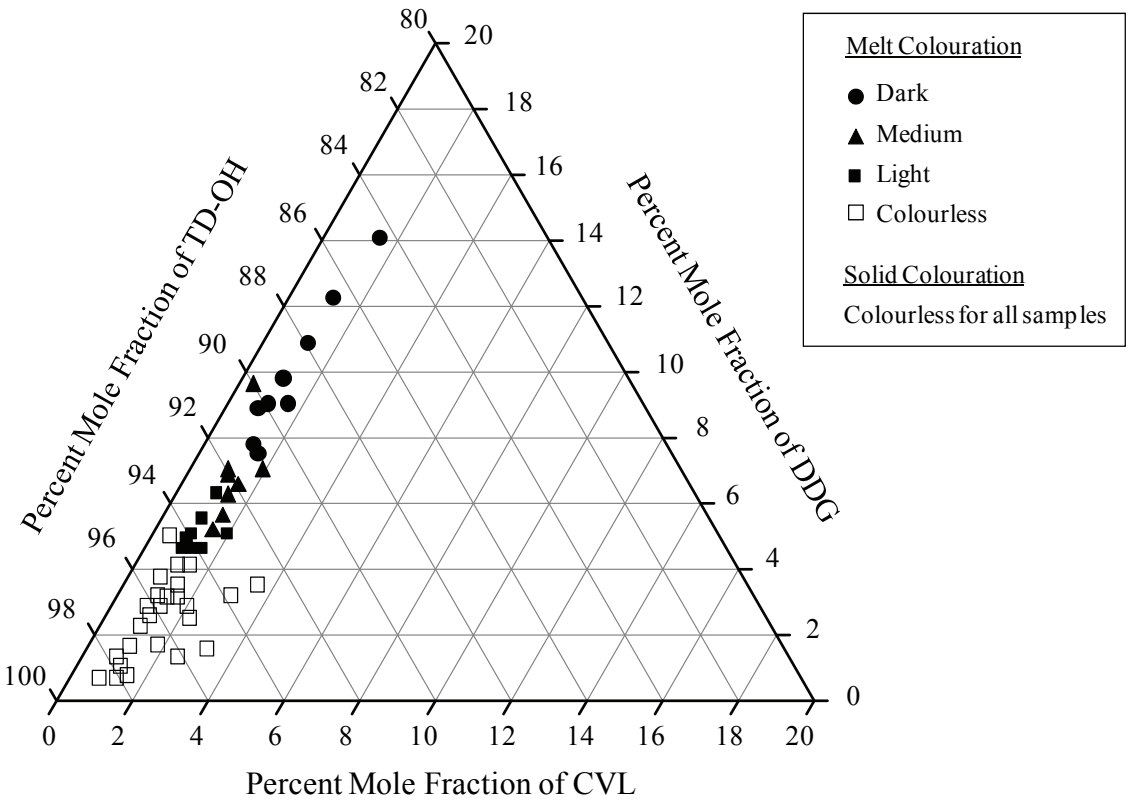

Figure 7.5. A portion of the ternary thermochromic phase diagram of the CVL:DDG:TD-OH system, showing the melt colouration. The equilibrium solids were all colourless.

The highest colour density and colour contrast values for the molten phase obtained *via* observational spectroscopy were observed for the [1:10:60] sample (x_{CVL} = 1.4%, x_{DDG} = 14.1%, $x_{TD\text{-}OH}$ = 84.5%) which had ΔCD_{max} = 1.8. The colour density values obtained *via* observational spectroscopy and colour photo analysis are not easily comparable due to the fact that the observational spectroscopy analysis lacked normalization against a white reference material, therefore optical effects associated with stray light, different brightness of ambient lighting, *etc.*, could have played a role in modifying the degree of observed colour in observational spectroscopy measurements. The highest colour density and colour contrast observed *via* colour photo analysis was

seen for the [1:9:90] sample (x_{CVL} = 1.0%, x_{DDG} = 9.0%, $x_{TD\text{-}OH}$ = 90.0%), which gave a maximum colour contrast of ΔCD_{Max} = 0.8.

7.2.2.2 CVL:DDG:HD-OH Thermochromic Phase Diagram

The CVL:DDG:HD-OH ternary system was also examined by both MacLaren *et al*.[101,110] and by Tang *et al*.[102,181] In their studies of this system, both examinations treated CVL:DDG:HD-OH mixtures in the same fashion as the CVL:DDG:TD-OH mixtures; the equilibrium solid was less strongly coloured than the melt and melt-darkened thermochromism was observed in both studies.[101,102] Their experiments used thermal quenching to force the coloured molten state into a darker metastable solid state, and then measured the colour fade rate as a function of time after quenching.[101,102] The colour fade rates were observed to be substantially slower for HD-OH mixtures than in the related TD-OH system,[101] and the equilibrium solids generally retained light colouration, which resulted in this ternary system being deemed of poor thermochromic quality.[101,110]

It was observed in this work that CVL:DDG:HD-OH could in fact become decoloured in the melt if the solvent concentration was sufficiently high and the developer concentration was sufficiently low. In such mixtures, light to medium coloured equilibrium solids melted to form decoloured melts. Conversely, melt-darkened thermochromism was obtained in mixtures with high developer concentrations and relatively low solvent concentrations. Figure 7.6 shows a portion of the ternary phase diagram of the CVL:DDG:HD-OH system. At low developer concentrations (*e.g.*, when x_{DDG} = 0.5 to 3%), virtually all samples studied showed melt-lightened thermochromism. At high developer concentrations (*e.g.*, when x_{DDG} > 8%), melt-darkened thermochromism

was observed for most samples, although due to the high colour density of the equilibrium solid state, the colour contrast between the solid and melt was rather low.

Included in Figure 7.6 are schematic representations of the hypothesized structural organization of the dye, developer, and solvent molecules in three-component systems demonstrating poorly matched alkyl chain lengths, and both melt-darkened and melt-lightened thermochromism. Figure 7.6 (a) and (c) show schematic representations of the equilibrium solid state. Due to the difference in chain length between the developer and solvent, the developer does not pack into the solvent structure as efficiently as in the case of well-matched chains (*e.g.*, as in CVL:ODG:OD-OH mixtures, see Figure 7.4 (a)). This mismatch allows the developer to interact with the dye in the solid state, and generate colour. It is likely that in some instances the developer can interact with the solid solvent, thereby reducing the colour density of the solid state compared with mixtures containing alkyl chains with a larger degree of chain length mismatch. In general, the larger the mismatch in alkyl chain length, the stronger the colour of the solid state.

On heating, two different cases are illustrated (Figure 7.6 (b) and (d)). When the developer concentration is low and the solvent concentration is high (*e.g.*, when $x_{DDG} < 4\%$ and $x_{HD\text{-}OH} > 92\%$), little to no colour is observed in the melt due to the high dilution of the colour-forming components (Figure 7.6 (d)). Increasing the developer concentration results in the formation of a coloured molten state, with the colour density of the mixture dependent on the developer concentration (Figure 7.6 (b)).

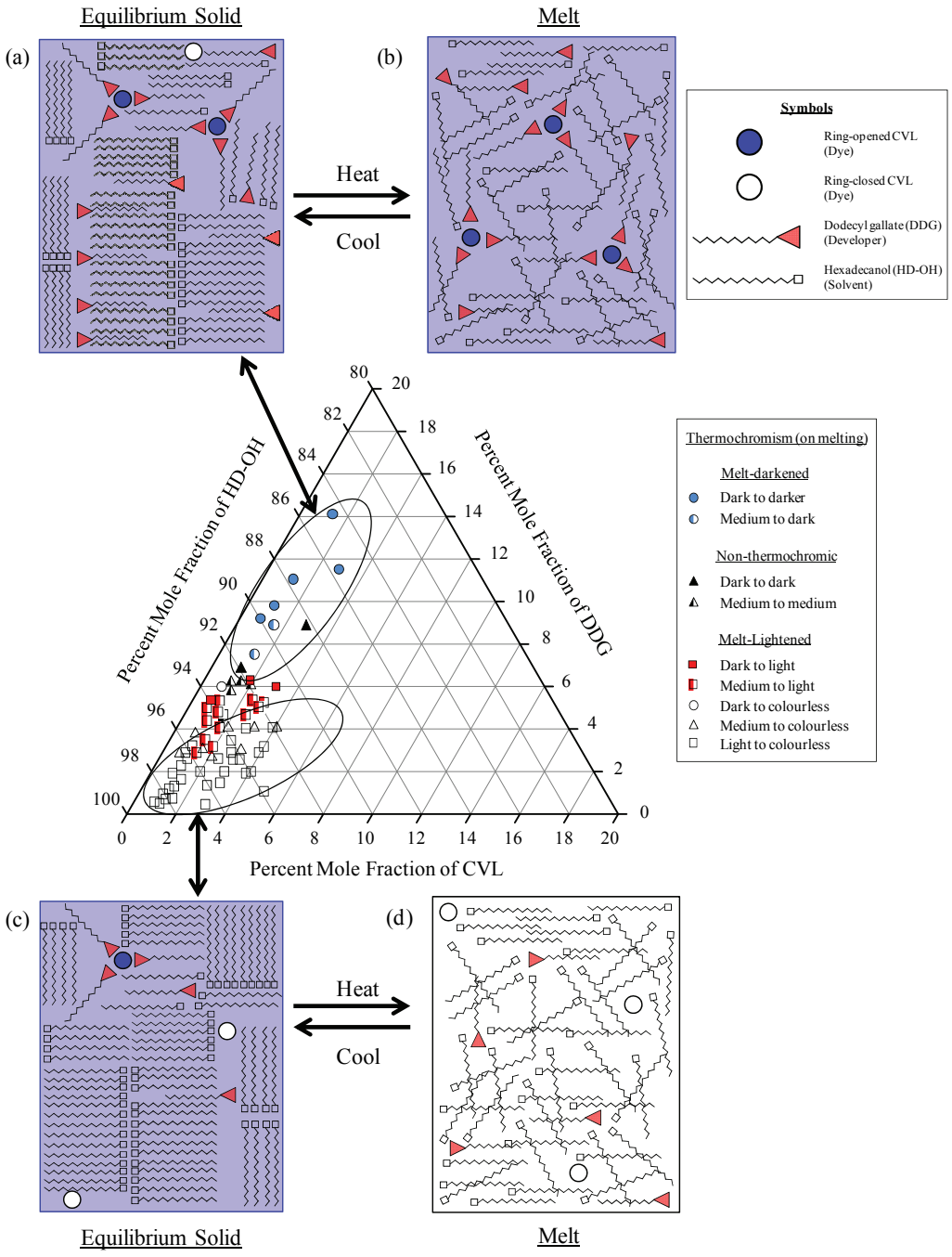

Figure 7.6. A portion of the ternary thermochromic phase diagram of the CVL:DDG:HD-OH system. Samples with high developer concentrations (*e.g.*, when $x_{DDG} > 7\%$) were coloured in (a) the solid state and (b) formed darker molten phases on heating, demonstrating melt-darkened behaviour. Samples with low developer concentrations (*e.g.*, when $x_{DDG} < 5\%$) were (c) coloured in the solid state and (d) became decoloured upon melting, demonstrating melt-lightened thermochromism. In between these regions (*e.g.*, when $x_{DDG} = 6$ to 7%), samples were sometimes not thermochromic. In the schematic diagrams, the number of dye and developer molecules is shown as being the same for both the solid and melt but, for the ease of drawing, the number of solvent molecules is not conserved.

A particularly interesting region of the CVL:DDG:HD-OH ternary phase diagram exists between the melt-lightened and melt-darkened regimes. Figure 7.7 shows a close-up of this region of the ternary phase diagram. At relatively low developer concentrations (*e.g.*, when $x_{DDG} \leq 5\%$), melt-lightened thermochromism was observed. Most of the samples studied demonstrated light-to-colourless (when $x_{DDG} < 3\%$) or medium-to-light (when $3\% < x_{DDG} < 5\%$) colour changes, although a few samples within these ranges demonstrated medium-to-colourless colour changes, which could be useful for thermochromic applications due to the moderate colour contrast values. In the range of $1\% < x_{CVL} < 2\%$ and $6\% < x_{DDG} < 7\%$, medium-to-medium and dark-to-dark transitions were observed, indicating that the developer concentration threshold value for inversion of colouring behaviour lies within this region of the phase diagram.

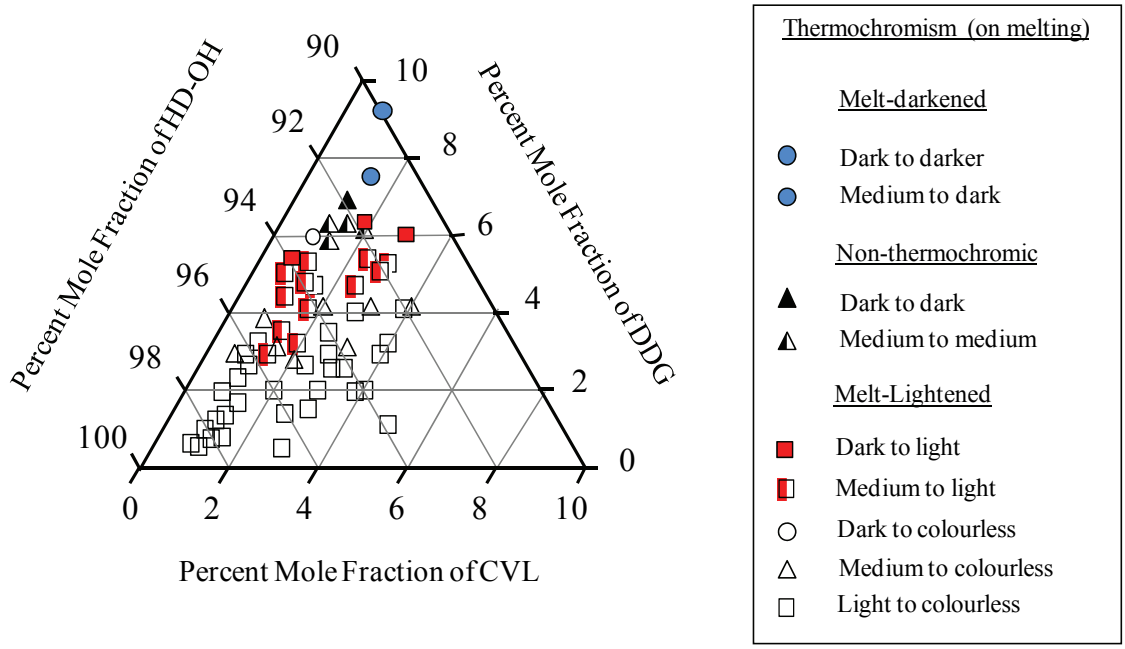

Figure 7.7. A close-up view of the solvent-rich region of the ternary thermochromic phase diagram of CVL:DDG:HD-OH mixtures. In this region, the colouring behaviour was observed to change from melt-lightened behaviour (when $x_{DDG} \leq 5\%$) to melt-darkened behaviour (when $x_{DDG} > 7\%$). In the intermediate region ($x_{DDG} \approx 6$ to 7%), the colour contrast between the equilibrium solid and the melt was near zero.

The highest colour contrast values observed *via* observational spectroscopy were seen for samples demonstrating melt-darkened thermochromism, in which a medium- or dark-coloured solid state melted to form an intensely coloured melt. The [1:10:60] sample (x_{CVL} = 1.4%, x_{DDG} = 14.1%, $x_{HD\text{-}OH}$ = 84.5%), for example, had medium colour density in the equilibrium solid (CD_{Equil} = 0.5) and melted to form an intensely coloured melt (CD_{Melt} = 1.5), yielding high colour contrast (ΔCD_{max} = 1.0). On the other hand, melt-lightened thermochromism generally demonstrated lower colour contrast as the colour density of the equilibrium solid was generally much lower (CD_{Equil} = 0.3 for the [1:2:90] sample (x_{CVL} = 1.1%, x_{DDG} = 2.1%, $x_{HD\text{-}OH}$ = 96.8%)) compared to melt-darkened samples. Although the melt was colourless in such mixtures, the low colour density of the equilibrium solid resulted in mixtures with low colour contrast (ΔCD_{max} = 0.3 to 0.5).

Using the knowledge gained from observation spectroscopy measurements, melt-lightened CVL:DDG:HD-OH mixtures with enhanced colour contrast values were prepared and studied by colour photo analysis. It must be reiterated here that the colour photo analysis of CVL:DDG:HD-OH samples lacked the use of a white reference material for colour normalization, and as such the colour densities reported here are overestimated. Nevertheless, efficient decolourization of the equilibrium solid was noted in most samples examined in section 4.3.2.3 (regarding the colour photo analysis of CVL:DDG:HD-OH mixtures). In particular, the [1:3:96] and [1:5:94] samples showed high equilibrium colour densities (CD_{Equil} = 0.9 to 1.1) and near complete decolouration of the melt (CD_{Melt} = 0.0 to 0.1), resulting in very good colour contrast values (ΔCD_{Max} = 0.9 to 1.0).

7.2.2.3 CVL:DDG:OD-OH Thermochromic Phase Diagram

Figure 7.8 shows a portion of the ternary phase diagram of the CVL:DDG:OD-OH system. At low developer concentrations (*e.g.*, when $x_{DDG} < 5\%$), most of the samples demonstrated light or medium colouration in the solid state, and melted to form decoloured melts. The colour contrast associated with melt-lightened thermochromism was rather low ($\Delta CD_{max} = 0.4$ to 0.5) due to the low colour density of the equilibrium state in such mixtures. The colour contrast obtained for melt-darkened samples was also rather low in the compositional range studied, with $\Delta CD_{max} = 0.5$ to 0.7 for the [1:10:90] ($x_{CVL} = 1.0\%$, $x_{DDG} = 9.9\%$, $x_{OD\text{-}OH} = 89.1\%$) and [1:10:80] ($x_{CVL} = 1.1\%$, $x_{DDG} = 11\%$, $x_{OD\text{-}OH} = 87.9\%$) samples, respectively.

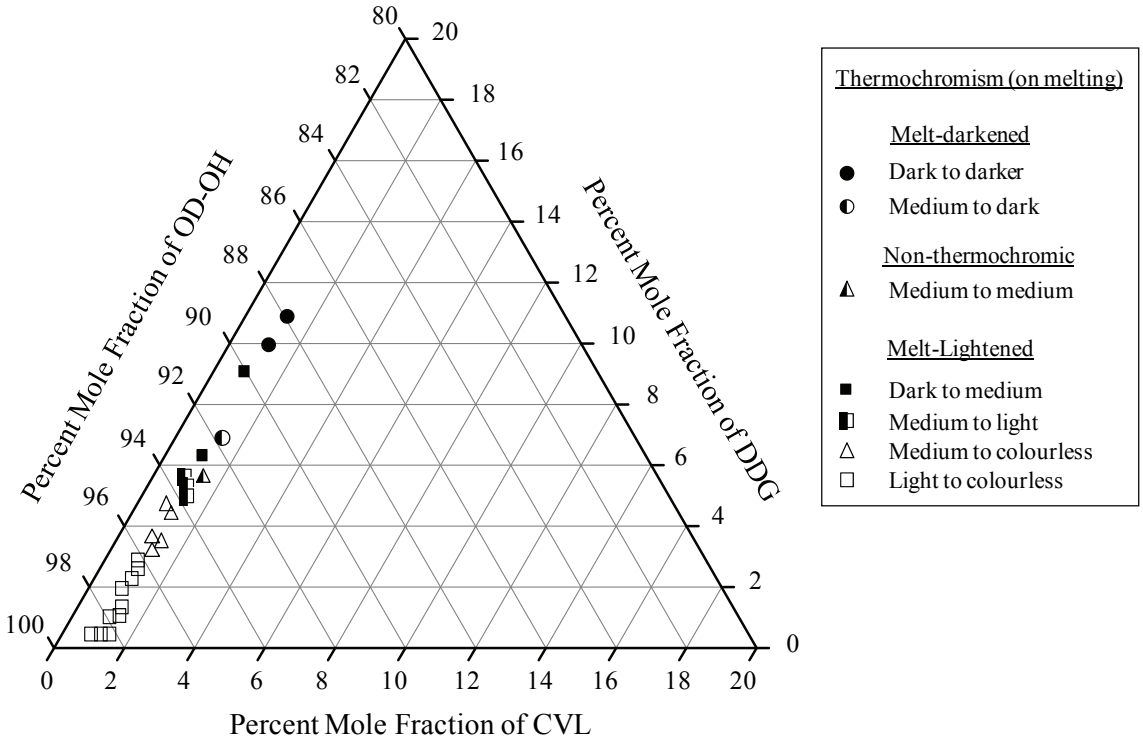

Figure 7.8. A portion of the ternary thermochromic phase diagram of the CVL:DDG:OD-OH system. Samples with high developer concentrations (*e.g.*, when $x_{DDG} > 10\%$) demonstrated melt-darkened thermochromism. Samples with low developer concentrations (*e.g.*, when $x_{DDG} < 5\%$)

demonstrated melt-lightened thermochromism. In between these regions (*e.g.*, when $x_{DDG} \approx 6\%$), samples were sometimes not thermochromic.

7.2.2.4 Summary of CVL:DDG:Alcohol Thermochromic Phase Diagrams

The colouring behaviour of mixtures in the CVL:DDG:alcohol systems changed as a function of solvent alkyl chain length. CVL:DDG:TD-OH mixtures demonstrated melt-darkened thermochromism at all compositions, whereas CVL:DDG:HD-OH and CVL:DDG:OD-OH mixtures demonstrated colouring behaviour that varied with composition. At high developer concentrations, melt-darkened thermochromism was observed, and at low developer concentrations, melt-lightened thermochromism was observed.

The colour contrast observed for CVL:DDG:TD-OH mixtures was high, and was similar to that of the CVL:ODG:alcohol mixtures discussed in section 7.2.1. The colour contrast in CVL:DDG:HD-OH and CVL:DDG:OD-OH mixtures was lower due to the light to medium colour density of the equilibrium solid over a large compositional range, and due to the fact that melt-darkened mixtures generally were dark in the solid state. The colour density and maximum colour contrast values obtained for DDG-containing mixtures are summarized in Table 7.3 (observation spectroscopy results) and Table 7.4 (colour photo analysis results).

Table 7.3. The colour density and colour contrast values obtained *via* observational spectroscopy for DDG-containing mixtures, showing data for the samples demonstrating the highest colour contrast for each ternary system.

Components	Composition	CD_{Equil}	CD_{Melt}	ΔCD_{Max}
CVL:DDG:TD-OH	[1:10:60] x_{DDG} = 14% $x_{TD\text{-}OH}$ = 85%	0.0	1.8	1.8
CVL:DDG:HD-OH	[1:10:60] x_{DDG} = 14% $x_{HD\text{-}OH}$ = 85%	0.5	1.5	1.0
CVL:DDG:HD-OH	[1:1:22.9] x_{DDG} = 4% $x_{HD\text{-}OH}$ = 92%	0.3	0.0	0.3
CVL:DDG:OD-OH	[1:10:80] x_{DDG} = 11% $x_{OD\text{-}OH}$ = 88%	0.7	1.4	0.7
CVL:DDG:OD-OH	[1:3:80] x_{DDG} = 3.6% $x_{OD\text{-}OH}$ = 95.2%	0.4	0.0	0.4

Table 7.4 The colour density and colour contrast values obtained *via* colour photo analysis for DDG-containing mixtures, showing data for the samples demonstrating the highest colour contrast for each ternary system.

Components	Composition	CD_{Equil}	CD_{Melt}	ΔCD_{Max}
CVL:DDG:TD-OH	[1:9:90] x_{DDG} = 9% $x_{TD\text{-}OH}$ = 90%	0.0	0.8	0.8
CVL:DDG:HD-OH	[1:5:94] x_{DDG} = 5% $x_{HD\text{-}OH}$ = 94%	1.1	0.1	1.0

7.2.3 Thermochromic Phase Diagrams for OG-Containing Mixtures

Due to the difference in chain length between octyl gallate (8 carbon atoms) and the three alcoholic solvents used (14 to 18 carbon atoms), melt-lightened thermochromism was observed over a wide range of compositions for CVL:OG:alcohol

mixtures. The best melt-lightened colour contrast observed for OG-containing mixtures was seen in mixtures that contained intermediate developer concentrations and that melted to give colourless molten phases. Melt-darkened thermochromism was obtained by vastly increasing the developer concentration, but due to the dark colour of the equilibrium solid in such mixtures, colour contrast values for melt-darkened thermochromic mixtures were very low.

7.2.3.1 CVL:OG:TD-OH Thermochromic Phase Diagram

Figure 7.9 shows a portion of the ternary phase diagram of the CVL:OG:TD-OH system. Colourless melts were formed when the percent mole fraction of OG was $x_{OG} <$ 6%, with very good colour contrast ($\Delta CD_{Max} = 0.8$) observed for the $[1:6.2:103.2]$ sample ($x_{CVL} = 0.9\%$, $x_{OG} = 5.6\%$, $x_{TD\text{-}OH} = 93.5\%$), which showed a dark-to-colourless transition upon melting. Melt-lightened thermochromism was observed for all samples with $x_{OG} < 8\%$, although at $x_{OG} \approx 8\%$ the melt was light in colour. The developer concentration threshold value lies somewhere in the vicinity of the $x_{OG} = 10\%$, as evidenced by the sample with $x_{OG} \approx 10\%$ that underwent a medium-to-medium colour change on melting. Vastly increasing the developer concentration (*e.g.*, when $x_{OG} \approx 18\%$) resulted in the appearance of melt-darkened thermochromism, although the colour contrast associated with this transition was relatively low ($\Delta CD_{max} = 0.4$).

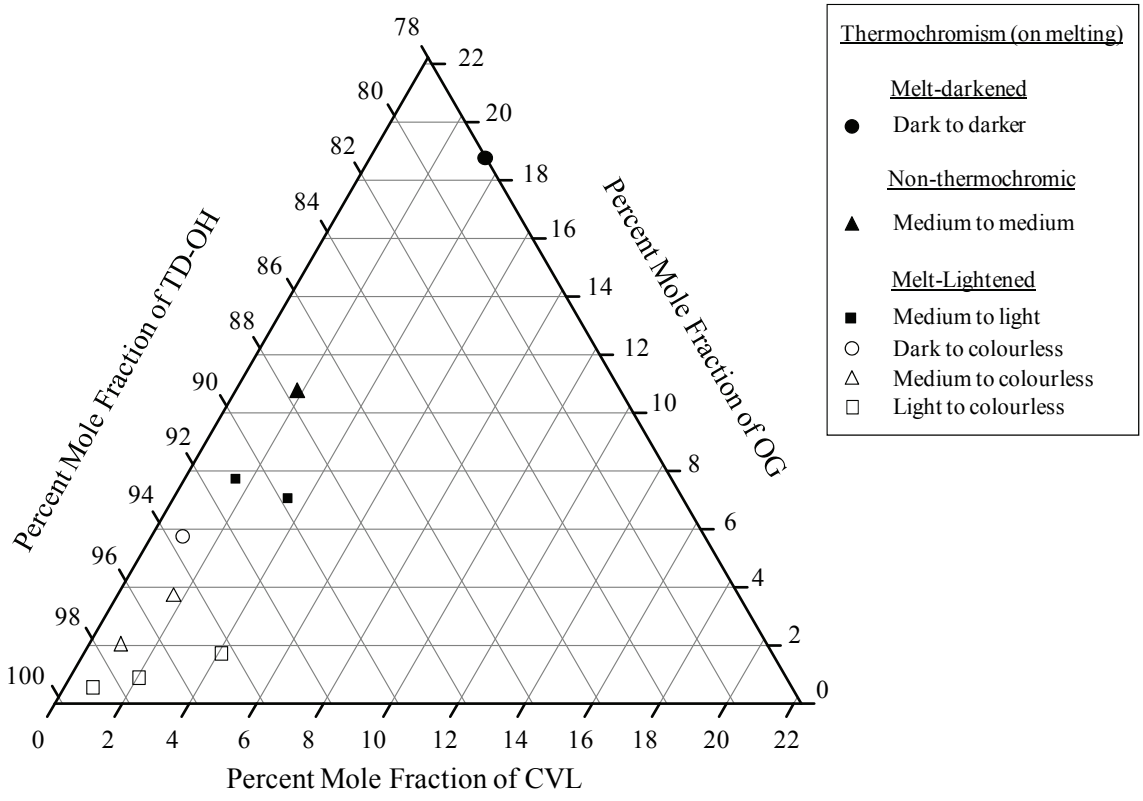

Figure 7.9. A portion of the ternary thermochromic phase diagram of the CVL:OG:TD-OH system. Samples with high developer concentrations (*e.g.*, when $x_{OG} \approx 18\%$) demonstrated melt-darkened thermochromism. Samples with low developer concentrations (*e.g.*, when $x_{OG} < 8\%$) demonstrated melt-lightened thermochromism. In between these regions (*e.g.*, when $x_{OG} \approx 11\%$), a non-thermochromic sample was obtained.

7.2.3.2 CVL:OG:HD-OH Thermochromic Phase Diagram

Figure 7.10 shows a portion of the ternary phase diagram of the CVL:OG:HD-OH system, which closely resembles the phase diagram obtained for the CVL:OG:TD-OH system. Colourless melts were formed when the OG mole fraction was below $x_{OG} < 6\%$, with good colour contrast ($\Delta CD_{Max} = 0.6$) observed for the [1:6.2:102.9] sample ($x_{CVL} = 0.9\%$, $x_{OG} = 5.7\%$, $x_{HD\text{-}OH} = 93.4\%$), which showed a medium-to-colourless colour change upon melting. Melt-lightened thermochromism was observed for all samples with $x_{OG} < 8\%$, although at $x_{OG} \approx 8\%$ the melt was light in colour. The developer concentration

threshold value lies somewhere in the vicinity of the x_{OG} = 10%, as evidenced by the sample which underwent a medium-to-medium colour change on melting at this concentration. Vastly increasing the developer concentration (*e.g.*, when $x_{OG} \approx 17\%$) resulted in the appearance of melt-darkened thermochromism, although the colour contrast associated with this transition was very low ($\Delta CD_{Max} = 0.1$).

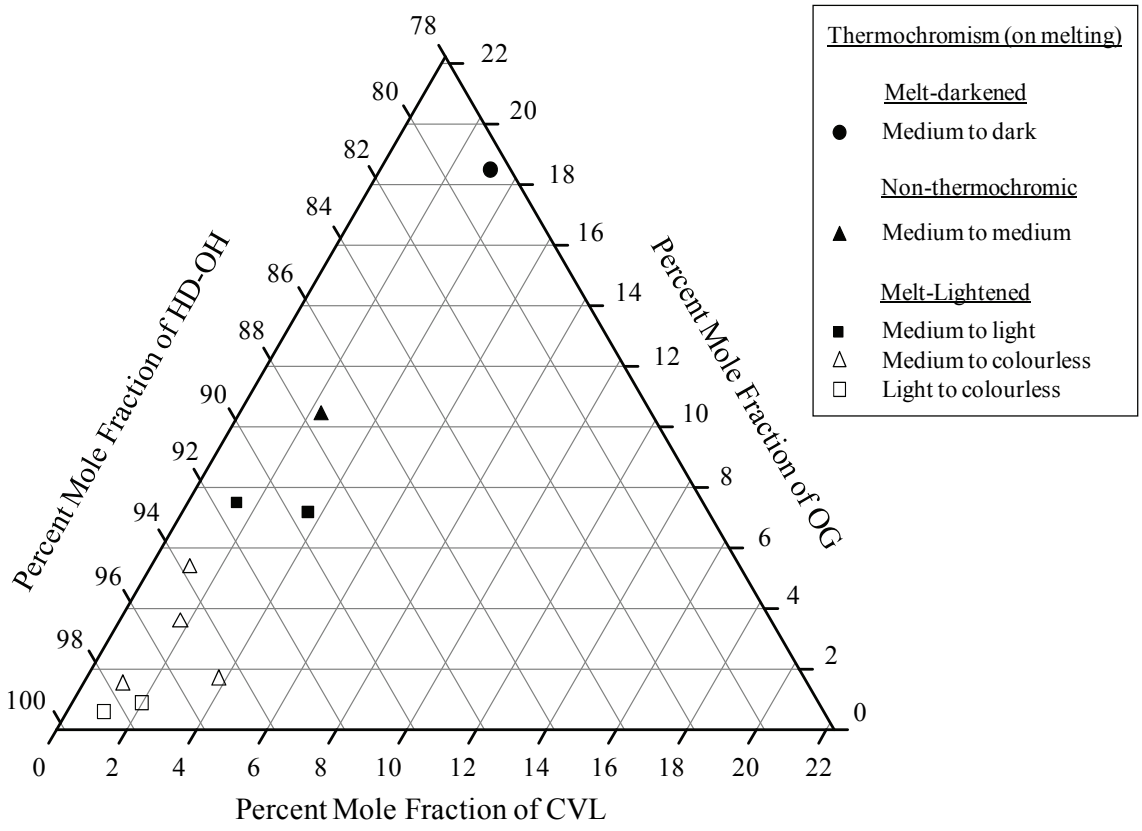

Figure 7.10. A portion of the ternary thermochromic phase diagram of the CVL:OG:HD-OH system. Samples with high developer concentrations (*e.g.*, when $x_{OG} \approx 18\%$) demonstrated melt-darkened thermochromism. Samples with low developer concentrations (*e.g.*, when $x_{OG} < 8\%$) demonstrated melt-lightened thermochromism. In between these regions (*e.g.*, when $x_{OG} \approx 10\%$), a non-thermochromic sample was obtained.

7.2.3.3 CVL:OG:OD-OH Thermochromic Phase Diagram

Figure 7.11 shows a portion of the ternary phase diagram of the CVL:OG:OD-OH system. The equilibrium colour densities observed for this system generally were higher than those of the TD-OH and HD-OH systems, and as such colour contrast values tended to be larger for melt-lightened samples. Colourless melts were formed when the OG mole fraction was below $x_{OG} < 6\%$, with very good colour contrast ($\Delta CD_{Max} = 0.8$) observed for the [1:5.9:86.5] sample ($x_{CVL} = 1.1\%$, $x_{OG} = 5.6\%$, $x_{OD\text{-}OH} = 93.3\%$), which showed a dark-to-colourless transition upon melting. Melt-lightened thermochromism was observed for all samples with $x_{OG} < 11\%$, although a number of samples across this compositional range demonstrate light colouration in the melt. The developer concentration threshold value lies between $x_{OG} = 10$ to 17%, since the $x_{OG} = 10\%$ sample showed melt-lightened thermochromism while the $x_{OG} = 19\%$ sample showed melt-darkened thermochromism, although the colour contrast associated with the melt-darkened thermochromic transition was, again, very low ($\Delta CD_{Max} = 0.1$).

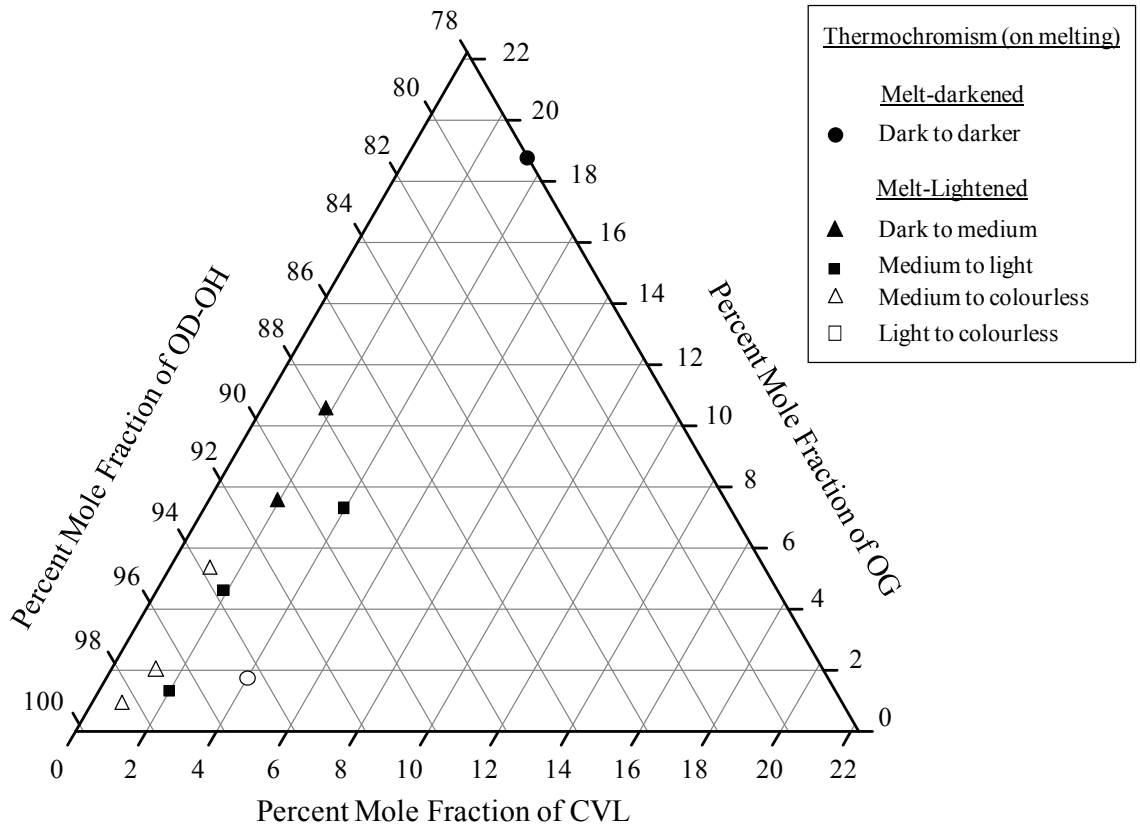

Figure 7.11. A portion of the ternary thermochromic phase diagram of the CVL:OG:OD-OH system. Samples with high developer concentrations (*e.g.*, when $x_{OG} \approx 19\%$) demonstrated melt-darkened thermochromism. Samples with low developer concentrations (*e.g.*, when $x_{OG} < 11\%$) demonstrated melt-lightened thermochromism. No non-thermochromic samples were obtained for this ternary system.

7.2.3.4 Summary of CVL:OG:Alcohol Thermochromic Phase Diagrams

The colouring behaviour of mixtures in the CVL:OG:solvent systems was consistent across the three alcohol solvents employed, as expected due to the poorly matched developer and solvent alkyl chain lengths. In all three systems, the equilibrium solid states had medium to dark colouration at all compositions studied, and both melt-lightened and melt-darkened behaviour was observed, although the colour contrast of melt-darkened behaviour was exceptionally low, even at high developer mole fractions

(*e.g.*, $x_{OG} \approx 18\%$). Melt-lightened thermochromism in this system was observed across a fairly wide compositional range ($x_{OG} \leq 8\%$), and high colour contrast was obtained owing to the high colour density of the solid state. The maximum colour contrast values obtained for each of the three-component OG-containing systems are summarized in Table 7.5.

Table 7.5. The colour density and colour contrast values obtained *via* colour photo analysis for OG-containing mixtures, showing data for the samples demonstrating the highest colour contrast for each ternary system listed in the table.

Components	Composition	CD_{Equil}	CD_{Melt}	ΔCD_{Max}
CVL:OG:TD-OH	[1:6.2:103.2] $x_{OG} = 5.6\%$ $x_{TD\text{-}OH} = 93.5\%$	0.8	0.0	0.8
CVL:OG:HD-OH	[1:6.2:102.9] $x_{OG} = 5.7\%$ $x_{HD\text{-}OH} = 93.4\%$	0.6	0.0	0.6
CVL:OG:OD-OH	[1:5.9:86.5] $x_{OG} = 5.6\%$ $x_{OD\text{-}OH} = 93.3\%$	0.8	0.0	0.8

7.2.4 Thermochromic Phase Diagrams of PG-Containing Mixtures

The alkyl chain lengths in mixtures containing propyl gallate (3 carbon atoms) and alkyl alcohols (14 to 18 carbon atoms) were very poorly matched, even more so than in the OG:alcohol systems, therefore melt-lightened thermochromism was hypothesized for these mixtures. Indeed melt-lightened thermochromism was observed over a wide range of compositions. The best colour contrast observed for PG-containing mixtures was seen in mixtures with intermediate developer concentrations that melted to give colourless molten phases. Melt-darkened thermochromism was again obtained in mixtures containing very high developer concentrations coupled with low solvent

concentrations, but due to the dark colour of the equilibrium solid in such mixtures, colour contrast values for melt-darkened thermochromic mixtures was very low.

7.2.4.1 CVL:PG:TD-OH Thermochromic Phase Diagram

Figure 7.12 shows a portion of the ternary phase diagram of the CVL:PG:TD-OH system. Colourless melts were formed when the percent mole fraction of PG was x_{PG} < 4%, with high colour contrast (ΔCD_{Max} = 0.9) observed for the [1:2.1:99.6] sample (x_{CVL} = 1.0%, x_{PG} = 2.0%, $x_{TD\text{-}OH}$ = 97.0%), which showed a dark-to-colourless transition upon melting. Melt-lightened thermochromism was observed for all samples with x_{PG} < 8%, although between 5% < x_{PG} < 8%, the melt retained light colouration. The developer concentration threshold value was observed to lie in the vicinity of x_{PG} = 10%, as evidenced by the sample which underwent a dark-to-dark colour change on melting. Vastly increasing the developer concentration (*e.g.*, when $x_{PG} \approx 18\%$) yielded melt-darkened thermochromism, although the colour contrast associated with this transition was relatively low (ΔCD_{Max} = 0.3).

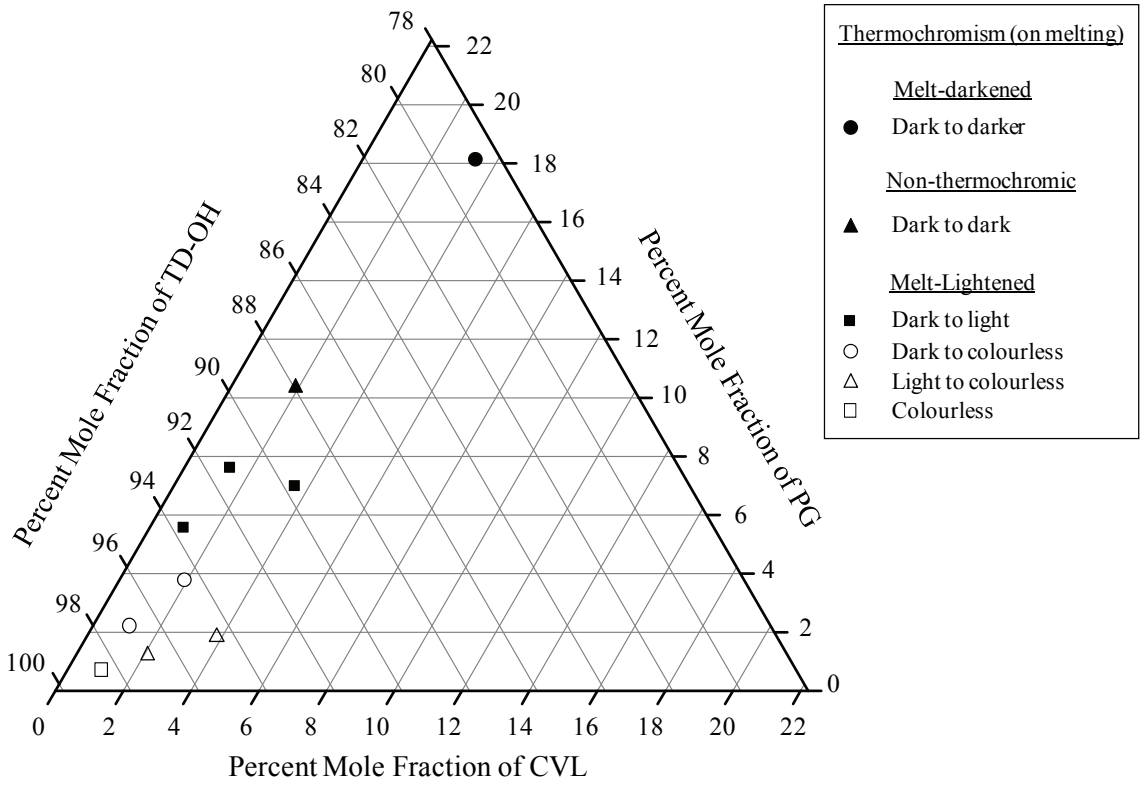

Figure 7.12. A portion of the ternary phase diagram of the CVL:PG:TD-OH system. Samples with high developer concentrations (*e.g.*, when $x_{PG} \approx 18\%$) demonstrated melt-darkened thermochromism. Samples with low developer concentrations (*e.g.*, when $x_{PG} < 8\%$) demonstrated melt-lightened thermochromism. In between these regions (*e.g.*, when $x_{PG} \approx 10\%$), a non-thermochromic sample was obtained.

7.2.4.2 CVL:PG:HD-OH Thermochromic Phase Diagram

Figure 7.13 shows a portion of the ternary phase diagram of the CVL:PG:HD-OH system, which was similar to that of the CVL:PG:TD-OH system. Colourless melts were formed when $x_{PG} < 4\%$, with excellent colour contrast ($\Delta CD_{Max} = 1.2$) observed for the [1:2:100.8] sample ($x_{CVL} = 1.0\%$, $x_{PG} = 1.9\%$, $x_{HD\text{-}OH} = 97.1\%$), which showed a dark-to-colourless transition upon melting. All of the samples with $x_{PG} < 4\%$ demonstrated complete decolouration of the melt yielding a range of samples demonstrating excellent colour contrast, although the samples containing less solvent (*e.g.*, when $x_{HD\text{-}OH} < 96\%$)

were plagued by high melt opacity due to incomplete dissolution of PG in the molten solvent.

Included in Figure 7.13 are schematic representations of the hypothesized structural organization of the dye, developer, and solvent molecules in three-component systems demonstrating very poorly matched alkyl chain lengths and melt-lightened thermochromism. Figure 7.13 (a) and (c) show a schematic representation of the equilibrium solid state. Due to the difference in chain length between the developer and solvent, the developer is essentially excluded from the solid-state structure of the solvent. This liberates the developer to interact with the dye in the solid state generating strong colouration in the solid state.

On heating, two different cases are illustrated (Figure 7.13 (b) and (d)). When the developer concentration was low and the solvent concentration is high (*e.g.*, when $x_{PG} <$ 4% and $x_{HD\text{-}OH} > 94\%$), little to no colour is observed in the melt due to the high dilution of the colour-forming components (Figure 7.13 (d)). Increasing the developer concentration resulted in the formation of a coloured molten state, with the colour density of the mixture dependent on the developer concentration (Figure 7.13(b)).

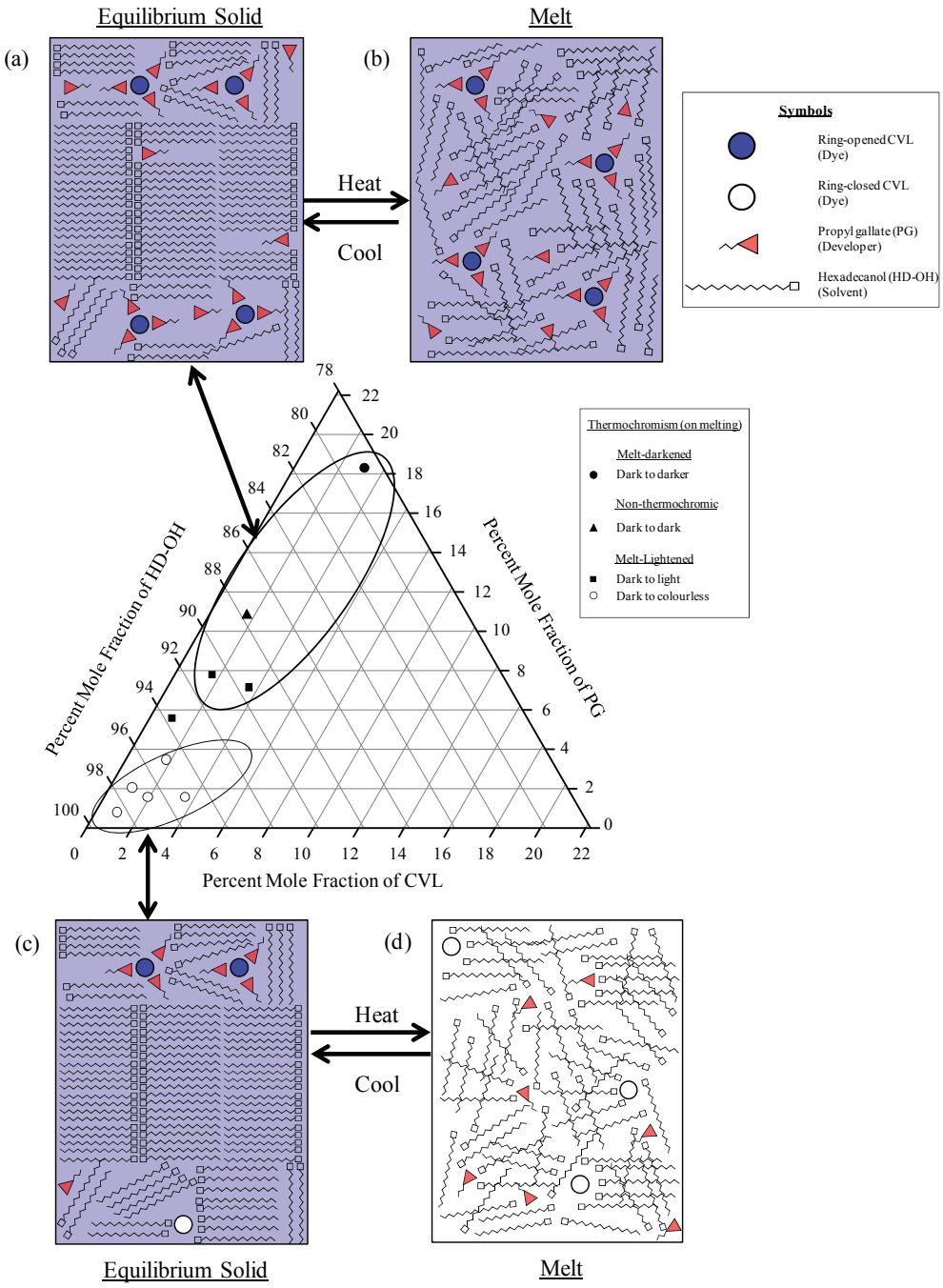

Figure 7.13. A portion of the ternary thermochromic phase diagram of the CVL:PG:HD-OH system. Samples with high developer concentrations (*e.g.*, when $x_{PG} \approx 7\%$) were coloured in (a) the solid state and (b) retained colour upon melting, yielding melt-darkened thermochromism at very large developer concentrations ($x_{PG} > 18\%$). Samples with low developer concentrations (*e.g.*, when $x_{PG} < 4\%$) were coloured in (c) the solid state and (d) became decoloured upon melting, demonstrating melt-lightened thermochromism. In the schematic diagrams, the number of dye and developer molecules is shown as being the same for both the solid and melt but, for the ease of drawing, the number of solvent molecules is not conserved.

Melt-lightened thermochromism was observed for all samples with $x_{PG} < 8\%$, although between $5\% < x_{PG} < 8\%$, the melt retained light colouration. The developer concentration threshold value was observed to lie in the vicinity of $x_{PG} = 10\%$, as evidenced by the sample which underwent a dark-to-dark colour change on melting. Vastly increasing the developer concentration (*e.g.*, when $x_{PG} \approx 18\%$) resulted in the appearance of melt-darkened thermochromism, although the colour contrast associated with this transition was relatively low ($\Delta CD_{Max} = 0.4$).

7.2.4.3 CVL:PG:OD-OH Thermochromic Phase Diagram

Figure 7.14 shows a portion of the ternary phase diagram of the CVL:PG:OD-OH system. Colourless melts formed below $x_{PG} < 4\%$, with excellent colour contrast ($\Delta CD_{Max} = 1.1$) observed for the [1:2.5:102.7] sample($x_{CVL} = 0.9\%$, $x_{PG} = 2.3\%$, $x_{TD\text{-}OH} = 96.7\%$), which showed a dark-to-colourless transition upon melting. All of the samples with $x_{PG} < 4\%$ demonstrated complete decolouration of the melt yielding a range of samples demonstrating excellent colour contrast, similar to the behaviour observed for CVL:PG:HD-OH mixtures. In the CVL:PG:OD-OH system, a wider range of compositions demonstrated light colour in the molten phase (*e.g.*, where $4\% \leq x_{PG} < 8\%$), reducing the overall colour contrast of thermochromic transitions in this compositional region.

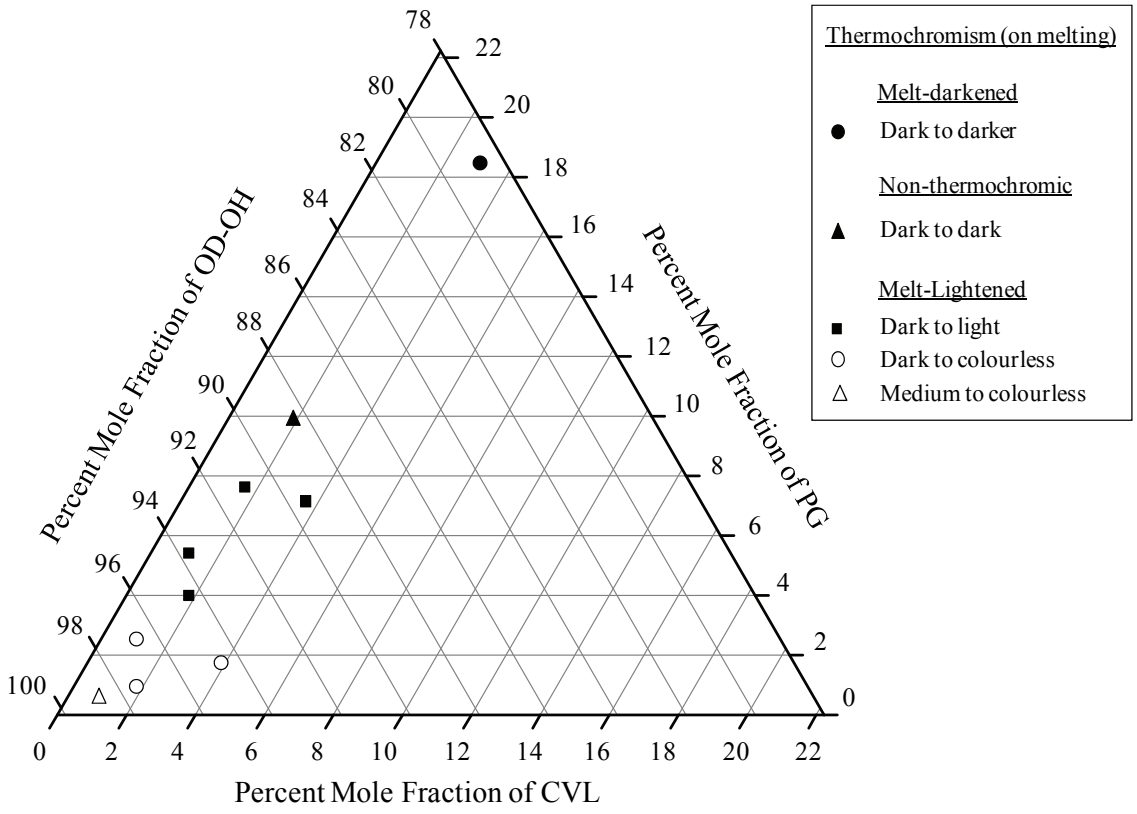

Figure 7.14. A portion of the ternary thermochromic phase diagram of the CVL:PG:OD-OH system. Samples with high developer concentrations (*e.g.*, when $x_{PG} \approx 18\%$) demonstrated melt-darkened thermochromism. Samples with low developer concentrations (*e.g.*, when $x_{PG} < 8\%$) demonstrated melt-lightened thermochromism. In between these regions (*e.g.*, when $x_{PG} \approx 10\%$), a non-thermochromic sample was obtained.

At $x_{PG} = 10\%$, there was no change in the colour density upon melting, as evidenced by a dark-to-dark "transition" on melting, indicating that a developer concentration threshold for inversion of colouring behaviour exists within this compositional range. Vastly increasing the developer concentration (*e.g.*, when $x_{PG} \approx 18\%$) resulted in the appearance of melt-darkened thermochromism, although the colour contrast associated with this transition was extremely low ($\Delta CD_{Max} = 0.1$).

7.2.4.4 Summary of CVL:OG:Alcohol Thermochromic Phase Diagrams

The colouring behaviour of mixtures in the CVL:PG:solvent systems was very consistent for the three solvents used in this work. In all three systems, the equilibrium solid states had medium to dark colouration at all compositions studied, and both melt-lightened and melt-darkened behaviour was observed, although the colour contrast of melt-darkened behaviour was exceptionally low, even at high developer concentrations (*e.g.*, when $x_{PG} \approx 18\%$).

Melt-lightened thermochromism in this system was observed across a fairly wide compositional range ($x_{PG} \leq 8\%$), although the formation of colourless melts was more limited ($x_{PG} \leq 4$ to 8%) than in the OG-containing mixtures. Higher colour contrast was also observed for PG mixtures ($\Delta CD_{max,PG} = 0.9$ to 1.2) compared to OG mixtures ($\Delta CD_{max,OG} = 0.6$ to 0.8) due to the darker colour of the solid state. The highest colour contrast values and associated colour density values, obtained for the PG-containing systems, are summarized in Table 7.6.

Table 7.6. The colour density and colour contrast values obtained *via* colour photo analysis for PG-containing mixtures, showing data for the samples demonstrating the highest colour contrast for each ternary system listed in the table.

Components	Composition	CD_{Equil}	CD_{Melt}	ΔCD_{Max}
CVL:PG:TD-OH	[1:2.1:99.6] $x_{PG} = 2.0\%$ $x_{TD\text{-}OH} = 97.0\%$	0.9	0.0	0.9
CVL:PG:HD-OH	[1:2.0:100.8] $x_{PG} = 1.9\%$ $x_{HD\text{-}OH} = 97.1\%$	1.2	0.0	1.2
CVL:PG:OD-OH	[1:2.5:102.7] $x_{PG} = 2.3\%$ $x_{OD\text{-}OH} = 96.7\%$	1.1	0.0	1.1

7.2.5 Thermochromic Phase Diagrams for CVL:BPA:HD-OH and CVL:DHB:HD-OH Mixtures

7.2.5.1 Thermochromic Behaviour of BPA- and DHB-Containing Mixtures

The CVL:BPA:HD-OH and CVL:DHB:HD-OH mixtures discussed in Chapter 6 demonstrated melt-lightened thermochromic behaviour at all compositions studied. Since both ternary systems behaved nearly identically, both systems are discussed concurrently in this section. The high colour density of the equilibrium solid state was the result of weak interactions between the developer and HD-OH, which prevented the formation of the colour-disrupting developer:solvent interactions that were observed to cause decolouration in the solid state of CVL:DDG:TD-OH mixtures (*i.e.*, mixtures with matched alkyl chain lengths).[101] In the solid state, BPA (or DHB) molecules are not sequestered by the solvent component (*e.g.*, HD-OH) and are free to develop the blue colour of CVL, thereby producing the strongly coloured solid states observed for all BPA and DHB samples at relatively low solvent concentrations (*e.g.*, when $z \leq 100$).

Upon melting, decolouration of these mixtures was observed due to the heightened molecular mobility associated with the liquid form of the solvent, which caused separation of the dye:developer complex, primarily due to dissolution of the developer. In some instances, insoluble developer remained visible in the molten solvent, and although its presence was noted, it did not generate colour in the melt. Additionally, conversion from the LO-phase to the R-phase of the solvent on heating initiated colour loss as the heightened degree of dynamical disordered associated with the orientationally disordered R-phase allowed for phase separation of the dye and developer, returning the leuco form of the dye and disrupting colour formation.

As a result of these decolourization features, all of the samples studied in the CVL:BPA:HD-OH and CVL:DHB:HD-OH ternary systems became nearly completely decoloured on solvent melting. Since the decolourization behaviour of these mixtures at low solvent loadings ($z \leq 100$) was essentially invariant with composition, other chemical/physical properties of these mixtures were considered for phase diagram determination. It was noted that when the solvent loading was very low ($z \approx 25$), insoluble CVL and developer were visually observed in the molten mixture. At intermediate solvent loading ($z \approx 50$ to 60), only insoluble developer was observed, and when the solvent loading was near $z \approx 100$, many mixtures became completely transparent. Therefore the phase diagrams for CVL:BPA:HD-OH and CVL:DHB:HD-OH at low solvent concentrations (*e.g.*, when $z \leq 100$) examine the presence of insoluble materials as a function of composition.

7.2.5.2 Thermochromic Phase Diagrams for BPA- and DHB-Containing Mixtures

Figure 7.15 shows a portion of the ternary phase diagram of the CVL:BPA:HD-OH system at relatively low solvent concentrations (*e.g.*, when $z \leq 100$) and Figure 7.16 shows a portion of the ternary phase diagram of the CVL:DHB:HD-OH system in the same compositional range. When the mole fraction of CVL was $x_{CVL} > 3\%$, both CVL and BPA became partially insoluble in the melts of both ternary systems. The compositional regions in which only the developer was insoluble overlapped for the two ternary systems. In CVL:BPA:HD-OH mixtures, insoluble BPA was observed when $1\% < x_{CVL} <$

2% and 1% < x_{BPA} < 2%, while in the CVL:DHB:HD-OH system this range was 2% < x_{CVL} < 3% and 2% < x_{BPA} < 6%.

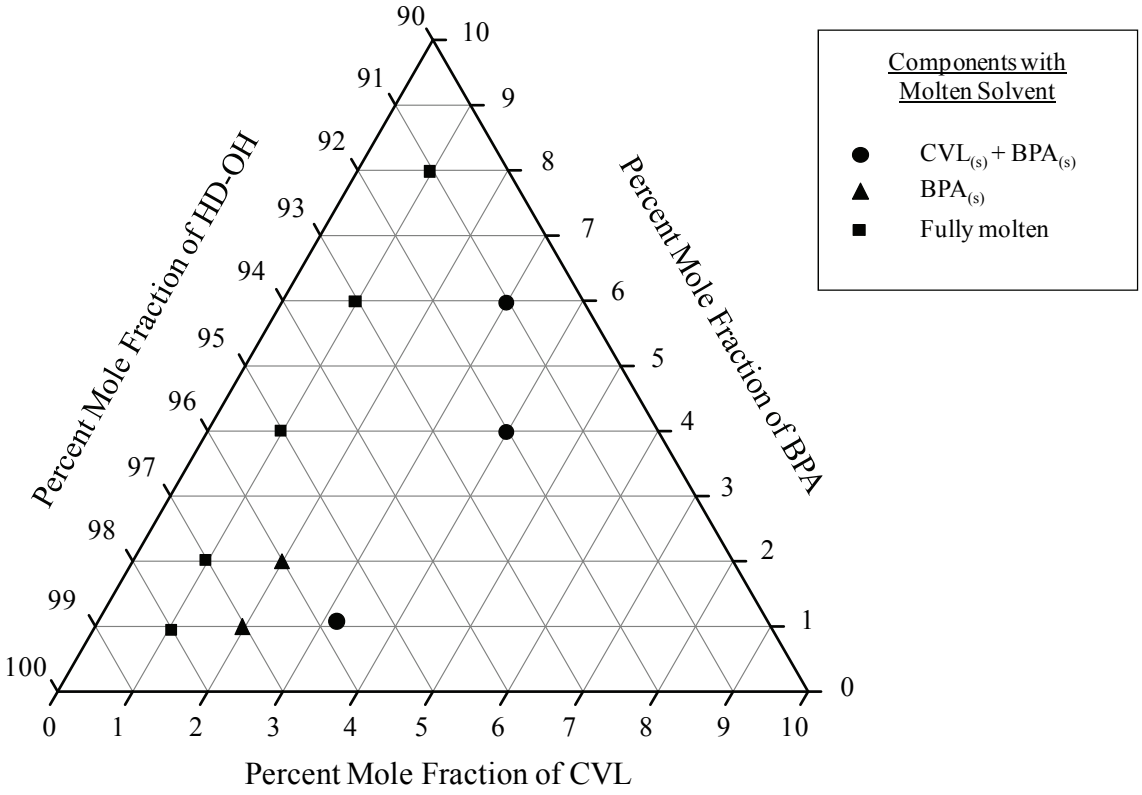

Figure 7.15. A portion of the ternary thermochromic phase diagram of the CVL:BPA:HD-OH system, showing the melt phase(s) at relatively low solvent concentrations (where $z \approx 25$ to 100).

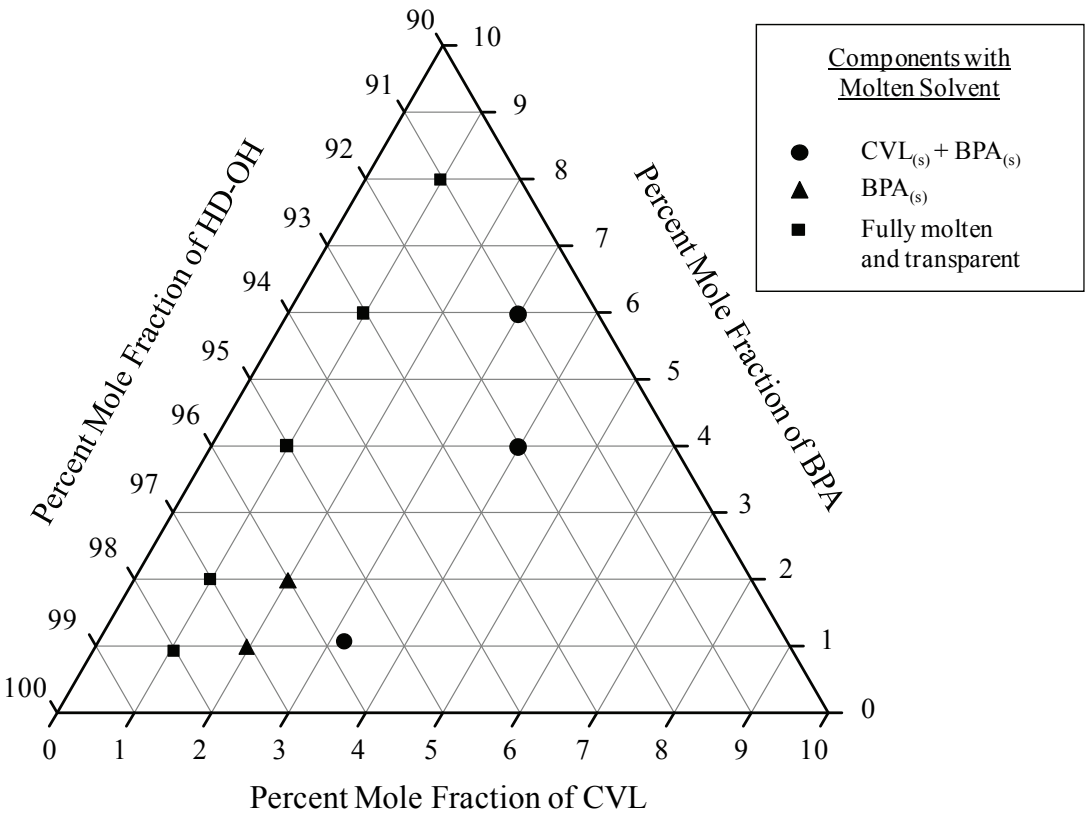

Figure 7.16. A portion of the ternary thermochromic phase diagram of the CVL:DHB:HD-OH system, showing the melt phase(s) relatively low solvent concentrations (where $z \approx 15$ to 100).

Rather surprisingly, both ternary systems demonstrated complete dissolution of all components when the percent mole fraction of CVL was $x_{CVL} = 1\%$ regardless of the percent mole fraction of developer. This behaviour was unexpected for samples with high developer loadings (*e.g.*, when $x_{DEV} \geq 4\%$) because samples with similar percent mole fractions of solvent and developer, yet slightly higher CVL loading, contained large amounts of insoluble developer (*e.g.*, the samples at [3:6:91] of both Figure 7.15 and Figure 7.16). This behaviour gives a strong indication that the concentration of CVL in fact plays an important role in defining the solubility of the developer, where a "salting-out" type of effect might be occurring as a result of the relatively poor solubility of BPA and DHB in molten HD-OH. The practical consequence is that the concentration of CVL

must be kept relatively low, or conversely the solvent concentration must be very high, to ensure that the developer fully dissolves in, and does not precipitate inhomogeneously from, the melt in such mixtures.

To ensure the complete dissolution of the dye and developer in the molten solvent, CVL:BPA:HD-OH and CVL:DHB:HD-OH mixtures at very high solvent concentrations (*e.g.*, where $160 \leq z \leq 2650$) were examined. Indeed, all of the mixtures prepared at these high solvent concentrations were completely transparent in the molten phase, indicating dissolution of the colouring components. However, the substantially reduced dye and developer concentrations caused the equilibrium solid colour density to drop significantly; therefore, it is more useful to describe the ternary phase diagrams in terms of the change in observed colour of these samples.

Figure 7.17 shows a portion of the ternary phase diagram of the CVL:BPA:HD-OH system at high solvent concentrations (*e.g.*, where $z \geq 160$). At low percent mole fraction of developer (*e.g.*, where $x_{DHB} \leq 0.2\%$) many of the samples displayed light to medium colour density in the solid state. Also, in general, when the percent mole fraction of CVL exceeded that of BPA, the mixtures had low equilibrium colour density. Dark equilibrium solids were only obtained when the mole fraction of BPA exceeded that of CVL; the reported stoichiometry of CVL:BPA complexes indicates that four molecules of BPA are required to fully develop the coloured form of each CVL molecule.[175,179]

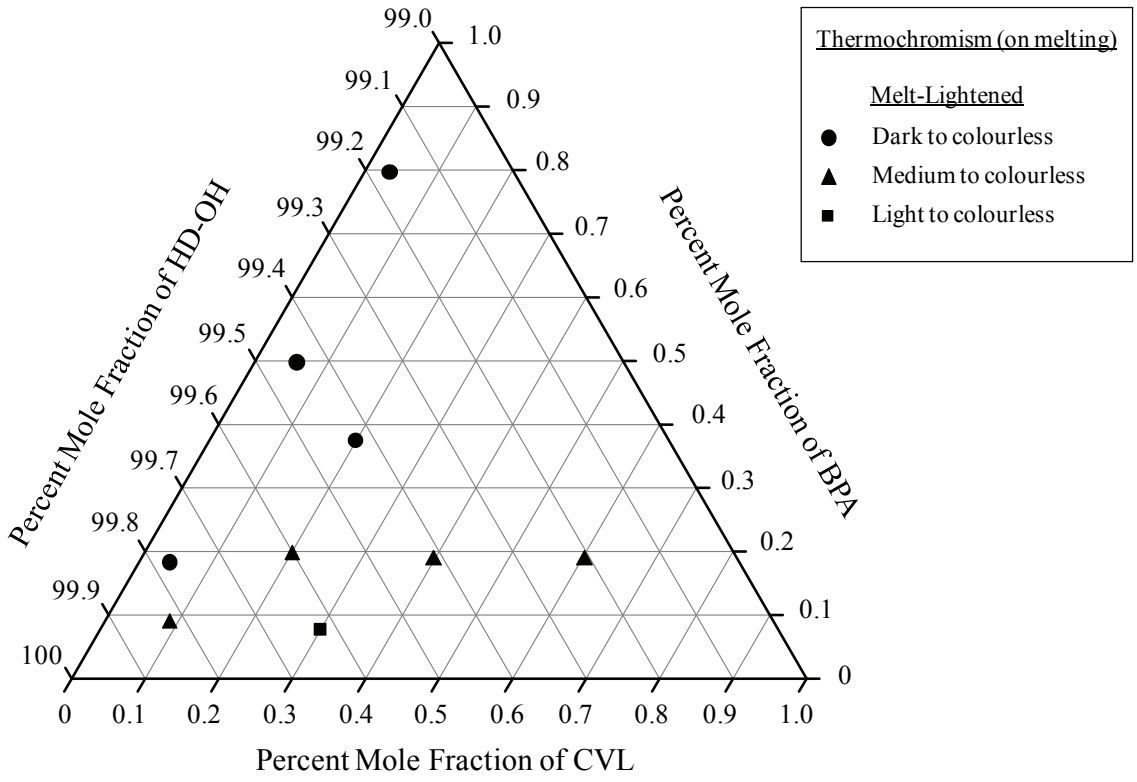

Figure 7.17. A portion of the ternary thermochromic phase diagram of the CVL:BPA:HD-OH system at high solvent concentration (where $z \approx 160$ to 2250). Melt-lightened behaviour was observed for all compositions.

Figure 7.18 shows a portion of the ternary phase diagram of the CVL:DHB:HD-OH system at high solvent concentrations (*e.g.*, where $z \geq 160$). Once again, all of the samples shown here were transparent in the melt; therefore, it is more useful to examine the change in observed colour of these mixtures. In general, weaker colour was observed in this system compared with BPA mixtures at similar compositions. BPA is one of the most effective developers for generating the ring-opened form of leuco dyes, therefore the reduced colour density of DHB mixtures compared with their BPA-containing counterparts was not surprising.[188] When the percent mole fraction of DHB was less than that of CVL, light colour was observed in the solid state. Increasing the DHB

concentration caused the solid to become more intensely coloured, with the only dark coloured samples containing very high DHB loading (*e.g.*, when $x_{DHB} \geq 0.9\%$).

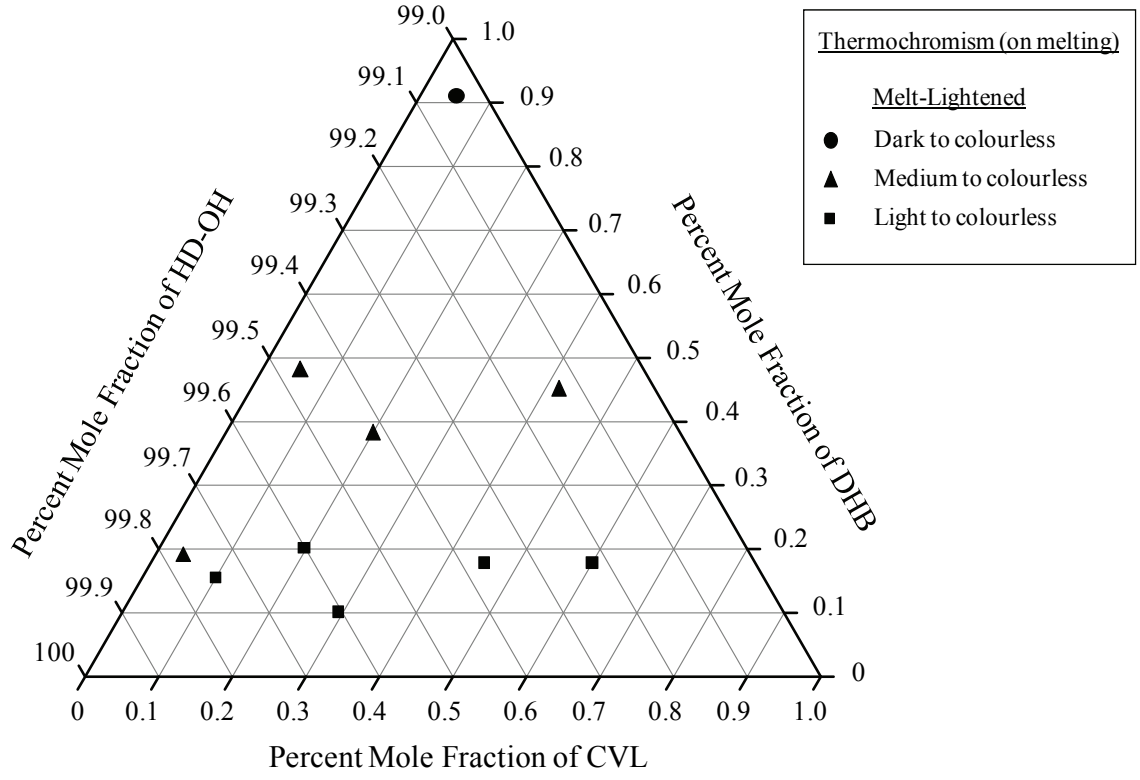

Figure 7.18. A portion of the ternary phase diagram of the CVL:DHB:HD-OH system at high solvent concentration (where $z \approx 160$ to 2650). Melt-lightened behaviour was observed for all compositions.

7.2.5.3 Summary of Thermochromic Phase Diagrams for BPA- and DHB-Containing Mixtures

Thermochromic mixtures containing BPA or DHB as the developer component became completely decoloured upon solvent melting at all of the compositions studied in this work. When the solvent concentration was relatively low ($z \leq 100$), the dye and/or the developer were noted to remain insoluble in the melt when $x_{CVL} > 1\%$. In mixtures containing similar CVL and developer concentrations (*i.e.*, $x_{CVL} \approx x_{DEV}$), the CVL appeared to have a type of "salting-out" effect on the developer, and only insoluble

developer was observed. When the CVL concentration exceeded that of the developer, both insoluble CVL and developer were observed in the molten solvent.

Completely colourless, transparent molten phases were obtained when the percent mole fraction of CVL in low solvent concentration samples was $x_{CVL} \leq 1\%$, and transparent melts were observed at all compositions when the solvent concentration was vastly increased (*e.g.*, when $z > 150$). The substantial increase in solvent concentration, however, had the detrimental effect of reducing colour density in the equilibrium solid, thereby reducing the overall colour contrast of the thermochromic colour change. Nevertheless, high colour contrast melt-lightened thermochromism was obtained in both the CVL:BPA:HD-OH and CVL:DHB:HD-OH ternary systems. Table 7.7 lists the highest colour contrast values obtained for the CVL:BPA:HD-OH and CVL:DHB:HD-OH systems at both high and low solvent concentrations; the colour contrast values observed for these samples at low solvent concentrations represent the best colour contrast observed in the present work for melt-lightened thermochromic mixtures.

Table 7.7. The colour density and colour contrast values obtained *via* colour photo analysis for PG-containing mixtures, showing data for the samples demonstrating the highest colour contrast for each ternary system.

Components	Composition	CD_{Equil}	CD_{Melt}	ΔCD_{Max}
CVL:BPA:HD-OH	[1:8.1:91]	1.4	0.0	1.4
CVL:BPA:HD-OH	[1:16:1985] x_{BPA} = 0.79% $x_{HD\text{-}OH}$ = 99.16%	1.1	0.0	1.1
CVL:DHB:HD-OH	[1:8:91]	1.5	0.0	1.5
CVL:DHB:HD-OH	[1:16:1685] x_{DHB} = 0.92% $x_{HD\text{-}OH}$ = 99.02%	0.6	0.0	0.6

7.2.6 Thermochromic Phase Diagram for CVL:DDG:OD-SH Mixtures

CVL:DDG:OD-SH mixtures showed a wide range of thermochromic behaviour due to the large range of concentrations studied. Both melt-lightened and melt-darkened thermochromism were observed for CVL:DDG:OD-SH mixtures, similar to the behaviour of the CVL:gallate:alcohol systems containing poorly matched alkyl chain lengths, however, the concentration of solvent required for decolouration of the melt was an order of magnitude larger in CVL:DDG:OD-SH mixtures.

Figure 7.19 shows a portion of the ternary thermochromic phase diagram of the CVL:DDG:OD-SH system. At very high solvent concentrations (*e.g.*, $x_{OD\text{-}SH} \approx 99.6$ to 99.9%), decolourization of the melt was observed for samples with $x_{CVL} < 0.2\%$, although the colour of the equilibrium solid was often light. The best colour contrast obtained for melt-lightened mixtures was obtained at $x_{CVL} = 0.05\%$, and when $0.2 \leq x_{DDG} \leq 0.4\%$. In this region, medium and dark coloured equilibrium solids melted to form colourless, transparent molten phases. Increased developer concentrations (*e.g.*, $x_{DDG} > 0.4\%$) and

dye concentrations (*e.g.*, $x_{CVL} \geq 0.1\%$) caused retention of colour into the molten phase, which reduced the colour contrast of melt-lightened mixtures.

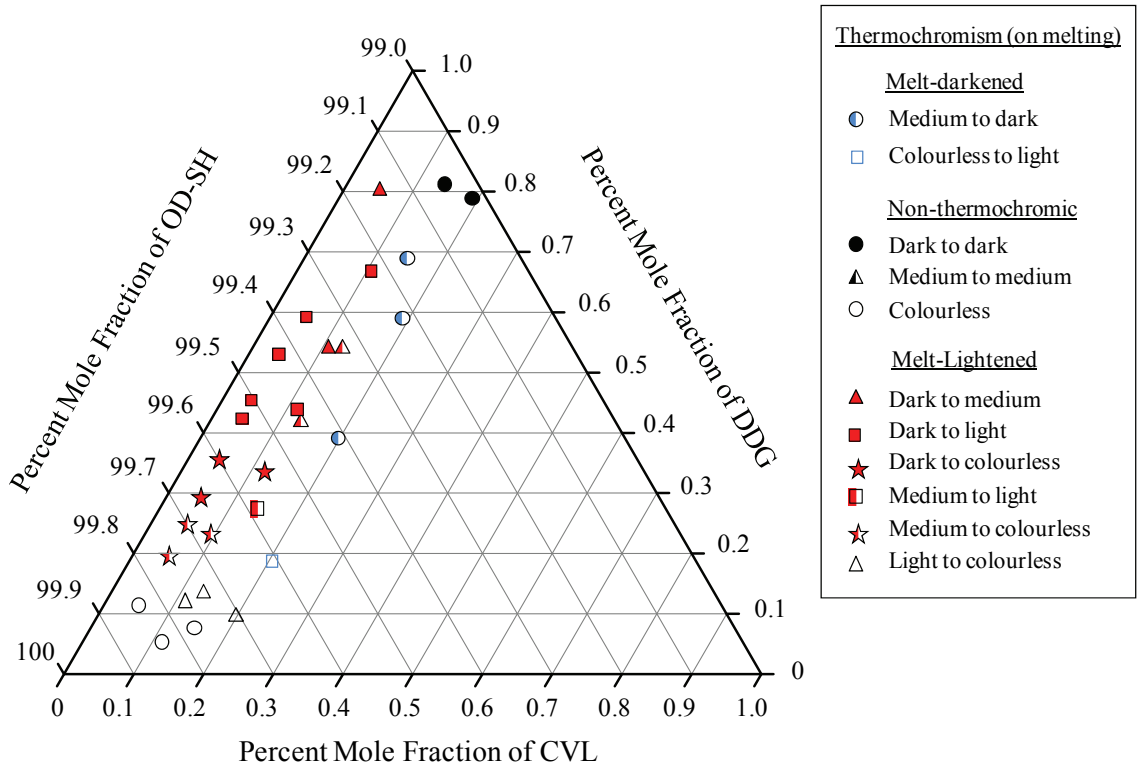

Figure 7.19. A portion of the ternary thermochromic phase diagram of the CVL:DDG:OD-SH system at very high solvent concentrations (where $z \geq 500$). Melt-darkened thermochromism was obtained at relatively high CVL and DDG concentrations (*e.g.*, when $x_{CVL} > 0.2\%$ and $x_{DDG} \geq 0.4\%$). Samples with low developer concentrations (*e.g.*, when $x_{DDG} < 0.5\%$) demonstrated melt-lightened thermochromism. Some samples were non-thermochromic at high developer concentrations (*e.g.*, when $x_{DDG} \approx 0.8\%$).

Increasing the dye and developer concentrations to much higher values caused the colouring behaviour to change from melt-lightened to melt-darkened thermochromism. At high DDG concentrations (*e.g.*, when $x_{DDG} > 0.6\%$) and high CVL concentrations (*e.g.*, when $x_{CVL} > 0.1\%$), melt-darkened thermochromism was observed at virtually all compositions. The transition region from melt-darkened to melt-lightened behaviour was very narrow in this system owing to the need for extremely high dilution of the colouring components to generate the decoloured form of the dye in the melt. Two samples

showing medium-to-medium transitions were observed in the region of $x_{CVL} \approx 0.12\%$, and $0.4 \leq x_{DDG} \leq 0.6\%$, indicating that the region of transition between thermochromic behaviour possibly lies somewhere in this compositional range.

The thermochromic behaviour of CVL:DDG:OD-SH mixtures was shown to change as a function of mixture composition, with samples containing very high solvent concentrations (*e.g.*, when $x_{OD\text{-}SH} \approx 99.6$ to 99.9%) demonstrating melt-lightened thermochromism, and samples containing relatively high dye and developer concentrations demonstrating melt-darkened thermochromism (*e.g.*, when $x_{CVL} > 0.1\%$ and $x_{DDG} > 0.6\%$). Similar behaviour was noted in the CVL:gallate:alcohol systems containing poorly matched alkyl chain lengths, however the lack of strong interaction between DDG and OD-SH resulted in the need for very high dilution of the colouring components to give rise to melt-lightened behaviour.

The colour contrast values for CVL:DDG:OD-SH mixtures were relatively low compared with the PG-, BPA-, and DHB-containing mixtures due to the low concentration of the colour-forming components. The practical consequence is that OD-SH containing mixtures are not particularly suitable for use in melt-lightened thermochromic applications, as high colour contrast is a basic requirement of good thermochromic materials.[101] The maximum colour contrast values, obtained *via* observational spectroscopy, for melt-lightened samples in the CVL:DDG:OD-SH ternary system are summarized in Table 7.8.

Table 7.8. The colour density and colour contrast values obtained *via* observational spectroscopy for CVL:DDG:OD-SH mixtures, showing data for the samples demonstrating the highest colour contrast for each compositional range studied listed in the table.

Components	Composition	CD_{Equil}	CD_{Melt}	ΔCD_{Max}
CVL:DDG:OD-SH	[1:6:2070] x_{DDG} = 0.29% $x_{OD\text{-}SH}$ = 99.67%	0.8	0.0	0.8
CVL:DDG:OD-SH	[1:2:900] x_{DDG} = 0.22% $x_{OD\text{-}SH}$ = 99.66%	0.7	0.1	0.6
CVL:DDG:OD-SH	[1:1:715] x_{DDG} = 0.14% $x_{OD\text{-}SH}$ = 99.72%	0.2	0.0	0.2
CVL:DDG:OD-SH	[1:0.5:500] x_{DDG} = 0.10% $x_{OD\text{-}SH}$ = 99.7%	0.2	0.0	0.2

7.3 Conclusions Regarding Thermochromic Phase Diagram Determination

Thermochromic phase diagrams can be used to map out the colouring behaviour of three-component rewritable thermochromic mixtures. Comparing the colour density of the equilibrium solid state to that of the molten mixture allows for the determination of the colour contrast between the two states. The colour contrast of the thermochromic transition is considered to be among the most important properties of thermochromic materials, therefore mapping out the change in colour contrast as a function of composition is a fruitful endeavour.

Throughout this work, it has been shown that CVL:alkyl gallate:alkyl alcohol mixtures can display different types of thermochromism. When the alkyl chains attached to the developer and solvent are well-matched in length, melt-darkened thermochromism can be obtained. High colour contrast in such mixtures, which include the

CVL:ODG:alcohol and CVL:DDG:TD-OH systems, can be obtained when the developer concentration is sufficiently high to generate a coloured melt. Due to the strong interaction of developer and solvent molecules in the solid state, which results from the similar length of the alkyl chains, the equilibrium solid states of such mixtures are virtually always decoloured.

CVL:alkyl gallate:alkyl alcohol mixtures that contain alkyl chains of vastly different lengths generally become strongly coloured in the solid state. The colour densities in the solid state, at similar mixture compositions, were shown to increase as the degree of alkyl chain length mismatch increases. Propyl gallate-containing mixtures demonstrated the highest equilibrium solid colour densities of the CV:alkyl gallate:alkyl alcohol mixtures, and when the solvent concentration was sufficiently large to cause decolourization of the melt, they also showed the highest colour contrast values. CVL:DDG:HD-OH and CVL:DDG:OD-OH mixtures have been shown in previous work to undergo relatively strong attractive interactions in the solid state,[101,110,143] and as a result the colour density of these mixtures was substantially lower compared to PG- and OG-containing mixtures.

In mixtures containing poorly matched alkyl chain lengths, melt-darkened thermochromic behaviour was also accessible, however very high developer concentrations were required to generate darker melts. Since the equilibrium solid state of such mixtures was coloured at virtually all compositions, the colour contrast of melt-darkened thermochromism was generally rather low. The colour contrast of melt-darkened thermochromism was also noted to decrease as the difference in alkyl chain

length increased, which is understandable given that mixtures containing alkyl chains of similar lengths generally had less strongly coloured solid states.

Mixtures containing BPA or DHB as the developer component were strongly coloured in the solid state at most compositions owing to the lack of attractive interactions occurring between the developer and solvent. These mixtures were also effectively decoloured upon melting of the solvent due to disruption of the dye:developer complex. However, at relatively low solvent concentrations (*e.g.*, $z \leq 100$), the dye and/or developer often remained insoluble in the molten mixture as a result of poor solubility of the two components. Vastly increasing the solvent concentration (*e.g.*, $z > 150$) reduced melt opacity at the cost of lowered solid state colour density.

In summary, high colour contrast mixtures that displayed the two types of thermochromic colour change, melt-lightened and melt-darkened thermochromism, were obtained by selecting appropriate developer and solvent components, and by modifying mixture composition. Ideal melt-darkened thermochromism was obtained for mixtures containing well-matched developer and solvent alkyl chain lengths (*e.g.*, DDG with TD-OH, ODG with OD-OH, *etc.*) when the developer concentration was very high. Alternatively, ideal melt-lightened thermochromism was obtained in systems that contained poorly matched alkyl chain lengths (*e.g.*, PG- and OG-containing systems, *etc.*) and in systems with chemically dissimilar developer and solvent components (*e.g.*, BPA or DHB with HD-OH) due to the intense colouration of the solid state. By mapping thermochromic colour changes and component solubility behaviour of such mixtures onto ternary thermochromic phase diagrams, the compositional regions of ideal

thermochromic behaviour can be quickly identified and used in the preparation of mixtures with optimal thermochromic properties.

Chapter 8 Thermally Erasable Ink-Jet Printer Inks[‡‡]

8.1 Introduction and Background

8.1.1 Thermally Erasable Laser-Jet Toner - e-blue™

8.1.1.1 Background

In 2003, Toshiba Co. announced the launch of a thermally erasable laser-jet toner, e-blue™, which can be decoloured (*i.e.,* erased) by heating.[41,42,201,206,207,214] The main driving force behind the development of this technology has been the potential reduction in energy consumption and greenhouse gas production associated with reducing the amount of office paper sent to recycling facilities.[215,216] Although e-blue™ has seen use in Japan, the product was not launched globally as a result of technical limitations which include substantial post-erase shadows (*i.e.,* ghost images remaining on the page), low image colour density, expensive specialized equipment, reduced paper quality after multiple erasings, and limited colour options (only blue toner is available).[105,140,188]

8.1.1.2 Composition and Function

The e-blue™ toner is composed of a white-to-blue colour-changing leuco dye, a phenolic developer, a chemical "erasing agent", and a polymeric binder resin used to hold the components together.[41,42,206,207] The structure of the leuco dye used in e-blue™, blue 203, is shown in Figure 8.1. In the presence of an acidic developer, *leuco*-blue 203

[‡‡] This work was carried out at Toshiba Co. RDC in Kawasaki, Japan

(Figure 8.1 (a)) can be converted to the ring-opened coloured form, which is blue (Figure 8.1 (b)).

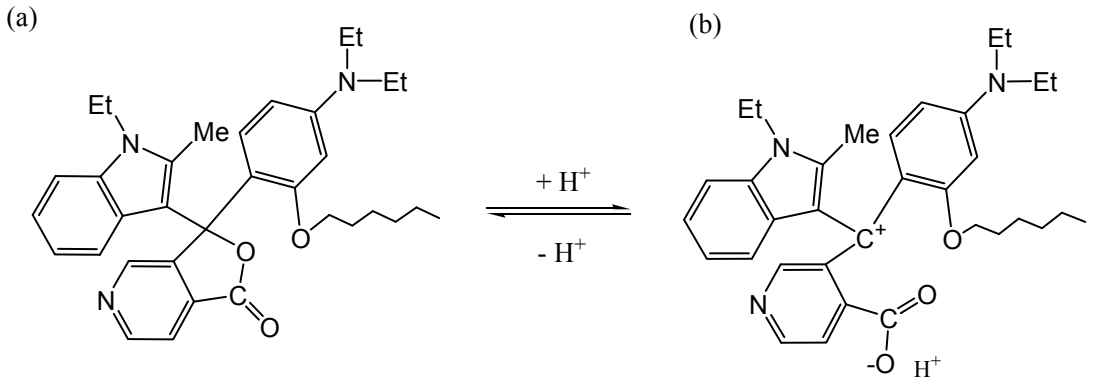

Figure 8.1. The structure of the e-blue™ dye, blue 203. (a) The leuco form of blue 203. (b) The ring-opened form of blue 203, which is formed in the presence of an acidic developer.

The developer used in e-blue™, ethyl gallate, is a low molecular weight member of the alkyl gallate family of phenolic developers, discussed extensively in this document. The e-blue™ toner is blue prior to printing indicating that the dye and developer have already interacted to convert *leuco*-blue 203 to the ring-opened, coloured form. Polystyrene is used as a plastic binder resin which forms the majority of the mixture (> 90 mass %) and is used as both a transfer medium and to hold the components together during printing.[41,42,206,207]

Although the exact structure of the erasing agent added to e-blue™ was not explicitly disclosed for trade secrecy reasons, chemicals suitable for application as erasing agents have been described in the patent literature.[217] A commonly stated example is the bile salt cholic acid, which is a cholesterol-derived, steroid-like compound produced in the liver.[217]

The function of the erasing agent is to trap the phenolic developer during the erasing process (*i.e.,* heating) and sequester it from the dye. Ethyl gallate (MW = 198.17

g mol^{-1}) has a low molecular mass compared to blue 203 (MW = 539.71 g mol^{-1}) and the low molecular mass steroids (400 – 500 g mol^{-1}), giving the developer heightened mobility within the toner particle. Upon heating, the dye-developer interaction is disrupted and the developer diffuses to and binds with the erasing agent. This not only removes colour during erasing, but also prevents colour reformation after cooling. The increased effectiveness of "oven-erasing" compared with "iron-erasing" can be explained by this phenomenon, since the heating time in the oven is substantially longer than the heating time with the iron allowing for more complete diffusion of the developer away from the dye.[41,140]

8.1.1.3 Technical Problems with Erasable Printing Inks

There are numerous technical drawbacks associated with e-blue™ which have prevented widespread use. An exhaustive list of the technical issues is out of the scope of this work, so this section will focus on the problems associated with e-blue™ that are potentially transferable to ink-jet printing applications.

Perhaps the most challenging technical problem associated with erasable printing applications is the maintenance of paper quality across multiple print/erase cycles.[105] Paper can become degraded in many ways, viewed as two categories: unavoidable damage from regular use and avoidable damage due to limitations with the erasable ink technology.

Unavoidable damage to printing paper includes (1) folds and creases on the page which prevent the page from being fed into the printer, (2) damage around the edges of the page from staples, paper clips, etc., which can also prevent proper feeding into the

printer, (3) the use of permanent inks on the page that can obscure future printing, and (4) reduced sharpness of printed images due to build-up of ink on the page.

Avoidable damage is highly dependent on the method of printing employed and the erasable ink system used. When using the erasable laser-jet toner, the polymeric binder resin remains on the surface of the page.[41,105] This presents two issues: (1) the polymeric binder is not completely transparent and can be seen as a grey shadow (*i.e.*, ghost image) after erasing,[218] and (2) after numerous printings, the polymeric binder forms a relatively thick layer on the surface of the paper which gives the page a stiff, brittle feeling. The stiffness of the page can create problems with the feeding mechanism of the laser-jet printer and is also unpleasant to the touch. The page can also be damaged by repeated application of heat as a result of the erasing process leading to problems such as paper browning and curling, both which prevent re-use of the sheet.[105]

There are other issues associated with e-blue™ which preclude it from widespread use. These include the high cost of purchasing a new laser-jet printer which can use the e-blue™ toner, purchasing and housing the 'oven', foul odours associated with heating a ream of paper inside an office, and the lack of other colours for erasable laser-jet toners. Some of these issues are transferable to ink-jet printing applications (*e.g.,* foul odours, paper browning, shadowing effects, etc.) but some can be avoided entirely (*e.g.,* paper will not become brittle since there is no binder, no need for an expensive printer, many colours become available, etc.). It is the avoidance of these technical issues that led to the project to study the development of the thermally erasable ink jet printer (IJP) ink at Toshiba Co. RDC.

8.1.2 Thermally Erasable Ink-Jet Printer Inks

8.1.2.1 Composition and Function

Erasable IJP inks are very similar to e-blue™ in both composition and function, although the transport medium was changed to accommodate the different deposition method.[201,209] In the case of e-blue™, the transport medium was the polystyrene binder; in the case of IJP inks, an aqueous/organic volatile solvent blend was used to carry the colour-forming components to the page.[201,209] IJP inks are generally colourless when dissolved in the volatile solvent with colour formation occurring on the page as the volatile solvent evaporates.[201]

As was the case for e-blue™, the colour-forming components in IJP inks are a combination of leuco dye and phenolic developer.[201] The dyes and developers used in IJP inks must be soluble in the volatile aqueous/organic solvent, which places constraints on the types of dyes and developers that can be used in this technology. As a result of the different deposition method, the colouring agents in IJP inks need to have a much deeper colour (*i.e.*, large molar absorption coefficient, ε, than dyes which can be used in laser-jet printing.[201,209]

The reason for requiring high molar absorption coefficient dyes for IJP inks is described schematically in Figure 8.2. In laser-jet printing, the toner is deposited directly onto the surface of the page with minimal ink penetration (Figure 8.2 (a)). As a result, most of the light incident on the page is reflected back to the observer after interaction with the dye, and little light intensity is lost due to scattering within the page. Conversely, IJP inks are able to easily penetrate into the page due to the mobility of the volatile solvent. This movement can carry the colour-forming components deep into the

page causing a reduction in the observed colour density compared to an equivalent amount of dye deposited by laser-jet printing (Figure 8.2 (b)). Incident light striking a portion of the page with little dye present will reflect without significant spectral modification causing the printed image to appear lighter. Additionally, dye particles found deep in the page can scatter light within the page, preventing the light from reflecting back to the observer, decreasing overall image brightness and quality.[219,220]

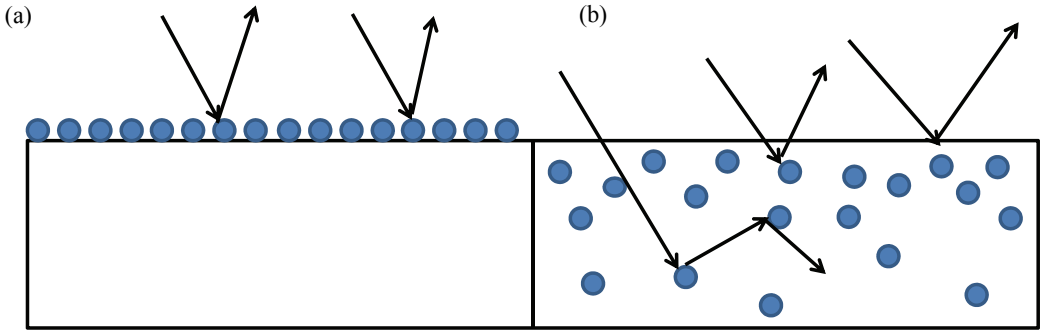

Figure 8.2. (a) Laser-jet toner is deposited on the surface of the page, incident light is reflected back to the observer, and little light intensity is lost to scattering within the page. (b) IJP inks penetrate deeply into the page due to the high mobility of the volatile solvent. Dye molecules found deep in the page appear with less contrast due to scattering of light within the page, and reflective losses from the surface of the page further reduce image colour density.[220]

The other major difference between e-blue™ and IJP inks is the volatile solvent. The major component of the solvent used in IJP inks is ethanol, which is deemed to be one the safest organic solvents available that is capable of dissolving the colour-forming components.[201,209] Ethanol also is preferred due to its low boiling point (T_{vap} = 78 °C), high volatility at room temperature, relatively pleasant odour, miscibility with water, and very low cost.[221]

The use of ethanol as the volatile solvent does present some challenges. Many leuco dyes are highly hydrophobic in nature due to their extended π-conjugated networks and therefore have limited solubility in pure ethanol. To increase the solubility of such

leuco dyes, solvent modifiers such as propylene glycol monomethyl ether (PGMME) and *iso*propanol can be added.[201] Additionally, IJP inks need to be filtered prior to addition to the printer cartridge to prevent clogging of printer heads (*i.e.,* print nozzles). An aqueous surfactant solution also is added to the solvent to prevent clogging of the printer heads.[201]

Due to the impact of ink penetration on the colour density of IJP inks, the viscosity of ethanol must be considered. The viscosity of ethanol at room temperature is rather low, being only slightly higher than that of water (η_{EtOH} = 1.074 x 10^{-3} Pa s^{-1}, η_{H_2O} = 8.94 x 10^{-4} Pa s^{-1}).[221] As a result, deposition of large amounts of ink can cause page wetting and extensive ink penetration, even through the entire thickness of the page.[222] Ink penetration creates technical problems including reduced image colour density, poor image quality and sharpness, difficult erasing, and the prevention of double-sided printing which eliminates some of the benefits of erasable printing (*i.e.*, reduced paper consumption).[215,216,223,224] Viscosity modifiers such as soluble polymers (*e.g.*, poly(vinyl alcohol)) and higher viscosity solvents (*e.g.*, PGMME) can be added to increase solvent viscosity and reduce ink penetration and page wetting.[201]

8.1.2.2 Colour Density Threshold Values

To determine if a dye-developer combination was suitable for further study, colour density threshold values were established. The lower bound of the optimal colour density of printed images is considered to be $CD = 0.4$. At these colour densities, the printed image is dark enough to be easily read at arm's length under most lighting conditions. The optimal colour density after erasure is considered to be $CD \leq 0.08$. At these colour densities, the printed image is considered completely erased and is

essentially invisible to the naked eye.[188] A troublesome consequence of increasing the printed colour density is that the erased colour density usually increases also.

8.2 Results and Discussion

8.2.1 Enhancement of the Colour Density of IJP Inks

One of the biggest limitations associated with e-blue™ was the poor colour density of printed samples and, as described in section 8.1.2.2, this issue is magnified in IJP inks. A number of ink compositions had been prepared and tested at RDC prior to the start of the internship and the best of these compositions was used as a starting point during the internship.

8.2.1.1 IJP Inks Containing CVL

The first ink composition studied in this work had been previously prepared by researchers at Toshiba RDC and was known to have high printed colour density and good erasability, but suffered from spontaneous colour loss within the first few days after printing. The colour former in this ink was CVL and the developer was bisphenol F. The structure of the latter is shown in Figure 8.3. CVL is preferred as a dye due to its large molar absorptivity ($\varepsilon = 2.8 \times 10^4$ L mol^{-1} cm^{-1} in CH_3CN, developed with acetic acid)[25] and low cost, while bisphenol F was used due to its high solubility in ethanol, lack of colour (very faint pink), ability to develop most leuco dyes, and reduced endocrine-mediated properties (*i.e.,* less disruptive to the endocrine system) compared to its analogue bisphenol A.[203,225]

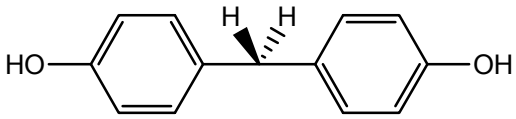

Figure 8.3. The structure of the phenolic developer, bisphenol F.

Five inks were prepared using CVL as the colour former; the exact compositions are shown in Table 8.1. Different solvent compositions were used to modify the amount CVL present in the printed image, to change the evaporation rate of the solvent, and to change the viscosity of the solvent. Figure 8.4 shows the colour density fade curves for the various CVL-containing inks as a function of time after printing (note that Day 0 is the day samples were printed).

Table 8.1. The compositions of CVL inks.

Sample Name	Mass of CVL / g	Mass of Bisphenol F / g	Mass of Ethanol / g	Mass of Sanizole Solution / g	Mass of PGMME / g
CVL Ink #1	0.05	0.6	7.5	1.5	1
CVL Ink #2	0.05	0.6	10	1	0.5
CVL Ink #3	0.05	0.6	8.5	1.1	1
CVL Ink #4	0.05	0.6	8.5	1	0.5
CVL Ink #5	0.05	0.7	8.5	1	0.5

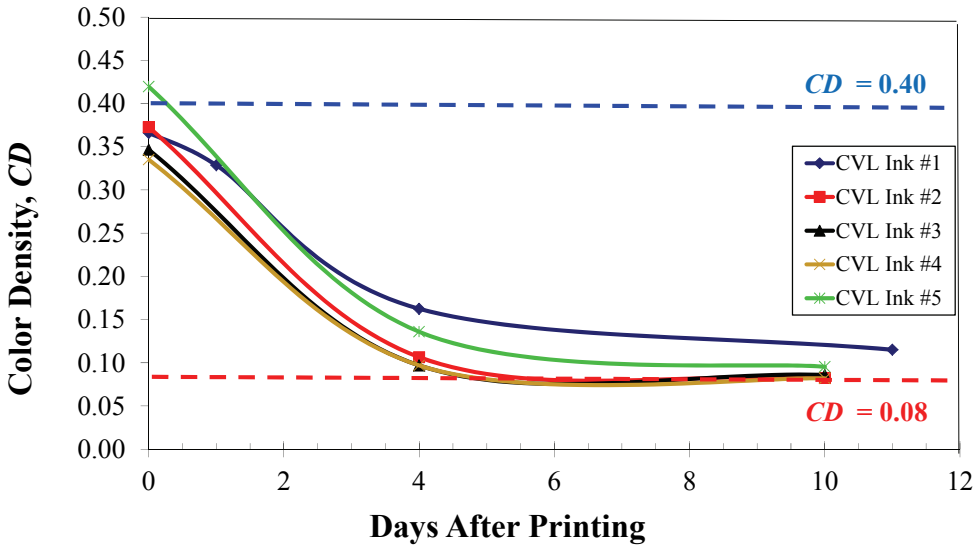

Figure 8.4. Colour density fade of CVL-containing IJP inks as a function of time. Rapid colour loss was observed within the first few days after printing. Note: lines are added as a guide to the eye.

Although most of the inks prepared approach the *CD* = 0.4 threshold, indicating very good initial colour density, it is apparent that these CVL containing inks demonstrate very poor colour stability over time. Within four days of printing, inks #2, #3, and #4 were completely erased (*CD* ≈ 0.08) and the other two were essentially erased on sitting for two weeks.

8.2.1.2 IJP Inks Containing Blue 63 and Blue 203

The results presented in section 8.2.1.1 indicate that CVL likely is not a suitable dye for use in erasable IJP inks due to very poor colourfastness (*i.e.*, resistance to colour fade).[106] To mitigate issues with poor colourfastness, the leuco dyes blue 63 and blue 203 (structures shown in Figure 8.5) were tested to determine if the colour densities of these dyes could match that of CVL inks. blue 203 is the dye used in e-blue™ and is known to have good colourfastness, while blue 63 is also expected to demonstrate good

colourfastness due to its structural similarities to blue 203. The only difference in structure between the two compounds is the length of the alkoxy chain attached to the "free" aminophenyl moiety.

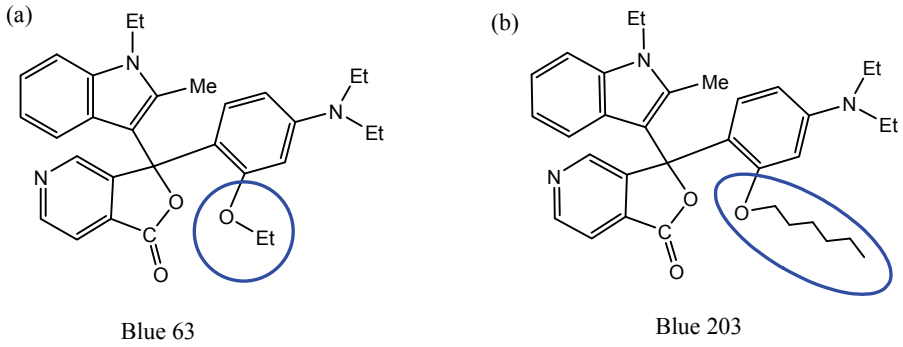

Figure 8.5. The structures of (a) blue 63 and (b) blue 203. The highlighted regions indicate the structural differences between the two leuco dyes.

Three inks were prepared using bisphenol F as the developer, two containing blue 203 with the other containing blue 63. The compositions of these inks are given in Table 8.2. Figure 8.6 shows the colour fade behaviour of blue 63 and blue 203 inks, with CVL ink #5 presented for comparison. The colourfastness properties of blue 63 and blue 203 inks were indeed much better than CVL inks; however, the initial colour densities were substantially lower. The initial colour density of the blue 203 inks ($CD \approx 0.32$) was higher than that of the blue 63 ink ($CD \approx 0.28$), but both fell short of the $CD = 0.4$ threshold needed for optimal initial image colour density. The excellent colourfastness properties associated with blue 203 were negated by the low initial colour densities which led to the study of other blue leuco dyes.

Table 8.2. The compositions of blue 63 and blue 203 inks.

Sample Name	Mass of Dye / g	Mass of Bisphenol F / g	Mass of Ethanol / g	Mass of Sanizole Solution / g	Mass of PGMME / g	Mass of *iso*-propanol / g
Blue 63 Ink #1	0.058	0.6	9.5	1.5	0.5	0
Blue 203 Ink #1	0.065	0.6	9.5	1.5	0.5	0
Blue 203 Ink #2	0.08	0.65	9	1.5	1	0.25

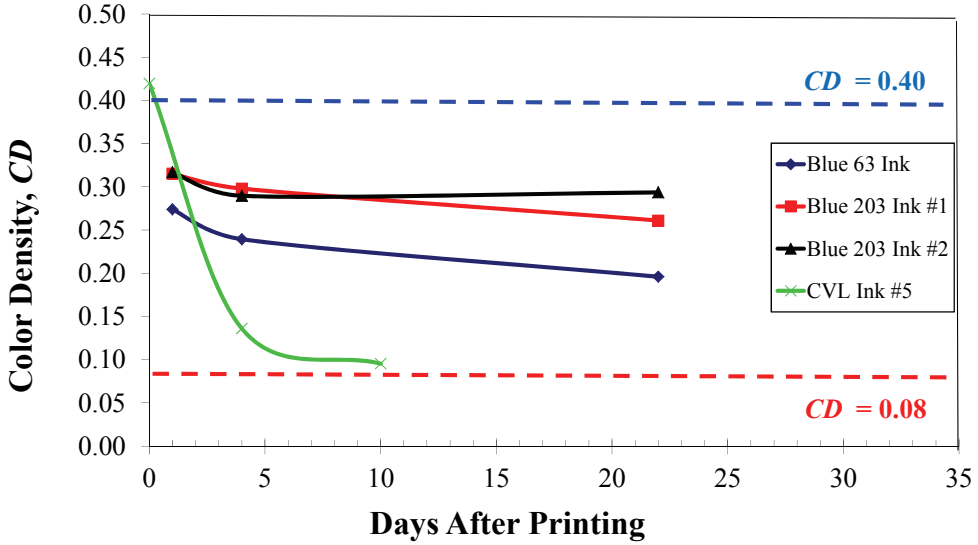

Figure 8.6. Colour fade of blue 63 and blue 203 inks as a function of time. CVL ink #5 is presented for comparison. Although little colour fade was observed in these inks, the initial colour density was low. Note: lines are added as a guide to the eye.

8.2.1.3 IJP Inks Containing Blue C4OH, Blue C6NH2 and PS-Blau

The final set of blue leuco dyes tested was selected due to their strong blue colouration in the ring-open form and lack of colour in their leuco forms. Figure 8.7 shows the structures of blue C4OH, blue C6NH2, and PS-blau.

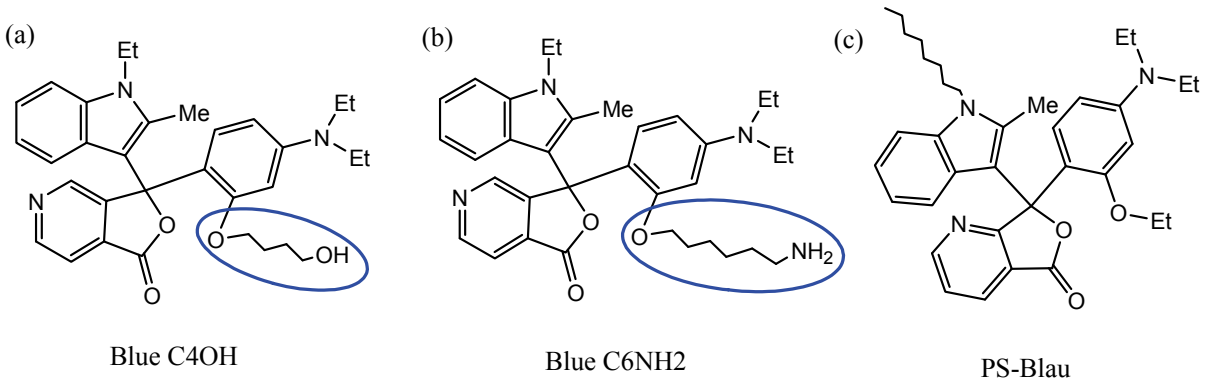

Figure 8.7. The structures of the leuco dyes (a) blue C4OH, (b) blue C6NH2, and (c) PS-blau. The highlighted regions indicate the structural differences between blue C4OH and blue C6NH2.

These three dyes, along with blue 63 and blue 203, all share a common backbone structure with modifications occurring on the "free" aminophenyl moiety and/or on the indole moiety. The influence of the side-chains on the stability of the ring-opened form of a leuco dye, and subsequently the colourfastness of printed images, is not well understood, but there are marked differences in the behaviour of the dyes when subtle changes in the molecular structure are introduced.[104]

Comparing blue 63 to blue 203, the only structural difference between the two compounds is the length of the carbon chain of the ether attached to the aminophenyl moiety. The blue 63 ink is shown (see Figure 8.6) to have a lower initial colour density than the blue 203 inks, which could be a consequence of enhanced solubility of blue 203 due the presence of the longer alkyl chain attached to the ether oxygen.

In the case of blue C4OH and blue C6NH2, it is possible that the presence of an –OH or $–NH_2$ group on the ether chain provides additional hydrogen bonding sites for the ring opened form, stabilizing it and giving rise to better colourfastness in the ring-open form. The presence of polar –OH and $–NH_2$ groups might also enhance solubility in solvents such as ethanol and water due to additional hydrogen bonding sites. CVL lacks

functional group modifications (*i.e.*, no ether oxygen, hydroxyl or amino groups) in the vicinity of the lactone ring, which could provide an explanation for the poor colourfastness demonstrated by CVL inks; the lack of additional hydrogen bonding sites due absence of oxygen and nitrogen atoms reduces the stability of the open form, which causes the ring-opening equilibrium to shift to the leuco form.

The compositions of blue C4OH, blue C6NH2, and PS-blau inks are given in Table 8.3. Note that a PVA solution (0.35 mg per 1 g water) was used in these inks to modify the viscosity of the solvent. An analysis of the impact of viscosity modification is given in section 8.2.3.

Table 8.3. The compositions of blue C4OH, blue C6NH2 and PS-blau 203 inks.

Sample Name	Mass of Dye / g	Mass of Bisphenol F / g	Mass of Ethanol / g	Mass of Aqueous PVA Solution / g	Mass of PGMME / g
Blue C4OH Ink	0.06	0.525	6	3	3
Blue C6NH2 Ink	0.06	0.525	6	3	3
PS-Blau	0.06	0.525	6	3	3

Figure 8.8 shows the colour fade behaviour of the inks containing blue C4OH, blue C6NH2, and PS-blau. The best colour density properties observed in this work belong to inks containing blue C4OH and blue C6NH2. Both these inks demonstrate high initial colour density, matching that of CVL containing inks and exceeding the $CD = 0.4$ threshold required for ideal image quality. Inks containing blue C4OH and blue C6NH2 also demonstrated good colourfastness as the colour density remained near $CD = 0.3$ for up to 10 days after printing. The inks containing blue 203 were able to maintain $CD = 0.3$ for up to three weeks after printing, but the initial colour density ($CD \approx 0.3$) was substantially less than that of blue C4OH inks ($CD \approx 0.45$). The ink containing PS-Blau

behaved very similarly to inks containing CVL, but with better colourfastness coupled with lower initial colour density.

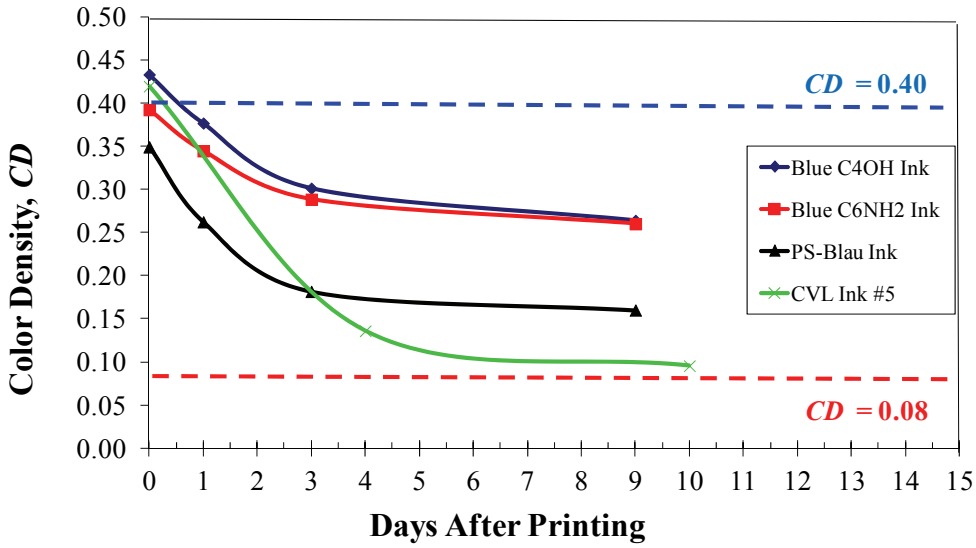

Figure 8.8. Colour fade of inks containing blue C4OH, blue C6NH2 and PS-blau as a function of time. CVL ink #5 is presented for comparison. Initial colour densities in the blue C4OH and blue C6NH2 inks exceeded the *CD* = 0.4 threshold, and colourfastness was substantially better than in CVL inks. Note: lines are added as a guide to the eye.

8.2.2 Effectiveness of Erasing – IJP Inks

A useful erasable ink needs to be just that: erasable. The following sections discuss the effectiveness of erasing of the inks discussed in section 8.2.1. The reader is referred to the subsections of section 8.2.1 for ink compositions. Printed samples generally were erased on the same day they were printed, with Day 0 being the day of printing and erasing. Two characteristics were examined during the erasing studies; (1) the reduction of colour density caused by the erasing procedure (*CD* = 0.08 is considered fully erased) and (2) the resistance to colour reformation over time, which is required to

maintain the erased image. Unless otherwise noted, all erasing was carried out using the "oven".

8.2.2.1 IJP Inks Containing CVL

The effectiveness of erasing for inks containing CVL is shown in Figure 8.9. These samples were erased using the "iron-eraser", which is known to be less effective than the "oven-eraser". Nevertheless, all five of the CVL containing inks demonstrated very good erasure immediately after printing and were able to maintain the erased state for an extended period of time. CVL ink #1 demonstrated a slight increase in colour density within the first few days after printing; this increase was attributed to being the first attempt at erasing samples using the hot iron, resulting in less than ideal erasing. CVL inks were expected to be easily erased based on the results presented in section 8.2.1.1, since CVL inks were shown to spontaneously decolour over time. As will be demonstrated in the following sections, there is a correlation between poor colourfastness and effective erasing, and *vice versa*.

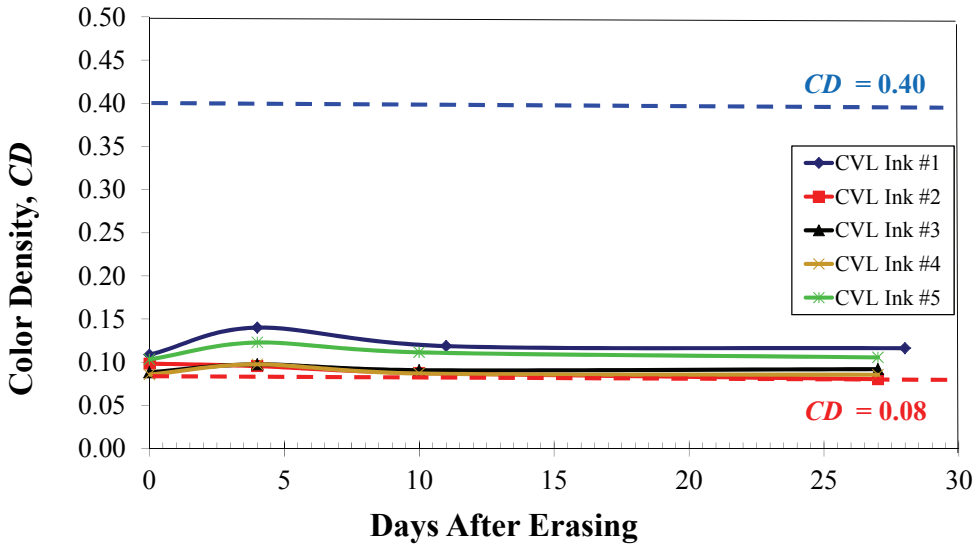

Figure 8.9. Colour density versus time after erasing for CVL inks. The erasing of these samples was carried out using the "iron-eraser". Initial colour densities before erasure were *CD* ≈ 0.35 to 0.40. Note: lines are added as a guide to the eye.

8.2.2.2 IJP Inks Containing Blue 63 and Blue 203

IJP inks containing blue 63 and blue 203 were shown (section 8.2.1.2) to have very good resistance to colour fade over time. Unfortunately, this good fade resistance was coupled with poor initial colour density. Figure 8.10 shows the change in colour density after erasing as a function of time for "oven-erased" samples. It is evident that the erased colour density approached the *CD* ≈ 0.08 threshold immediately after erasing. A slight increase in the colour density was observed in blue 203 ink #2 over the course of a few weeks. A consequence of this was the reappearance of visible images on the page that could obscure future printing.

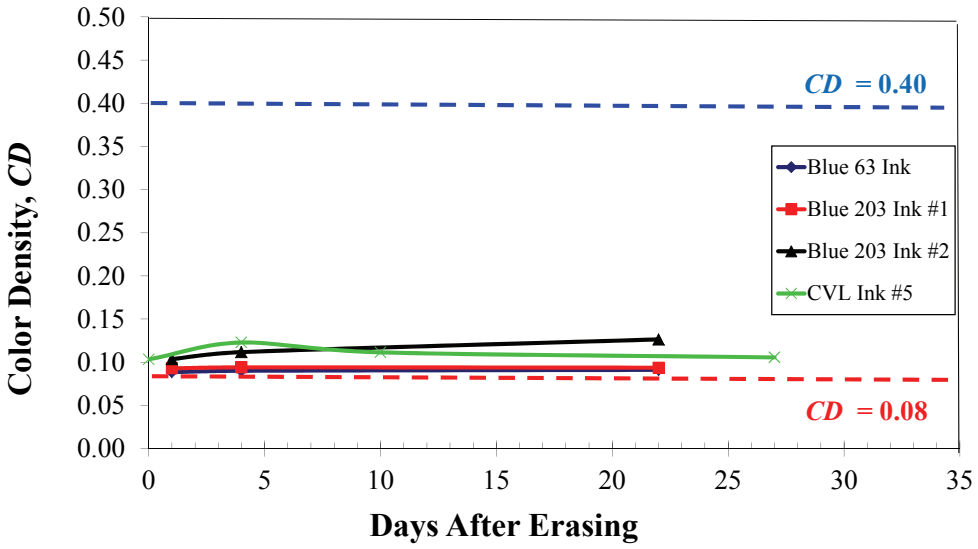

Figure 8.10. Colour density versus time after erasing for inks containing blue 63 and blue 203. All three inks show good colour erasure and maintain the erasure over time. Initial colour densities before erasure were *CD* ≈ 0.25 to 0.30. CVL ink #5 is shown for comparison. Note: lines are added as a guide to the eye.

The blue 63 ink demonstrated good erasing behaviour despite also having good colourfastness. This is likely due to the low initial colour density of the blue 63 ink, which makes it much easier to reduce the colour density to the *CD* = 0.08 threshold than would be possible for an ink with equivalent colourfastness but higher initial colour density.

8.2.2.3 IJP Inks Containing Blue C4OH, Blue C6NH2 and PS-Blau

IJP inks containing blue C4OH and blue C6NH2 demonstrated very promising initial colour density values as well as good resistance to colour fade over time. Figure 8.11 shows the colour erasure behaviour of these inks. The promising blue C4OH and blue C6NH2 inks demonstrated poor initial colour erasure and also suffered from poor resistance to colour reappearance over time. As discussed in section 8.2.2.1, there appears to be a correlation between good colourfastness and poor erasing. The practical

consequence of this correlation is that an ink demonstrating good initial colour density and good resistance to colour fade will often also suffer from poor erasing and poor maintenance of the erased state, as observed for the blue C4OH and blue C6NH2 inks.

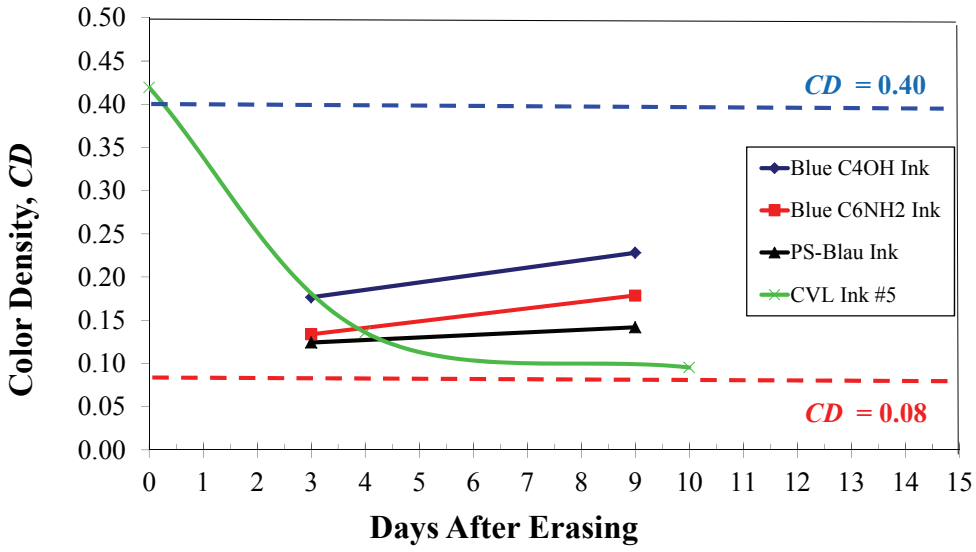

Figure 8.11. Colour density versus time after erasing for inks containing blue C4OH, blue C6NH2 and PS-blau. The three inks show fairly poor colour erasure and do not maintain the erased state over time. Initial colour densities before erasure were *CD* ≈ 0.35 to 0.45. The colour fade behaviour of CVL ink #5 is shown for comparison. Note: lines are added as a guide to the eye.

8.2.3 Modification of the Viscosity of IJP Inks

The viscosity of IJP inks is known to play an important role in the quality of printed images. Low-viscosity inks can be deposited on the page at a much higher rate than high-viscosity inks due to the deposition method employed in IJP printing (the printer literally fires a jet of liquid ink onto the page).[181] High penetrability of low viscosity inks results in a number of detrimental effects that reduce the quality of printed images including print mottle (uneven colour density across an image), decreased colour density, and the appearance of the image on the opposite side of the page.[226] In an effort

to increase the viscosity of IJP inks, viscosity modifiers such as PVA, gelatine, and corn starch were added to the inks. PVA was used most extensively in this work and therefore it is the only viscosity modifier discussed in detail.

8.2.3.1 IJP Inks Containing CVL Modified With PVA

A series of six inks containing varying amounts of PVA were prepared and tested for colour fade rate and erasing effectiveness. CVL (50 mg) was used as the dye for these studies in an effort to enhance the colourfastness of CVL inks and to take advantage of the low cost of CVL. The developer used in these inks was bisphenol F (500 mg). PVA was added, in the form of a stock solution (0.35 mg PVA per 1 g of water), in varying amounts to create a range of PVA concentrations. The final concentrations of PVA in the six inks are listed in the legend of Figure 8.12, which shows how colour density changes as a function of time after printing.

It is apparent from the data shown in Figure 8.12 that there is little correlation between the initial colour density and the PVA concentration, as well as little modification of the colour fade rate. All of the curves follow the same colour fade behaviour and only one ink (PVA = 0.05 mg/g) had a colour density matching that of the previously studied CVL-containing inks. The increased initial colour density in the 5 mg/g ink compared with the other PVA-containing inks is not fully understood. One explanation is that the increased PVA concentration caused the viscosity of the ink to increase, reducing ink penetration and causing the colour density of the printed image to become larger due to the fact that more of the dye remained near the surface of the page. The final colour density after less than a week on the bench approached $CD = 0.08$ for all

inks, indicating that these inks demonstrated very poor colourfastness and would be easily erased.

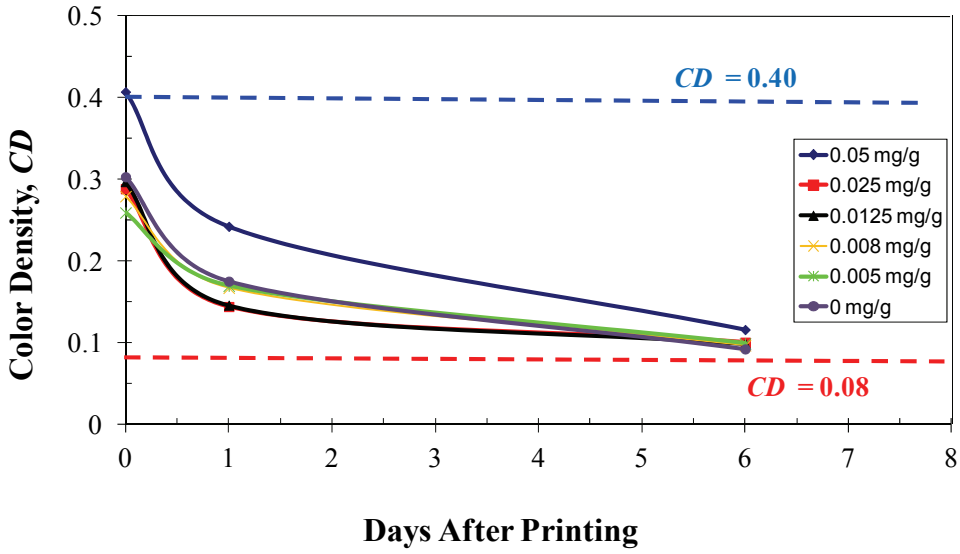

Figure 8.12. Colour density fade as a function of time after printing of CVL-containing inks to which PVA was added. The legend indicates the concentration of PVA in the final ink mixture. There appears to be little correlation between PVA loading and colourfastness as all samples behave similarly. Note: lines are added as a guide to the eye.

There was essentially no difference in the colour erasing behaviour between the samples, as demonstrated by the results shown in Figure 8.13. All of the samples were well erased ($CD \approx 0.1$) and none of the images showed colour reappearance over time. From the data reported in Figure 8.12 and Figure 8.13, it appears that PVA generally had little influence on the colouring behaviour of CVL-containing inks. A potential explanation is that the PVA concentration was too low to affect any change in the system. To further study the influence PVA might have on the colouring behaviour of erasable IJP inks, Blue C4OH inks containing PVA were prepared.

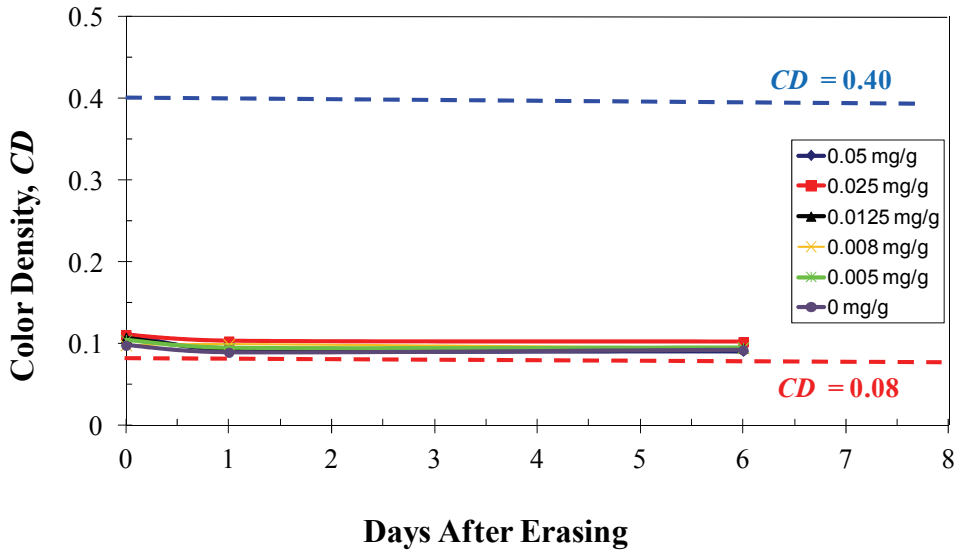

Figure 8.13. Colour density after erasing for CVL inks containing PVA. The legend indicates the concentration of PVA in the final ink mixture. All of the samples demonstrate very good erasing and no colour reformation over time. Initial colour densities before erasure were *CD* ≈ 0.25 to 0.40. Note: lines are added as a guide to the eye.

8.2.3.2 IJP Inks Containing Blue C4OH Modified With PVA

A similar set of inks was prepared using blue C4OH (50 mg) as the dye and bisphenol F (500 mg) as the developer. A new PVA stock solution in water (3 mg/g) was prepared to increase the concentration of PVA in the inks. From the data shown in Figure 8.14 (colour fade) and Figure 8.15 (colour density after erasing), it is apparent that there was little correlation between PVA concentration and colour change behaviour in these inks. This finding matches the results obtained in section 8.2.3.1 for CVL-containing inks. In this instance, the ink containing 0.1 mg/g PVA (in the final ink mixture), which was the intermediate PVA concentration, had the highest initial colour density. This is in contrast to the inks shown in Figure 8.12, in which the ink with the highest PVA concentration had the highest initial colour density, further demonstrating that the colouring behaviour of IJP inks was not strongly dependent on PVA concentration.

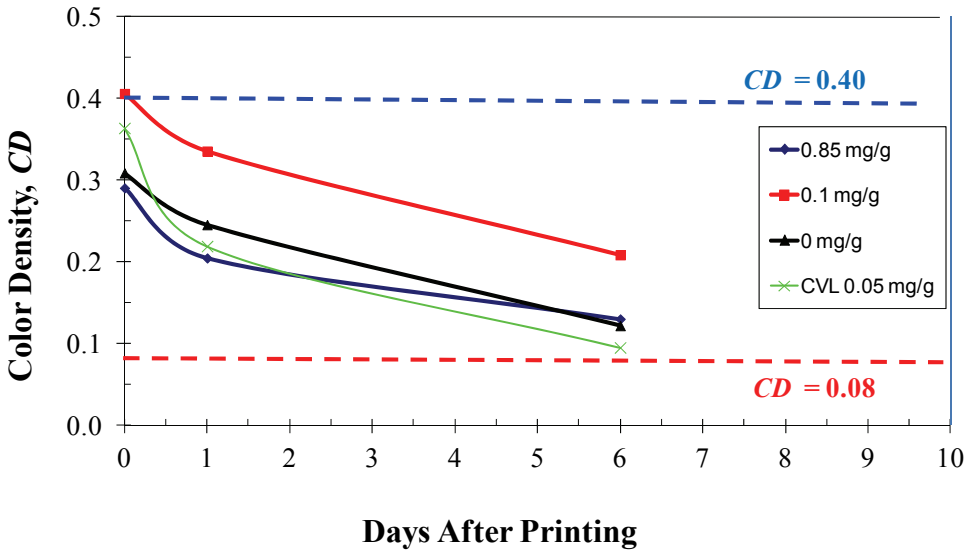

Figure 8.14. Colour density fade as a function of time after printing for blue C4OH inks modified with PVA. The legend indicates the concentration of PVA in the final ink mixture. There appears to be no correlation between PVA loading and colourfastness as all curves behave similarly. A CVL-containing ink, modified with PVA, is shown for comparison. Note: lines are added as a guide to the eye.

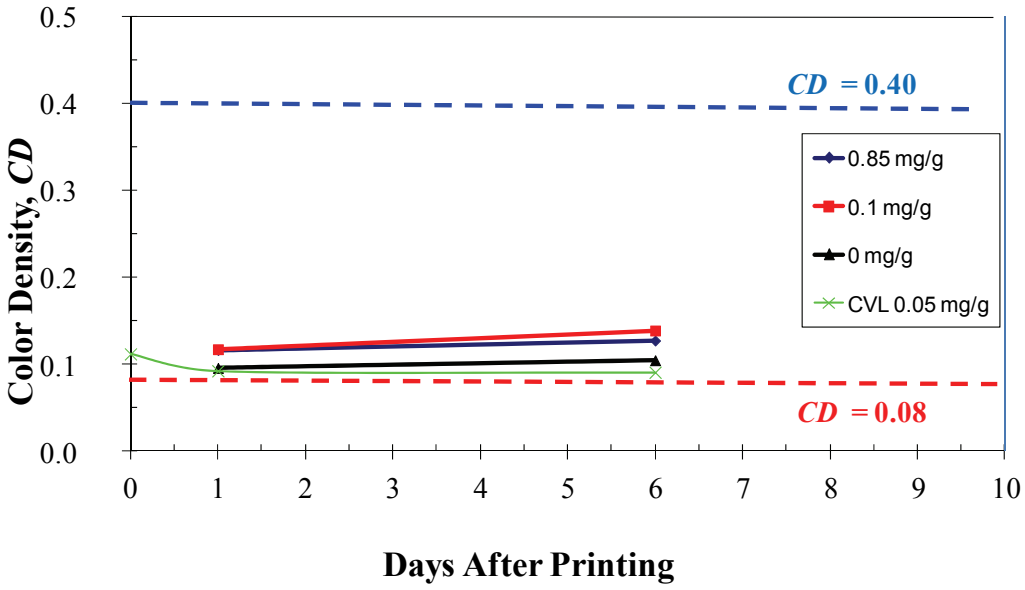

Figure 8.15. Colour density after erasing for blue C4OH inks modified with PVA. The legend indicates the concentration of PVA in the final ink mixture. All of the samples demonstrate good erasing with little colour reformation over time. Initial colour densities before erasure were *CD* ≈ 0.30 to 0.40. A CVL-containing ink, modified with PVA, is shown for comparison. Note: lines are added as a guide to the eye.

It is possible that the concentration of PVA was simply too low to have a detectable effect on the penetrability of IJP inks. High water temperatures (*e.g.*, 80 to 90 °C) and long mixing times (*e.g.*, over 60 minutes) may be required to fully dissolve PVA into water at high PVA concentrations (> 10 mass%),[227] therefore extended studies of the influence of PVA on IJP inks were considered to be too time-consuming for the purposes of the internship.

Nevertheless, the higher PVA concentration stock solution (3 mg/g) was added to the inks discussed in subsequent sections. On visual inspection of inks containing PVA compared with inks lacking PVA, it appeared that sharper printed images were obtained with PVA present in the ink. This was likely due to slightly increased viscosity, which reduced ink penetrability into the page, causing the ink to become less laterally dispersed during printing and, therefore, sharpened the printed image. However, neither the concentration dependence of the colouring behaviour, nor the concentration dependence of the sharpness of the printed image, was studied further.

8.2.4 Best Ink Prepared During the Internship

The best set of inks prepared during the internship contained blue C4OH as the leuco dye (50 mg) and 2,4-dihydroxybenzophenone (DHB, see section 6.1.2.2 and Figure 6.2 for structure) as the developer (500 mg). DHB was not used during earlier studies of IJP inks due to its yellow colour, however when coupled with blue C4OH the initial colour density is very high ($CD \approx 0.4$) and the post-erase shadow was so faint that it was barely visible to the naked eye. The inks containing blue C4OH with DHB also showed good colourfastness, with the final colour density values falling in the range of $CD = 0.2$

to 0.25 up two weeks after printing, as shown in Figure 8.16. The main reason these inks were selected as the best (of those prepared during the internship) is the excellent erasing behaviour demonstrated by these inks, evidenced by the data shown in Figure 8.17.

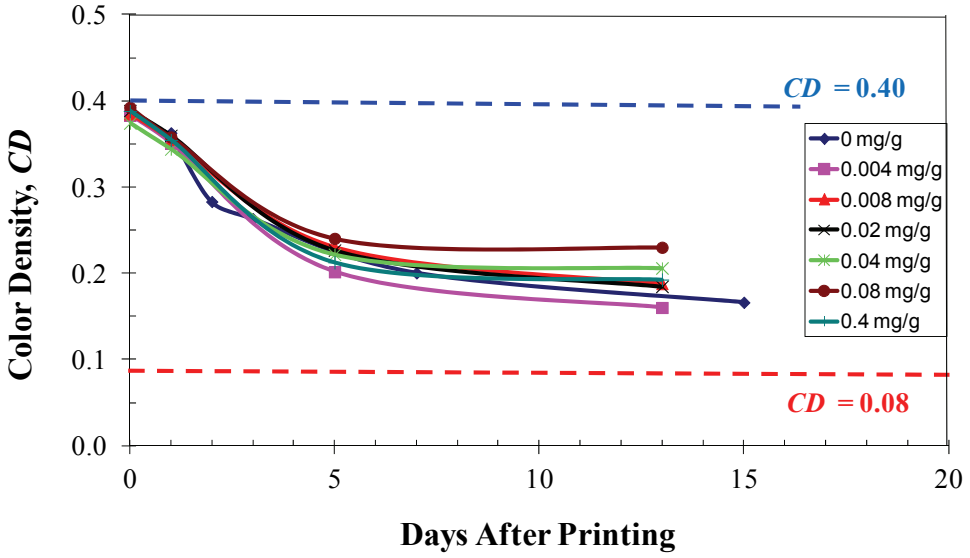

Figure 8.16. Colour density fade as a function of time after printing for blue C4OH/DHB inks modified with PVA. The legend indicates the concentration of PVA in the final ink mixture. Note: lines are added as a guide to the eye.

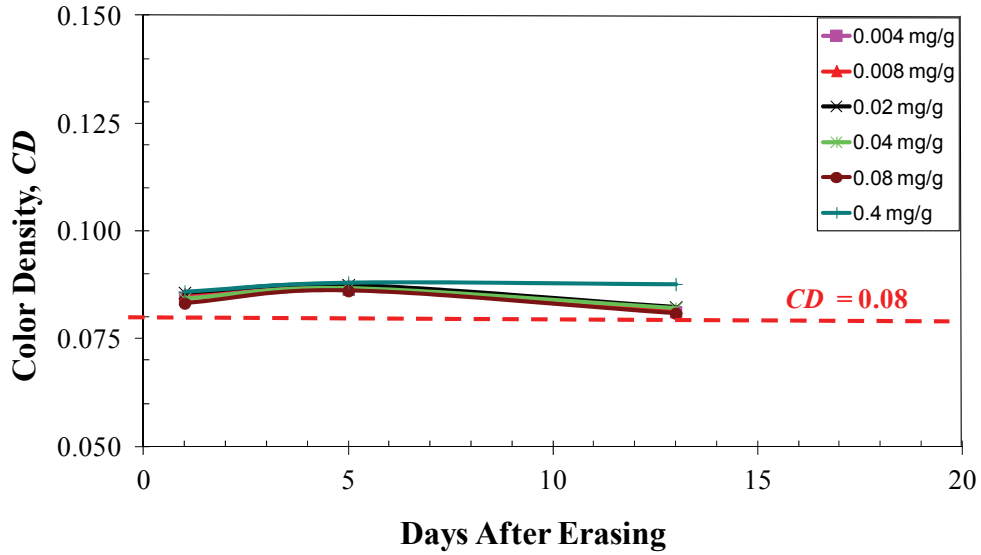

Figure 8.17. Colour density after erasing for blue C4OH/DHB inks modified with PVA. The legend indicates the concentration of PVA in the final ink mixture. All of the samples demonstrate very good erasing and essentially no colour reappearance over time. Initial colour densities before erasure were *CD* ≈ 0.35 to 0.40. Note: lines are added as a guide to the eye.

One additional modification to the ink composition was made during the final stages of the internship: the addition of acetic acid. Addition of acetic acid (1 g of a 1 M aqueous solution to an ink with a total solvent mass of 15 g) resulted in a darkening of the printed image as acetic acid is able to easily convert the leuco form of blue C4OH to the coloured form. The addition of acetic acid does not influence the erasing ability of the ink due to its volatility ; the heat treatment in the oven causes the acetic acid to evaporate (T_{vap} = 118 °C).[221] Initial concerns about paper browning due to the presence of acetic acid were unfounded as the acetic acid did not degrade the paper at this low concentration.[140] The colour fade and erasing properties of the acetic acid-modified blue C4OH/DHB ink are shown in Figure 8.18. Erasing was nearly ideal (*CD* ≈ 0.08*)* with this ink, and the initial (*CD* = 0.4) colour density and the value after a week (*CD* ≈ 0.3) was among the best observed during the internship.

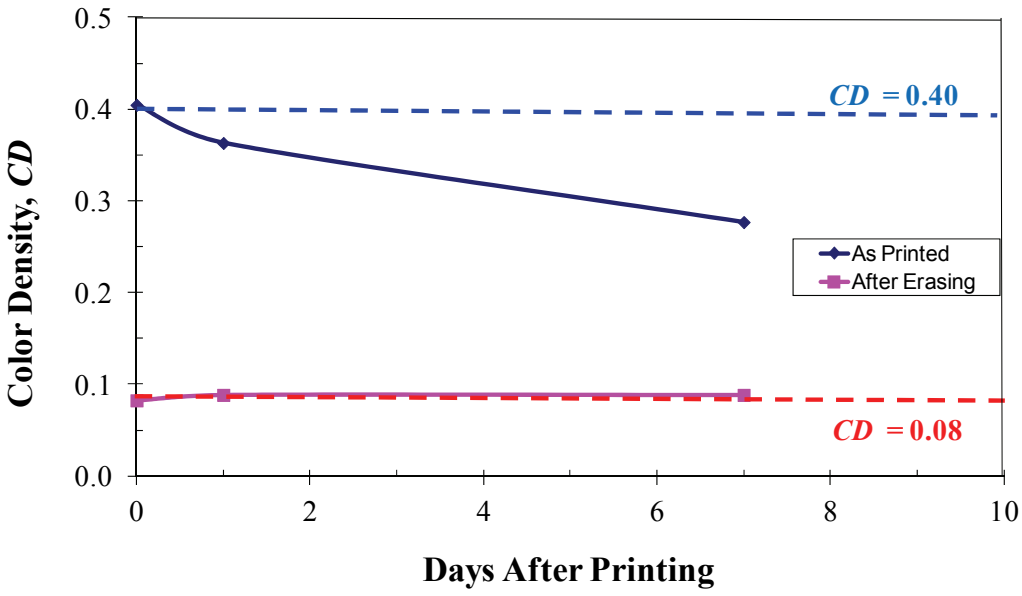

Figure 8.18. The best ink prepared during the internship containing blue C4OH as the dye, DHB as the developer, PVA as a viscosity modifier, and acetic acid as a colour deepener. Note: lines are added as a guide to the eye.

Figure 8.19 shows examples of the printed and erased images obtained *via* printed with the blue C4OH/DHB ink, modified with both acetic acid and PVA. The printed images (Figure 8.19 (a)) were sharp, the initial colour density is very good, and the ink did not penetrate through the entire thickness of the page. The dark colour of the images allows the page to be easily read, even in low light conditions. The increased viscosity of the inks, and concomitant reduction in ink penetrability, allows for double-sided printing.

The erased images (Figure 8.19 (b)) were almost completely invisible to the naked eye (an extremely weak yellow shadow is visible if the page is held very close to the eye) and colour did not reform in these samples over the observation period (two weeks). Although some technical issues associated with colour fade remain, the high quality of printed images and the excellent erasing demonstrated by the blue C4OH/DHB inks indicate that erasable IJP ink technologies might be close to commercialization.

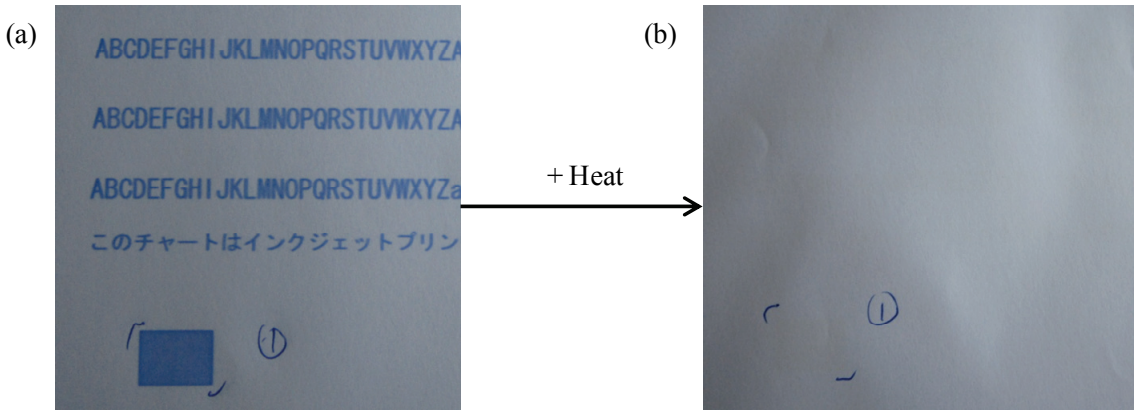

Figure 8.19. (a) Printed image and (b) erased image created with the blue C4OH/DHB ink modified with both PVA and acetic acid. The printed image has good colour density and the text is sharp. The box marked (1) was used as a placeholder, so that when the ink is erased it was possible to record the colour density of the erased image. No residual shadows are observable on the erased image.

8.3 Conclusions Regarding Thermally Erasable Ink-Jet Printer Inks

A number of conclusions about the design and function of erasable IJP inks can be drawn from the results presented in this chapter. First and foremost, the development of erasable ink technologies is very difficult as the optimization of one property (*e.g.,* colourfastness) is often detrimental to another property (*e.g.,* erasing ability).[201,209] In general, inks that were resistant to colour fade over time were also more difficult to erase. Many of the inks tested were not very resistant to colour fade over time, especially inks containing CVL, and were subsequently easily erased.

Attempts to modify the colouring behaviour of IJP inks by modifying the viscosity of the solvent ultimately proved inconclusive. There was little correlation observed between the amount of PVA added to an ink and the initial printed colour density or colour fade rate. This could be the result of PVA concentrations being too low or the PVA not modifying the viscosity of the ink enough to change penetration depths. Although viscosity of the inks was not quantified during the internship (or in this thesis), inks containing a large amount of PVA (*e.g.*, 0.4 mg/g) were generally sharper than images printed with inks that lacked PVA. The increased sharpness of images printed with PVA-containing inks does provide indirect evidence for viscosity modification as higher-viscosity IJP inks, which penetrate less deeply into the sheet, usually produce sharper images.[228]

There are a number of factors at play that can influence the colour fade rate, and although some of these factors can be easily controlled (*e.g.,* exposure to light can cause photobleaching,[25] so samples were stored in the dark), some factors are beyond control

(*e.g.,* humidity in the air can decrease initial colour density). Water is known to play an important role in the colouring and erasing reactions in these systems.[105] Unfortunately, control of atmospheric humidity in the laboratory was very difficult to maintain due to governmental limitations placed on electricity consumption in the wake of the 2011 Tohoku earthquake and tsunami which disrupted the electrical grid throughout Japan.

The blue C4OH/DHB inks modified with PVA and acetic acid showed the best colour properties of the inks studied during the internship, and represented a culmination of the progress in the understanding of the chemical processes that give rise to the colouring behaviour observed in erasable IJP inks. Resistance to colour fade and colour erasing ability were inversely related; inks that were easily erased were less resistant to spontaneous colour fade. Colour deepeners, such as acetic acid, can be used to enhance the initial colour density of inks that were initially weakly coloured, without detrimental impacts on the erasing ability. Low solvent viscosity arising from the use of ethanol and *iso*-propanol, which are much less toxic than more effective halocarbon solvents, caused poor image sharpness and extensive page-wetting. These two detrimental effects can be overcome by modification of the viscosity of the solvent with polymeric materials such as PVA. The identification of technical issues, and the development of potential solutions, allowed for the engineering for thermally erasable ink-jet printer inks that demonstrated high initial colour density, good resistance to colour fade, sharp image formation on printing, and excellent erasing ability.

Chapter 9 Summary, Conclusions, and Future Work

9.1 Summary of Reversible Thermochromism in Three-Component Mixtures

The influence of the length of the alkyl chains attached to the alkyl gallate developer and the alkyl alcohol solvent on the reversible thermochromic properties of CVL:gallate:alcohol mixtures was examined in the present work. Two colour determination methods, observational spectroscopy and colour photo analysis, were used to study the change in colour density of these mixtures upon transition from the equilibrium solid state to the molten state. Chapter 4 examined the influence of modifying the solvent alkyl chain length, Chapter 5 examined the influence of modifying the developer alkyl chain length, and Chapter 6 explored the influence of other developers and solvents on the thermochromic properties of three-component, reversible thermochromic mixtures. Chapter 8 discussed studies on the properties of thermally erasable ink-jet printer inks. The following sections briefly summarize the most important results obtained in the present work.

9.1.1 Influence of the Solvent Alkyl Chain Length

In Chapter 4, the thermochromic behaviour of CVL:DDG:alcohol mixtures was shown to be dependent on the difference in length of the alkyl chains attached to DDG and the alcohol solvent. When the alkyl chain lengths were well-matched (*e.g.*, two carbon atom difference in CVL:DDG:TD-OH mixtures), melt-darkened thermochromism was observed. Increasing the length of the solvent alkyl chain caused the alkyl chain lengths to become mismatched (*e.g.*, four carbon atom difference in CVL:DDG:HD-OH

mixtures, and six carbon atom difference in CVL:DDG:OD-OH mixtures). This range resulted in melt-lightened thermochromism at low developer and high solvent concentrations for HD-OH and OD-OH mixtures. In the same systems, melt-darkened thermochromism could be obtained by increasing the developer concentration and decreasing the solvent concentration.

CVL:DDG:TD-OH mixtures were shown to display melt-darkened thermochromism over a wide compositional range (*e.g.*, $2 < y < 10$ and $25 < z < 100$). The solid state usually was colourless since DDG and TD-OH undergo strong attractive interactions,[101] which sequester the developer from the dye and prevent colour formation in the solid state. Coloured molten phases were obtained when the concentration of the developer was sufficiently large to generate the coloured form of CVL. A graphical summary of the observed behaviour of CVL:DDG:TD-OH mixtures at high solvent concentrations (*e.g.*, $z \geq 80$) is shown in Figure 9.1.

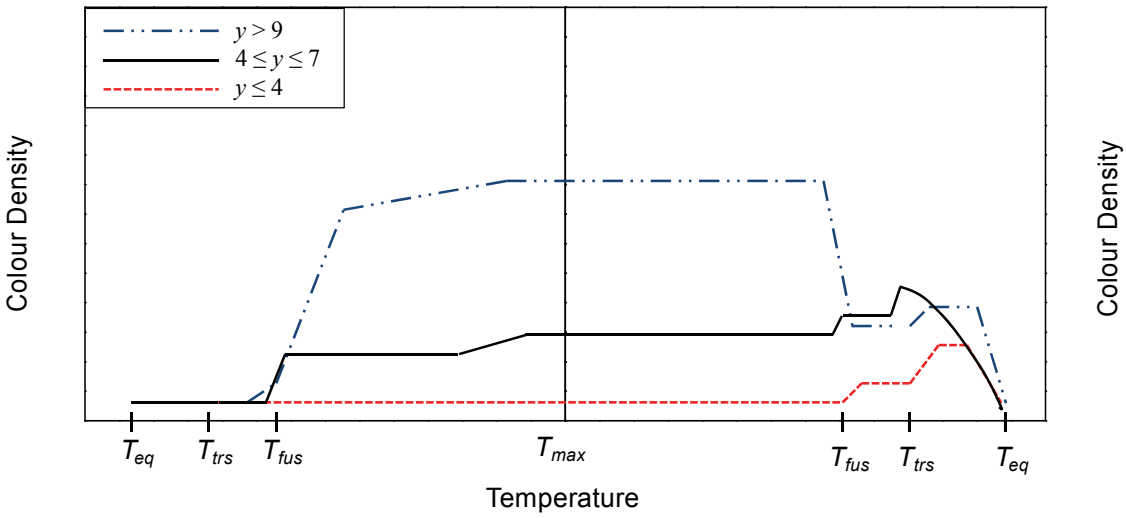

Figure 9.1. A stylized summary of the observed thermochromic behaviour of CVL:DDG:TD-OH mixtures at high solvent concentrations (*e.g.*, when $z \geq 80$). The equilibrium solid state was always colourless, and melt-darkened thermochromism could generate a coloured melt at high developer concentrations (*e.g.*, $y > 9$).

The CVL:DDG:HD-OH and CVL:DDG:OD-OH systems demonstrated both melt-lightened and melt-darkened thermochromism, depending largely on the concentration of the developer and solvent. Between these two regions, some samples did not display any colour change on melting and were considered non-thermochromic. The general features of thermochromic behaviour for CVL:DDG:HD-OH and CVL:DDG:OD-OH mixtures, for high solvent concentrations (*e.g.*, z = 80 to 100), are shown in Figure 9.2. Melt-darkened thermochromism was observed at high developer concentrations (*e.g.*, $y \approx 6$ to 10), melt-lightened thermochromism was observed at low developer concentrations (*e.g.*, $y \approx 0.5$ to 4), and non-thermochromic behaviour was obtained at intermediate developer concentrations (*e.g.*, $y \approx 4$ to 6).

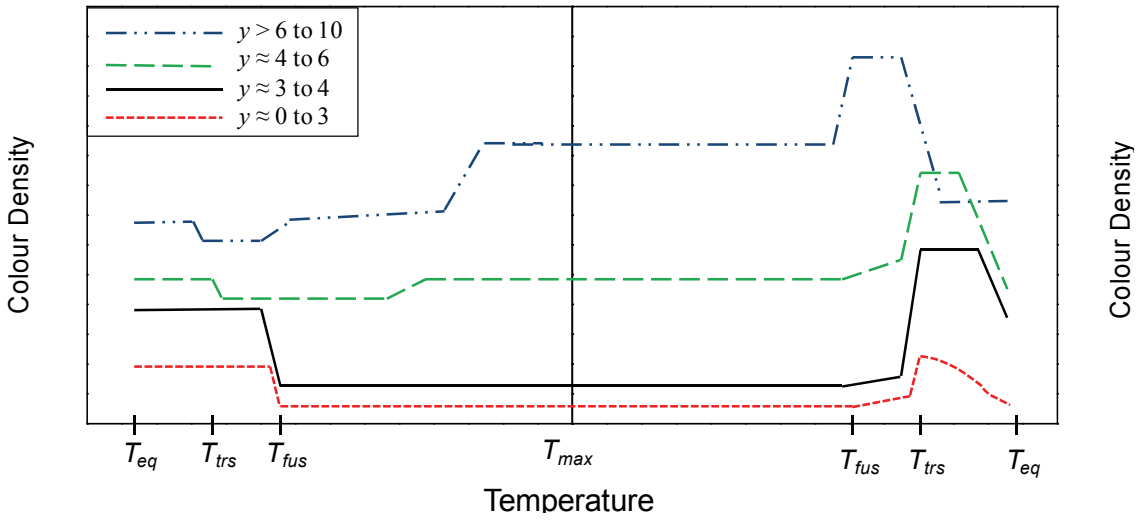

Figure 9.2. A stylized summary of the thermochromic behaviour of CVL:DDG:HD-OH and CVL:DDG:OD-OH mixtures at high solvent concentrations (*e.g.*, when $z \approx 80$ to 100). The equilibrium solid state usually was coloured, with melt-darkened thermochromism occurring at high developer concentrations (*e.g.*, $y \approx 6$ to 10), and melt-lightened thermochromism occurring at low developer concentrations (*e.g.*, $y \approx 0.5$ to 4).

9.1.2 Influence of the Developer Alkyl Chain Length

Chapter 5 explored the influence of changing the alkyl chain length of the gallate developer on the thermochromic properties of three-component systems. CVL:ODG:alcohol mixtures demonstrated melt-darkened thermochromism in the compositional ranges examined in this work. Due to the similarity in alkyl chain length for ODG:OD-OH (zero carbon atom difference) and ODG:HD-OH (two carbon atom difference) mixtures, melt-lightened thermochromism was expected, but melt-darkening was observed. The behaviour of the CVL:ODG:TD-OH system was somewhat surprising given that the difference in alkyl chain length was the same as the CVL:DDG:HD-OH system (which demonstrated melt-lightened thermochromism at most compositions). The longer alkyl chain of the ODG, therefore, stabilized the developer:solvent complex in the solid state of CVL:ODG:TD-OH mixtures more than in CVL:DDG:HD-OH mixtures. Figure 9.3 summarizes the thermochromic behaviour of CVL:ODG:alcohol mixtures at the low solvent concentrations (*e.g.*, $z \approx 25$), for which the best colour contrast was observed.

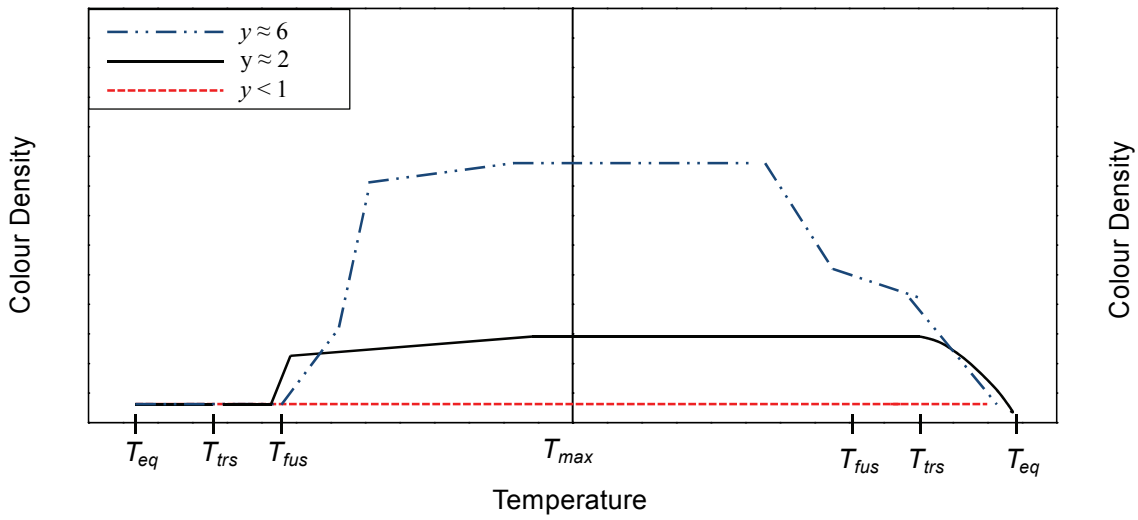

Figure 9.3. A stylized summary of the observed thermochromic behaviour of CVL:ODG:solvent mixtures at low solvent concentrations (*e.g.*, when $z \approx 25$). The equilibrium solid state was always colourless, and melt-darkened thermochromism generated high melt colour density at high developer loading (*e.g.*, $y \approx 6$).

Mixtures containing octyl gallate (OG) and propyl gallate (PG) as the developer demonstrated melt-lightened thermochromism over a much wider compositional range than the CVL:DDG:HD-OH and CVL:DDG:OD-OH mixtures. The large degree of alkyl chain length mismatch in octyl gallate (six to 10 carbon atoms) and propyl gallate (11 to 15 carbon atoms) caused the attractive interactions between the developer and solvent in the solid state to be substantially weakened. This resulted in the formation of deeply coloured equilibrium solid states at virtually all compositions studied in this work. It was therefore difficult to obtain melt-darkened thermochromism, whereas complete decolouration of the melt was obtained when the solvent concentration was sufficiently large (*e.g.*, $z \approx 100$). PG- and OG-containing mixtures demonstrated some of the best colour contrast observed in this work due to the formation of strongly coloured solid states and fully decoloured melts. Figure 9.4 summarizes the observed thermochromic

behaviour for PG- and OG-containing mixtures at high solvent concentrations (*e.g.*, $z \approx$ 85 to 100).

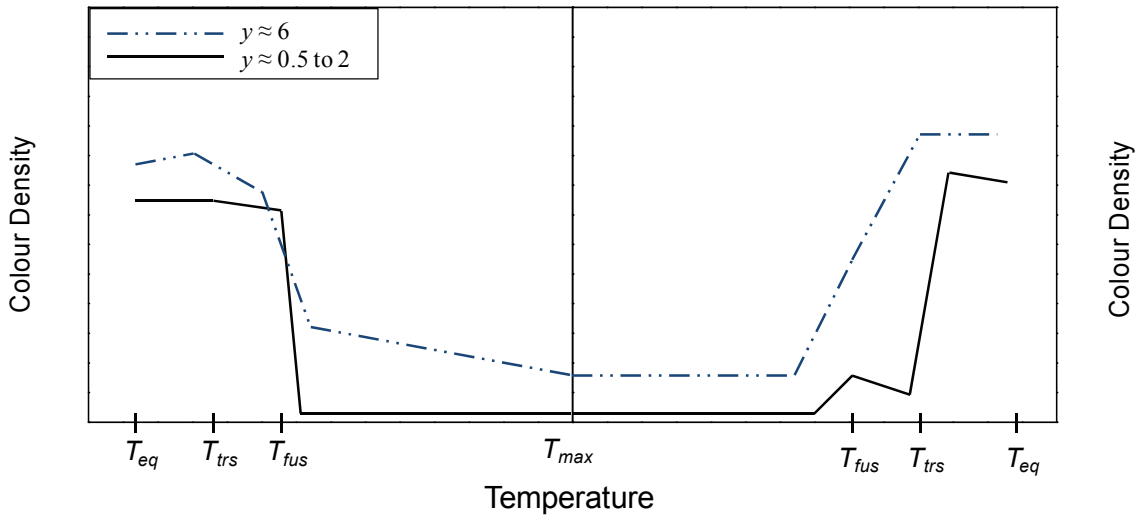

Figure 9.4. A stylized summary of the thermochromic behaviour of CVL:PG:alcohol and CVL:OG:alcohol mixtures at high solvent concentrations (*e.g.*, when $z \approx$ 85 to 100). The equilibrium solid state always was coloured, with melt-lightened thermochromism occurring at virtually all developer concentrations (*e.g.*, $y \approx$ 0.5 to 6), and complete decolourization of the melt occurring when $y \leq 2$.

Mixtures containing gallic acid (GA) provided an interesting example of some of the technical difficulties associated with poorly soluble developer components. Prior to solvent melting in the TD-OH system, no colour was observed. Solvent melting generated colour, which was maintained on cooling. In the HD-OH system, the colour density was high in both the equilibrium solid and molten phases, yielding effectively no colour change. In the OD-OH system, the colour density in the equilibrium solid and in the high temperature melt was low, whereas strong colouration formed just above the melting point of OD-OH. All of the gallic acid mixtures examined were plagued by low reproducibility of the colouring behaviour and high melt opacity.

9.1.3 Other Developer and Solvent Components

Bisphenol A (BPA) and 2,4-dihydroxybenzophenone (DHB) were used as developers and showed that a low degree of structural similarity between the developer and solvent is sufficient to generate mixtures demonstrating high contrast, melt-lightened thermochromism. In BPA and DHB mixtures, the equilibrium solid state was coloured at all compositions studied, with low solvent concentration samples (*e.g.*, $z \leq 100$) demonstrating high equilibrium colour density. DSC experiments showed that both BPA and DHB experience a weak attractive interaction with HD-OH, which was insufficiently strong to generate compound formation, as had been observed in the DDG:TD-OH system. Consequently, the solvent was not able to sequester the developer from the dye in BPA and DHB three-component mixtures, and strong colouration of the equilibrium solid was observed at all compositions. Figure 9.5 summarizes the observed thermochromic behaviour for BPA and DHB-containing mixtures at low solvent concentrations (*e.g.*, $z \leq 100$).

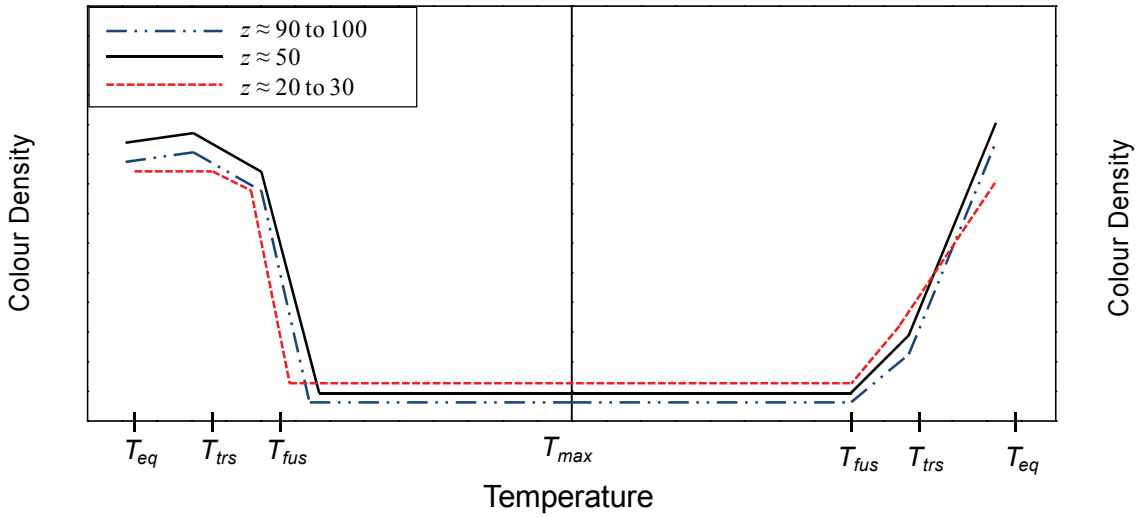

Figure 9.5. A stylized summary of the thermochromic behaviour of CVL:BPA:HD-OH and CVL:DHB:HD-OH mixtures at low solvent concentrations (*e.g.*, when $z \leq 100$). The equilibrium solid state always was coloured, with melt-lightened thermochromism occurring at all compositions.

At low solvent concentrations (*e.g.*, $z = 25$ to 60), CVL and/or BPA (or DHB) did not become fully dissolved in the molten solvent. Solid CVL was observed at very low solvent concentrations (*e.g.*, $z < 30$) and solid BPA (or DHB) was observed at intermediate solvent concentrations (*e.g.*, when $z \approx 45$ to 60). To reduce the opacity of the melt, the solvent concentration was vastly increased (*e.g.*, $z = 110$ to 2600). Although the opacity of the melt was reduced, the colour density of the solid state also was reduced, generating mixtures with lower colour contrast than the $z \leq 100$ mixtures. Figure 9.6 summarized how the colour density of the solid state varied with solvent and developer concentrations at high solvent concentrations (*e.g,*. $z = 110$ to 2600) for BPA and DHB mixtures.

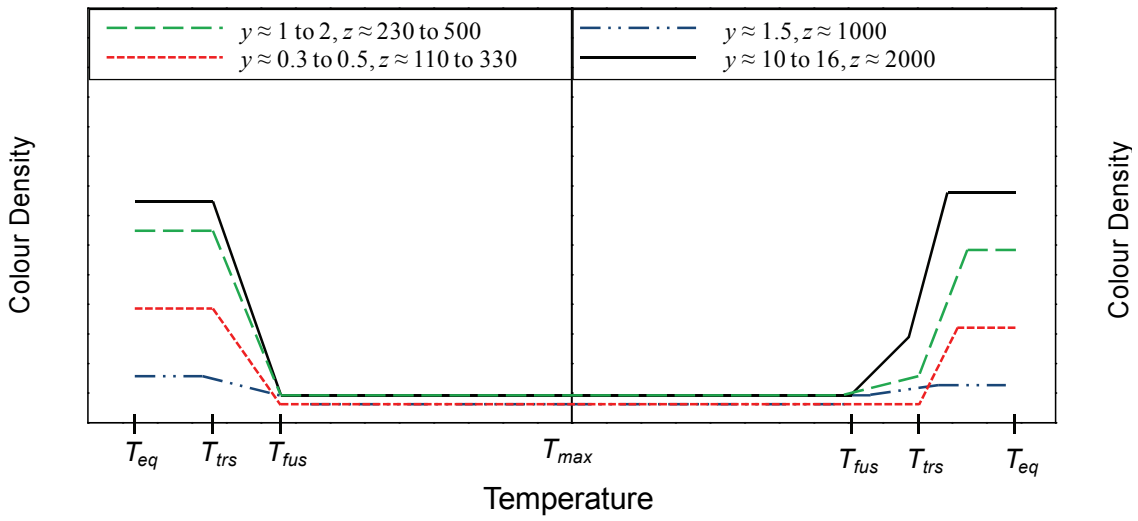

Figure 9.6. A stylized summary of the thermochromic behaviour of CVL:BPA:HD-OH and CVL:DHB:HD-OH mixtures at high solvent concentrations (*e.g.*, when $z > 100$). High solid-state colour densities were obtained at high developer ($y = 10$ to 16) and low solvent ($z \leq 500$) concentrations. Low solid state colour density was observed at very low developer (*e.g.* $y = 0.3$ to 0.5) and high solvent (*e.g.*, $z \approx 1000$) concentrations.

Finally, octadecanethiol (OD-SH) was used as a solvent component in three-component mixtures to examine the influence of the solvent end-group. CVL:DDG:OD-SH mixtures demonstrated melt-darkened thermochromic behaviour over a wide range of compositions (*e.g.*, where $z < 100$). Very high dilution of the colouring components (*e.g.*, $z \geq 500$) was required to obtain melt-lightened thermochromic behaviour. DSC analysis showed that DDG and OO-SH do not experience any attractive interactions in binary mixtures, therefore the developer was not sequestered by the solvent in the solid state in ternary mixtures, and consequently the equilibrium solid state was strongly coloured at virtually all compositions. Very high solvent concentrations (*e.g.*, $z > 900$) were required to cause consistent decolourization of the melt, allowing for melt-lightened thermochromism to occur. Figure 9.7 summarizes the change in thermochromic behaviour for CVL:DDG:OD-SH mixtures, $y \approx 5$ to 6 and $500 \leq z \leq 2000$, with melt-

lightened behaviour observed at high solvent loading, and melt-darkened behaviour observed at low solvent loading.

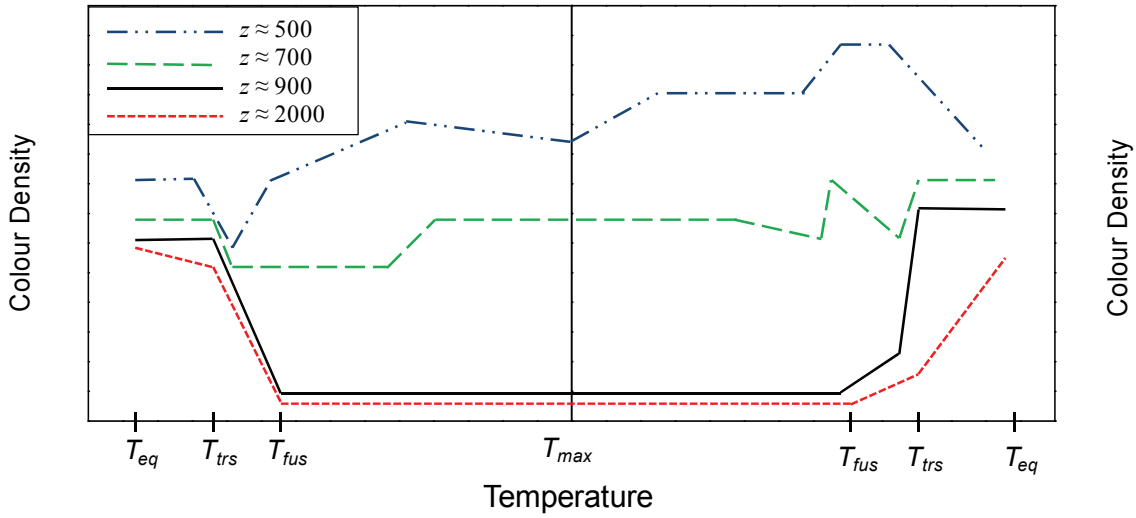

Figure 9.7. A stylized summary of the thermochromic behaviour of CVL:DDG:OD-SH mixtures at high developer loading ($y \approx 5$ to 6). Melt-darkened thermochromism was obtained at low solvent concentrations ($z \leq 500$). Melt-lightened thermochromism was obtained at high solvent concentrations ($900 \leq z \leq 2000$). Between these two regimes, $z \approx 700$, non-thermochromic behaviour was observed.

9.1.4 Influence of the Solvent Rotator Phase

The rotator phase of the solvent was shown to play a role the decolourization of coloured equilibrium solids as the solvent was heated from the low temperature ordered phase (LO-phase) to the rotator phase (R-phase). In mixtures that displayed melt-lightened thermochromism from a coloured solid state, the heightened degree of orientational disorder of the solvent R-phase allowed for heightened molecular mobility of the developer and/or dye in the solid state. This allowed the developer to dissociate away from the dye, similar to the mode of decolourization in the melt where the dye and

developer dissociate away from one another, causing the solid mixture to become decoloured when the solvent transitioned into the R-phase.

Another feature associated with the solvent R-phase was the anomalous increase in colour density in the solid state near the low end of the LO-to-R phase transition temperature range for the pure solvent. This feature was most pronounced in the CVL:DDG:HD-OH system. As the solvent transitioned into the R-phase, slight decolouration of the coloured equilibrium solid occurred. Upon removing the sample from the water bath, the solvent transitioned back into the LO-phase due to sample cooling near the exterior of the sample vial. Conversion to the LO-phase was noted, for most samples, to generate strong colouration in the solid state due to the formation of a metastable solid; this was akin to the thermal quenching technique employed by MacLaren, Tang, and White to generate thermochromism in previous studies.[101,102] Further heating returned the R-phase of the solvent with concomitant colour loss.

On cooling, the R-phase of the solvent was formed immediately on solvent solidification and generally did not substantially impact the colour density of the mixture. Melt-lightened mixtures usually maintained low colour density on transition from the melt to the R-phase of the solvent, with large increases in colour density occurring on transition into the LO-phase of the solvent.

9.1.5 Melt-Lightened vs. Melt-Darkened Thermochromism and Maximum Colour Contrast

The colour contrast between the equilibrium solid state and the melt is one of the most important physical properties of a thermochromic material. To obtain high colour contrast, either the melt or the equilibrium solid state should be fully decoloured. For melt-darkened mixtures, decolouration of the solid state was reliant on strong attractive interactions between the developer and solvent components. This was possible when the solvent and developer alkyl chain lengths were well-matched (*e.g.*, for DDG:TD-OH and ODG-containing mixtures). Conversely, melt-lightened mixtures required decolourization of the melt to allow for high colour contrast. Melt decolourization was obtained by increasing the solvent concentration (*e.g.*, $z \geq 100$), which resulted in destruction of the coloured dye:developer complex by dissociation of the colouring components initiated by dissolution into the molten solvent.

Maximum colour contrast values obtained for each ternary system examined in the present work are listed below. The results obtained *via* colour photo analysis are presented separately from those obtained *via* observational spectroscopy. Additionally, melt-darkened mixtures and melt-lightened mixtures are presented separately for ease in comparing the colour contrast values.

Table 9.1 lists the colour contrast values and equilibrium and melt colour densities for melt-darkened samples analyzed *via* colour photo analysis. The CVL:ODG:TD-OH mixture demonstrated the highest colour contrast ($\Delta CD_{max} = 1.1$), while the other systems demonstrated moderate colour contrast values ($\Delta CD_{max} = 0.7$ to 0.8). The excellent colour contrast and decoloured solid state observed for the

CVL:ODG:TD-OH system is a promising result when considering applications in thermochromic materials.

Table 9.1 Colour contrast values and equilibrium solid and melt colour densities obtained *via* colour photo analysis for melt-darkened thermochromic mixtures. The samples listed demonstrated the highest colour contrast observed here for each ternary system.

Components	Composition	CD_{Equil}	CD_{Melt}	ΔCD_{max}
CVL:DDG:TD-OH	[1:9:90]	0.1	0.8	0.7
CVL:ODG:TD-OH	[1:6.4:26.7]	0.1	1.2	1.1
CVL:ODG:HD-OH	[1:6.1:25.8]	0.2	1.0	0.8
CVL:ODG:OD-OH	[1:5.9:25.2]	0.1	0.9	0.8

Table 9.2 lists the colour contrast values and equilibrium and melt colour densities for melt-darkened samples analyzed *via* observational spectroscopy. The highest colour contrast for these samples ($\Delta CD_{max} = 1.8$) was for the CVL:DDG:TD-OH, which is unsurprising given that only this system contained well-matched alkyl chain lengths. The solid states of CVL:DDG:HD-OH and CVL:DDG:OD-OH were coloured as a result of the weakened interaction of DDG with the solvent component. Although the colour density of the melt of the CVL:DDG:HD-OH sample was very high ($CD_{Melt} = 1.5$), the increased solid-state colouration ($CD_{Equil} = 0.4$) was detrimental to the overall thermochromic effect (since one state should be fully decoloured). CVL:DDG:HD-OH and CVL:DDG:OD-OH are more suitable melt-darkened mixtures since the solid state was coloured at virtually all compositions.

Table 9.2 Colour contrast values and equilibrium solid and melt colour densities obtained *via* observational spectroscopy for melt-lightened thermochromic mixtures. The samples listed demonstrated the highest colour contrast observed here for each ternary system.

Components	Composition	CD_{Equil}	CD_{Melt}	ΔCD_{max}
CVL:DDG:TD-OH	[1:10:60]	0.0	1.8	1.8
CVL:DDG:HD-OH	[1:10:60]	0.4	1.5	1.1
CVL:DDG:OD-OH	[1:10:90]	1.0	1.7	0.7

Table 9.3 lists the colour contrast values and equilibrium and melt colour densities for melt-lightened samples analyzed *via* colour photo analysis. The colour density of the solid state as observed to increase upon changing the developer from octyl gallate to propyl gallate. Propyl gallate mixtures experienced weaker developer:solvent interactions in the solid state, allowing for more intense colouration. A consequence of this was the retention of colour into the melt due to the reduced solubility of the developer, as evidenced by the melt colour density of the CVL:PG:HD-OH sample (CD_{Melt} = 0.2 for [1:6.2:99.0]). Decreased developer concentrations were required to fully decolour the melt in PG-containing mixtures.

Table 9.3 Colour contrast values and equilibrium solid and melt colour densities obtained *via* colour photo analysis for melt-lightened thermochromic mixtures. The samples listed demonstrated the highest colour contrast observed here for each ternary system. Note: the CVL:DDG:HD-OH mixture was measured without the use of a white reference material for brightness normalization and, therefore, the colour densities are artificially high.

Components	Composition	CD_{Equil}	CD_{Melt}	ΔCD_{max}
CVL:DDG:HD-OH	[1:5:94]	1.1	0.1	1.0
CVL:OG:TD-OH	[1:6.2:103.2]	0.8	0.0	0.8
CVL:OG:HD-OH	[1:6.2:102.9]	0.6	0.0	0.6
CVL:OG:OD-OH	[1:5.2:86.5]	0.8	0.0	0.8
CVL:PG:TD-OH	[1:2.1:99.6]	0.9	0.0	0.9
CVL:PG:HD-OH	[1:6.2:99.0]	1.2	0.2	1.0
CVL:PG:OD-OH	[1:2.5:102.7]	1.0	0.0	1.0

Table 9.4 lists the colour contrast values and equilibrium and melt colour densities for melt-lightened samples containing BPA and DHB. These mixtures demonstrated the highest colour contrast observed in this work as a result of the intense colouration of the solid state and complete decolouration of the melt. Weak solid-state interaction between BPA/DHB and HD-OH was responsible for the high colour density in the equilibrium solid state.

Table 9.4 Colour contrast values and equilibrium solid and melt colour densities obtained *via* colour photo analysis for melt-lightened mixtures containing BPA and DHB. A sample from the low solvent concentration regime (*e.g.* $z \leq 100$) and high solvent concentration regime (*e.g.* $z \geq 150$) is listed for both systems.

Components	Composition	CD_{Equil}	CD_{Melt}	ΔCD_{max}
CVL:BPA:HD-OH	[1:8:91]	1.4	0.0	1.4
CVL:BPA:HD-OH	[1:10:1990]	1.2	0.0	1.2
CVL:DHB:HD-OH	[1:8:91]	1.5	0.0	1.5
CVL:DHB:HD-OH	[1:16:1685]	0.6	0.0	0.6

Table 9.5 lists the colour contrast values and equilibrium and melt colour densities for melt-lightened samples analyzed *via* observational spectroscopy. The colour contrast values observed for these samples were substantially lower than those of PG-containing mixtures due to enhanced interaction between DDG and the long chain alcohols in the solid state, and the need for very high dilution of the OD-SH samples due to the lack of interaction of DDG and OD-SH in the solid state. OD-SH mixtures were often strongly coloured in both the equilibrium solid and the melt, and therefore good colour contrast was difficult to obtain in this system.

Table 9.5 Colour contrast values and equilibrium solid and melt colour densities obtained *via* colour photo analysis for melt-lightened thermochromic mixtures. The samples listed demonstrated the highest colour contrast observed here for each ternary system.

Components	Composition	CD_{Equil}	CD_{Melt}	ΔCD_{max}
CVL:DDG:HD-OH	[1:1:23]	0.3	0.0	0.3
CVL:DDG:OD-OH	[1:5:90]	0.8	0.1	0.7
CVL:DDG:OD-SH	[1:8:1910]	0.8	0.1	0.7

9.2 General Conclusions Concerning Reversible Thermochromic Behaviour in Three-Component Mixtures

Three-component mixtures containing CVL as the dye, alkyl gallates as the developer, and alkyl alcohols as the solvent can undergo both melt-lightened and melt-darkened thermochromism. When the alkyl chains attached to the developer and solvent, are well matched in terms of length, melt-darkened behaviour is exclusively observed. When the alkyl chain lengths are poorly matched, both melt-lightened and melt-darkened behaviour can be observed, with melt-lightened behaviour generally demonstrating higher colour contrast due to the formation of a decoloured molten phase.

When the alkyl chain lengths are well-matched (*e.g.*, CVL:DDG:TD-OH, CVL:ODG:solvent), the solid state of the mixture is decoloured. This results from the formation of a strong developer:solvent complex in the solid state (compound formation was previously observed in DDG:alcohol mixtures),[101,102,110] which prevents the developer from interacting with the dye in the solid state. Melting of the solvent liberates the developer from the developer:solvent complex and both the dye and developer can dissolve in the molten solvent. If the developer concentration is too low, no colour forms in the melt. Therefore, high developer concentrations are required to develop the colour of melt-darkened mixtures.

When the alkyl chain lengths are poorly matched (*e.g.*, PG- and OG-containing mixtures), the solid-state developer:solvent interaction is weak, and the developer is not sequestered by the solvent. This situation allows the developer to interact with the dye to generate the coloured form of the dye. In general, mixtures with poorly matched alkyl chains always show strongly coloured solid states, even at low developer concentrations. To obtain good colour contrast in these mixtures, a fully decoloured melt is required. Since the developer:solvent interaction is weak, the developer tends to show low solubility in the melt, which not only causes colour retention after melting but also high melt opacity. To counteract this effect, high solvent concentrations are required to fully dissolve the developer.

In mixtures containing BPA and DHB, very weak interactions between the developer and solvent components resulted in the observation of intensely coloured solid states, coupled with fully decoloured melts. Such mixtures demonstrated the best colour contrast observed in this work (ΔCD_{Max} = 1.4 to 1.5) due to the extremely high colour

density of the solid state and complete decolourization of the melt. DSC analysis demonstrated that weak solid-state interactions between the developer and solvent precluded the formation of strong developer:solvent complexes, allowing the developer to generate the coloured form of the dye in the equilibrium solid state.

Finally, the rotator phase of the solvent was shown to play a role in the colouring behaviour of the solid state in three-component thermochromic mixtures, particularly on heating. The heightened degree of orientational disorder in the R-phase, compared with the LO-phase of the solvent promotes the dissociation of coloured dye:developer complex prior to solvent melting. This effect was most significant in mixtures demonstrating melt-lightened thermochromism (*e.g.*, PG-containing mixtures and BPA /DHB with HD-OH).

9.3 Conclusions Regarding Thermally Erasable Ink-Jet Printer Inks

A number of conclusions about the design and function of erasable IJP inks can be drawn from the results presented in Chapter 8. The development of erasable ink technologies is very difficult as the optimization of one property (*e.g.,* colourfastness) is often detrimental to another property (*e.g.,* erasing ability).[201,209] In general, inks that were easy to thermally erase were also poorly resistant to colour fade. CVL-containing inks were particularly prone to colour fade; on the other hand, they were easily erased.

Attempts to modify the colouring behaviour of IJP inks by modifying the viscosity of the solvent ultimately proved inconclusive. No correlation between the concentration of PVA and the initial printed colour density or colour fade rate was

observed. Nevertheless, the increased sharpness of images printed with PVA-containing inks does provide indirect evidence for viscosity modification as higher viscosity IJP inks usually produce sharper images.[228]

The blue C4OH/DHB inks modified with PVA and acetic acid showed the best colour properties measured during the internship, and represented a culmination of the progress towards understanding the chemical processes that gave rise to the colouring behaviour observed in erasable IJP inks. The identification of technical issues, and the development of potential solutions, allowed for the engineering for thermally erasable ink-jet printer inks that demonstrated high initial colour density, good resistance to colour fade, sharp image formation on printing, and excellent erasing ability.

9.4 Future Work

The present research has been useful in developing a more complete picture of the mechanisms for colour generation in reversibly thermochromic, three-component systems. Nevertheless, questions remain about some of the fundamental aspects of colour generation in multi-component mixtures. The following sections detail some suggestions of potentially useful future directions for thermochromism research.

9.4.1 Compilation of Thermochromic Phase Diagrams Using Combinatorial Methods

The determination of thermochromic phase diagrams allowed for the identification of compositional regions of interest by mapping a few data points (*i.e.*, sample compositions) over a wide compositional range. The methods of analysis employed in this work, while more rapid and time-efficient than those used in previous studies, were still very time- and labour-intensive. With the development of highly automated combinatorial sample preparation methods, it should be possible to more quickly map out the thermochromic phase diagrams for similar systems in the near future.

An attempt at using a solution-based, nanolitre dispensing robot to generate large libraries of combinatorially produced samples (akin to ink-jet printing) was considered during the early stages of the present research, however, the minute sample size proved problematic for obtaining reproducible, thermochromic behaviour. Moving forward, automated mixing of large sample masses could provide a more rapid method of sample preparation, and across a much wider compositional range, which could aid in the rapid identification of compositions of interest.

9.4.2 Structural Analysis Using X-Rays

Another interesting avenue for research is the application of small angle scattering (SAXS) experiments to the study of the structure of the dye:developer and developer:solvent complexes. The general principle behind small-angle scattering is that the scattering angle of an X-ray beam (or light and neutron beams) due to elastic collisions of the X-rays with particles in a sample is proportional to the inverse of the

particle size. For very small particles (*e.g.*, atoms and molecules) scattered beams would be collected at fairly large angles (10 to 90 °) due to small interatomic distances, bond lengths, and crystallographic lattice parameters (1 to 10 Å).

X-rays scattered from larger particles (~10 to 100 nm) will have scattering at much lower angles (~0.1° to 10°) and need a specialized instrument for their detection. For this reason, SAXS instruments were developed to study macromolecular complexes and other large scale physical objects. Two predicted structures for the metastable coloured state, shown in Figure 2.10, suggest the formation of macromolecular complexes on appropriate size scales for study with SAXS. It is possible that by studying the system using SAXS, aggregates of different size scales might be observed. This would undoubtedly provide further understanding of the underlying mechanisms controlling colour formation and erasure in three-component thermochromic mixtures. As with other techniques, some experimental hurdles will likely arise from the need for controlled heating and cooling during colour formation and erasure; both of these issues can be overcome with clever cell design.

X-Ray diffraction studies as a function of temperature could also be carried out to determine the exact temperature of the phase transition from the LO-phase to the R-phase as the two crystalline phases have different diffraction patterns. XRD correlated with colour measurements of the mixtures might provide more insights into the role of the R-phase during heating and cooling. The influence of the solvent R-phase in thermochromic mixtures has not been studied in any great detail in the literature.

9.4.3 Thermal Analysis

DSC experiments carried out in the present work, and in previous studies,[110] demonstrated that weak solid-state interactions between the developer and solvent components were integral in the formation of a strongly coloured solid state. Strong solid-state interactions between the developer and solvent have previously been suggested to be responsible for the decolouration of the solid state due to the formation of developer:solvent complexes[101,110]; therefore, analysis of the strength of solid-state interactions between candidate developer and solvent components could be used to predict the thermochromic behaviour of three-component mixtures containing those components.

The impact of the R-phase of the solvent could also be further explored *via* extended DSC analysis. Techniques such as isothermal DSC, which maintains a constant sample temperature while measuring heat flow into the sample, could be used to correlate colour density changes with transition into and out of the R-phase. Other considerations include exploring the impact of super-cooling of alkyl gallates, as observed for DDG and ODG, and the potential impact of alkyl gallate R-phases (observed for HDG, but not DDG).

9.4.4 Extension of Design Rules

The variation in thermochromic behaviour of three-component systems as the developer alkyl chain length was modified, and as the developer and solvent components were changed, provided strong evidence that by controlling the strength of the developer:solvent solid-state interaction, a variety of thermochromic behaviours can be

obtained. With this knowledge, the preparation of high-contrast thermochromic materials can be aided through the predictive use of binary interaction strengths, chemical compatibility of developer and solvent components based on molecular structure, and developer effectiveness based on pK_a values, dielectric constants, and solubility coefficients. The knowledge gained through such studies, combined with previous studies reported in the literature, will undoubtedly aid in the future design of three-component mixtures demonstrating reversible, high colour contrast thermochromism.

References

1. T. B. Harsch, *International Liquid Xtal Co.*, US Patent No. 3785721 A, **1974**.

2. P. R. W. Jones, US Patent No. 3494524 A, **1970**.

3. R. M. Christie, *Chromic Materials for Technical Textile Applications*, Chapter 1 in Issue 138, "Advances in the Dyeing and Finishing of Technical Textiles" of the Woodhead Publishing Series in Textiles, M. L. Gulrajani (Ed.), Woodhead Publishing Ltd.: Cambridge, UK, **2013**.

4. P. Bamfield and M. G. Hutchings, *Chromic Phenomena: Technological Applications of Colour Chemistry*, 2nd Edition, RSC Publishing: Cambridge, UK, **2010**.

5. K. Nassau, *The Physics and Chemistry of Color: The Fifteen Causes of Color*, 2nd Edition, in Wiley Series of Pure and Applied Optics, John Wiley and Sons, Inc.: New York, **2001**.

6. D. N. Batchelder, *Contemporary Physics*, **1988**, 29, 3-31.

7. M. A. White, *Physical Properties of Materials*, 2nd Edition, CRC Press, Taylor & Francis Group: Boca Raton, Fl., USA, **2012**.

8. R. M. Christie, *Colour Chemistry*, RSC Publishing: Cambridge, UK, **2001**.

9. A. Usui and H. Watanabe, *NEC Corporation*, US Patent No. 4680602 A, **1984.**

10. D. M. Chapin, C. S. Fuller, and G. L. Pearson, *Journal of Applied Physics*, **1954**, 25, 676-677.

11. T. H. Lowry and K. H. Richardson, *Mechanism and Theory in Organic Chemistry*, 3rd Edition, Harper Collins: New York, **1987**.

12. A. Samat and V. Lokshin, *Thermochromism of Organic Compounds*, Chapter 10 in "Organic Photochromic and Thermochromic Compounds, Volume 2", J. C. Crano and R. J. Guglielmetti (eds.), Kluwer Academic/Plenum Publishers: New York, USA, **1999**.

13. B. Breiten, I. Biaggio, and F. Diederich, *Chimia*, **2010**, 64, 409-413.

14. E. Kleinpeter, U. Boelke, and J. Kreicberga, *Tetrahedron*, **2010**, 66, 4503-4509.

15. D. A. McQuarrie, *Quantum Chemistry*, University Science Books: Sausalito, **1983**.

16. D. Aitken, S. M. Burkinshaw, J. Griffiths, and A. D. Towns, *Review of Progress in Coloration and Related Topics*, **1996**, 26, 1-8.

17. P. M. S. Monk, R. J. Mortimer, and D. R. Rosseinsky, *Electrochromism and Electrochromic Devices*, Cambridge University Press: Cambridge, UK, **2007**.

18. N. Arakuwa, Y. Fujii, K. Machida, N. Murayama, and T. Sakagami, US Patent No. 4756973 A, **1988**.

19. J. Vitry, *Chimieet Industrie – Genie Chimique*, **1969**, 102, 1333-1349.

20. T. L. Dawson, *Coloration Technology*, **2010**, 126, 177-188.

21. M. Lidén and U. Eriksson, *Journal of Biological Chemistry*, **2006**, 281, 13001–13004.

22. J. Nathans, D. Thomas, and D. S. Hogness, *Science*, **1986**, 232, 193–202.

23. H. Beecken, E.-M. Gottschalk, U. van Gizycki, H. Krämer, D. Maassen, H.-G. Matthies, H. Musso, C. Rathjen, and U. I. Zdhorszky, *Biotechnic & Histochemistry*, **2003**, 78(6), 289-302.

24. M. M. Sidky, *Chemia Stosowana*, **1983**, 3, 165-182.

25. N. S. Allen, N. Hughes, and P. Mahon, *Journal of Photochemistry*, **1987**, 37, 379-390.

26. J. C. Crano, R. J. Guglielmetti (eds.), *Organic Photochromic and Thermochromic Compounds, Volume 2*, Kluwer Academic/Plenum Publishers: New York, USA, **1999**.

27. M. A. Invernale, Y. Ding, and G. A. Sotzing, *Coloration Technology*, **2011**, 127, 167-172.

28. Y. Ding, M. A. Invernale, and G. A. Sotzing, *ACS Applied Materials & Interfaces,* **2010**, 2, 1588-1593.

29. J. H. Day, *Chemical Reviews*, **1963**, 63, 65-80.

30. J. H. Day and A. Joachim, *Journal of Organic Chemistry*, **1965**, 30, 4107-4111.

31. M. A. White and A. Bourque, *Colorant, Thermochromic*, in "Encyclopedia of Color Science and Technology", R. Luo (ed.), Springer: New York, USA, **2013**.

32. C. B. Greenberg, "*Chromogenic Materials (Thermochromism)*" in Kirk-Othmer Encyclopedia of Chemical Technology, 4th Ed., Vol. 6, John-Wiley & Sons; New York, **1993**.

33. H. H. Baum, NCR Corporation, US Patent No. 4151748, **1979**.

34. B. K. Green and L. Schieicher, U.S. Patent No. 2800457, **1957**.

35. B. K. Green, U.S. Patent No. 2800458, **1957**.

36. M. A. White, *Journal of Chemical Education*, **1998**, 75, 1119-1120.

37. M. Bide, *ChemMatters*, **1992**, October, 8-11.

38. M. A. White and M. Leblanc, *Journal of Chemical Education*, **1999**, 76, 1201-1205.

39. D. J. Campbell, W. B. Bosma, S. J. Bannon, M. M. Gunter, and M. K. Hammar, *Journal of Chemical Education*, **2012**, 89, 526-528.

40. T. Kito, N. Nakasuji, T. Kataoka, H. Inagaki, and Y. Shibahashi, *Pilot Ink Co., Ltd.*, US Patent No. 4720301, **1988**.

41. S. Takayama, M. Shigeru, and K. Sano, *Kabushiki Kaisha Toshiba*, European Patent No. EP 0932084 A1, **1999**.

42. K. Sano, S. Takayama, S. Fujioka, T. Okuyama, and S. Machida, *Kabushiki Kaisha Toshiba*, US Patent No. 6017386, **2000**.

43. M. Tanaka, H. Hayashi, S. Matsonoto, S. Kashino, and K. Mogi, *Bulletin of the Chemical Society of Japan*, **1997**, 70, 329-337.

44. J. H. Sun, K. C. Leong, and C. Y. Liu, *Heat and Mass Transfer*, **1997**, 33, 121-127.

45. T. Sugawara and I. Takasu, *Advances in Physical Organic Chemistry*, **1999**, 32, 219-264.

46. T. Fujiwara, J. Harada, and K. Ogawa, *Journal of Physical Chemistry B*, **2004**, 108, 4035-4038.

47. H. Meyer, *Chemische Berichte*, **1909**, 42, 143-145.

48. A. Schönberg and O. Schutz, *Chemische Berichte*, **1928**, 61, 478-479.

49. P. U. Biedermann, J. J. Stezowski, and I. Agranat, *Chem. Commun.*, **2001**, 954-955.

50. Y. Tapuhi, O. Kailisky, and I. Agranat, *Journal of Organic Chemistry*, **1979**, 44, 1941-1948.

51. V. I. Minkin, A. V. Tsukanov, A. D. Dubonosov, and V. A. Bren, *Journal of Molecular Structure*, **2011**, 998, 179-191.

52. F. Robert, P.-L. Jacquemin, B. Tinant, and Y. Garcia, *Crystal Engineering Communications*, **2012**, 14, 4396-4406.

53. F. Robert, A. D. Naik, B. Tinant, and Y. Garcia, *Inorganica Chimica Acta*, **2012**, 380, 104-113.

54. R. Muthyala and X. Lan, *The Chemistry of Leuco Triarylmethanes*, Chapter 5 in "Chemistry and Applications of Leuco Dyes", R. Muthyala (Ed.), Plenum Press: New York, USA, **1997**.

55. V. V. Jarikov and D. C. Neckers, *Journal of Organic Chemistry,* **2001**, 66, 659-671.

56. F. Azizian, A. J. Field, B. M. Heron, and C. Kilner, *Chemical Communications*, **2012**, 48, 750-752.

57. Y. Takahashi, A. Shirai, T. Segawa, T. Takahashi, and K. Sakakibara, *Bulletin of the Chemical Society of Japan*, **2002**, 75, 2225-2231.

58. V. Raditoiu, A. Raditoiu, L. Wagner, V. Amariutei, and C. A. Nicolae, *Revista de Chimie*, **2013**, 64(2), 147-151.

59. R. Dickinson and I. M. Heilbron, *Journal of the Royal Society*, **1927**, 1699-1705.

60. M. R. di Nunzio, P. L. Gentili, A. Romani, and G. Favaro, *Journal of Physical Chemistry C*, **2010**, 114, 6123-6131.

61. G. Berkovic, V. Krongauz, and V. Weiss, *Chemical Reviews*, **2000**, 100, 1741-1753.

62. K. Kinashi, T. Horiguchi, K. Tsutsui, K. Ishida, and Y. Ueda, *Journal of Photochemistry and Photobiology A*, **2010**, 213, 189-193.

63. J. T. C. Wojtyk, A. Wasey, N.-N. Xiao, P. M. Kazmaier, S. Hoz, C. Yu, R. P. Lemieux, and E. Buncel, *Journal of Physical Chemistry A*, **2007**, 111, 2511-2516.

64. K. Ito, M. Kuwabara, K. Fukunishi, and Y. Fujiwara, *Dyes and Pigments*, **1997**, 34, 297-306.

65. R. Kulčar, M. Friškovec, M. K. Gunde, and N. Knešaurek, *Colouration Technology*, **2011**, 127, 411-417.

66. M. Friškovec, R. Kulčar, and M. K. Gunde, *Colouration Technology*, **2013**, 129, 214-222.

67. D. Zhang, *Polymers Paint Colour Journal*, **2008**, 198, 36-38.

68. M. A. Chowdhury, B. S. Butola, and M. Joshi, *Colouration Technology*, **2013**, 129, 232-237.

69. D. C. Short, A. B. Ouimet, and B. S. Short, US Patent No. 8182430 B2, **2012**.

70. N. Sekar, *Colourage*, **1998**, 45, 39-42.

71. K. Tsutsui, T. Yamaguchi, and K. Sato, *Japanese Journal of Applied Physics*, **1994**, 33, 5925-5928.

72. I. Sage, *Liquid Crystals*, **2011**, 38, 1551-1561.

73. E. Reinitzer, quoted by O. Z. Lehmann, *Phyiskalische Chemie*, **1889**, 4, 462-472.

74. D. Pauluth and E. F. Wachtler, *Synthesis and Applications of Chiral Liquid Crystals*, Chapter 13 in "Chirality in Industry II", A. N. Collins, G. N. Sheldrake, and J. Crosby (Eds.), John Wiley & Sons: West Sussex, England, **1997**.

75. C.R. Smith, D.R. Sabatino, and T.J. Praisner, *Experiments in Fluids*, **2001**, 30, 190-201.

76. M. Kertesz, C. H. Choi, and S. J. Yang, *Chemical Reviews* **2005**, 105, 3448-3481.

77. P. M. Beaujuge and J. R. Reynolds, *Chemical Reviews*, **2010**, 110, 268-320.

78. N. Hirota, N. Hisamatsu, S. Maeda, H. Tsukahara, and K. Hyodo, *Synthetic Metals*, **1996**, 80, 67-72.

79. X. Chen and J. Yoon, *Dyes and Pigments*, **2011**, 80, 194-198.

80. J. Liu, J. W. Y. Lam, and B. Z. Tang, *Chemical Reviews*, **2009**, 109, 5799-5867.

81. L. Yu and S. L. Hsu, *Macromolecules*, **2012**, 45, 420-429.

82. L. Liu, S. Peng, W. Wen, and P. Sheng, *Applied Physics Letters*, **2007**, 90, 213508 1-3.

83. C. Yang, F. P. Orfino, and S. Holdcroft, *Macromolecules*, **1996**, 29, 6510-6517.

84. C. Phollookin, S. Wacharasindhu, A. Ajavakom, G. Tumcharern, S. Ampornpun, T. Eaidkong, and M. Sukwattanasinitt, *Macromolecules*, **2010**, 43, 7540-7548.

85. H. Tachibana, R. Kumai, N. Hosaka, and Y. Tokura, *Chemistry of Materials*, **2001**, 13, 155-158.

86. M. Wenzel and G.H. Atkinson, *Journal of the American Chemical Society*, **1989**, 111, 6123-6127.

87. M. Tanaka, *Bulletin of the Chemical Society of Japan*, **1993**, 70, 3171-3174.

88. D. Yan, J. Lu, J. Ma, M. Wei, D. G. Evans, and X. Duan, *Angewandte Chemie International Edition*, **2011**, 50, 720 –723.

89. P. M. Alvey, J. J. Reczek, V. Lynch, and B. L. Iverson, *Journal of Organic Chemistry*, **2010**, 75, 7682–7690.

90. J. H. Day, *Chemical Reviews*, **1968**, 68, 649-657.

91. V. Melnik, I. Khatsevych, V. Kladko, A. Kuchuk, V. Mikirin, and B. Romanyuk, *Materials Letters*, **2012**, 68, 215-217.

92. Y. Ma, B. Zhu, and K. Wu, *Journal of Coatings Technology*, **2000**, 72, 67-71.

93. C.G. Granqvist, P.C. Lansåker, N.R. Mlyuka, G.A. Niklasson, and E. Avendaño, *Solar Energy Materials & Solar Cells*, **2009**, 93, 2032-2039.

94. Y. Ma, B. Zhu, and K. Wu, *Solar Energy*, **2001**, 70, 417-422.

95. J. Schwiertz, A. Geist and M. Epple, *Dalton Transactions*, **2009**, 2921-2925.

96. M. Marinković, R. Nikolić, J. Savović, S. Gadžurić, and I. Zsigrai, *Solar Energy Materials & Solar Cells*, **1998**, 51, 401-411.

97. S. Gadžurić, M. Vraneš, and S. Dožić, *Solar Energy Materials & Solar Cells*, **2012**, 105, 309-316.

98. R. R. Mather, *Review of Progress in Coloration and Related Topics*, **2001**, 31, 36-41.

99. K. Naito, *Applied Physics Letters*, **1995**, 67(2), 211-213.

100. S. M . Burkinshaw, J. Griffiths, and A. D. Towns, *Journal of Materials Chemistry*, **1998**, 8, 2677-2683.

101. D. C. MacLaren and M. A. White, *Journal of Materials Science*, **2005**, 40¸ 669-676.

102. H. Tang, D. C. MacLaren, and M. A. White, *Canadian Journal of Chemistry*, **2010**, 8, 1063-1070.

103. H. Xiaoxiu, W. Na, Y. Xing, and S. Cheng, *Advanced Materials Research*, **2012**, 380, 7-10.

104. H. Oda, *Sen'I Gakkaishi*, **2007**, 63, 81-86.

105. T. Gotanda, S. Takayama, Y. Sekiguchi, K. Sano, K. Maeda, and Y. Imamura, *Journal of Imaging Science and Technology*, **2006**, 50, 509-515.

106. H. Oda and T. Kitao, *Japanese Society of Dyers and Colorists*, **1989**, 105, 257-261.

107. C. F. Zhu and A. B. Wu, *Thermochimica Acta*, **2005**, 425, 7-12.

108. L. Van der Schueren and K. de Clerck, *Coloration Technology*, **2011**, 128, 82-90.

109. M. A. Chowdhury, M. Joshi, and B. S. Butola, *Asian Dyer*, **2012**, 59-62.

110. D. C. MacLaren, *PhD Thesis*, Department of Chemistry, Dalhousie University, **2003**.

111. H. Oda and T. Kitao, *Dyes and Pigments*, **1991**, *16,* 1-10.

112. C. R. Theocharis and W. Jones, *Journal of Crystallographic and Spectroscopic Research*, **1984**, 14, 121-128.

113. G. Rihs and C. D. Weis, *Dyes and Pigments*, **1991**, 15, 107-127.

114. M. Kuzuya, T. Usui, S. Ito, F. Miyake, S. Nozawa, and T. Okuda, *Chemical Pharmacology Bulletin*, **1980**, 28, 3561-3569.

115. D. A. Hinckley, P. G. Seyfold, and D. P. Berris, *Spectrochimica Acta*, **1986**, 42A, 747-754.

116. M. Yanagita, I. Aoki, and S. Tokita, *Bulletin of the Chemical Society of Japan*, **1997**, 70, 2757-2763.

117. K. Takaoka, S. Maeda, H. Miura, K. Endo, and D. P. Chong, *Bulletin of the Chemical Society of Japan*, **1998**, 71, 807-816.

118. G. Lingjie, Z. Tianzeng, Q. Hailin, and F. Jingguo, *Chinese Journal of Magnetic Resonance*, **1995**, 12, 607-611.

119. Y. Sekiguchi, S. Takayama, T. Gotanda, and K. Sano, *Chemistry Letters*, **2006**, 35, 458-459.

120. D.A. Hinckley and P.G. Seyfold, *Spectrochimica Acta*, **1988**, 44A, 1053-1059.

121. K. Hideaki, K. Keishi, K. Tsutsui, H. Goto, E. Kawamura, H. Kuboyama, S. Maruyama, I. Sawamura, M. Shimada, and T. Yamaguchi, *Ricoh Co. Ltd*., European Patent No. 576015, **1994**.

122. S. Maruyama, H. Goto, E. Kawamura, M. Shimada, K. Kubo, K. Tsutsui, H. Ema, T. Yamaguchi, H. Kuboyama, I. Sawamura, and K. Taniguchi, *Ricoh Co. Ltd.*, US Patent No. 5395433, **1995**.

123. K. Sano, S. Takayama, T. Gotanda, and Y. Sekiguchi, *Kabushiki Kaisha Toshiba*, US Patent No. 2010/0021840 A1, **2010**.

124. T. Gotanda, S. Takayama, Y. Sekiguchi, and K. Sano, *Kabushiki Kaisha Toshiba*, European Patent No. EP 2515175 A1, **2012**.

125. J.-M. Yan and D.-Y. Yan, *Chinese Science Bulletin*, **1994**, 39, 1448-1451.

126. E. Takai, A. Hirano, and K. Shiraki, *Journal of Biochemistry*, **2011**, 150, 165-171.

127. J. S. Wright, E. R. Johnson, and G.A. DiLabio, *Journal of the American Chemical Society*, **2001**, 123, 1173-1183.

128. S. G. Morris and R. W. Riemenschneider, *Journal of the American Chemical Society,* **1946**, 68, 500-501.

129. S. G. Morris, L. A. Kraekel, D. Hammer, J. S. Myers, and R. W. Riemenschneider, *Journal of the Americal Oil Chemists' Society*, **1947**, 309-311.

130. G. J. M. van der Kerk, J. H. Verbeek, and J. C. F. Cleton, *Recueil des Travaux Chimiques des Pays-Bas et de la Belgique*, **1951**, 70, 277-284.

131. L. A. Savi, P. C. Leal. T. O. Vicira, R. Rosso, R. J. Nunes, R. A. Nunes, T. B. Creczynski-Pasa, C. R. M. Barardi, and C. M. O. Slmoes, *Arzneimittel Forschung*, **2005**, 55, 66-75.

132. L.S. Vartanyan and E.M. Gonikberg, *Izvestiya Akademii Nauk SSSR, Seriya Khimicheskaya*, **1963**, 11, 2047-2049.

133. Calculated using Advanced Chemistry Development (ACD/Labs) Software V11.02 (© 1994-2013 ACD/Labs). Retrieved November, 2013.

134. A.A. Hasanein, M.S. Masoud, and M.M. Habeeb, *Spectroscopy Letters*, **1988**, 21, 481-83.

135. B. Sas, B. Coppens, and J. Van hemel, US Patent No. 6297396, **2001**.

136. N. Okabe and H. Kyoyama, *Acta Crystallographica E*, **2002**, E58, o245-o247.

137. N. Okabe and H. Kyoyama, *Acta Crystallographica E*, **2002**, E58, o442-o444.

138. G.A. Jeffrey and Y. Yeon, *Acta Crystallographica E*, **1990**, B46, 519-524.

139. K. Yammane and M. Nishioka, *OJI Paper Co.*, US Patent No. 5928988, **1999**.

140. S. Takayama and K. Sano, *Journal of the Imaging Society of Japan*, **2006**, 45, 142-145.

141. H. Furuya, M. Torii, K. Tsutsui, and M. Shimada, *Ricoh Co. Ltd.*, US Patent No. 6001159, **1999**.

142. S. Takayama, F. Sawoko, T. Okuyama, H. Nishizawa, H. Miyamoto, and M. Sugiuchi, *Kabushiki Kaisha Toshiba*, US Patent No. 5849651, **1998**.

143. D. C. MacLaren and M. A. White, *Journal of Materials Chemistry*, **2003**, 13¸ 1701-1704.

144. A. Watanabe, *Bulletin of the Chemical Society of Japan*, **1961**, 34, 398-402.

145. A. Watanabe, *Bulletin of the Chemical Society of Japan*, **1961**, 34, 1728-1734.

146. D. G. Kolp and E. S. Lutton, *Journal of the American Chemical Society*, **1951**, 5593-5595.

147. K. Růžička, M. Fulem, V. Růžička, and M. Zábranský, *Thermochimica Acta*, **2004**, 421, 35-41.

148. E. B. Sirota and X. Z. Wu, *Journal of Chemical Physics*, **1996**, 105, 7763-7773.

149. V. C. van Miltenburg, H. A. J. Oonk, and L. Ventola, *Journal of Chemical Engineering Data*, **2001**, 46, 90-97.

150. K. Tanaka, T. Sato, and T. Hayashida, *Bulletin of the Institute for Chemical Research, Kyoto University*, **1958**, 35, 123-128.

151. J. D. Hoffman and C. P. Smyth, *Journal of the American Chemical Society*, **1949**, 71, 431-439.

152. N. G. Parsonage and L. A. K. Staveley, *Disorder in Crystals*, Oxford University Press: Oxford, England, **1978**.

153. L. Ventola, M. Ramirez, T. Calvet, X. Solans, M. A. Cuevas-Diarte, P. Negrier, D. Mondieig, J. C. van Mittenburg, and H. A. J. Oonk, *Chemistry of Materials*, **2002**, 14, 508-517.

154. M. Soutzidou, V.-A. Glezakou, K. Viras, M. Helliwell, A. J. Masters, and M. A. Vincent, *Journal of Physical Chemistry B*, **2002**, 106, 4405-4411.

155. L. Ventolà, T. Calvet, M. A. Cuevas-Diarte, M. Ramirez, H. A. J. Oonk, D. Mondieig, and Ph. Negrier, *Physical Chemistry Chemical Physics*, **2004**, 6, 1786-1791.

156. C. Mosselman, J. Mourik, and H. Dekker, *Journal of Chemical Thermodynamics*, **1974**, 6, 477-487.

157. T. Yamamoto, K. Nozaki, and T. Hara, *Journal of Physical Chemistry*, **1990**, 92, 631-641.

158. F. Michaud, L. Ventola, M. T. Calvet, M. A. Cuevas-Diarte, X. Solans, and M. Font-Bardia, *Acta Crystallographica*, **2000**, C56, 219-211.

159. M. G. Broadhurst, *Journal of the Research of the National Bureau of Standards A*, **1962**, 66A, 241-249.

160. M. Tasumi, T. Shimanouchi, A. Watanabe, and R. Goto, *Spectrochimica Acta*, **1964**, 20, 629-666.

161. A. Ammar and D. A. Young, *Molecular Crystals and Liquid Crystals*, **1974**, 27, 207-215.

162. J. Xing, Z.-C. Tan, Q. Shi, S.-X. Wang, and Y.-S. Li, *Journal of Thermal Analysis and Calorimetry*, **2008**, 92, 375-380.

163. S. Ishikawa and I. Ando, *Journal of Molecular Structure*, **1993**, 291, 183-190.

164. D. C. MacLaren and M. A. White, *Journal of Materials Chemistry*, **2003**, 13¸ 1695-1700.

165. K. Tsutsui, T. Yamaguchi, and K. Sato, *Ranliao Gongye*, **1995**, *1*, 68-73.

166. K. Naito, *Kabushiki Kaisha Toshiba*, US Patent No. 5869420, **1999**.

167. K. Fujita and Y. Ono, *Pilot Ink Co. Ltd.*, US Patent No. 5919404, **1999**.

168. H. Furuya, M. Torii, K. Tsutsui, and M. Shimada, *Ricoh Co. Ltd.*, US Patent No. 5866505, **1999**.

169. K. Fujita and K. Senga, *Matsushita Electric Industrial Co.*, European Patent No. EP 1084860, **2001**.

170. J. Maruyama and H. Sano, *Mitsubishi Paper Mills Ltd.*, US Patent No. 6184180 B1, **2001**.

171. J. M. Jacobson and J. Sun, *Massachusetts Institute of Technology*, US Patent No. 6022648, **2000**.

172. M. Yanagita, S. Kanda, and S. Tokita, *Molecular Crystals and Liquid Crystals*, **1999**, 327, 49-52.

173. M. Yanagita, S. Kanda, and S. Tokita, *Molecular Crystals and Liquid Crystals*, **1999**, 327, 53-56.

174. K. Ibata, K. Iriishi, T. Otsuka, and S. Saito, *IS&T's Eigth Internation Congress on Advances in Non-Impact Printing Technologies*, **1992**, 376-380.

175. J. Luthern and A. Peredes, *Journal of Materials Science Letters*, **2000**, 19, 185-188.

176. J. Luthern and A. Peredes, *Journal of Materials Science Letters*, **2003**, 22, 881-884.

177. D. Lin-Vlen, N.B. Colthup, W.G. Fateley, and J.G. Grasselli, *The Handbook of Infrared and Raman Characteristic Frequencies of Organic Molecules*, Academic Press: Boston, US, **1991**.

178. G. Varsanyi, *Assignments for Vibrational Spectra of Seven Hundred Benzene Derivatives*, Vol. 1, John Wiley & Sons: New York, US, **1974**.

179. Y. Takahashi, A. Iwasaki, and K. Toyofuku, *IS&T's Tenth International Congress on Advances in Non-Impact Printing Technologies*, **1994**, 361.

180. S. Kubota, T. Mori, N. Matsuo, and Y. Shono, *Journal of Pesticide Science*, **2011**, 36, 63-65.

181. H. Tang, *MSc Thesis*, Department of Chemistry, Dalhousie University, **2007**.

182. GIMP 2.0, GNU Image Manipulation Program, http://www.gimp.org. Last accessed July 15, 2013.

183. ImageJ, Image Processing and Analysis in Java, National Institutes of Health, USA, http://rsbweb.nih.gov/ij/. Last accessed July 15, 2013

184. EasyRGB colour conversion program, http://www.easyrgb.com. Last accessed July 15, 2013.

185. Minolta CR-300 Chroma Meter, Color Guide and Operation Manual, Konica Minolta, **1991**.

186. Charles Poynton, Color FAQ, **2009**, http://poynton.com/ColorFAQ.html. Last accessed July 15, 2013.

187. X-Rite Inc., "The Color Guide and Glossary", http://www.xrite.com/documents/literature/en/L11-029_color_guide_en.pdf. Last accessed July 15, 2013.

188. Private Communication with Dr. Kenji Sano, Toshiba Corporation, **2011**.

189. M. A. White, *Thermal Analysis and Calorimetry*, Chapter 4 in Volume 8 "Physical Methods in Supramolecular Chemistry", J. Ripmeester and J.E. Davies (Eds.) in "Comprehensive Supramolecular Chemistry", J.-M. Lehn, J.L. Atwood, D.D. MacNicol, J. E. D. Davies, and F. Vogtle (Eds.), Pergamon: Oxford, UK, **1996**.

190. V. J. Griffin and P.G. Laye, *Differential Thermal Analysis and Differential Scanning Calorimetry*, Chapter 2 in "Thermal Analysis Techniques and Applications", E. L.Charsley and S. B. Warrington (Eds.), Royal Society of Chemistry: Cambridge, UK, **1992**.

191. B. Wunderlich, *Thermal Analysis*, Academic Press Inc.: Boston, US, **1990**.

192. M. B. Johnson and M. A. White, *Thermal Methods*, Chapter 2 in "Inorganic Materials: Multi-Length Scale Characterisation", D. W. Bruce, D. O'Hare, and R. I. Walton (Eds.), John Wiley & Sons, Ltd.: West Sussex, UK, **2014**.

193. X. Hao, N. Wei, X. Yin, and C. Sun, *Advanced Materials Research*, **2012**, 380, 7-10.

194. S. Yamamoto, H. Furuya, K. Tsutsui, S. Ueno, and K. Sato, *Crystal Growth & Design*, **2008**, 8, 2256-2263.

195. W. Laguardia and D. Laguardia, *Cups Unlimited Llc*., US Patent No. US 20070053406 A1, **2007**.

196. C. J. Scott and C. Y. Straka, US Patent No. US 20090183669 A1, **2009**.

197. C. Carrot, S. Mbarek, M. Jaziri, Y. Chalamet, C. Raveyre, and F. Prochazka, *Macromolecular Materials and Engineering*, **2007**, 292, 693-706.

198. J. M. R. C. A. Santos, and James T. Guthrie, *Journal of Materials Chemistry*, **2006**, 16, 237-245.

199. J. S. Grebowicz, *Journal of Thermal Analysis*, **1996**, 46, 1151-1166.

200. W. K. Waldron, G. B. McKenna, and M. M. Santore, *Journal of Rheology*, **1995**, 39, 471-497.

201. K. Sano, Y. Sekiguchi, S. Takayama, and T. Gotanda, *Toshiba TEC Kabushiki Kaisha* and *Kabushiki Kaisha Toshiba*, US Patent No. US 2012/0266778 A1, **2012**.

202. T. Mendum, E. Stoler, H. VanBenschoten, and John C. Warner, *Green Chemistry Letters and Reviews,* **2011***,* 4, 81-86.

203. T. Geens, D. Aerts, C. Berthot, J.-P. Bourguignon, L. Goeyens, P. Lecomte, G. Maghuin-Rogister, A.-M. Pironnet, L. Pussemier, M.-L. Scippo, J. Van Loco, and A. Covaci, *Food and Chemical Toxicity*, **2012**, 50, 3725-3740.

204. T. Geens, L. Goeyens K. Kannan, H. Neels, and A. Covaci, *Science of the Total Environment*, **2012**, 435-436, 30-33.

205. B. Borrell, *Nature*, **2010**, 464, 22, 1122-1124.

206. S. Machida, A. Takayama, K. Sano, K. Tsunemi, and S. Sato, *Toshiba Corp.*, Japanese Patent No. JP 2000019770 A, **2000**.

207. K. Sano, A. Takayama, S. Machida, S. Ikeda, and T. Urano, *Toshiba Corp.*, Japanese Patent No. JP 2000160041 A, **2000**.

208. A. Takayama, K. Sano, T. Gotanda, and Y. Sekiguchi, *Toshiba Corp.*, Japanese Patent No. JP 2010190973 A, **2010**.

209. Y. Sekiguchi, K. Sano, A. Takayama, T. Gotanda, T. Madono, and N. Sunada, *Toshiba Corp.* and *Yamada Chemical Co., Ltd.*, Japanese Patent No. JP 2013028727 A, **2013**.

210. K. Nozaki, M. Munekane, T. Yamamoto and Y. Ogawa, *Journal of Materials Science*, **2006**, 4, 3935-3946.

211. G. M. Anderson and D. A. Crerar, *Thermodynamics in Geochemistry: The Equilibrium Model*, Oxford University Press: Oxford, UK, **1993**.

212. I. Prigogine and R. Defay, *Chemical Thermodynamics,* Longmans: London, UK, **1965**.

213. H. A. J. Oonk, *Phase Theory: The Thermodynamics of Heterogeneous Equilibria*, Elsevier: Amsterdam, Holland, **1981**.

214. Toshiba Co. e-blue Press Release, December 2, 2003. http://www.toshiba.co.jp/about/press/2003_12/pr0201.htm. Last accessed July 16, 2003.

215. Tanaka, K. Sano, K. Minakami, N. Takeyama, H. Kagami and K. Haruki, "*Environmental Load of Decolorable Ink with an LCA Perspective*", Internal Communication, Toshiba Corporation, **2003**.

216. T. A. M. Counsell, and J. M. Allwood, *Resources, Conservation and Recycling*, **2007**, 49, 340-352.

217. K. Sano, K. Maito, S. Takayama, S. Fujioka, T. Okuyama, and S. Machida, *Kabushiki Kaisha Toshiba*, US Patent No. 6277208 B1, **2001**.

218. S. Takayama, T. Gotanda, and K. Sano, *Journal of the Imaging Society of Japan*, **2005**, 44, 326-331.

219. L. Yang, R. Lanz, and B. Kruse, *Journal of the Optical Society of America*, **2001**, A18, 360-366.

220. L. Yang and B. Kruse, *Journal of Imaging Science and Technology*, **2004**, 48.

221. W. M. Haynes, ed., *CRC Handbook of Chemistry and Physics*, 94th Edition, CRC Press/Taylor and Francis: Boca Raton, Forida, USA, **2013**.

222. Ch. Kappel, U. Hirn, M. Donoser, and W. Bauer, *94th Annual Meeting, Pulp and Paper Technical Association of Canada*, **2006**, B539-B542.

223. T. A. M. Counsell, *Ph.D. Thesis*, Department of Engineering, Clare College, University of Cambridge, **2007**.

224. D. R. Leal-Ayala, J. M. Allwood, and T. A. M. Counsell, *Applied Physics A*, **2011**, 105, 801-818.

225. N. Higashihara, K. Shiraishi, K. Miyata, Y. Oshima, Y. Minobe, and K. Yamasaki, *Archives of Toxicology*, **2007**, 81, 825-832.

226. L. Yang, *Journal of the Optical Society of America A*, **2003**, 20, 1149-1154.

227. J. Tao, *MSc Thesis*, Department of Materials Science and Engineering, Worcester Polytechnic Institute, **2003**.

228. P.Puukko, A. Ilmonen, T. Lamminmaki, and S. Sundqvist, *NIP25 and Digital Fabrication 2009 – Technical Program and Proceedings*, **2009**, 566-569.

Appendix

Permissions for Reproduced Figures

Permission for reproduction of Figure 1.9

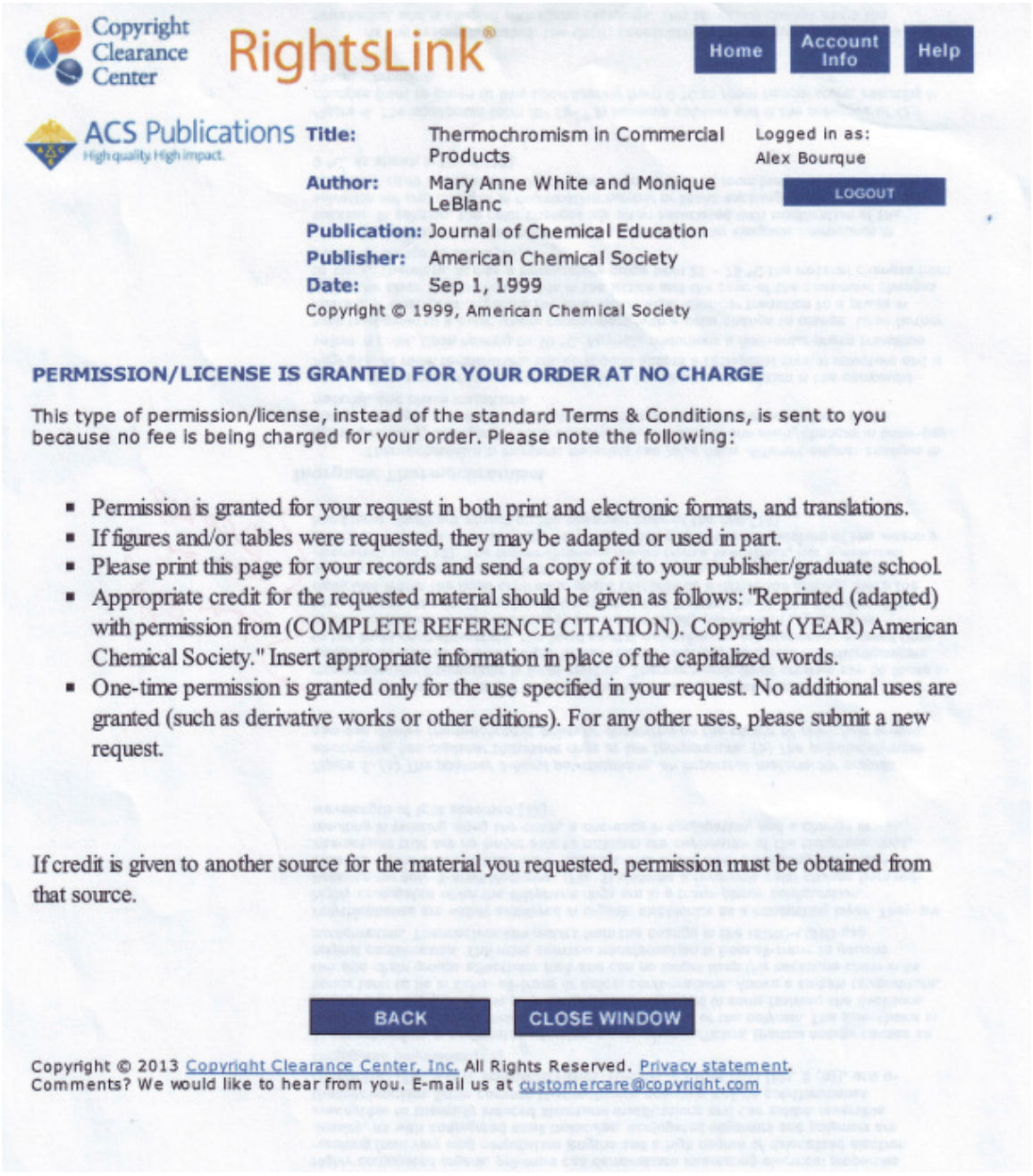

Copyright Clearance Center RightsLink®

Home | Account Info | Help

ACS Publications High quality. High impact.

Title: Thermochromism in Commercial Products

Author: Mary Anne White and Monique LeBlanc

Publication: Journal of Chemical Education

Publisher: American Chemical Society

Date: Sep 1, 1999

Copyright © 1999, American Chemical Society

Logged in as: Alex Bourque

LOGOUT

PERMISSION/LICENSE IS GRANTED FOR YOUR ORDER AT NO CHARGE

This type of permission/license, instead of the standard Terms & Conditions, is sent to you because no fee is being charged for your order. Please note the following:

- Permission is granted for your request in both print and electronic formats, and translations.
- If figures and/or tables were requested, they may be adapted or used in part.
- Please print this page for your records and send a copy of it to your publisher/graduate school.
- Appropriate credit for the requested material should be given as follows: "Reprinted (adapted) with permission from (COMPLETE REFERENCE CITATION). Copyright (YEAR) American Chemical Society." Insert appropriate information in place of the capitalized words.
- One-time permission is granted only for the use specified in your request. No additional uses are granted (such as derivative works or other editions). For any other uses, please submit a new request.

If credit is given to another source for the material you requested, permission must be obtained from that source.

BACK | CLOSE WINDOW

Copyright © 2013 Copyright Clearance Center, Inc. All Rights Reserved. Privacy statement.
Comments? We would like to hear from you. E-mail us at customercare@copyright.com

Permission for reproduction of Figure 2.1.

SPRINGER LICENSE
TERMS AND CONDITIONS

Feb 18, 2014

This is a License Agreement between Alex Bourque ("You") and Springer ("Springer") provided by Copyright Clearance Center ("CCC"). The license consists of your order details, the terms and conditions provided by Springer, and the payment terms and conditions.

All payments must be made in full to CCC. For payment instructions, please see information listed at the bottom of this form.

License Number	3332040820742
License date	Feb 18, 2014
Licensed content publisher	Springer
Licensed content publication	Journal of crystallographic and spectroscopic research
Licensed content title	Crystal structure of 3,3-(p-N,N-dimethylaminophenyl)-6-N,N-dimethylaminophthalide, (crystal-violet lactone)
Licensed content author	Charis R. Theocharis
Licensed content date	Jan 1, 1984
Volume number	14
Issue number	2
Type of Use	Thesis/Dissertation
Portion	Figures
Author of this Springer article	No
Order reference number	
Title of your thesis / dissertation	Investigations of Reversible Thermochromism in Three-Component Systems
Expected completion date	May 2014
Estimated size(pages)	300
Total	0.00 USD
Terms and Conditions	

Introduction

The publisher for this copyrighted material is Springer Science + Business Media. By clicking "accept" in connection with completing this licensing transaction, you agree that the following terms and conditions apply to this transaction (along with the Billing and Payment terms and conditions established by Copyright Clearance Center, Inc. ("CCC"), at the time that you opened your Rightslink account and that are available at any time at http://myaccount.copyright.com).

Permission for reproduction of Figure 2.3

ELSEVIER LICENSE
TERMS AND CONDITIONS

Feb 13, 2014

This is a License Agreement between Alex Bourque ("You") and Elsevier ("Elsevier") provided by Copyright Clearance Center ("CCC"). The license consists of your order details, the terms and conditions provided by Elsevier, and the payment terms and conditions.

All payments must be made in full to CCC. For payment instructions, please see information listed at the bottom of this form.

Supplier	Elsevier Limited The Boulevard,Langford Lane Kidlington,Oxford,OX5 1GB,UK
Registered Company Number	1982084
Customer name	Alex Bourque
Customer address	Dalhousie University Halifax, NS B3H4R2
License number	3327240141095
License date	Feb 13, 2014
Licensed content publisher	Elsevier
Licensed content publication	Journal of Photochemistry
Licensed content title	Photochemical fading and photostabilization of the crystal violet lactone colour former system
Licensed content author	Norman S. Allen,Nigel Hughes,Paul Mahon
Licensed content date	May 1987
Licensed content volume number	37
Licensed content issue number	2
Number of pages	12
Start Page	379
End Page	390
Type of Use	reuse in a thesis/dissertation
Portion	figures/tables/illustrations
Number of figures/tables/illustrations	1
Format	both print and electronic
Are you the author of this Elsevier article?	No

Will you be translating?	No
Title of your thesis/dissertation	Investigations of Reversible Thermochromism in Three-Component Systems
Expected completion date	May 2014
Estimated size (number of pages)	300
Elsevier VAT number	GB 494 6272 12
Permissions price	0.00 USD
VAT/Local Sales Tax	0.00 USD / 0.00 GBP
Total	0.00 USD
Terms and Conditions	

Figures 2.6 and 2.7 are reproduced under the fair use clause of the Creative Commons open license.

Creative Commons

Attribution 2.0 England and Wales

CREATIVE COMMONS CORPORATION IS NOT A LAW FIRM AND DOES NOT PROVIDE LEGAL SERVICES. DISTRIBUTION OF THIS LICENCE DOES NOT CREATE AN ATTORNEY-CLIENT RELATIONSHIP. CREATIVE COMMONS PROVIDES THIS INFORMATION ON AN "AS-IS" BASIS. CREATIVE COMMONS MAKES NO WARRANTIES REGARDING THE INFORMATION PROVIDED, AND DISCLAIMS LIABILITY FOR DAMAGES RESULTING FROM ITS USE.

Licence

THE WORK (AS DEFINED BELOW) IS PROVIDED UNDER THE TERMS OF THIS CREATIVE COMMONS PUBLIC LICENCE ("CCPL" OR "LICENCE"). THE WORK IS PROTECTED BY COPYRIGHT AND/OR OTHER APPLICABLE LAW. ANY USE OF THE WORK OTHER THAN AS AUTHORIZED UNDER THIS LICENCE OR COPYRIGHT LAW IS PROHIBITED. BY EXERCISING ANY RIGHTS TO THE WORK PROVIDED HERE, YOU ACCEPT AND AGREE TO BE BOUND BY THE TERMS OF THIS LICENCE. THE LICENSOR GRANTS YOU THE RIGHTS CONTAINED HERE IN CONSIDERATION OF YOUR ACCEPTANCE OF SUCH TERMS AND CONDITIONS.

This Creative Commons England and Wales Public Licence enables You (all capitalised terms defined below) to view, edit, modify, translate and distribute Works worldwide, provided that You credit the Original Author.

'The Licensor' [one or more legally recognised persons or entities offering the Work under the terms and conditions of this Licence]

and

'You'

agree as follows:

1. Definitions

a. **"Attribution"** means acknowledging all the parties who have contributed to and have rights in the Work, Derivative Work or Collective Work under this Licence.

b. **"Collective Work"** means the Work in its entirety in unmodified form along with a number of other separate and independent works, assembled into a collective whole.

c. **"Derivative Work"** means any work created by the editing, modification, adaptation or translation of the Work in any media (however a work that constitutes a Collective Work will not be considered a Derivative Work for the purpose of this Licence). For the avoidance of doubt, where the Work is a musical composition or sound recording, the synchronization of the Work in timed-relation with a moving image ("synching") will be considered a Derivative Work for the purpose of this Licence.

d. **"Licence"** means this Creative Commons England and Wales Public Licence agreement.

e. **"Original Author"** means the individual (or entity) who created the Work.

f. **"Work"** means the work protected by copyright which is offered under the terms of this Licence.

g. For the purpose of this Licence, when not inconsistent with the context, words in the singular number include the plural number.

2. Licence Terms

2.1 The Licensor hereby grants to You a worldwide, royalty-free, non-exclusive, Licence for use and for the duration of copyright in the Work.

You may:

- copy the Work;
- create one or more Derivative Works;
- incorporate the Work into one or more Collective Works;
- copy Derivative Works or the Work as incorporated in any Collective Work; and
- publish, distribute, archive, perform or otherwise disseminate the Work, Derivative Works or the Work as incorporated in any Collective Work, to the public in any material form in any media whether now known or hereafter created.

Permission for reproduction of Figures 2.10, 2.11, 2.12, 2.13, 2.14, 2.16, 2.17, 5.13

Re: Permission to Use Figures

douglas.c.maclaren@esso.ca

Fri 2/25/2011 5:47 PM

To: Alex Bourque;

Of course, Alex. You have my permission to use any and all materials in my Ph.D. thesis to support materials to support your project work - preliminary report, papers, presentations, final thesis.

Best of luck in the prelim... It is a lot of work, but if well drafted it can serve as a good framework to get your thesis kickstarted!

Cheers,

D.C. (Doug) MacLaren

Section Head - Research Support Section

Imperial Oil Ltd.
Sarnia Research Centre
453 Christina St. S.
Sarnia, ON, CANADA
N7T 8C8

Tel. (519) 339-2283
Cell (519) 328-0905
Fax. (519) 339-4048
Email: douglas.c.maclaren@esso.ca

Permission for reproduction of Figure 2.15.

ROYAL SOCIETY OF CHEMISTRY LICENSE TERMS AND CONDITIONS

Feb 21, 2014

This is a License Agreement between Alex Bourque ("You") and Royal Society of Chemistry ("Royal Society of Chemistry") provided by Copyright Clearance Center ("CCC"). The license consists of your order details, the terms and conditions provided by Royal Society of Chemistry, and the payment terms and conditions.

All payments must be made in full to CCC. For payment instructions, please see information listed at the bottom of this form.

License Number	3333631509786
License date	Feb 21, 2014
Licensed content publisher	Royal Society of Chemistry
Licensed content publication	Journal of Materials Chemistry
Licensed content title	Dye–developer interactions in the crystal violet lactone–lauryl gallate binary system: implications for thermochromism
Licensed content author	Douglas C. MacLaren,Mary Anne White
Licensed content date	May 9, 2003
Volume number	13
Issue number	7
Type of Use	Thesis/Dissertation
Requestor type	academic/educational
Portion	figures/tables/images
Number of figures/tables/images	3
Format	print and electronic
Distribution quantity	10
Will you be translating?	no
Order reference number	
Title of the thesis/dissertation	Investigations of Reversible Thermochromism in Three-Component Systems
Expected completion date	May 2014
Estimated size	300
Total	0,00 USD

Terms and Conditions

This License Agreement is between {Requestor Name} ("You") and The Royal Society of Chemistry ("RSC") provided by the Copyright Clearance Center ("CCC"). The license consists of your order details, the terms and conditions provided by the Royal Society of Chemistry,

Permission for reproduction of Figure 7.1.

Re: Permission to use Figures

Hong Tang <HN807758@dal.ca>

Tue 3/29/2011 10:13 AM

To: Alex Bourque;

Sorry to respond late. Yes, you can use the figures and let me know if you have more questions.

Good luck!

Hong